Rho GTPase Signalling in Cilia and Blood Vessel Lumen Formation

Gary Grant

Submitted in accordance with the requirements for the degree of
Doctorate of philosophy (PhD)

The University of Leeds
Leeds institute of Cancer Studies and Pathology
School of Medicine

February 2017

The candidate confirms that appropriate credit has been given within the thesis where reference has been made to the work of others.

Acknowledgements

Many people have contributed to me completing my research degree and I would like to start by thanking my Fiancé Gillian Ward for all of the support and advice she provided through this process and for the huge part she played in me completing this PhD project. I would also like to thank my parents and family for their support and encouragement thorough my entire educational journey not only my PhD studies.

I would like to thank my primary supervisor Dr. Georgia Mavria for her help and support throughout my PhD study. Her widespread knowledge and passion for research has given me inspiration to develop a love for scientific research which will be invaluable in any future endeavours. I am also extremely grateful to my co-supervisor Prof. Colin Johnson, whose expert advice and interest in his subject area left me with a revitalised desire to continue a career in scientific research.

I would also like to acknowledge all the past and present members of the Mavria research group especially Marghe Scarcia, Kathyrn McMahon and Anne Sanford for the training they gave me at the beginning of my PhD. I would like to thank of all of the staff and students on level five of the Wellcome Trust Brennor Building who have provided not only scientific advice but also provided four years of great laughs which has made the process of this research degree a lot easier.

Finally, I would like to thank all of the collaborators who made this project possible though provision of methods, materials, or expert advice. I would like to thank the group of Prof Christopher Marshall at the Institute of Cancer Research London, including Maggie Yeo for her instrumental help with the ROCK project. I am thankful to Filomena Estevez for her help with embryos analysis and all the members of the LIMM imaging team.

Abstract

Vascular endothelial cells, the cells that line blood vessels, play roles both in the development of the circulatory system through providing blood vessel integrity, and its homeostasis through responding to changes in the local environment. During development, the acquisition of functionality of new blood vessels, some of which form from pre-existing ones through the process of angiogenesis, requires generation of endothelial lumens to carry the blood, during a process known as lumenogenesis. Throughout new blood vessel formation, endothelial cells go through coordinated and complex cell shape changes and polarity changes driven by Rho GTPase activity. Rho GTPases control intracellular actin dynamics and therefore affect all stages of new vessel growth. Precise control of Rho GTPase signalling is through a range of upstream activator and downstream effector proteins.

Here we have investigated the role of two proteins involved in the antagonistic Rho/ Rac pathways during angiogenesis and lumen formation. Results presented in this thesis describe a role for the Rac guanine nucleotide exchange factor (GEF) DOCK4, and Cdc42 GEF DOCK9, in controlling lumen formation in an organotypic *in vitro* angiogenesis assay, through both common and distinct cellular mechanisms. The RhoA effector ROCK1/2 controls RhoA-mediated cytoskeletal remodelling and have been shown to control angiogenesis in tissue culture assays. Here we use *in vivo* knockout mouse model to show that ROCK2 controls actin-based filopodia formation and vessel integrity, as well as other cytoskeletal processes such as ciliogenesis. Further investigation showed that loss of ROCK2 results in aberrant lumen formation. We also highlight a new role for ROCK2 signalling in primary cilia growth and abundance in endothelial cells which may also impact on lumen formation.

In summary, this work has identified novel molecular pathways that control lumen formation in endothelial cells. These results build on the current understanding of molecular mechanisms involved in lumen formation, and may also lead to better understanding of the function of ROCK, a potential therapeutic target in therapeutic angiogenesis strategies.

Table of Contents

Acknowledgements ..... **iii**

Abstract ..... **iv**

Table of Contents ..... **v**

List of Figures ..... **ix**

List of Tables ..... **xii**

List of Abbreviations ..... **xiii**

Chapter 1 ..... **1**

Introduction **1**

1. Blood vessel formation **2**

1.1 The circulatory system 2

1.2 Developmental angiogenesis **3**

1.2.1 Mechanisms of angiogenesis 4

1.3 Pathological angiogenesis **7**

1.4 Angiogenic signalling **9**

1.5 Lumen formation **11**

1.5.1 Cellular mechanisms of blood vessel lumen formation 11

1.5.2 Molecular mechanisms of lumen formation 20

1.6 Actin **24**

1.6.1 Actin machinery 26

1.6.1.1 ARP2/3 26

1.6.1.2 Formins 27

1.6.1.3 Profilin 27

1.6.1.4 ADF/Cofilin 28

1.6.1.5 Myosins 29

1.6.2 The actin cytoskeleton 29

1.6.3 Rho GTPases 30

1.6.3.1 Cdc42 30

1.6.3.2 Rac1, 2, 3 31

1.6.3.3 RhoA, B and C 32

1.6.4 Guanine nucleotide exchange factors (GEFs) 35

1.6.4.1 DOCK4 36

1.6.4.2 DOCK9 37

1.6.5 Rho effectors 39

1.7 Primary cilia **43**

1.7.1 Primary cilia structure and function 43
1.7.2 Endothelial cilia and their role in sensing blood flow 47
1.7.3 Cilia and actin cytoskeleton 49
1.7.3.1 Cilia and ROCK 50
1.8 Aims 51
1.8.1 Preliminary work leading to this thesis 51
Chapter 2 53
Materials and Methods 53
2.1 Cell culture basics 54
2.1.1 Plate coating 54
2.1.2 Cell lines 54
2.1.3 Freezing and thawing cells 55
2.1.4 Standard solutions 56
2.1.5 Bacterial cell culture 57
2.1.5.1 DNA plasmid preparation 58
2.1.5.2 DOCK9 shRNA sequences 58
2.2 Cell culture techniques 58
2.2.1 Production of Lentiviral Vectors in 293T cells 58
2.2.2 Virus titre assay 58
2.2.3 HUVEC lentiviral transduction 59
2.2.4 HUVEC cell sorting via FACS sort 59
2.2.5 HUVEC-HDF coculture assay 59
2.2.6 In-vitro ciliogenesis assay 60
2.2.7 Apical membrane initiation site assay (AMIS assay) 60
2.3 Imaging techniques 60
2.3.1 Embryo fixation and staining (immunofluorescence) 60
2.3.2 Co-culture fixation and immunofluorescence staining 60
2.3.3 Cilia assay fixation and staining 61
2.3.4 AMIS assay fixation and staining 61
2.3.5 Immunohistochemistry staining 61
2.3.5.1 Embryo immunohistochemistry 61
2.3.6 Confocal imaging 61
2.3.6.1 HUVEC-HDF Co-culture imaging 62
2.3.6.2 Wholemount angiozone embryo imaging 62

2.3.6.3 Cilia imaging 62
2.3.6.4 AMIS imaging 62
2.3.7 Bright field imaging of Immunohistochemistry stained sections 62
2.3.8 Live imaging 63
2.3.9 Phalloidin staining of cells 63
2.4 Image analysis 64
2.4.1 HUVEC-HDF Co-culture lumen measure 64
2.4.2 HUVEC-HDF nuclei per length counts 64
2.4.3 Cilia analysis (ciliogenesis assay) 65
2.4.4 Lumen and filopodia measuring via immunofluorescence (Embryo analysis) 65
2.4.5 Cilia count in the embryo immunohistochemistry sections 65
2.4.6 Lumen measure in the embryo immunohistochemistry sections 65
2.5 Biochemical techniques 66
2.5.1 Western blotting analysis 66
2.5.1.1 Protein quantification by BCA protein assay 66
2.5.1.2 SDS-PAGE 66
2.5.1.3 Western blotting and detection 66
2.5.1.4 Stripping and reprobing 67
2.6 Statistical methods 67
Chapter 3 68
Rac GEF DOCK4 and Cdc42 GEF DOCK9 Control Tubule Lumen Formation 68
3.1 Introduction 69
3.2 Optimisation of the organotypic coculture assay to model angiogenesis in vitro 69
3.3 Analysis of lumen formation in the coculture assay 74
3.4 DOCK4 is necessary for lumen formation in the coculture assay 78
3.5 Generation of lentiviral shRNAs for DOCK9 knockdown studies 83
3.6 Analysis of the effect of DOCK9 knockdown on endothelial cell shape and proliferation 85
3.7 DOCK9 knockdown inhibits lumen formation in the coculture assay 88
3.8 DOCK9 localises with the apical surface in spreading HUVEC in vitro 93
3.9 Conclusions 98
Chapter 4 100
The role of ROCK2 in Sprouting and Lumen Formation *in vivo* 100

4.1 Introduction **101**
4.2 Loss of global *ROCK2* is embryonically lethal at E13.5 ..... **101**
4.3 Characterising of embryonic brain blood vessels E12.5 vs E13.5 ..... **105**
4.4 ROCK2 controls endothelial cell filopodia formation and vascular integrity **109**
4.5 ROCK2 controls the morphology of the major vessels during development **113**
4.6 ROCK2 controls blood vessel diameter and lumen density during angiogenic development **116**
4.7 Conclusions **120**

Chapter 5 ..... **122**

The role of Rho-associated kinases in Cilia Formation in Endothelial Cells **122**
5.1 Introduction **123**
5.2 Cultured human vascular endothelial cells ciliate in the organotypic angiogenesis assay **123**
5.3 Microvascular endothelial cells assemble primary cilia during brain development ... **126**
5.4 Investigating the role of ROCK in ciliogenesis using an *in vitro* ciliogenesis assay **130**
5.5 Rho kinase (ROCK1/2) controls cilia length and density **133**
5.6 Inhibition of components of the ROCK pathway in *Rock2* $^{-/-}$ MEFs **143**
5.7 ROCK2 controls endothelial ciliogenesis and orientation in blood vessels **146**
5.8 Conclusions **151**

Chapter 6 ..... **154**

Final discussion **154**
6.1 Introduction **155**
6.2 Rac GEF DOCK4 and Cdc42 GEF DOCK9 control lumen formation **156**
6.3 Role of Rock2 in blood vessel morphogenesis **158**
6.4 Role of Rock2 in ciliogenesis **161**
6.5 Concluding remarks **163**

References **164**

List of Figures

Figure 1.1 Stages of sprouting angiogenesis and lumen formation 6

Figure 1.2 Cellular mechanisms of tube formation 14

Figure 1.3 Endothelial lumen formation - chord hollowing. 19

Figure 1.4 Actin structure and assembly 25

Figure 1.5 Overview of Rho/Rho kinase signalling 34

Figure 1.6 DOCK4 and DOCK9 protein domain maps 38

Figure 1.7 ROCK1 and ROCK2 structure, homology and phosphorylation sites. 42

Figure 1.8 The structure and compartments of the primary cilium. 45

Figure 3.1 Organotypic angiogenesis assay and overview of stages leading to tube formation 71

Figure 3.2 Tubule growth in the HUVEC-HDF coculture assay at 5 days 72

Figure 3.3 Still images from time-lapse movies depicting stages of tubule growth 73

Figure 3.4 Onset of lumen formation in mature tubules in the coculture assay 75

Figure 3.5 VE-cadherin and podocalyxin localization in mature tubules in the coculture assay 76

Figure 3.6 Lumen formation in the coculture assay 77

Figure 3.7 The effect of DOCK4 knockdown on tubule lateral adhesions 79

Figure 3.8 DOCK4 knockdown controls endothelial cell numbers in tubules 80

Figure 3.9 DOCK4 knockdown inhibits lumen formation in the coculture assay 81

Figure 3.10 Quantification of the effect of DOCK4 knockdown on lumen formation 82

Figure 3.11 Stable knockdown of DOCK9 by means of lentiviral transduction 84

Figure 3.12 DOCK9 knockdown does not affect HUVEC spreading or bipolarity 86

Figure 3.13 DOCK9 does not control endothelial cell proliferation or VE-cadherin expression 87

Figure 3.14 EGFP-HUVEC forming tubules in the coculture 89

Figure 3.15 DOCK9 controls lumen formation in the coculture assay 90

Figure 3.16 DOCK9 knockdown does not affect endothelial density in tubules 91

Figure 3.17 Validation of the DOCK9 antibody in HUVEC 92

Figure 3.18 Apical proteins localise to the AMIS domain during early spreading in HUVEC 95

Figure 3.19 DOCK9 localises with the AMIS apical domain in spreading HUVEC 96

Figure 3.20 DOCK9 knockdown does not affect apical localisation of podocalyxin 97

Figure 4.1 Morphology of embryos with global *Rock2* deletion at E13.5 103

Figure 4.2 ROCK2 staining of sections from wild type and *Rock2* knockout embryos. 104

Figure 4.2 Sprouting and lumen formation at E12.5 and E13.5 in wild type embryos 107
Figure 4.3 Increased filopodial sprouting in cerebral blood vessel in *Rock2* knockout embryos 110
Figure 4.4 Altered vascular integrity in cerebral blood vessel in *Rock2* knockout embryos . 111
Figure 4.5 *Rock2* knockout embryos show increased filopodia formation in developing blood vessels at the heart level..... 112
Figure 4.6 *Rock2* controls vascular integrity in the heart..... 114
Figure 4.7 Loss of *Rock2* affects aortic diameter and expansion 115
Figure 4.8 *Rock2* controls blood vessel diameter in the parenchyma during development . 117
Figure 4.9 *Rock2* controls lumen opening and lumen dynamics during development 118
Figure 4.10 Mural cell coverage is not affected in *Rock2*$^{-/-}$ parenchymal vessels..... 119
Figure 5.1 Cilia identification on endothelial cells growing in a monolayer and in the HUVEC-HDF coculture model 125
Figure 5.2 Endothelial cilia identification in the angiozone of developing embryos 127
Figure 5.3 Endothelial cilia identification in vessels at the foramen of Monro..... 128
Figure 5.4 Lack of primary cilia in the developing aorta visualised at the heart level..... 129
Figure 5.5 bEnd3 and HCMEC ciliate under serum starvation in culture 131
Figure 5.6 hTERT-RPE1 cells ciliate readily under serum starvation in culture 132
Figure 5.7 Rho/ROCK pathway and inhibitors 135
Figure 5.8 Y27632 causes loss of stress fibres in hTERT-RPE1 cells in the *in vitro* ciliogenesis assay..... 136
Figure 5.9 Effect of treatment of hTERT-RPE1 cells with the ROCK inhibitor Y27632..... 137
Figure 5.10 Treatment with the ROCK inhibitor Y27632 increases ciliary length and reduces the number of ciliated hTERT-RPE1 cells 138
Figure 5.11 Treatment with LIM kinase inhibitors, blebbistatin, or the actin depolymerising agent, latrunculin B increases ciliary length in hTERT-RPE1 cells..... 139
Figure 5.12 Treatment with LIM kinase inhibitors, blebbistatin or the actin depolymerising agent, latrunculin B increases ciliary length in hTERT-RPE cells 141
Figure 5.13 Effect of ROCK pathway inhibitors on wild-type mouse embryonic fibroblasts (MEFs) 144
Figure 5.14 Isolated *Rock2* $^{-/-}$ mouse embryonic fibroblasts (MEFs) have increased ciliary length and fewer ciliated cells compared with wild-type MEFs 145
Figure 5.15 Endothelial cell cilia of the vasculature of the E13.5 *Rock2* $^{-/-}$ mice..... 147
Figure 5.16 Endothelial cell cilia are reduced in the vasculature of the E13.5 *Rock2* $^{-/-}$ mice 148

Figure 5.17 Treatment with the ROCK inhibitor Y27632 increases ciliary length in HCMEC. 150
Figure 6.1 Model for the roles of DOCK4 and DOCK9 in blood vessel lumen formation 157
of pathway downstream of VEGF controlling lumen formation. 158
Figure 6.2 Model for the role of ROCK2 in ciliogenesis and lumen formation 162

List of Tables

Table 2.1 Standard solutions used throughout this thesis 57

Table 2.2 List of primary antibodies used for immunofluorescence..... 63

Table 2.3 List of secondary antibodies used for immunofluorescence 64

Table 2.4 List of antibodies used in this thesis for immunoblot assays 67

Table 4.1. Angiogenic growth and lumen formation at embryonic days E12.5 and E13.5.... 108

List of Abbreviations

AMIS	Apical membrane invagination site
ARL13B	ADP-Ribosylation Factor-like Protein 13B
BCA	Bicinchonic Acid
bEnd3	Mouse brain endothelial cells
DMEM	Dulbecco's Modified Eagle's Medium
DMSO	Dimethylsulfoxide acid
DOCK	Dedicator of cytokinesis
DTT	Dithiothreitol
ECL	Enhanced Chemilumenescence
ECM	Extra Cellular Matrix
ECs	Endothelial Cells
ERM	Ezrin/radixin/moesin
EV	Empty Vector
FACS	Fluorescence activated cell sorting
FACS	Fluorescence Activated Cell Sorting
FBS	Fetal Bovine Serum
g	gravitational acceleration
GAP	GTPase Activating Protein
GAPDH	Glycerinaldehyde-3-Phosphate-Dehydrogenase
GDI	GDP Dissociation Inhibitor
GEF	Guanine Nucleotide Exchange Factor
GFP	Green Fluorescent Protein
HCMEC	Human cerebral microvascular endothelial cells
HDF	Human Dermal Fibroblasts
HEK-293T	Human Embryonic Kidney Cells
HIFs	Hypoxia Inducible factors
hTERT-RPE	Human retinal pigmented epithelial
HUVEC	Human Umbilical Vein Endothelial Cells
IFT	Intraflagellar transport
ISV	Intersegmental Vessel
KO	Knockout
LVEM	Large Vessel Endothelial Medium
MEF	Mouse Embryonic Fibroblasts

Non-S	Non Silencing
Par	Partitioning defective
PBS	Phosphate Buffered Saline
PBX	Phosphate buffered saline – Triton X100
PFA	Paraformaldehyde
PFA	Paraformaldehyde
ROCK	Rho associated coiled-coil protein kinase
rpm	revolutions per minute
RT	Room Temperature
SDS-PAGE	Sodium Dodecyl Sulfate Polyacrylamide Gel Electrophoresis
shRNA	Short Hairpin Ribonucleic Acid
siRNA	Small Interfering Ribonucleic Acid
TBS	Tris Buffered Saline
TBS	Tris Buffered Saline
TBST	Tris Buffered Saline – Tween 20
VE-Cadherin	Vascular Endothelial – Cadherin
VE-PTP	Vascular Endothelial - Protein Tyrosine Phosphatase
VEGF	Vascular Endothelial Growth Factor
VEGF	Vascular Endothelial Growth Factor
VEGFRs	Vascular Endothelial Growth Factor Receptors
WT	Wild Type

Chapter 1

Introduction

1. Blood vessel formation

1.1 The circulatory system

The circulatory system plays a fundamental role in homeostasis through circulation of blood providing tissues with oxygen and nutrients, and removal of waste products. It also plays roles in transporting immune cells, growth factors, and inflammatory cytokines to distant sites within the body (Adams and Alitalo, 2007). In smaller and more simple organisms, these functions can take place through diffusion, without the need for a closed circulatory system. However, larger and more complex organisms require a closed circulatory system, capable of transporting blood further and deeper into tissues. Closed circulatory systems comprise a pump, the heart, and a network of blood vessels that contain the blood which is carried to distant cells and tissues. Blood vessels are lined by a specialized layer of endothelial cells. In humans, the complex network of blood vessels is almost 60,000 miles long, composed of arteries, veins, and capillaries, each with unique functions (Pugsley and Tabrizchi, 2000). The largest vessels, arteries, function in transporting large volumes of oxygenated blood away from the heart to distance tissues. Smaller vessels, veins, then return deoxygenated blood from the tissues back to the heart. Capillaries function in delivering blood deeper into tissues and cells; this is made possible by their small size but large surface areas.

The development of the circulatory system begins in the embryo and continues throughout adult life. The first stages of its development occur through a process known as vasculogenesis. During vasculogenesis, endothelial cell precursors, known as angioblasts, develop in the mesodermal compartment and form islands of cells which eventually form tubes (Risau and Flamme, 1995). This process takes place in the absence of blood flow and is thought to be guided by genetics and local environmental and mechanical inputs (Jones, le Noble and Eichmann, 2006). This *de novo* network of vessels becomes sufficient to supply the developing embryo with blood and oxygen. As the embryo develops, the need for oxygen and nutrients increases beyond this initial network's capability. The primitive vascular network is now further expanded through a different form of blood vessel development termed angiogenesis.

1.2 Developmental angiogenesis

Angiogenesis is defined as the growth and development of new vessels from pre-existing ones. After the initial vascular plexus is formed in the embryo, the majority of new growth takes place via angiogenesis (Risau, 1997). During this highly dynamic process, endothelial cells lining the vessels go through diverse cellular processes including sprouting, migration, proliferation and polarization; all in response to external stimuli (Risau, 1997; Carmeliet and Jain, 2011). This type of growth allows massive expansion, and intricate specialisation of the developing network through growth, pruning, and remodelling of blood vessels.

The circulatory system is the first organ to develop in vertebrates, highlighting its evolutionary importance. It is necessary early in development, to provide oxygen and nutrients to the rapidly growing new tissue and organs (Patel-Hett and D'Amore, 2011). Angiogenesis first occurs after the early primitive vascular structures are formed via vasculogenesis. These new angiogenic vessels sprout and reshape the entire circulatory system into a functional organ capable of reaching every tissue in the body. To fulfil this role certain vessels must take on specific and specialized roles within the vasculature. One important step during developmental angiogenesis is the specialization of vessels. Environmental factors including flow, pressure, speed and pattern of blood flow affect this process called arteriovenous differentiation (Kwei *et al.*, 2004). The arteries that carry blood away from the heart must be capable of operating under huge pressure and accelerated flow. During development veins and arteries are seen to express distinct molecular markers. Pre-arterial vessels express higher levels of EphrinB2 and NRP1 in response to pulsate flow and other environmental cues. In turn these vessels increase calibre and mural cell coverage (Adams and Alitalo, 2007). The venous system, which is exposed to lower pressures and flow rates, are seen to express higher levels of EphB4 and in turn develop valves to control flow direction and show poorer mural cell coverage. In support, altering of flow rates in the vasculature of the chick yolk sac has been shown to reverse arterial expression of EphrinB2 and NRP1 (le Noble *et al.*, 2004). Establishment of the functional vascular system in development is an intricate process controlled by genetic predetermines, signalling molecules and environmental ques.

In the adult the growth of blood vessel ceases except for in wound healing, the menstrual cycle and pregnancy, and also in disease states discussed in detail in the pathological angiogenesis section (1.3).

1.2.1 Mechanisms of angiogenesis

There are two major mechanisms of angiogenesis: sprouting angiogenesis and intussusceptive angiogenesis. Sprouting angiogenesis involves activation of endothelial cells within pre-existing vessels, to break away from the vessel wall, and migrate and sprout in order to form new conduits. Sprouting angiogenesis extends new vessels into hypoxic regions, or regions devoid of blood supply. Conversely, intussusceptive angiogenesis is the process by which a single vessel pinches in the middle and separates to form two new vessels side-by-side. Intussusceptive angiogenesis increases vessel number more rapidly and without the need for endothelial proliferation.

1.2.1.1 Sprouting angiogenesis

Sprouting angiogenesis is a multi-stage process that results in newly formed vessels linking pre-existing vessels, or vascularizing new areas of tissue. Within vessel walls, endothelial cells remain quiescent with luminal-ablumenal (apical-basal) polarity and orientation in line with blood flow (Richards, Hetheridge and Mellor, 2015). Growth factor stimulation of these endothelial cells causes release of matrix metallo-proteases (MMPs) that breakdown the surrounding basement membrane to allow for cell sprouting (van Hinsbergh and Koolwijk, 2008). Driven by local gradients of growth factors, the activated endothelial cells degrade the local extracellular matrix to sprout (Figure 1.1) (Gerhardt *et al.*, 2003). Upregulation of VEGFR2 signalling also causes weakening of cell-cell junctions by endocytosis of VE-cadherin, allowing cell detachment from its neighbouring cells (Gavard and Gutkind, 2006). The leading tip cell polarizes with its migrating front, extending actin rich filopodial and lamellipodial protrusions that probe the extracellular environment for directional ques and growth factors. The position of the tip cell is a competitive one, and under the control of local growth factors. High levels of VEGF signalling in the tip cell cause repression of tip cell fate for the trailing stalk cells, through a negative signal sent to the trailing stalk cells via the Dll4-Notch system, which prevents trailing cells from responding to VEGF (Blanco and Gerhardt, 2013). The stalk endothelial cells go through complex and controlled rearrangements and proliferate to extend the growing sprout. They elongate, align and gain apical-basal polarity. Polarized endothelial tubules then open to form a hollow lumen capable of supporting blood flow. Finally, the newly formed vessels mature by deposition of basement membrane, and mural cell coverage.

The tip cell continues migration towards the VEGF-driven stimulus until it reaches another vessels or tip cell, and a connection is formed by anastomosis. In order to anastomose successfully, tip cells must downregulate their high migratory and dynamic behaviour to form secure connections with the new vessel. This phenotypic conversion is reported to be mediated by VEGFC-expressing macrophages, which migrate to the sites of anastomosing vessels. VEGFC binding to VEGFR3 on tip cells increases notch signalling within the tip and downregulates its sensitivity to VEGF to enable anastomosis (Fantin *et al.*, 2010; Tammela *et al.*, 2011). The tip cell continues migrating towards the VEGF-driven stimulus until it reaches another vessel or tip cell and a connection is formed by anastomosis. Prior to anastomosis, lumen formation takes place behind the leading sprout front. Continuation of this process will enable the functionality of the vessel in carrying blood flow to new conduits. Lumen formation, which is described in more detail in section 1.3, is a highly complex process involving multiple inputs from signalling pathways controlled by cell junctions, polarity, and extracellular matrix proteins, to mechanical stimulus like blood flow, pressure, and tissue architecture. These cues may result in endothelial cell morphological changes mediated by Rho GTPases and their control on the actin cytoskeleton.

In addition to the aforementioned processes taking place during new blood vessel formation, further organization of vessels takes place via vessel regression. Vessel regression describes the pruning of unconnected, or unnecessary vascular branches or sprouts, and is thought to be a consequence of withdrawal of growth factors or insufficient blood flow.

1.2.1.2 Intussusceptive angiogenesis

Distinct from sprouting angiogenesis, which relies on proliferation and growth of vessels, intussusceptive angiogenesis involves the splitting of a pre-existing vessels. The initial stage involves the pinching of vessel walls to allow two opposing endothelial cells to make contact. This contact becomes known as a 'trans-vascular pillar'. Generation of the trans-vascular pillars within vessels then allow invagination of the basal membrane and redistribution of cell borders and junctional molecules to form two new vessels side-by-side (Djonov *et al.*, 2000). This behaviour allows for expansion of vascular networks without the need for proliferation as with sprouting angiogenesis. Commonly seen in the growth of vascular beds and plexuses, intussusceptive angiogenesis is tightly associated with high blood pressure and changes in flow patterns (Burri, Hlushchuk and Djonov, 2004).

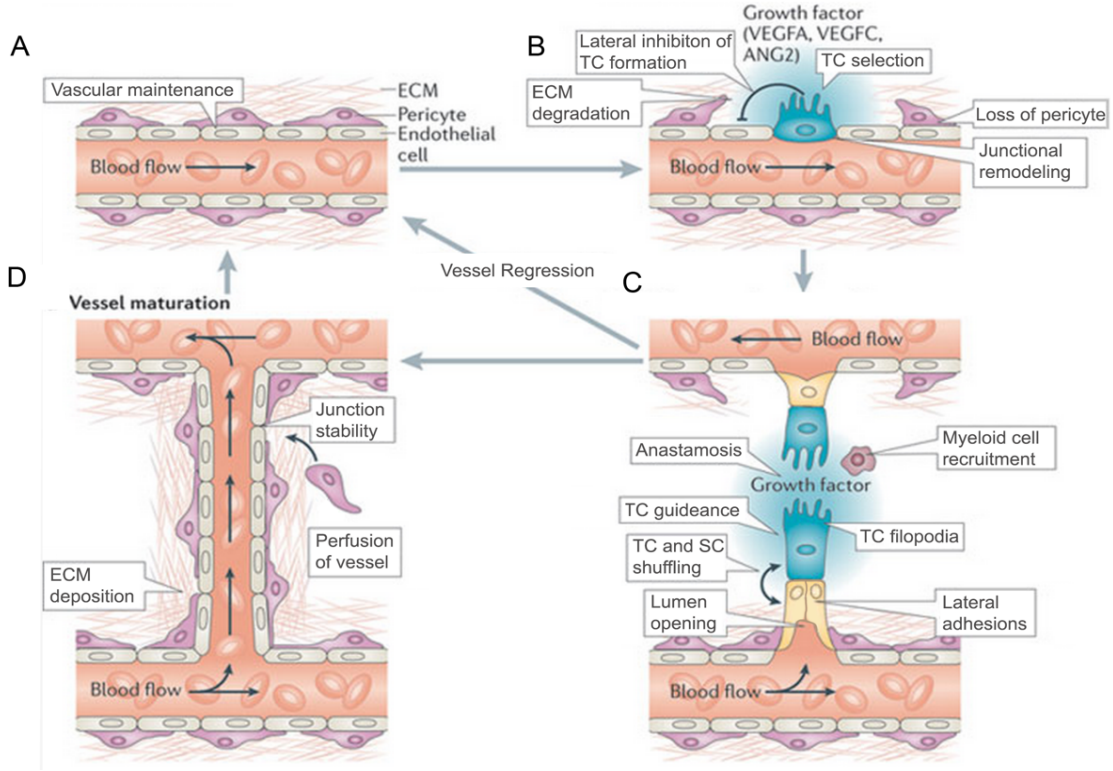

Figure 1.1 Stages of sprouting angiogenesis and lumen formation

Sprouting angiogenesis requires activation of endothelial cells within pre-existing vessel wall, growth of the sprout, and formation of a functional lumen. A) Pre-existing vessels lined with elongated quiescent endothelial cells. B) Initiation of sprouting angiogenesis through growth factor stimuli from the surrounding environment such as VEGF. The tip cell degrades the extracellular matrix and sprouts into the extracellular matrix. C) Stalk cells behind the leading tip, suppressed by Notch-Dll4 signalling, proliferate and align next to each other to form multicellular chords. Stalk cells gain apical lateral adhesions where lumens will eventually open. Tip cells anastomose with neighbouring tips or established blood vessels. D) Lumens open typically at sites with later cell-cell adhesions. Blood vessels become perfused and mature via extracellular matrix deposition and mural cell coverage. Adapted from Herbert and Stainier (Herbert and Stainier, 2011).

1.3 Pathological angiogenesis

Due to the importance of angiogenesis during development, defects in its regulation can result in a variety of diseases including ischemic and inflammatory conditions. Vascular abnormalities contribute to the pathology of diseases including primary and metastatic tumour growth, diabetic retinopathy, and macular degeneration, and cardiovascular disease.

The vasculature can provide tumours with the nutrients and oxygen they require and also provide a direct route for metastasis to distant sites in the body. As cancerous tumours increase in size, above a million cells or more, they need to take advantage of this angiogenic process (Gupta and Qin, 2003). By manipulating the pro- and anti-angiogenic signalling molecules, tumours encourage growth and development of their own blood supply from nearby vessels through sprouting angiogenesis.

Many tumours have been shown to express high levels of pro-angiogenic growth factors, including VEGF, through genetic mutation. They can also stimulate angiogenesis through other mechanisms like increased inflammation, mobilization of host cells like microphages, and release of hypoxic molecules (Gupta and Qin, 2003). However, due to consistently high levels of angiogenic signalling in the tumour, the resulting vasculature remains highly active with high permeability, and becomes leaky and functions sub-optimally (Nagy *et al.*, 2009). Failure of endothelial cells within the vessels to quiesce and form mature junctions, basement membranes and attract mural cell coverage, all lead to vascular instability seen within tumours. Poor penetration of blood vessels thorough tumours results in many of the problems encountered in treating this disease including reduced chemotherapeutic delivery, hypoxic regions resistant to radiotherapy, and high likelihood of circulation of cancer cells through leaky vessels. As this process is such a vital element of tumour growth, many attempts have been made to target the tumour vasculature with relatively high success and anti-angiogenic therapy is now standard of care for many cancers including metastatic colorectal cancers, non-small cell lung cancers and metastatic renal cell cancers.

Bevacizumab (Avastin) is a humanised monoclonal antibody that targets all isoforms of VEGF-A. Clinical use of Avastin has been shown to slow angiogenesis and increase survival, and consequently Avastin has been approved for use in colorectal, kidney and lung cancer (Petrovic, 2016). Although successful in slowing growth of those cancers, other trials have shown less promising results for treatment of cancers including metastatic breast cancers and

pancreas cancers (El-Kenawi and El-Remessy, 2013). This may possibly be due to high levels of heterogeneity within tumours and the range of angiogenetic signalling molecules available, as many tumours find ways to overcome the initial effects of these inhibitors on blood vessel growth. Recent evidence has also shown the growth of cancer around blood vessels can take place without the induction of angiogenesis, through co-option of vessels. Endothelial cells are known to cleave kinins like bradykinin, which has been shown to increase migration and invasion of patient-derived glioma cells towards blood vessels without the need for angiogenesis (Montana and Sontheimer, 2011). However, co-option of these vessels by glioma cells may lead to regression, hypoxia and subsequent initiation of angiogenesis. This highlights the importance of timing of treatments and further understanding of pro-angiogenic switch which takes place in the tumour environment.

Defective angiogenesis in the eye can lead to a range of pathological conditions which have detrimental effects on vision including, diabetic retinopathy and macular degeneration. Diabetic retinopathy (DR) is the leading cause of vascular related sight loss in the world and results as one of the consequences of poorly controlled diabetes mellitus. Damage to blood vessel in the retina occurs from exposure to high blood sugar levels and leads to eventual loss of vision. Release of VEGF by damaged vessels stimulates angiogenesis and leakage of healthy vessels which can lead to further sight loss. Intravitreal injections of anti-angiogenic inhibitors such as Avastin (bevacizumab) have shown efficacy in treating later stages of proliferative diabetic retinopathy (PDR) (di Lauro *et al.*, 2010). The blocking of the VEGF receptor through Avastin treatment decreases vessel leakage and angiogenic sprouting and may improve the sight or allow a window for other approaches like laser treatment.

A number cardiovascular diseases are associated with narrowing or closing of blood vessels and loss of blood supply to affected areas. Therapeutic angiogenesis in cardiovascular disease is a method used to re-supply blood flow through stimulating regrowth of vessels using growth factor or cell based therapies (Deveza, Choi and Yang, 2012). Delivery of genes, proteins or cells have shown promising therapeutic results in animal models to date but translation to the clinic has been less successful for a number of reasons including growth factors delivery methods and lack of maturation of these new vessels.
Intramuscular injection of angiogenic tissue growth factors or bone marrow stem cells has shown short term efficiency in animal models of critical limb ischemia with no off-target angiogenesis or occult growth of tumours (Ko and Bandyk, 2014).

Other therapeutic approaches include the targeting of individual molecules responsible for cardiovascular diseases or their associated symptoms. Signalling molecules involved in the Rho GTPase signalling pathways (discussed in detail in section 1.6.3) including the Rho kinases (ROCK1 and ROCK2) (discussed in detail in section 1.6.5) have been shown to play roles in many cardiovascular function due to their control of the actin cytoskeleton and in proliferation, contraction, migration and adhesion. RhoA/ROCK signalling has been highlighted as a major player in the pathogenesis of many cardiovascular related diseases and therefore efforts have been made to target ROCK activity. Promising results using ROCK inhibitors (such as Y27632 or Fasudil) in animal models have shown this to be effective in reducing blood pressure and vasoconstriction in models of cardiovascular disease (see review (Surma, Wei and Shi, 2011)). Fasudil is the only Rho kinase inhibitor currently approved for clinical use and only available in Japan where it is used to treat vasospasm after acute ischemic stroke.

1.4 Angiogenic signalling

Multiple signalling pathways control the complex process of angiogenesis, which is highly regulated under the control of pro- and anti-angiogenic factors. The VEGF receptor system signalling under the control of hypoxia and Dll4-Notch signalling are some of the most important and best characterized angiogenic signalling pathways.

Angiogenesis is controlled by a large number of soluble growth factors and molecules released by hypoxic, growing or damaged tissues. Angiogenic behaviour is organized by gradients of pro- and anti-angiogenic signals which modulate how vessels develop and mature. Other effectors of angiogenic behaviour include mechanical cues such as blood flow and pressure within vessels.

The VEGF family of growth factors and their receptors are key regulators of both angiogenesis and vasculogenesis (Ferrara, Gerber and LeCouter, 2003). There are 6 VEGF family members, VEGF-A to D, the related placental growth factor (PLGF), and VEGF-E which is a virally encoded growth factor (Li and Eriksson, 2001). VEGF-A is highly conserved throughout evolution and is the most important member of the family in controlling blood vessel growth (Tischer *et al.*, 1991). VEGF family members show varying affinities towards multiple VEGF receptors: VEGFR1 (Flt-1), VEGFR2 (KDR, Flk-1) and VEGFR3 (Flt-4). VEGFR1 and VEGFR2 are mainly expressed on

vascular endothelial cells while VEGFR3 is mostly expressed on lymphatic endothelial cells. VEGF-A binds strongest to VEGFR2 and this signalling is thought to be the main driving force for angiogenic growth. When a VEGF ligand binds its receptor, the receptors may form homo- or hetero-dimers, which activate the receptors through auto-phosphorylation of multiple tyrosine residues within the intracellular domains. Signalling downstream of VEGFR2 activates multiple signalling pathways that collectively promote cell proliferation, survival, migration and changes in gene expression (Dvorak *et al.*, 1995). VEGFR1 is thought to act as a decoy receptor with an inhibitory role in angiogenesis through its interaction with VEGF but subsequent weak ability to transmit downstream signals. Furthermore, a soluble, catalytically inert form of VEGFR1 may also sequester VEGF and inhibit angiogenic signalling through VEGFR2 (Kendall and Thomas, 1993). Recently, it was shown that VEGFR1 is expressed in the stalk cells of a sprouting tubules, thus also inhibiting response by VEGFR2 (Chappell, Mouillesseaux and Bautch, 2013).

Hypoxia is one of the main drivers of angiogenic growth in regions lacking adequate oxygen for survival, through regulation of VEGF. Endothelial cells react in hypoxic regions by stabilizing hypoxia inducible factors (HIFs) which are a set of transcription factors that control the formation of blood vessels as well as a number of other roles in other cell types (Shweiki *et al.*, 1992). HIF1 is a heterodimeric transcription factor that contains two subunits, HIF1α and HIF1β. During normoxic conditions, HIF1α gets degraded by the ubiquitin-proteasome pathway through binding to the tumour suppressor von Hippel-Lindau protein (Ratcliffe *et al.*, 1999). This binding is under the control of enzymes that use cellular O_2 as a substrate. Under hypoxic conditions this binding is disrupted due to reduced cellular O_2 levels and HIFα is able to accumulate in the cytoplasm and translocate to the nucleus where it dimerizes with HIFβ and binds to target genes at hypoxia response elements (HREs) (Semenza *et al.*, 1996). Target genes include a huge range of genes involved in angiogenic responses to hypoxia including upregulation of VEGF (Wang *et al.*, 1995; Forsythe *et al.*, 1996).

The Notch signalling pathway plays an important role in regulating VEGF signalling in stalk cells during angiogenic sprouting. During sprouting angiogenesis, the selected tip cell, stimulated by VEGF, upregulates its expression of Delta like ligand 4 (DLL4) (Liu *et al.*, 2003). DLL4 is a transmembrane ligand for Notch, and binds Notch expressed on trailing stalk cells. Notch then signals to downregulate levels of VEGFR2 in the stalk cells, hence reducing competition for tip

cell position in the growing sprout; a process necessary for proper vascular patterning (Phng and Gerhardt, 2009).

1.5 Lumen formation

A lumen is defined as the central cavity space inside of a tubular structure or hollow tissue like a blood vessel or the intestine. Many tissues and organs within the body need to form tubes within lumens to carry out their physiological function. The importance of these tubular structures is in the transport of a luminal cargo isolated from the surrounding tissues. In blood vessels for example, the transport of blood and its cargo takes place inside vascular lumens, which transport oxygen and nutrients to distant sites and deep into tissues.

There are different mechanisms for lumen development and growth within the body depending on tissue and function. Lumens in blood vessels and lymphatic vessels are lined by endothelial cells, whereas cavities in the gastrointestinal tract, kidneys, liver, lungs or the salivary glands are lined by epithelial cells. Defective lumen development or maintenance can result in disease such as cardiovascular disease for example, in the case of blood vessel lumens.

1.5.1 Cellular mechanisms of blood vessel lumen formation

To meet the demand for the wide range of vital processes that lumens take part in, such as delivering nutrients, oxygen and circulating antibodies and immune cells, diverse mechanisms are in operation for their formation: cord hollowing, cell hollowing, plasma membrane invagination and sheet folding shown in Figure 1.2 operating in both blood vessel and epithelial lumen formation (Sigurbjörnsdóttir, Mathew and Leptin, 2014). Endothelial lumen formation is similar to epithelial lumen formation in that it originates by some of the mechanisms previously discussed. Namely, chord hollowing, cell hollowing and membrane invagination have been described in the literature for both *in vitro* and *in vivo* endothelial cell lumen formation. Other similarities include the necessity for acquisition of polarity and the importance of cell-cell junctions.

Different processes are thought to operate during the formation of different calibre blood vessels (Arispe and Davis Dev Cell 2009), but the same mechanisms are often seen within the

same vascular bed, as for example in the case of intersegmental vessels in zebrafish embryos where both cord and cell hollowing mechanisms are in operation (Gebala *et al.*, 2016).

A Chord hollowing

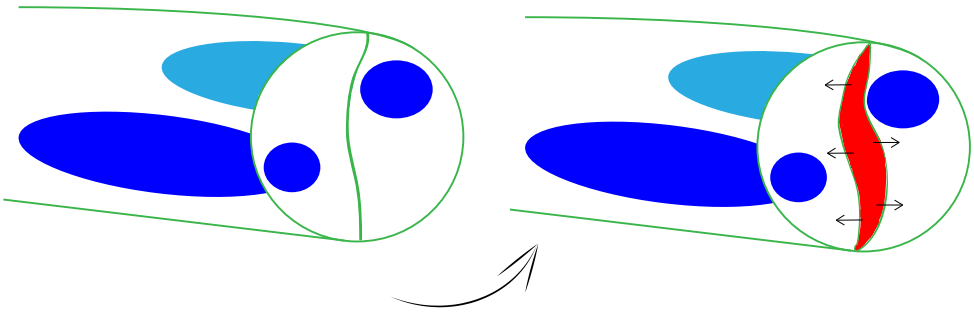

Cell hollowing

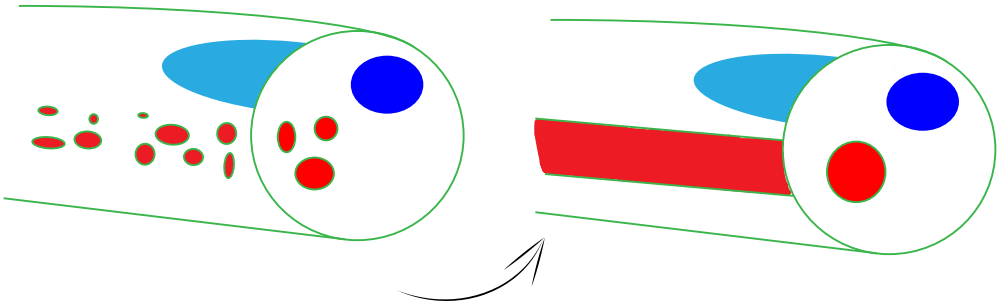

Plasma membrane invagination

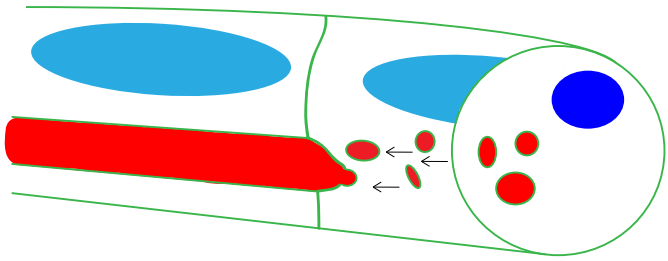

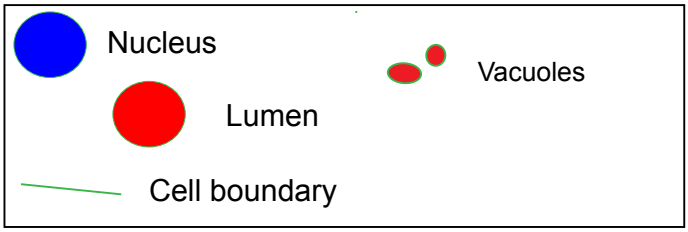

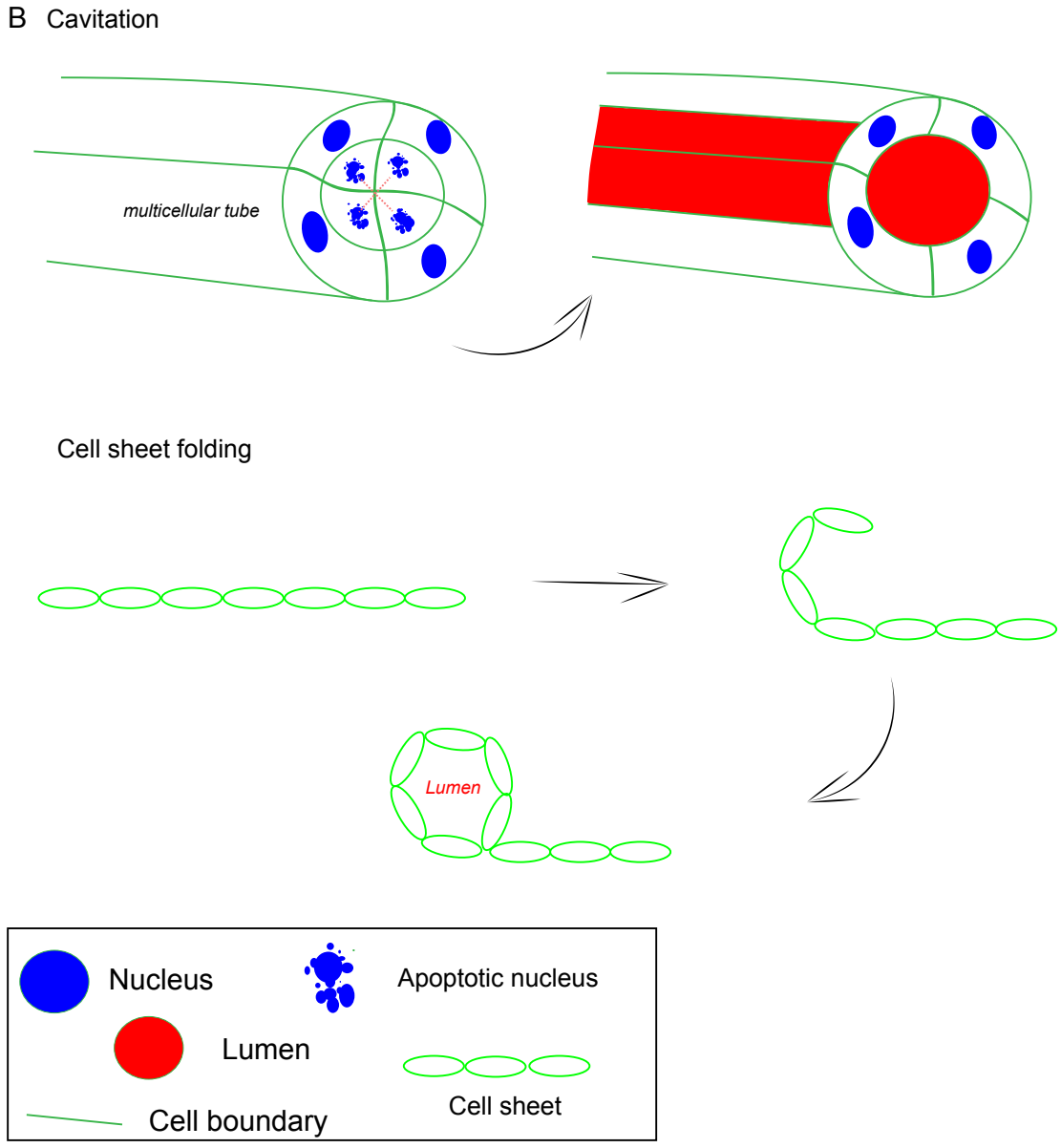

Figure 1.2 Cellular mechanisms of tube formation
(A) Chord hollowing takes place when multicellular tubes rearrange their junctions to form a lumen surrounded by at least two cells. Apical proteins are delivered to the cell-cell junctions were they are involved in separation of apical junctions and lumen formation. Cell hollowing occurs in single cells when intracellular vacuoles coalesce to form a lumen inside the cell. This small lumen then expands and joins with adjacent cells to create seamless lumens. Membrane invagination involves the invagination of the outer plasma membrane to form an intracellular space. This lumen invagination is aided by the addition of intracellular vacuoles. (B) Cavitation is the hollowing of a multicellular tube via death/apoptosis of the central most cells. Sheet folding describes formation of a lumen by a layer of cells folding back on its self to enclose a hollow region. Adapted from (Strilić *et al.*, 2009).

1.5.1.1 Chord hollowing

Chord hollowing describes a mechanism involving multicellular tubes forming lumens between cells with lateral adhesions (Figure 1.2 A). This process takes place between at least two polarized cells, where lateral cell-cell junctions have formed and apical (lumenal) proteins start localizing at those junctions. An important aspect of chord hollowing is the redistribution of junctional proteins to the outer membrane (Figure 1.2 A).

During the cord hollowing process of lumen formation opposing cells polarize and gain apical-basal (lumenal-ablumenal) polarity. The cell-cell junctions become the site of apical specification where the new lumen forms (Figure 1.2A). This mechanism therefore relies on endothelial cells having lateral adhesions where apical proteins localize prior to lumen formation.

Strilic et al showed that the mouse aorta develops through chord hollowing (Strilić *et al.*, 2009) (Lammert & Axnick 2012). The aortic lumen was shown to develop extracellularly between adjacent endothelial cells (Figure 1.2A). Endothelial cell junctions enriched with vascular endothelial cadherin where shown to be necessary for the initial stages of formation of a multicellular lumen through recruitment of apical proteins to the cell junctions. Localization of highly negatively charged CD34-sialomucins such as podocalyxin to this early lumenal site and re-distribution of junctional proteins to the lateral positions allows opening of the lumen potentially through electrostatic repulsion (Figure 1.2A). Further work from Strillic and co-workers demonstrated that the role of podocalyxin is fundamental for lumen development, and that its negative charge does indeed drive electrostatic repulsion between apposing cells to initiate lumen opening. In those experiments sialidases were injected into the mesenchyme of developing embryos to remove sialic acid before aortic lumen opening (Gelberg H1, Healy L, Whiteley H, Miller LA, 1996). This resulted in loss of electrostatic repulsive forces and fewer lumenised aorta compared with controls, confirming the role of sialomucins in lumen formation in this system (Strilić *et al.*, 2010). Importantly, the defect could be rescued through addition of another apical binding negatively charged protein, dextran sulfate, into mouse embryos, confirming that requirement for sialomucins is dependent on their charge (Strilić *et al.*, 2010). In addition to aortic lumen formation multicellular lumens can also be observed in intersegmental vessels (ISVs) in zebrafish embryos (Blum *et al.*, 2008) (Gebala *et al.*, 2016), suggesting that that the mechanism of chord holloing may not limited to larger calibre vessels.

Cavitation describes the death of cells within the centre of a multicellular tube and it is another way by which a multicellular lumen may form (Figure 1.2 B). This form of lumen formation is seen in much larger scale lumens in epithelial cells (Qi *et al.*, 2015) however there has been no evidence that it may operate in the formation of blood vessel lumens.

1.5.1.2 Cell hollowing

In contrast to chord hollowing, cell hollowing describes formation of a lumenal space within a single cell, thus negating the need for multicellular tubes and takes place in individual endothelial cells. This is typically achieved through coalescing of intracellular vacuoles, which combine to form the lumenal space without the need for multiple cells. Vacuoles develop within endothelial cells lined head-to-tail that coalesce and fuse to form a small intracellular lumen (Figure 1.2A). (Bayless, Salazar and Davis, 2000; Bayless and Davis, 2002; Davis, Koh and Stratman, 2007; Gore *et al.*, 2012). The vacuoles traverse cell boundaries to form tubes lacking cell junctions. These tubes are termed "seamless tubes" as they lack cell-cell junctions around their circumference (Figure 1.2 A). This mechanism has been observed in endothelial cells forming tubules in collagen (Bayless, Salazar and Davis, 2000; Koh, Mahan and Davis, 2008). In-vivo cell hollowing has been described in the intersomitic vessels (ISVs) within the developing zebrafish embryo (Kamei, W Brian Saunders, *et al.*, 2006). In this study vacuoles appeared and fused to form large intracellular spaces which took up most of the space within the cell. Using fluorescently labelled beads the authors were able to show continuation of the lumen starting at the dorsal aorta through these hollow cells proving that separate endothelial cells had become linked to create a common endothelial tube via vacuole formation (Kamei et al., 2006). However similar studies in ISVs by Blum and colleagues disagrees and strongly suggested that zebrafish ISVs are formed through the process of chord hollowing, as the lumen appears mostly juxtaposed by two endothelial cells containing lateral cell junctions (Blum *et al.*, 2008). Additional studies by Wang and co-workers showed similarly that the ISVs do indeed form via chord hollowing, particularly at the base of the ISV, while intracellular vacuoles were also observed which contributed at least in part to the expansion of the lumen (Wang *et al.*, 2010). A latest publication by the Gerhardt group confirmed that in the ISVs lumens are mostly multicellular, although unicellular segments were also observed, albeit to a much lesser extent (Gebala *et al.*, 2016).

Altogether these studies suggest that different mechanisms may operate in different blood vessels, or in the development of the same blood vessel. The cell hollowing mechanism may prevail in vessels with smaller diameter, single cell thick, which lack the thickness seen in lumen developing via chord hollowing; cell hollowing may also act as a lumen expansion mechanism by exporting intracellular vacuoles into an already formed extracellular lumen surrounded by at least two endothelial cells as proposed by Wang et al (Wang *et al.*, 2010).

1.5.1.3 Membrane invagination

Plasma membrane invagination involves expansion the apical cell membrane of one cell into the lumen of another cell to form a continuous lumen. This process was shown to play a role in lumen formation during anastomosis of a sprouting vessel with a pre-existing vessel (Herwig *et al.*, 2011). In this study, unicellular zebrafish ISVs where shown to have transcellular lumens that originated through plasma membrane invagination through anastomosis with the dorsal longitudinal anastomotic vessel (DLAV). The invaginating lumen forms a pouch in the cell it anastomoses with, expands its lumen through the entire length of the cell and fuses with the distal membrane to form a tube (Herwig *et al.*, 2011). This process may be accompanied by complex junctional and cell shape rearrangements which can also be aided formation of vacuoles that fuse with the invaginating membrane, resulting in overall expansion of the lumenal surface within the interior of the cell (Lenard *et al.*, 2013).

1.5.1.4 Inverse blebbing

A recent study by Gerhardt and co-workers showed both intracellular and extracellular lumens exist away from the base of the ISV, with extracellular lumens prevailing over intracellular lumens (Gebala *et al.*, 2016). Furthermore, while the provisional extracellular lumen forms at the base of the ISV in absence of blood flow (Wang *et al.*, 2010), expansion of the lumen along the ISV requires blood flow (Gebala *et al.*, 2016)

Interestingly, this blood pressure driven expansion of the lumen, termed inverse blebbing, was shown to take place through a common mechanism that operates both in single cells and laterally adjacent cells within the ISV. Inverse blebbing describes the process of blood pressure induced spherical deformations in the apical membrane of endothelial cells to which the cell

responds by local contraction that enables lumen expansion in one direction only (Gebala *et al.*, 2016).

The existence of diverse mechanisms of lumen formation depending on changes at the cellular level, cell rearrangements and blood flow, potentially also controlled spatially and temporally may be genetically driven, at least partially, depending on the final vessel morphology necessary for particular function. As the aforementioned mechanisms of lumen formation may occur under different conditions, the range of methods available to endothelial cells to form lumenised structures potentially reflects the importance of this dynamic process for the function of complex organ systems.

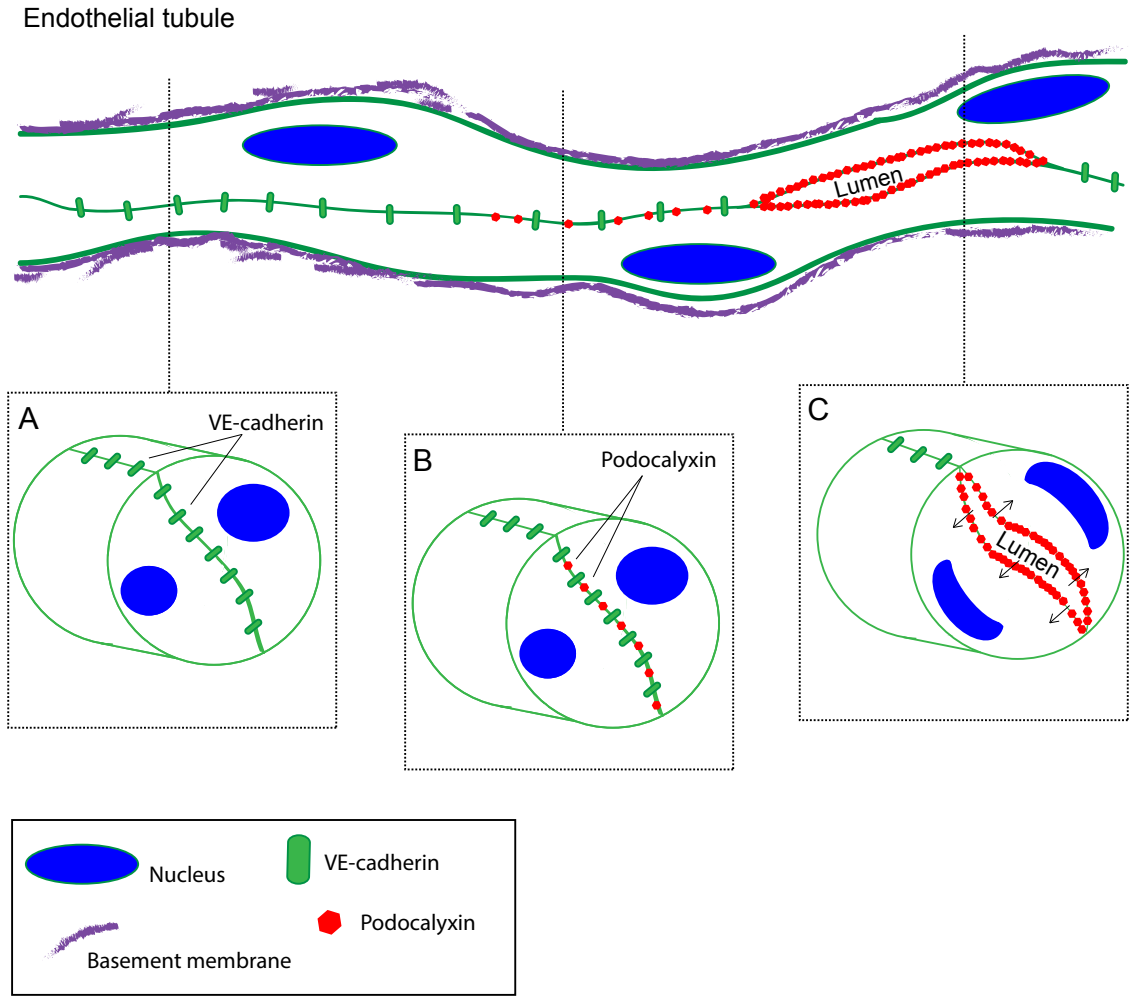

Figure 1.3 Endothelial lumen formation - chord hollowing

Schematic shows stages of lumen formation between two adjacent endothelial cells during chord hollowing. (A) Adjacent endothelial cells within tubes form lateral adhesions where VE-cadherin is expressed. (B) CD34 sialomucins (podocalyxin) are recruited to the developing apical membrane. (C) Accumulation of podocalyxin at the apical membrane results in lumen opening, potentially through electrostatic repulsive forces. Adapted from (Strilić *et al.*, 2009).

1.5.2 Molecular mechanisms of lumen formation

The signalling pathways that control lumen formation have been linked with many aspects of actin cytoskeletal dynamics. Not surprisingly such dramatic changes in cell shape and morphology are controlled by a plethora of cues including changes in extracellular matrix sensed by integrins and cell junctional organisation. Signalling pathways activated by these stimuli control the previously discussed cellular mechanisms of lumen formation.

1.5.2.1 Integrins

Endothelial cell interaction with the extracellular matrix (ECM) is conducted through integrins. These transmembrane proteins sense the surrounding environment and induce cytoskeletal changes in response to changes in the ECM. As most endothelial lumen studies have been carried out in *in vitro* 3D matrices that can be manipulated, a great of deal of knowledge has been gained regarding the role of integrin in migration, sprouting, and lumen formation in endothelial tubes. Engagement of collagen I and fibronectin by integrins has been shown to have proangiogenic effects (Davis and Senger, 2005; Iruela-Arispe and Davis, 2009), while engagement of basement membrane components such as collagen IV promotes quiescence and lumen formation (Davis & Senger, 2008; Iruela-Arispe & Davis, 2009).

The $\beta1$ family of integrins has been shown to be important in both epithelial and endothelial lumen formation. Inhibition of $\beta1$ integrin via blocking antibodies results in total loss of lumen formation in the aorta of chicken embryos (Drake, Davis and Little, 1992). Loss of endothelial recognition of the basement membrane through $\beta1$ integrin genetic deletion has been shown to impact on lumen formation in mice through defects in the polarity protein Par3 (Zovein *et al.*, 2010). The αv family of integrins have also been shown to control lumen formation through their interaction with extracellular matrix proteins such as collagen (Davis and Camarillo, 1996; Hood *et al.*, 2003). Davis and co-workers showed that the integrin $\alpha2\beta1$ controlled formation of intracellular vacuoles which coalesce and are involved in capillary lumen formation (Davis and Camarillo, 1996). Integrin engagement is also known to be key activator of Rho GTPase signalling involved in lumen formation (Bryan and D'Amore, 2007) which is discussed in detail in Section 1.6.5.

1.5.2.2 Junctional molecules

Cell-cell contact is prerequisite for most of the described mechanisms of lumen formation. Like epithelial cells, endothelial cells in contact form adherens junctions and tight junctions. Vascular endothelial cadherin (VE-cadherin) is an endothelial specific cadherin and is involved in different aspects of endothelial growth and behaviour such as adhesion, vascular permeability and leukocyte extravasation (Bazzoni and Dejana, 2004; Vestweber, 2008). Fundamental to endothelial cell behaviour it has been shown that loss of VE-cadherin *in vivo* results in major vascular defects due to loss of vascular morphogenesis including loss of lumens in mice (Carmeliet *et al.*, 1999; Gory-Faure *et al.*, 1999). Consistent with the notion that lateral cell-cell adhesion is important in vascular lumen formation, early work by Carmeliet and co-workers had shown that VE-cadherin genetic deletion or truncation of its cytosolic domain which binds β-catenin results in endothelial defects in remodelling, maturation and also tubule opening (Carmeliet *et al.*, 1999). Correct localization of VE-cadherin is known to regulate and organize the localization of important apical and basal proteins leading to lumen formation (Wang *et al.*, 2010) including, podocalyxin, moesin1, and collagen IV which all fail to localize properly when VE-cadherin is lost *in vitro* and *in vivo* (Strilić *et al.*, 2009; Lampugnani *et al.*, 2010; Wang *et al.*, 2010). Moesin1 has been shown to control endothelial cell polarisation in zebrafish ISVs and loss of moesin1 leads to complete failure of ISV lumenisation and also delayed aortic lumen formation in knockout mice in another study (Strilić *et al.*, 2009; Wang *et al.*, 2010). These moesin1 defects are hypothesised to be due to the organization of the actin cytoskeleton and its role in directing luminal/ablumenal polarity.

Interestingly, more recent work has shown that VE-cadherin localized at filopodia on migrating tip cells induces polarity changes in stable quiescent endothelial cells within a tube. Interaction of VE-cadherin at the tips with the basal (ablumenal) side of endothelial cells within an established blood vessel, resulted in re-distribution of apical proteins to that site and initiation of apical membrane invagination to begin the process of lumen formation (Lenard *et al.*, 2013).

1.5.2.3 Polarity complex

In order to form tubes, endothelial cells, like epithelial cells, gain apical-basal polarity (also described as lumenal-ablumenal polarity in endothelial cells). This acquisition of polarity orchestrates the correct localization of apical and basal proteins in order to commence the

process of lumen formation. Cell-cell junctions between endothelial cells act as sites of apical polarization where VE-cadherin plays an important role as well as the CD34 related protein podocalyxin (Lampugnani et al., 2010; Y. Wang et al., 2010). The CD34 sialomucin family members are known to localize to the apical membrane of endothelial cells where their electrostatic properties aid in lumen opening (Strilić *et al.*, 2009). At the same time cell-ECM contacts maintain basal (ablumenal) identity (Bryant and Mostov, 2008).

Loss of endothelial recognition of the basement membrane through β1 Integrin deletion has been shown to be critical for lumen formation in mice through defects in Partitioning defective 3, Par3 (Zovein *et al.*, 2010). β1 Integrin loss resulted in loss of endothelial cells shape and mislocalisation of apical proteins and adhesion proteins through transcriptional decreases in the Par3 (Zovein *et al.*, 2010). Par3 is a member of the Par complex which consists of Par-3, Partitioning defective 6 (Par-6), Atypical protein kinase C (aPKC), and Cdc42 which localises to tight junctions and has been shown to be essential during endothelial lumen formation (Lizama and Zovein, 2013). Par3 and VE-cadherin interaction (Iden *et al.*, 2006) has also been shown to regulate endothelial polarity and junctional organization which is subsequently necessary for lumen formation.

Integrin β1 loss also affected localization of VE-cadherin and podocalyxin known to be essential for lumen formation. After loss of integrin β1, VE-cadherin which is normally seen at cell-cell junctions, was now present around the entire circumference of the cell while podocalyxin had lost its specific localization at the apical membrane only (Zovein *et al.*, 2010). It is therefore evident that endothelial cell (EC) interaction with the ECM and other ECs regulate apical basal differentiation and signalling to polarity proteins like Par3. Par3, together with PAK2, PAK4 and PKC are known to interact with Cdc42 and other members of the Rho GTPase family which in turn control endothelial cytoskeletal changes necessary for lumen formation (Koh, Mahan and Davis, 2008). Additional studies, however, are needed to assess if these regulatory mechanisms exist *in vivo* due to the likelihood of multiple functions for these polarity proteins. Loss of or gain of function studies would need temporal and cellular control to fully assess roles of these molecules *in vivo*.

After polarization of cells within a tubule, trafficking of apical proteins to the apical membrane controls lumen formation and opening. As discussed earlier, the CD34 family of sialomucins are known to be involved in the initial opening of tubules through their highly glycosylated and

sialic acid adorned extracellular domain (Nielsen and McNagny, 2008). This domain provides a negative charge which pushes opposing apical membranes apart and initiates the opening of lumens. Deletion of one of the CD34 related family members, podocalyxin, results in delays or defects in lumen opening in epithelial lumens (Doyonnas *et al.*, 2001; Cheng *et al.*, 2005; Meder *et al.*, 2005). Interestingly, vascular endothelial cells within these podocalyxin deficient models develop normally, possibly through compensation by other sialomucins like CD34 (Doyonnas *et al.*, 2001).

1.5.2.4 Blood flow and sheer stress

Vessel diameter appears to be controlled genetically but it has been shown that flow and sheer stress are essential for the maintenance and the regulation of the diameter of blood vessels (Jones, le Noble and Eichmann, 2006). Not only does the physical effect of flow and pressure shape the developing lumen, but the recognition of flow-induced sheer stress by endothelial cells also controls vessel morphology. The endothelial response to shear stress is necessary to maintain the homeostasis of the circulatory system, and loss of this response can lead to the development of vascular diseases such as hypertension, thrombosis, aneurysms, and atherosclerosis (Ando and Yamamoto, 2013). Changes in lumen size can also be affected by levels of nitric oxide induced by blood flow and pressure. Recognition of flow-induced sheer stress by the calcium ion channel Piezo1 was shown to be essential for lumen formation (Li *et al.*, 2014). Loss of piezo was embryonically lethal after the heart had started beating while haploinsufficiency led to abnormalities in the major vessels (Li *et al.*, 2014).

An important property of endothelial lumens is their ability to sense and respond to internal flow and pressure. After lumen formation is complete, unlike epithelial lumens, vascular lumens remain highly dynamic and continue to remodel in response to forces. During vessel growth endothelial lined lumens must form behind a growing sprout when the growing sprout may be elongating and migrating at a high rate, while endothelial cells forming a new lumen must maintain integrity through dramatic increases blood pressure and flow (Pelton *et al.*, 2014). Being in direct contact with pulsate blood flow enables the endothelial cells to monitor flow rates and pressures and respond to these cues accordingly.

1.6 Actin

Actin monomers are one of the most important and abundant proteins within eukaryotic cells because of their ability to play roles in a huge range of cellular functions and processes. Whether found on its own as G-actin or coupled together as F-actin, the actin machinery is involved in all aspects of cell structure and shape changes. Therefore, it is evident that all processes of angiogenesis including, sprouting, migration, and lumen formation, which rely on tightly regulated control of cell shape require control of the actin machinery.

Actin is a highly conserved monomeric protein that has the ability to polymerize and form sheets, filaments and bundles involved in controlling cell morphology (Figure 1.4)(Roberto Dominguez and Kenneth C. Holmes, 2011). Actin filament growth begins at an actin nucleation site composed of 2 or more actin monomers. Assembled head to tail, actin monomers elongate into chains of F-actin filaments with pointed and barbed ends. The barbed end of the filament grows rapidly through addition of ATP bound actin which has weak GTPase activity. Chains of F-actin form by a process known as "actin filament treadmilling" where ATP-bound actin monomers join the elongating barbed end, get hydrolysed to ADP, and then disassociate off the pointed end (Wegner and Isenbergt, 1983) (Figure 1.4B). While in the filament actin monomers hydrolyse to ADP and inorganic phosphate, their affinity for each other weakens which results in dissociation (Bugyi and Carlier, 2010). The speed at which actin monomers are added or lost, as well as the abundance of actin monomers dictate weather filaments elongate or shrink. Through the growth and organization of these simple filament shapes more complex structures can form through actin branching and binding proteins (Figure 1.4 C-D).

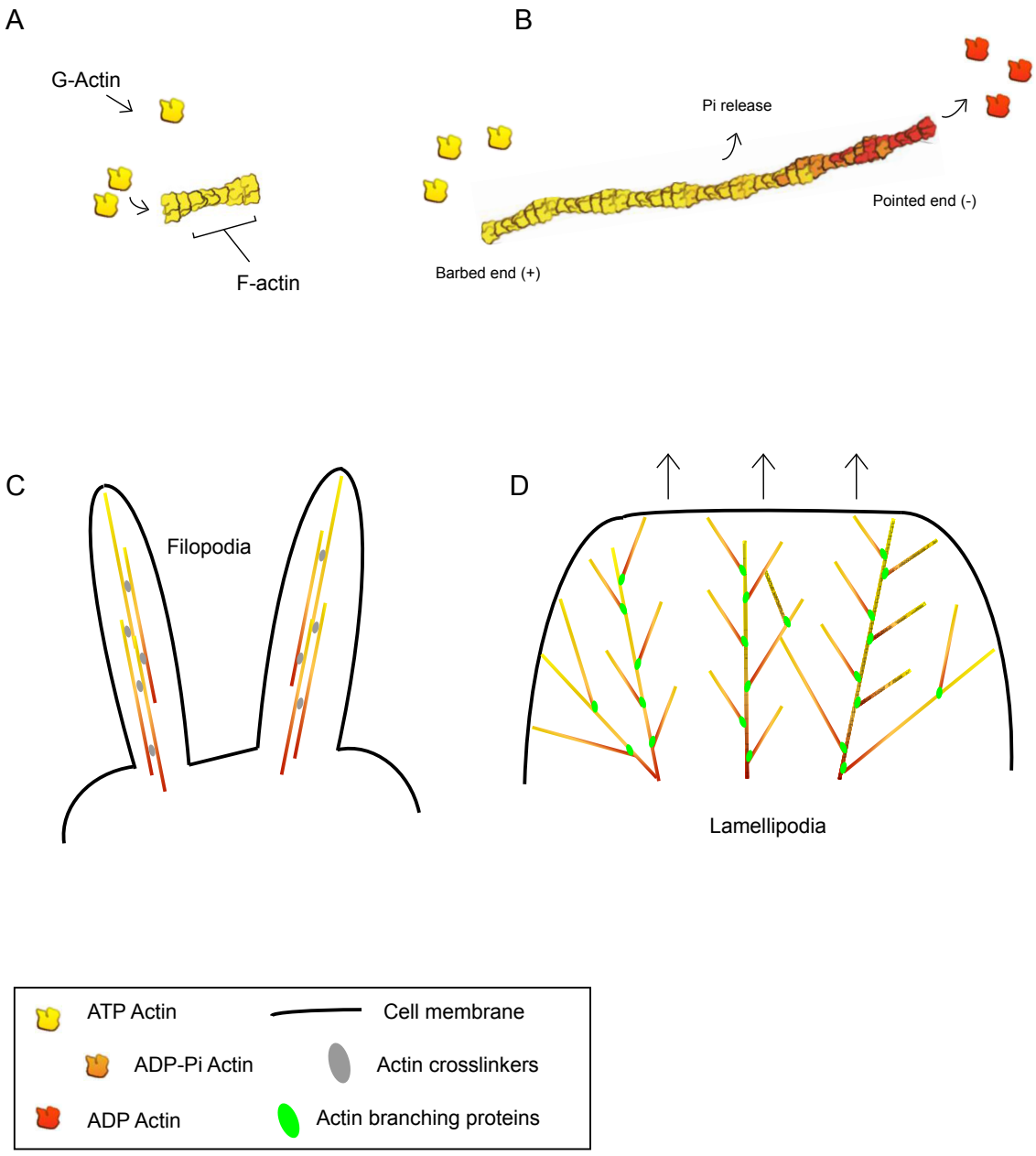

Figure 1.4 Actin structure and assembly

(A) Actin monomers combine in a helical structure to form filaments. ATP-actin is added at the barbed end of the filament. (B) The ADP gets hydrolysed in the filament, loses its strong affinity for actin monomers and gets removed from the pointed end; this turnover of actin is termed actin-treadmilling. Through this simple process more complex structures may be formed. (C) Filopodia are actin rich protrusions that extend from the cell membrane. Filaments are bundled together by actin binding proteins to form long unbranched protrusions. (D) Lamellipodia are actin dense flat sheets that protrude from the membrane. Actin filaments branch via actin binding proteins and form complex flat networks. Adapted from Blanchoin et al 2014 (Blanchoin *et al.*, 2014).

To create an actin filament, a nucleation point must be produced for the addition of monomeric actin to take place and grow the filament. This process is highly controlled within the cell and is under the influence of a range of actin nucleating, severing and elongation proteins and their associated factors.

1.6.1 Actin machinery

1.6.1.1 ARP2/3

The ARP2/3 complex is composed of 7 protein subunits of which two have close structural relationship with actin monomers. Of the seven subunits, Arp2 and Arp3 have the closest structural similarity to actin monomers and this is where the complex gets its name (RD, 2008). The Arp2/3 complex cannot initiate actin nucleation or polymerization without the help of actin nucleation promoting factors (NPFs). WASP, WAVE and WASH are some of the most well-studied NPFs and are regulated by Rho GTPase activity (Goley and Welch, 2006). They function through their WCA domain, binding ARP2/3 and presenting it with an actin monomer, which together with the 2 and 3 subunits form an actin nucleation point (Kelly *et al.*, 2006).

The Arp2/3 complex can also bind F-actin filaments and become activated. The complex drives actin branching activity through binding F-actin and increasing the number of barbed ends free for polymerization. By binding onto the side of a pre-existing actin filament at the pointed end, the Arp2 and Arp3 subunits form the base of a new branch of filament growing off the side at an angle of 70^{o} (Egile *et al.*, 2005). This behaviour results in highly branched networks seen in lamellipodia (Figure 1.4D). The complex also affects actin filaments by binding at the pointed ends and acting as a capping protein. This results in prevention of disassociation of actin monomers from the pointed end. Hydrolysis of ATP on Arp2 eventually leads to a decreased affinity of Arp2/3 for the pointed end, releasing itself, in turn allowing further disassociation of actin monomers (MF, 2003).

Branched actin filaments play roles in many areas of the cell depending on the desired outcome. The branching activity of Arp2/3 is controlled by NPFs which are in turn controlled by Rho GTPases. Specific localization of Arp2/3 NPFs control were branching will take place; for example, activation of Arp2/3 at the leading edge of a cell, by NPFs localized there, will result in the growth of lamellipodia (Campellone and Welch, 2010).

1.6.1.2 Formins

Formins function as actin regulators and play many different roles. They are identified by their FH2 domain which has actin nucleation and elongation capabilities (Pruyne *et al.*, 2002). Formins bind the barbed end of growing actin filaments and aid in elongation while protecting them from capping proteins (Kovar and Pollard, 2004). This process is much quicker than addition of cytosolic free actin monomers to the barbed end of a growing filament. As well as actin nucleation, formins also have the ability to control actin depolymerisation, bundling and severing (Breitsprecher and Goode, 2013). Rho GTPases are known to regulate formins.

Different GTPases have the ability to bind the same formin GTPase binding domain (GBD) resulting in activation in different cell compartments. Normally found in an autoinhibitory folded form, formins become activated when bound to active Rho GTPases which release the auto-inhibition. (Eisenmann *et al.*, 2005). Further activation may be needed for full formin activity, and actin binding may play a role in this process.

1.6.1.3 Profilin

Profilin is an another important actin binding protein that regulates actin monomer polymerization. Upon discovery, profilin was thought to be an actin depolymerizing protein as it bound monomeric actin *in vitro* (Carlsson *et al.*, 1976). Later it was shown that upon binding actin, profilin significantly accelerated the exchange of ADP for ATP thus providing more available actin for polymerization (Plank and Ware, 1987). It was also implicated in promoting binding of actin-profilin complexes to the barbed end over the pointed end of growing actin filaments (Pollard and Cooper, 1984). It is now known that profilin binds to actin monomers and is involved in the exchange of ADP for ATP (Goldschmidt-Clermont *et al.*, 1992). The affinity of profilin for phosphoinositides found in the plasma membrane, which has been shown to disrupt the profilin-actin binding, is suggested to be a mechanism for delivery of ATP-actin monomers to the plasma membrane ready for polymerization (Lassing and Lindberg, 1985; Witke *et al.*, 2001).

Profilin is regulated by Rho A and has been shown to be part of a complex with Rho A and p140mDia which is recruited to lamellipodia in fibroblasts and membrane ruffles in MDCK cells

controlling changes in the actin cytoskeleton (Watanabe *et al.*, 1997). Due to the importance of profilin in such fundamental processes, genetic knockout of profilin results in embryonic lethality as early as the two-cell stage due to severe defects in cytokinesis (Witke *et al.*, 2001). Recent studies have linked mutations in the profilin1 gene with pathological conditions including contribution to the pathogenesis of amyotrophic lateral sclerosis and neurodegeneration (Alkam *et al.*, 2016).

In addition to actin nucleation and elongation factors precise regulation of actin dynamics necessitates the action of actin severing and depolymerizing proteins. These proteins cleave actin filaments to prevent excessive growth and return actin monomers to the free pool available for incorporation into new filaments.

1.6.1.4 ADF/Cofilin

Cofilin is an actin binding protein involved in the de-polymerization of actin filaments. Cofilin can interact with both G-actin and F-actin and has a strong affinity for ADP-bound actin over the two other forms actin, ATP-actin and ADP-Pi-actin. Cofilin also plays a positive role in actin treadmilling through severing growing filaments and hence replenishing the monomeric actin pool for new filament growth.

Cofilin can nucleate actin filaments directly and also be involved in increasing or decreasing filament branching. Its severing activity on F-actin filaments creates new barbed ends available for nucleation and filament growth (Ichetovkin, Grant and Condeelis, 2002; Andrianantoandro and Pollard, 2006). After severing of F-actin filaments, cofilin allows for the binding and branching of these filaments through ARP2/3 mediated branching activities, as newly polymerized filaments allow for a 10-fold more stable branching over older ones (Ichetovkin, Grant and Condeelis, 2002; TD, 2006). Furthermore, it can sever ARP2/3 complex produced branches on older filaments. (TD, 2009). The severing activity shown by cofilin is known to take place between separate cofilin bound sections of F-actin filaments. Cofilin binding to F-actin alters the existing filaments' conformational twist. Its binding activity on the filament creates flexibility in the F-actin filament which can spread up the filament to regions unbound by cofilin. These unbound regions between cofilin molecules become weak and split as they lack the structural support given by cofilin mediated stabilization (Bravo-Cordero *et al.*, no date; Galkin, Orlova and Kudryashov, 2011).

Rho GTPase signalling controls at least in part the activity of cofilin. Rho GTPases effectors such as ROCK1/2, activate LIM-kinase which phosphorylates cofilin at its Ser 3 residue and render it inactive (Caroni *et al.*, 1998). Other kinases also control cofilin activity, such as testicular protein kinase (TESK), which also phosphorylates cofilin at Ser 3 independently of LIMK (Toshima *et al.*, 2001). The activity of cofilin can be further coordinated by phosphatases that control its reactivation. Slingshot (SSH1) for example is transported to the lamellipodia by coronin 1B and dephosphorylates cofilin, thus increasing its activity at lamellipodia (Niwa *et al.*, 2002). Balanced expression of kinases and phosphatases modulate cofilin activity at different cell sites.

1.6.1.5 Myosins

As well as playing a structural role within the cell, actin also contributes to cell contractility and trafficking. This is through the interaction of actin with myosins, motor proteins that move along actin filaments and hydrolyse ATP as they move. Myosins convert chemical energy in the form of ATP to mechanical energy, used to generate force and movement along actin filaments (Cooper, 2000). They can be involved in shuttling of cargo along F-actin chains, or in contractility by creating pulling forces (Schnittler *et al.*, 1990). The generated force is used in the contraction of stress fibres and pulling of the extracellular matrix that cells are attached to.

1.6.2 The actin cytoskeleton

The actin cytoskeleton functions not only as structural support for the cell, but also as a vital scaffold involved in important cellular functions. Through coordinated action of the actin machinery, cells control their shape changes, migration and morphology. Cell movement is necessary for the majority of cell functions and is accomplished through coordinated protrusion, adhesion and contraction of the cell membrane. The cell takes advantage of previously discussed actin regulators to modulate the cell shape for numerous processes. Filopodia are actin-rich cell protrusions that aid migration, through sensing of growth factors, extracellular matrix proteins, and cues from other cells. They protrude from the cell membrane through elongation of actin filaments linked by actin crosslinkers (Figure 1.4C). In endothelial cells, filopodia are highly dynamic and have high turnover rate. One of the main drivers of filopodial protrusions is the Rho GTPase Cdc42 (Ridley and Hall Cell, Cdc42 paper).

Lamellipodia on the other hand are flat sheets of actin-rich membrane which protrude from the cells edge to aid in migration (Figure 1.4 D). Actin branching behaviour is known to drive lamellipodia through ARP2/3 complex activity. Rac signalling is known to drive lamellipodia formation (Ridley *et al.*, 1992). Many of the important cellular actin cytoskeletal rearrangements are under the control of the Rho family of small GTPases.

1.6.3 Rho GTPases

Rho GTPases are small (~21kDa) signalling G proteins that act as molecular switches in signalling pathways. Rho proteins are known best for the control of the actin cytoskeleton but they also control many other processes including proliferation, survival, differentiation and gene expression, through actin dependent and independent mechanisms The Rho family of small GTPases are a subclass of the larger Ras superfamily which consists of over 150 members divided in to 5 subgroups Rho, Ras, Arf, Ran, and Rab (Madaule and Axel, 1985). Rho GTPases are highly conserved and have been found in yeast, plants, worms and flies (Jaffe and Hall, 2005).

Several studies have implicated Rho proteins in the process of angiogenesis (Hoang, Whelan and Senger, 2004; Mavria *et al.*, 2006; Bryan and D'Amore, 2007; Abraham *et al.*, 2009, 2015; Kaur *et al.*, 2011). The complex changes in shape undergone by endothelial cells during sprouting, migration and lumen formation require precise control of the actin cytoskeleton by Rho proteins. Within the family of small Rho GTPases, cell division control protein 42 homologue (Cdc42), Ras-related C3 botulinum toxin substrate, Rac (Rac 1, 2, and 3), and Ras homology gene family, Rho (Rho A, B, and C) are the best studied. Of these GTPases, CDC42 has been shown to control filopodia formation (Kozma *et al.*, 1995; Nobes and Hall, 1995), Rac shown to be involved in lamellipodia formation (Ridley *et al.*, 1992) and Rho to play roles in stress fibre formation and actomyosin contractility. With such important regulatory roles in diverse functions, deregulation of Rho GTPase signalling is seen in many cancers and numerous other diseases (Vega and Ridley, 2008).

1.6.3.1 Cdc42

Cdc42 was first discovered in yeast and shown to important for budding behaviour through its control of the actin cytoskeleton (Johnson and Pringle, 1990). Cdc42 is one of the main actin nucleator proteins and is therefore implicated in many cellular processes. Its best described

role in mammalian cells is the induction of filopodia formation but has also been implicated in controlling cell polarity, proliferation and migration through the control of actin polymerization, depolymerisation, branching, bundling and contractility (Erickson and Cerione, 2001; Peng *et al.*, 2003; Etienne-Manneville, 2004; Wilkinson, Paterson and Marshall, 2005; Derivery and Gautreau, 2010).

During angiogenesis, endothelial sprouting behaviour is led by filopodia-rich tip cells. As discussed in Section 1.6.2, filopodia are actin-rich structures that extend the membrane forward into the extracellular environment and help with detecting growth factor gradients necessary for directional migration (Gerhardt *et al.*, 2003). Extension of filopodia by endothelial cells is highly dynamic, and filopodia are turned over rapidly during endothelial sprouting.

Cdc42 endothelial-specific knockout mice show early embryonic death between E8.5 and E10.5 (Hu *et al.*, 2011; Barry *et al.*, 2015), only slightly later than lethality in the global Cdc42 knockout models (E7.5)(Chen *et al.*, 2000; Wang *et al.*, 2013). Early investigations in endothelial specific knockout embryos showed that embryos lacking endothelial Cdc42 are smaller with fewer blood vessels, suggesting an important role for Cdc42 in vascular development (Hu *et al.*, 2011). Barry et al. subsequently showed that early deletion of Cdc42 (E8.5) results in blocked endothelial lumen formation in the yolk sac, while later deletion (E14.5) results in defects in endothelial junctional organization and vascular integrity (Barry *et al.*, 2015). Their results suggested that Cdc42 plays a role in angiogenic remodelling, filopodia formation and sprouting through two mechanisms: through the effectors Pak2 and Pak4 and their control of the actin cytoskeleton through pMLC; and Cdc42 and N-WASP control on actin polymerization and EC junctions (Barry *et al.*, 2015).

1.6.3.2 Rac1, 2, 3

Rac1, 2 and 3 are all members of Rac subclass which are expressed differentially in tissues. Rac1 is ubiquitously expressed, Rac 2 is only expressed in hematopoietic cells, while Rac3 is only found in the nervous system during development. Rac1 is known to control lamellipodia and membrane protrusions. Association of Rac with the actin nucleator and branching complex ARP2/3 drives these protrusions and are both found localized at the front of the growing

protrusion (GG, 1999). Rac is involved in membrane ruffling thus impacting on migration and also controls focal adhesions (Hall, 1998; Steffen *et al.*, 2013).

During angiogenesis, Rac has been shown to control the actin cytoskeleton during capillary formation in vitro in a 3D angiogenesis assay (John O. Connolly‡ , Nandi Simpson,* Lindsay Hewlett, 2002). Endothelial Rac1 deletion using Tie2 Cre is embryonic lethal mid-gestation at E9.5 due to defects in the development of the major vessels, and abnormal loss of small branched vessels both in the yolk sac and embryo (Tan *et al.*, 2008). Endothelial cells isolated from the Rac1 knockout mice showed defects in a range of important processes necessary for angiogenesis including migration, adhesion and tubulogenesis (Tan *et al.*, 2008). However, in another study using Tie1 Cre recombinase to drive endothelial deletion, the investigators found that endothelial cell migration early during development was unaffected, whereas lymphangiogenesis was perturbed with Rac1 deletion. This was due to improper migration of endothelial progenitors away from the cardinal vein early in development to form the lymphatic vascular system, and resulted blood filled lymphatic vessels and death in utero (D'Amico *et al.*, 2009).

1.6.3.3 RhoA, B and C

RhoA also functions in the control and regulation of the actin cytoskeleton. As a member of the Rho subclass (Rho A, B and C), Rho A has been shown to control aspects of cell contractility (Ridley and Hall, 1992). Rho B on the other hand is involved in cytokine trafficking and cell survival while Rho C is important for cell motility and invasive behaviour (WHEELER and RIDLEY, 2004). The three members of the subclass share structural similarities and may interact with the same effectors.

RhoA is vital in development as evident by several mouse knockout studies (Herzog *et al.*, 2011; Jackson *et al.*, 2011; Melendez *et al.*, 2011). RhoA knockout embryonic fibroblasts show increased cell spreading in culture compared with wild type fibroblasts (Melendez *et al.*, 2011). RhoA loss in keratinocytes was shown to be essential for contraction and directed migration (Jackson *et al.*, 2011). Studies of mouse macrophages show that loss of RhoA or RhoB results in defects in tail end retraction during cell migration, and loss of the ability of the cell to retract lamellipodia resulting in extreme elongation (Koenigs *et al.*, 2014). Interestingly, migration was increased suggesting that Rho may play diverse roles in the regulation of migration (Koenigs *et*

al., 2014). The diversity of roles and also the report of some contradictory findings in the RhoA literature may be explained by an overlap in function of the three family members, and a level of redundancy amongst them.

Pharmacological inhibitors of the RhoA pathway are known to block angiogenesis *in vitro* (van Nieuw Amerongen *et al.*, 2003). In endothelial cells, RhoA has been shown to be essential for angiogenesis downstream of VEGF signalling (Bryan *et al.*, 2010). It has been suggested that through its effector ROCK, RhoA activation results in cytoskeletal changes necessary for angiogenesis driven by VEGF, while other studies have shown that ROCK inhibition stimulates endothelial sprouting and angiogenesis (Abraham *et al.*, 2009). In a mouse skin angiogenesis model, dominant negative RhoA-expressing endothelial cells, stimulated by VEGF, failed to form tubules while the active RhoA-expressing cells formed tubules with lumens (Hoang, Whelan and Senger, 2004). Interpretation of studies employing dominant negative counterparts of Rho GTPases may be complicated by interaction with GEFs that control different Rho family members.

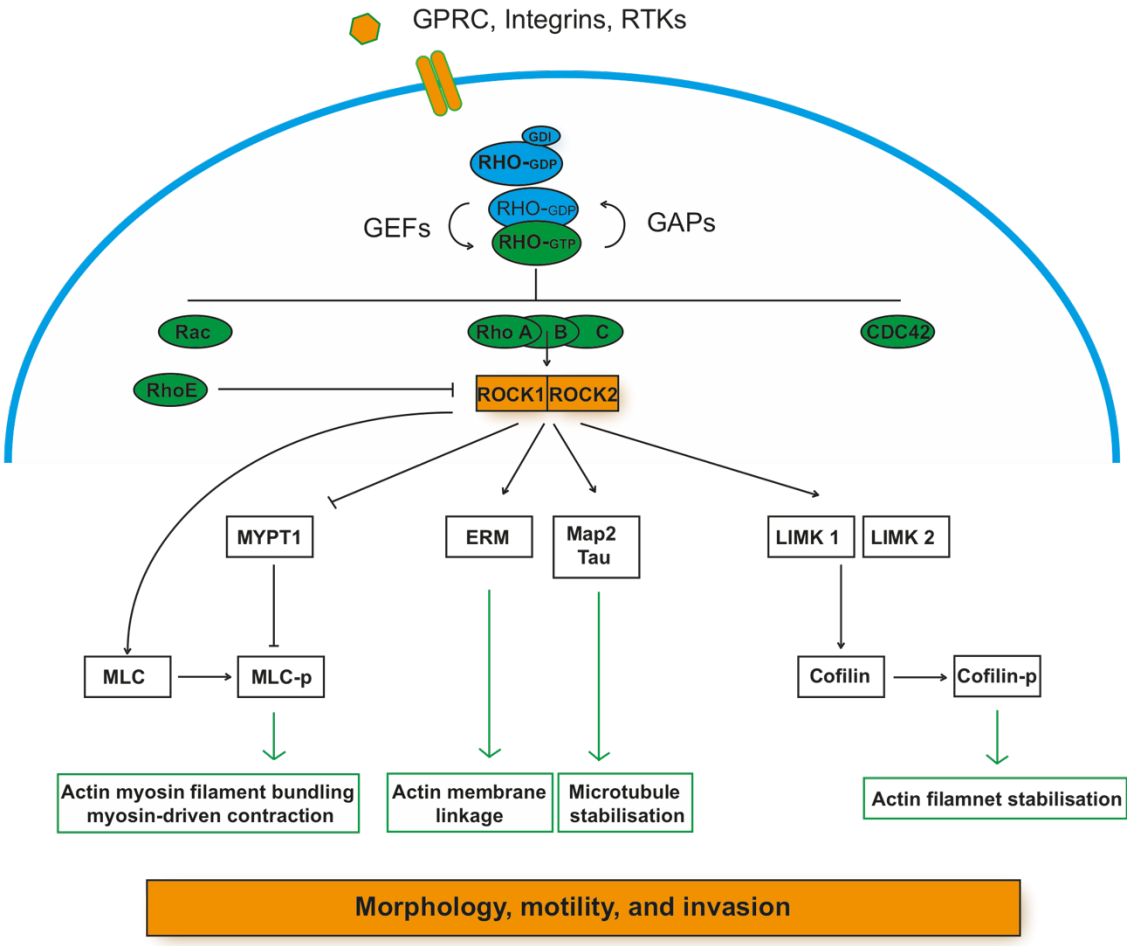

Figure 1.5 Overview of Rho/Rho kinase signalling
Schematic of Rho GTPase activation via guanine nucleotide exchange factors (GEFs) and downstream effectors and their function. Activated ROCKI/II phosphorylates Myosin light chain (MLC) directly or myosin phosphate target subunit 1 (MYPT1) of myosin phosphatase. They may also phosphorylate LIM kinase (LIMK1, 2) resulting in phosphorylation of Cofilin and inhibition of its actin severing activities. Ezrin, radixin, and moesin (ERM) phosphorylation leads to changes in actin membrane linkage while Map2 and Tau activation controls microtubule stabilization. Adapted from (Matsuoka and Yashiro, 2014).

1.6.4 Guanine nucleotide exchange factors (GEFs)

Rho GTPases cycle between two states: inactive when GDP bound, and active when GTP bound. Regulation of activation status is under control of three classes of proteins: positive regulators, specifically guanine nucleotide exchange factors (GEFs); negative regulators, such as GTPase activating proteins (GAPs); and guanine nucleotide dissociation inhibitors (GDIs). GEFs catalyse the exchange of GDP for GTP (Rossman, Der and Sondek, 2005), while GAPs promote the intrinsic GTPase activity of Rho proteins and dissociation of GTP to allow GDP binding which switching GTPases to their inactive state. GDIs bind to Rho GTPases in their GDP bound state and inhibit both activation by exchange to GTP, and translocation to the plasma membrane (Hoffman and Cerione, 2013). GEFs and GAPs introduce a high level of complexity to GTPase signalling cascades. There are over 80 Rho GEFs with many able to activate multiple GTPases.

There are two families of Rho GEFs, the larger Dbl homology-pleckstrin homology (DH-PH) GEFs, and the dedicator of cytokinesis (DOCK) 180 family GEFs. In the DH-PH GEFs the DH domain catalyses the exchange of GDP for GTP thus activating the GTPase, while the PH domain is thought to control localization of the GEFs at the plasma membrane, through binding phosphoinositides (Maffucci and Falasca, 2001). The Dbl family GEFs contain nucleotide and Mg^{2+} binding pockets. The nucleotide binding (GTP or GDP) controls the activity of the GEF while the Mg^{2+} pocket is involved in high-affinity binding of GTP and discharge of the activated Rho GTPase. A similar mechanism of catalysis of the activation process has been described for DOCK180 family GEFs (Yang *et al.*, 2009) despite the lack of sequence similarity between the activating domains of the two family GEFs. Other domains may vary considerably amongst different DH-PH GEFs, which are involved in tissue specificity, dictate what GTPases the GEFs activate, and also mediate interactions with other proteins, or mediate Rho GTPase independent functions.

The DOCK180 family GEFs, named after the prototypical member DOCK180 (DOCK1), comprise 11 family members (DOCK1-11). Nucleotide exchange is catalysed by the DOCKER, also known as DHR2 domain which bears no sequence similarity with the DH domain of DH-PH GEFs (Meller, Merlot and Guda, 2005). The DHR1 domain may be involved in the localization of DOCK180 proteins at the plasma membrane through binding to phosphatidylinositol 3,4,5-triphosphate (Meller et al., 2005).

DOCK180 family GEFs are subdivided into four categories depending on their amino acid sequence homology: DOCK-A comprising DOCK180, DOCK2 and DOCK5; DOCK-B comprising DOCK3 and DOCK4; DOCK-C (Zir; Zizimin like DOCKs) comprising DOCK6, DOCK7 and DOCK8; and DOCK-D comprising DOCK9 (zizimin 1), DOCK10 and DOCK11 (Meller, Merlot and Guda, 2005). Members of groups A and B possess a Src homology 3 (SH3) domain at the N-terminus and proline-rich motif at the C-terminus for protein interactions (Mayer, 2001). Groups A and B are Rac GEFs, while group D are Cdc42 GEFs. Group C are less well studied but have been shown to activate both Cdc42 and Rac (Miyamoto *et al.*, 2007).

Regulation of DOCK180 proteins is in part carried out through interaction with engulfment and motility (ELMO) proteins, ELMO1,2 and 3 are members of a family of scaffolding proteins. Studies have shown that DOCK180 is only active towards Rac when in complex with ELMO (Brugnera *et al.*, 2002). On the other hand, conflicting results have shown that an isolated DHR-2 domain of DOCK180 is sufficient for activation of Rac in the absence of ELMO (Côté and Vuori, 2002). This could be down to the localisation role ELMO is playing on DOCK180, delivering the complex to different compartments of the cell for Rac activation.

1.6.4.1 DOCK4

DOCK4 was first described as a tumour suppressor and activator of Rap GTPase in a mouse tumour model (Yajnik *et al.*, 2003). In this study, Yajnik and co-workers showed that genomic deletion of DOCK4 in mouse NF2 and TP53 tumour models resulted in defects in formation of adherens junctions which promote tumorigenesis, while DOCK4 mutations were also identified in human prostate and ovary tumours which failed to activate Rap1 (Yajnik *et al.*, 2003). Experiments in mouse osteocarcinoma cells lacking the endogenous Dock4 gene showed that expression of wild type but not mutant DOCK4 reduced tumour cell growth and migration in soft agar (Yajnik *et al.*, 2003).

Further studies showed DOCK4 has the ability to activate the Rho GTPase, Rac1 (Hiramoto, Negishi and Katoh, 2006). Hiramoto and co-workers showed that overexpression of DOCK4 in mouse fibroblasts induced Rac1 activation, which was further regulated by RhoG (Hiramoto, Negishi and Katoh, 2006). They went on to show that when the catalytic DHR2 domain (Figure 1.6) was deleted, there was reduced interaction between DOCK4 and Rac1. The RhoG effector ELMO facilitates this DOCK4 mediated activation of Rac1 by acting as a scaffolding protein.

RhoG activation promotes the binding of ELMO to the sh3 domain of DOCK4. This in turn allows translocation of DOCK4 to the plasma membrane where it activates Rac1 and drives cell migration (Hiramoto, Negishi and Katoh, 2006).

1.6.4.2 DOCK9

DOCK9 (Zizimin 1) is another member of the DOCK family of GEFs which belongs to group D of DOCK180 family GEFs. It was first discovered through an affinity proteomic approach looking at novel activators of Cdc42 in fibroblasts and was shown to be responsible for inducing filopodia (Meller *et al.*, 2002). Like DOCK4, DOCK9 contains a DHR1 and DHR2 domain (Yang *et al.*, 2009), and additionally a pleckstrin homology (PH) domain (Figure 1.6). Both the DHR1 and PH domains are involved in translocation of DOCK9 to the plasma membrane (Kuramoto, Negishi and Katoh, 2009).

DOCK9 has been shown to be responsible for cellular protrusive activity and essential for the growth of dendrites in neuronal cells, while depletion of DOCK9 in glioblastoma cells inhibits formation of pseudopodia resulting in reduced invasion *in vivo* (Kuramoto, Negishi and Katoh, 2009; Hirata *et al.*, 2012).

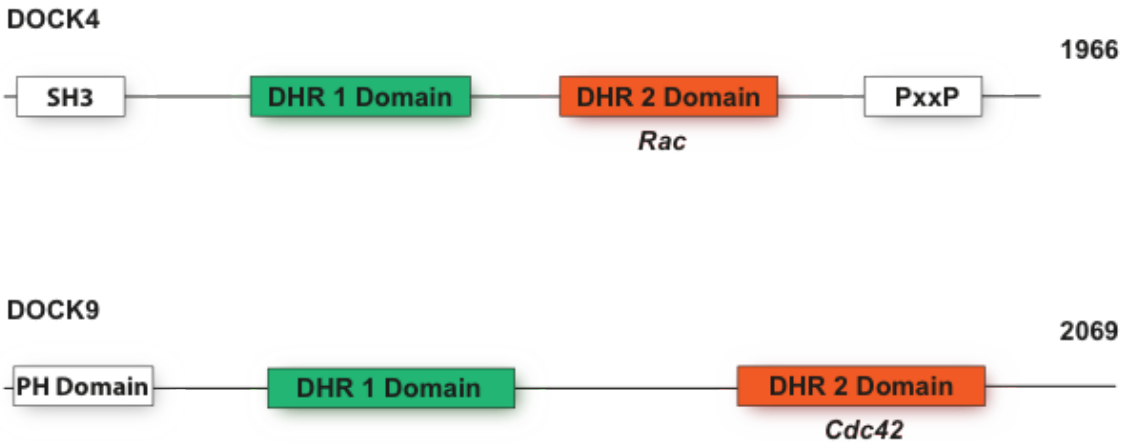

Figure 1.6 DOCK4 and DOCK9 protein domain maps
DOCK4 and DOCK9 are members of the DOCK family of GEFs and therefore contain the DHR1 and DHR2 domains. The DHR2 domain is responsible for activation of Rho GTPases while the DHR1 domain is involved in localization. DOCK4 belongs to the subgroup B of the DOCK GEFs and contains a N-terminal SH3 domain and C-terminal proline rich sequence motif that binds SH3 domains and mediate protein-protein interactions respectively. DOCK9 is a member of the D subclass (Zizimin) of DOCKs and possess a PH domain responsible for interaction with phosphoinositides and binding the plasma membrane.

1.6.5 Rho effectors

Rho GTPases are involved in a huge range of signalling pathways controlling diverse cellular functions. When activated, Rho proteins have the ability to interact with multiple downstream effectors which coordinate the diverse cellular responses and contribute to the specificity of a particular signal transmitted by a Rho protein. The effector proteins typically bind Rho GTPases in their GTP-bound form and may remain bound for activity, or gain activity by phosphorylation or binding to another activation protein (Bishop and Hall, 2000).

1.6.5.1 Rho associated coiled coil kinases (ROCK1 and 2)

The Rho associated kinases of which there are two, ROCK1 and ROCK2 (collectively referred to as ROCK), are highly conserved serine threonine kinases that are involved in signalling cascades that control actin dynamics. They share a 64% overall identity in humans with 89% identity in their kinase domains (Figure 1.7). Activation occurs through interaction with RhoA, B, or C, through the Rho binding domain (RBD), while inactivation can take place through interaction with RhoJ (another Rho family member), RAD (a member of the Ras family overexpressed in muscle of type II diabetic humans), and GEM (another Ras family member) at sites other than the RBD of the ROCK proteins (Riento and Ridley, 2003).

One of the most common mechanisms of effector activation by GTPases is disruption of auto-inhibitory interactions to expose functional domains within the effector (Bishop and Hall, 2000). This is true for ROCK, normally found folded in an auto-inhibitory conformation, which shields the kinase domain. Binding of Rho proteins to the Rho binding domain (RBD) of ROCK relieves auto-inhibition of the kinase domain for activity (Riento and Ridley, 2003). Auto-phosphorylation of ROCK1 at Ser1333 and ROCK2 at Ser1366 reflects the activation status of the kinases (Figure 1.7). Other phosphorylation sites on ROCK2 increase (Thr967, Ser1099, Ser1133, or Ser1374) or decrease (Thy722) its activation status (Hartmann, Ridley and Lutz, 2015).

ROCK is one of the main downstream effectors of Rho-mediated actin cytoskeleton rearrangements, stress fibres and focal adhesions (Chrzanowska-Wodnicka and Burridge, 1996). Through its kinase domain, ROCK phosphorylates and activates further downstream targets including the Lim kinases, Map2 tau and myosin light chain (MLC) which impact on actin polymerization, protrusive activity and cellular contractility. ROCKs may phosphorylate

MLC directly or indirectly through inhibitory phosphorylation of myosin phosphatase target subunit 1 (MYPT1) which dephosphorylates MLC2 (a regulatory light chain of myosin) (Figure 1.5)(Ito *et al.*, 2004). Hence, they increase actomyosin contractile force generation by phosphorylation of MLC2, which causes a ATP-dependant change in myosin structure and shifts its position in relation to actin, resulting in a contractile pulling on actin filaments. ROCK and myosin binding subunits play roles in many downstream Rho signalling outputs including stress fibres, focal adhesions, smooth muscle cell contraction and vasodilation of blood vessels (Hartmann, Ridley and Lutz, 2015). Another target of ROCK is LIM kinase 1 and 2, which upon phosphorylation, phosphorylate cofilin and inhibit its F-actin cleaving ability (Ohashi *et al.*, 2000) (Figure 1.5). Further reports have implicated ROCK and myosin light chain signalling in cadherin-based adhesion and regulation of morphological and permeability changes of endothelial cells (McKenzie and Ridley, 2007).

Expression of the two isoforms, ROCK1 and ROCK2, differs depending on the tissue. ROCK1 is ubiquitously expressed in all tissues except for the brain and muscles whereas ROCK2 is expressed heavily in the brain and muscles and also in the heart, blood vessels, lung and placenta (Nakagawa *et al.*, 1996; Montalvo *et al.*, 2013). Similar roles for each ROCK isoform have been reported including roles in actin cytoskeleton organization, migration, cellular morphology and progression of the cell cycle, apoptosis, and extracellular matrix assembly (ORLANDO, STONE and PITTMAN, 2006; Shi and Wei, 2007; Mong and Wang, 2009; Inaba *et al.*, 2010; Leong *et al.*, 2011). However, the knockdown of individual paralogues of either ROCK1 or ROCK2 and less use of the pan-ROCK inhibitors e.g. Y27632, have highlighted isoform-specific roles in endothelial cells. Co-staining for ROCK1 and ROCK2 in pancreatic islet endothelial cells *in vitro* has shown distinct localisation of both paralogues suggesting differing roles within this cell type. In the same study it was shown that ROCK2, and not ROCK1, was responsible for the phosphorylation of the actin regulating proteins MBS and cofilin, and also that ROCK2 knockdown cells displayed better survival rates under serum starvation when compared to ROCK1 (Montalvo *et al.*, 2013). This was shown to be due to a ROCK2 reduction in caspase 3 cleavage not seen with ROCK1.

ROCK1 and ROCK2 global knockout mice have also been generated and display distinct phenotypes. The ROCK2 global knockout was the first to be described (Thumkeo *et al.*, 2003) and showed that over 90% of *Rock2*$^{-/-}$ embryos died *in utero* due to defects in the placental-embryo interaction. The mice that survived were smaller but did not show any histological

difference to the wild type and subsequently caught up later in growth (Thumkeo *et al.*, 2003). ROCK1 global knockout mouse models showed a less severe phenotype than ROCK2. Deletion of ROCK1 resulted in global developmental defects including failure of closure of the eyelids and of the ventral body wall (Shimizu *et al.*, 2005). Defects in actin cytoskeletal organisation and MLC phosphorylation were shown to be responsible for this phenotype.

1.6.5.2 Rho signalling in angiogenesis and lumen formation

During lumen opening and expansion, control of Rho GTPase signalling responsible for actin based shape changes is essential. The regulation of RhoA has been shown to have effects on lumenisation, both positive and negative. Activation of RhoA has been shown to lead to lumen collapse *in vitro* through control of microtubules (Bayless and Davis, 2004). Xu et al showed that mice lacking Raspi1 had increased RhoA/ ROCK/ myosin II activity and blockade of Cdc42 and Rac1 and was responsible for the loss of lumens (Bayless and Davis, 2002; Xu *et al.*, 2011). The same effect was seen with downregulation of RhoA downstream of Rasip1 and ArhGAP29, which results in promotion of lumen formation in these mice (Xu *et al.*, 2011). Likewise, RhoA induced actomyosin contraction downstream of PP2A-Bα has shown to be a negative regulator of lumen formation (Martin *et al.*, 2013). Conversely, other reports have shown opposite roles for RhoA in lumen formation. Hoang et al showed that a dominant negative form of RhoA reduced the number of lumenised blood vessels in a mouse skin angiogenesis model (Hoang, Whelan and Senger, 2004), although these studies are complicated by potential interaction of dominant negative RhoA with GEFs for other GTPases. Another report suggested that during the formation of the mouse dorsal aorta, RhoA had an essential role in activation of ROCK and localization of myosin II to actin filaments surrounding the lumen to initiate cell shape changes and lumen opening (Strilić *et al.*, 2009).

Endothelial and mural cell contractility play important roles in regulating vessel stability and diameter. The actin-myosin interaction in endothelial cells is controlled by MLC phosphorylation (Cai *et al.*, 1998) and MLC phosphorylation in ECs is controlled by ROCKI/II (Abraham et al, 2009). Control of contractility through myosin plays important roles in endothelial permeability, sprouting (Abraham et al, 2009), and has also been shown recently to be important for cell curvature regulated branching morphogenesis in 3D collagen gels (Elliott *et al.*, 2015).

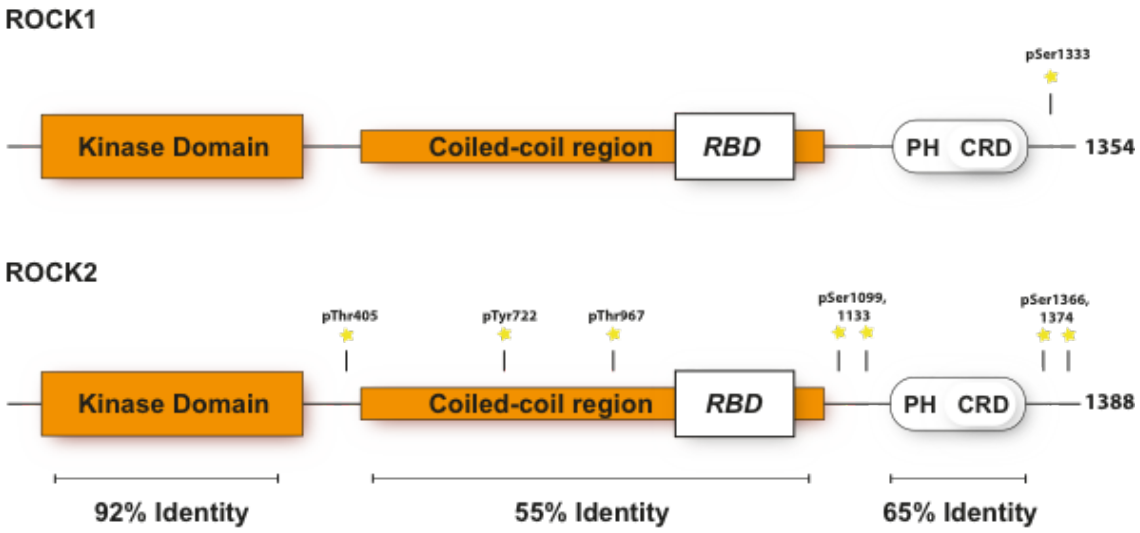

Figure 1.7 ROCK1 and ROCK2 structure, homology and phosphorylation sites.
Both ROCK1 and ROCK2 contain N-terminal kinase domain and C-terminal PH domain with a cysteine rich (CRD) domain therein. Between these domains the coiled-coil region contains the Rho binding domain (RBD). Activation of the kinases is through binding of Rho A, B, C to the RBD release of the auto inhibitory folding complex (not shown) they are held in, and freeing of the kinase for activity. ROCK1 and ROCK2 share 65% overall homology with the highest sequence homology in the kinase domains. Adapted from (Hartmann, Ridley and Lutz, 2015). Stars indicate phosphorylation sites.

1.7 Primary cilia

Cilia are specialized cell organelles found on nearly all cells of the body that function as extracellular antennae (Christensen *et al.*, 2007). They are microtubule-based organelles that have a wide range of diverse functions ranging from mechanical functions such as sensing of fluid flow and pressure, to sensing of chemicals and light (Singla, Veena, 2006). There are two separate forms of cilia described to date. The best-described form is the motile cilium, which can be present in large numbers on epithelial cells of the airways and oviduct. These cilia are motile and, in the case of the airway epithelium, act to move mucus away from the lungs. A second form of cilium is the non-motile sensory cilium, also known as the primary cilium. The vertebrate primary cilium is a solitary hair-like structure that protrudes from the plasma membrane into the extracellular space, and functions for detecting diverse chemical and mechanical stimuli (Christensen, Clement, Satir, & Pedersen, 2012, Praetorius & Spring, 2001). Primary cilia are intricately linked with the cell cycle as the base of the cilium is formed from the mother centriole and it is usually expressed during cell cycle arrest in G0 (Goto, Inoko and Inagaki, 2013).

1.7.1 Primary cilia structure and function

The microtubule configuration of both motile and non-motile cilia have been well-described and show minor differences. They consist of anchoring basal bodies which originate from the mother centriole and are situated near the plasma membrane. From this basal body anchor then protrudes the axoneme, composed of microtubules surrounded by specialized plasma membrane which protrudes beyond the cell boundary and out into the extracellular space (Figure 1.8). Between the basal body and the axoneme is a specialized region termed the transition zone which controls what molecules and proteins enter and exit the axonemal microtubules and the ciliary membrane. Both types of cilia are described and identified by their axonemal microtubule organisation. Motile cilia have a “9 + 2” microtubule make-up as their axoneme contains 9 pairs of microtubules surrounding an inner pair. Primary cilia lack this inner pair of microtubule, and have a “9 + 0” make up as well as lacking many of the structural components found in motile cilia including the dynein arms responsible for producing their motility.

Assembling of the primary cilia involves intricate transport of proteins and structural components up and down the microtubule axoneme. This shuttling is carried out by

intraflagellar transport proteins (IFTs) and comprises two modes of motion along ciliary microtubules though IFT-A and IFT-B complexes. IFT-B anterograde motion is towards the tip of the cilia and uses heterotrimeric kinesin-2 motors, while the IFT-A retrograde motion back towards the cilia base is carried out by cytoplasmic dynein 1b motors (Pedersen and Rosenbaum, 2008). Assembly of the primary cilium and transport of the necessary building blocks up the axoneme is carried out by the IFT-B complexes, while signalling components from the ciliary membrane are shuttled down the axoneme towards the cilium base by the IFT-A complexes (Pedersen and Rosenbaum, 2008). Due to the importance of these IFT proteins in construction and maintenance of primary cilia, defects in their regulation can lead to severe developmental defects.

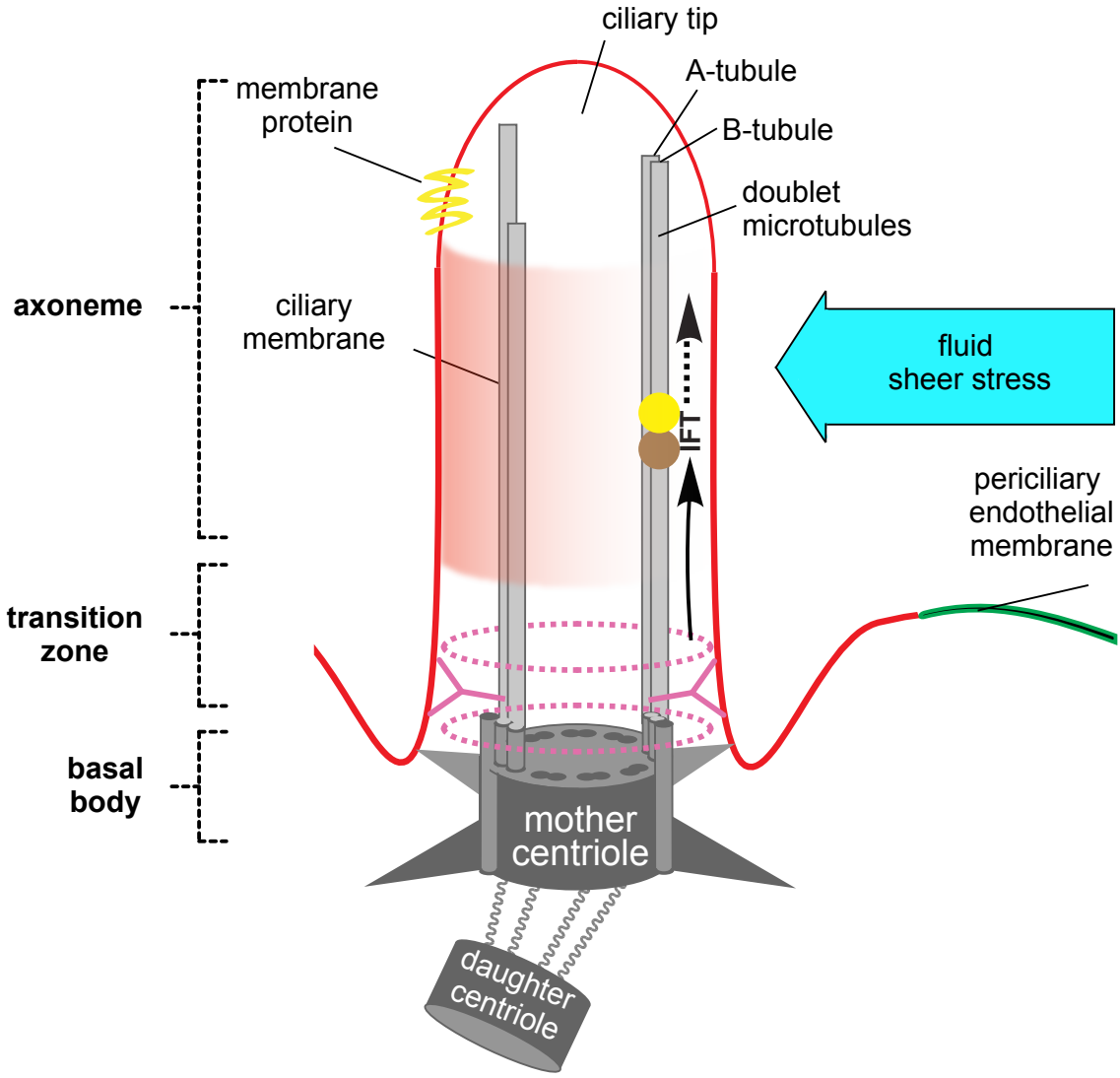

Figure 1.8 The structure and compartments of the primary cilium.
The primary cilium acts as a cellular antenna, responsible for detecting a wide range of external influences including sheer stress, pressure, and both chemical and mechanical ques. The primary cilium is anchored in the basal body by the mother and daughter centrioles from where doublet microtubules originate and grow through the transition zone to form the ciliary axoneme. Shipping of cargo up and down the ciliary microtubules is carried out by Intraflagellar transport proteins IFTs. The ciliary membrane is continuous with the cell plasma membrane, however, a selection of molecules to be displayed here takes place in the transition zone, resulting in exclusivity of expression of ciliary molecules on this membrane alone. Adapted from (Malicki and Johnson, 2016).

Once thought to be evolutionary defunct, the role of the primary cilia was recently highlighted by identification of a collection of genetic diseases where genes involved in cilia growth or function have been dysregulated or mutated. These rare recessive human disorders known as ciliopathies – complex developmental syndromes that can involve cystic kidneys, obesity, mental retardation, blindness, and various development malformations - have been shown to be caused by defects in proteins localized to cilia and ciliary basal bodies (Baker & Beales, 2009). Primary cilia are now known to play important regulatory roles in development and tissue homeostasis. Recent studies by Berbari et al. (Berbari, O'Connor, Haycraft, & Yoder, 2009) have shown that primary cilia are involved in regulating key signalling pathways during development. Primary cilia have been shown to be essential for the proper function of the Sonic Hedgehog (Shh) signalling pathway, the canonical Wnt/β-catenin signalling pathway and the PDGF signalling pathway (Christensen et al., 2007) to name a few of the best described.

The Hedgehog signalling pathway plays a fundamental role in mammalian development, and particularly in tissue morphogenesis and differentiation. As well as playing developmental roles, the Hedgehog pathway is also involved in maintaining adult stem cells and can become a driver of tumourigenesis if dysregulated. During Hedgehog signalling two of its most important proteins, Smoothened (SMO) and Patched (PTCH), have been shown to localise to the primary cilium (Jynho Kim *et al.*, 2015). Recently IFT proteins have been shown to drive this primary cilium Hedgehog signalling through responses to Hedgehog ligands that are mediated through receptors found on the primary cilium (He, Agbu and Anderson, 2016). In the absence of the Sonic Hedgehog ligand (SHH), SMO is unable to locate to the primary cilium membrane. However, when the SHH ligand is present, it binds PTCH and allows SMO translocation to the cilium and activation of the GLI transcription factors (Oro, 2007). Interestingly, Hedgehog signalling has been shown to play major roles in endothelial cell biology from regulating HUVEC survival (Zhu *et al.*, 2015), to mediating tumour associated angiogenesis and endothelial dysfunction leading to diabetic neuropathy (Chapouly *et al.*, 2016).

As with the Hedgehog pathway, the Wnt signalling pathway is highly conserved through evolution and fundamental in development through control of tissue patterning and cell differentiation lineages (Sineva and Pospelov, 2014). The Wnt signalling pathway has 3 arms: the canonical Wnt pathway, the non-canonical planar cell polarity pathway, and the non-canonical Wnt/calcium pathway. The planar cell polarity pathway has the most evidence for an interaction with primary cilia through Wnt signalling receptors like Frizzled, and other proteins

being located on the ciliary axoneme and at the ciliary base (Satir, Pedersen and Christensen, 2010).

Activation of the PDGF signalling pathway plays important roles in angiogenesis-related functions including development, wound healing and tumour angiogenesis (Bodle and Loboa, 2016). Similar to the Wnt pathway, ligands and receptor for PDGF signalling localize at the primary cilium. In fibroblasts, it has been shown that the PDGF receptor PDGFα localizes at the primary cilium during growth, and activation of this receptor stimulates downstream signalling to Akt and Mek1/2-Erk1/2 within and the cilium and at the basal body. Fibroblasts lacking the essential IFT protein IFT88 (also known as Tg737) fail to grow regular cilia and lose this PDGF signalling cascade (Schneider *et al.*, 2005).

An increasing number of developmental and homeostatic pathways are being linked to the structure and function of primary cilia. The extent of the importance of this cell organizing structure is still unclear, and further studies are likely to highlight further roles of the primary cilium, and how they may provide targets for novel therapies.

1.7.2 Endothelial cilia and their role in sensing blood flow

To date there have been no reports of endothelial cells bearing motile cilia, but primary cilia have been reported on endothelial cells in the literature for more than 40 years (Mollo, Canese, & Bartoli, 1969). Endothelial cells possess cilia that have the 9+0 microtubule bundle arrangement that extend from the basal body, and are therefore morphologically classified as primary cilia (Egorova, van der Heiden, Poelmann, & Hierck, 2012). Primary cilia found on endothelial cells are typically shorter than those on epithelial cells, in the range of 1 to 5μm, and have been described as being more embedded in the plasma membrane and within the ciliary pocket (Basten & Giles, 2013). The cilium typically protrudes from the luminal or apical side of the cell into the lumens of the vessels, although sometimes it appears to protrude from the basal side into the basement membrane and underlying extracellular matrix (Egorova et al., 2012).

Endothelial cells within the vascular network are in direct contact with blood and constantly exposed to flow. They are able to sense the frictional force exerted on the vessel walls, termed shear stress. Sensing of blood flow and pressure by endothelial cells is an important

physiological response that controls blood vessel diameter and patterning (Jones, le Noble and Eichmann, 2006; Ando and Yamamoto, 2013). The endothelial response to shear stress is necessary to maintain homeostasis of the circulatory system, while loss of the response can lead to the development of vascular diseases such as hypertension, thrombosis, aneurysms and atherosclerosis (Ando and Yamamoto, 2013). It has been shown that a sudden increase in sheer stress originating from blood flow may increase vessel diameter, while a reduction in diameter can be seen from the increased pressure within the blood vessel (Bolz *et al.*, 2000; Pyke and Tschakovsky, 2005). The exact mechanism by which endothelial cells sense flow is undetermined, but many hypotheses have been gaining experimental support, such as sensing flow through ion channels, G-proteins and their receptors; adhesion molecules, the cytoskeleton, hemodynamic drag of the nucleus caveolae; and primary cilia (Tkachenko *et al.*, 2013)(Ando and Yamamoto, 2013). These findings support the idea that endothelial cells can sense local changes in flow and pressure, and also act upon this cue by communicating a response to the surrounding mural cells to cause significant changes in vessel morphology.

Primary cilia have been identified *in vivo* on arteries and other blood vessels (Bystrevskaia, Antonov and Perov, 1987; Haust, 1987) and have been reported *in vitro* in cultured endothelial cells (Iomini *et al.*, 2004; Hierck *et al.*, 2008). Early studies have shown that endothelial cells *in vitro* can sense mechanical stimuli, such as sheer stress, through their primary cilium (Hierck *et al.*, 2008). Flow-sensing ion channels like the polycystin family (Pkd1 and Pkd2) localize to the ciliary membrane and are known to be able to mechanosense. Defects in either of these proteins leads to (ADPKD) autosomal dominant polycystic kidney disease, whereby their cells retain normal renal cilia but loss of flow recognition cause cysts to develop in the kidneys (Kotsis, Boehlke and Kuehn, 2013). These ion channels are also found on endothelial cilia (AbouAlaiwi *et al.*, 2009, 2011), and interestingly the majority of ciliopathies described to date all have a vascular phenotype. In endothelial cells isolated from mouse models which lack cilia (due to knock-out of *Ift88*, also known as *Tg737*), and from polycystic kidney mice (that retain cilia but have loss of polycystin1 and polycystin2) showed reduced or no response to fluid flow induced sheer stress *in vitro* (Nauli *et al.*, 2008). Similarly, removal of the primary cilium in MCDK cells abolishes their response to flow (Praetorius and Spring, 2003).

Very early flow sensing during vascular development, when forces are small, has also been linked with endothelial primary cilia in zebrafish (Goetz *et al.*, 2014). Studies identified primary cilia in the dorsal aorta of zebrafish bending under low levels of flow. They showed that a

number of zebrafish morphants (Zebrafish treated with a antisense oligonucleotide to temporarily knockdown a gene of interest) deficient in flow, contractile hearts, or the Pkd2 ion channel all had reduced levels of endothelial calcium signalling important for vasodilation, but also that this early hemodynamic response to flow is fundamental in downstream angiogenesis and loss of leads to defects in proper angiogenic sprouting, branching and looping (Goetz *et al.*, 2014). In another zebrafish model, loss of proper cilia response through mutant IFT proteins, increased the chances of intracranial haemorrhage which could be completely rescued by endothelial specific re-expression of the IFT genes (Kallakuri *et al.*, 2014). Interestingly, this research also linked the Hedgehog signalling pathway with vascular integrity through Hedgehog inhibition resulting in increased intracranial haemorrhage and activation rescuing of the phenotype (Kallakuri *et al.*, 2014).

1.7.3 Cilia and actin cytoskeleton

Cilia are primarily microtubule-based structures but exciting recent evidence is linking actin-related activities with ciliogenesis and cilia function. The exact mechanisms involved in actin-linked regulation and control of cilia are not well-described. In most cases and cell types, cells only ciliate while not actively proliferating. To induce ciliogenesis in cultured cells they are typically taken out of active cycling by either growth to a high confluence, serum starvation, or a combination of both. However, recent evidence also suggest that other factors like cell shape, spreading and extracellular matrix density may also have a significant influence on the cells ability to ciliate (Pitaval *et al.*, 2010). In most cases actin polymerisation has been shown to be an inhibitor of ciliogenesis, while destabilization of the actin cytoskeleton has the opposite effect and induces ciliogenesis. Controllers of actin cytoskeletal dynamics routinely show up as effectors of ciliogenesis. Large scale siRNA screens looking at genes involved in ciliogenesis have shown actin related genes to be both positive and negative regulators of ciliogenesis (Kim *et al.*, 2010; Wheway *et al.*, 2015). Actin branching and nucleation have been shown to decreases ciliogenesis, with components of the actin organizing complex, Arp2/3 which is known to control actin branching, having negative effects on ciliogenesis (Bershteyn *et al.*, 2010).

There are contradictory ideas as to how the actin cytoskeleton controls cilia formation and function, with bodies of evidence to support each. An intact and complete cytoskeletal network may be necessary for proper regulation of the shuttling of vesicles bound for the

ciliary region (basal body and the axoneme). This network of actin fibres may slow or limit the influx of vesicles in order to precisely control the growth and overall function of the cilium. This idea is supported by evidence that actin polymerisation or disassembly leads to elongated cilia and accumulation of vesicles at the base of the primary cilium (Kim *et al.*, 2010; Jongshin Kim *et al.*, 2015). Another mechanism involves the localization of disassembly factors to the base of the cilium by the actin network which may control tubulin acetylation and ultimately cilia length (Sánchez de Diego *et al.*, 2014; Malicki and Johnson, 2016). The final proposed mechanism involves activation of the transcriptional coactivator YAP/TAZ. YAP/TAZ activity is controlled through actin cytoskeleton remodelling and has been shown to control ciliogenesis (Wada *et al.*, 2011). When YAP/TAZ is concentrated in the cytoplasm ciliogenesis occurs as normal, while nuclear translocation or knockdown of YAP/TAZ suppresses ciliogenesis, possibly through HDAC6 recruitment which acts as a disassembly factor (Jongshin Kim *et al.*, 2015). Additionally, actin remodelling factors LIMK2 and TESK1 also had an effect on ciliogeneis through inhibiting vesicular trafficking to the ciliary base by controlling expression of YAP/TAZ target genes (Jongshin Kim *et al.*, 2015).

1.7.3.1 Cilia and ROCK

As described previously (section 1.2.3-5), the Rho signalling pathway has a major effect on actin dynamics and the cytoskeleton. ROCK1 and ROCK2 are two of the main downstream Rho effectors and therefore have many substrates, activation of which causes dynamic changes in actin organization.

Hyperactivation of RhoA signalling is seen in some ciliopathies. TMEM216 is a transmembrane protein that localizes to the base of primary cilia and when mutated causes a number of ciliopathies (Valente *et al.*, 2010). *TMEM216* mutant fibroblasts or knockdown results in defective ciliogenesis but also hyperactivation of RhoA signalling. Mutant cells also showed mislocalisation of actin cross linking proteins and stress fibres known to be controlled by ROCK signalling (Valente *et al.*, 2010).

Another report showed that the ciliopathy protein TMEM67, mutated as the cause for a range of human ciliopathies, plays a role in non-canonical Wnt (PCP) signalling and is required for actin cytoskeletal remodelling and Rho A activity (Dawe *et al.*, 2009). Loss of TMEM67 disrupted signalling through Wnt5a and Ror2, and resulted in non-canonical Wnt (PCP) defects

culminating in lung branching morphogenesis defects and aberrant stress fibre formation (Abdelhamed *et al.*, 2013). Lung branching and polarity defects were rescued by stimulation of Rho A signalling by calpeptin (Abdelhamed *et al.*, 2015).

It is therefore evident that a significant link between ciliogenesis and Rho signalling exists. As one of the major downstream effectors of Rho signalling, the Rho kinases (ROCK1 and ROCK2) may play important regulatory roles in many of the implicated functions of primary cilia. Intriguingly, the defects seen in stress fibre formation and localization in TMEM216-mutated patient fibroblast lines further link ROCK signalling with ciliogenesis and primary cilia function (Valente *et al.*, 2010).

1.8 Aims

The Aims of this project were to understand the detailed molecular mechanisms of vascular lumen formation and, in particular, the role of Rho GTPase signalling pathways. These have gained increasing recent prominence in the context of tubulogenesis. To provide insights into this process, I have used tissue culture and *in vivo* approaches to define the roles of Rac and ROCK signalling during vascular lumen formation. Recent work has suggested that primary cilia are involved in flow recognition and development of blood vessel lumens. I have therefore also explored links between the regulation of cilia growth by Rho GTPases and potential effects on blood vessel lumens.

1.8.1 Preliminary work leading to this thesis

Previous work by the Mavria group had identified DOCK4 as a regulator of lateral branches in a RNAi screen using the angiogenesis co-culture assay. Further work had gone on to show that DOCK4 regulates lateral tubule behaviour through its activation of Rac1, downstream of VEGF. This control of lateral behaviour was found to be through an interaction of DOCK4 with the Cdc42 GEF, DOCK9, which controlled filopodia formation. Preliminary data suggested a potential role for DOCK4 in lumen formation.

The Rho associated kinases (ROCK1 and ROCK2) modulate RhoA activity to mediate diverse effects on the actin cytoskeleton. Published work has suggested that ROCK signalling is an important mediator in a number of angiogenic processes. Development of a global ROCK2

genetic deletion mouse model prior to this study had shown that loss of ROCK2 was embryonically lethal at E13.5, and that *Rock2*$^{-/-}$ embryos at this stage exhibited extensive haemorrhaging and pooling of blood in the limb buds.

Recent published evidence has also suggested a potential role for primary cilia in endothelial cell biology and identified primary cilia within endothelial lumens. Primary cilia are already known to play roles in flow sensing and calcium signalling in other cell types, which are both important for lumen formation. A reverse genetic siRNA screen from the Johnson group and other workers has recently identified genes involved in control of the actin cytoskeleton as regulators of primary cilia formation. ROCK2 had the greatest effect on ciliogenesis from the entire whole genome screen carried out (Wheway *et al.*, 2015).

The objectives of the project were as follows:

1) Investigate the role of DOCK4 and DOCK9 in endothelial lumen formation (Chapter 3)

I performed assays in the angiogenesis co-culture model, with knockdown of DOCK4 or DOCK9 to determine the effect on lumen formation. Lumen formation at 14 days was assessed and compared with control tubules through immunoflourescent imaging and quantification.

2) Investigate the role of ROCK2 in angiogenesis and lumen formation *in vivo* (Chapter 4)

The study of ROCK2 in angiogenesis employed the use of the genetic knockout *Rock2* $^{-/-}$ mouse model available to the Mavria group. Studies using immunofluorescent and immunohistochemistry microscopy techniques assessed the effect of ROCK2 loss on *in vivo* developmental angiogenesis and subsequent lumen formation.

3) Investigate the role of ROCK signalling in endothelial cilia in blood vessels (Chapter 5)

The abundance and location of primary cilia were assessed in endothelial cells and tubules both *in vitro* and *in vivo*. The effect of ROCK signalling on cilia formation was assessed *in vitro* by pharmacological approaches, and *in vivo* by the *Rock2* $^{-/-}$ knockout mouse model.

Chapter 2

Materials and Methods

2.1 Cell culture basics

2.1.1 Plate coating

Gelatin coating for HDF on glass bottom plates: 2% [w/v] gelatin solution (Sigma Aldrich-tissue culture grade) was diluted to 0.1% with sterile PBS. Coated plates were kept at room temperature for 30 minutes and excess gelatin was rinsed off with PBS. Gelatin coated glass bottom plates were used for confocal and live imaging of co-cultures.

Collagen I coating for HEK 293T expansion after thawing from frozen. T75 tissue culture flasks were coated with filter sterilized 50μg/ml collagen-rat tail (BD Bioscience) diluted from 3μg/ml stock with 0.02M acetic acid (made from 17M stock acetic acid). 6mls was added to each flask and left for 1 hour at room temperature to solidify before being rinsed three times with sterile PBS. Plates were used immediately or stored in PBS at 4 degrees for up to 24 hours.

2.1.2 Cell lines

Angio-tested HDF (Human Dermal Fibroblast - tested to perform in the angiogenesis co-culture assay) were obtained from TCS CellWorks (Buckingham, UK). HDFs purchased at passage 8 were cultured in Dulbeccos' Modified Eagle's Medium (DMEM) with 10% [v/v] fetal calf serum (FCS, Biosera Ltd) supplemented with 100mg/ml L-glutamine and 100μg/ml penicillin/streptomycin (Sigma Aldrich). HDFs were thawed in the water bath at 37°C and cultured in plastic tissue culture T75 flasks in 15ml media. HDFs were split 1:5 when they reached 90% confluency. HDF cells were used up to passage 12 for co-culture assays.

Angiogenesis tested HUVEC (Human Umbilical Vein Endothelial Cells – tested to perform in the angiogenesis co-culture assay) were also obtained from TCS CellWorks (Buckingham, UK) and were cultured in Large Vessel Endothelial Basal Medium (LV) (TCS CellWorks) supplemented with supplied antibiotics (1000X amphotericin B/gentamycin) and growth supplements (TCS Cellworks). HUVEC were purchased at P1 before being thawed into T75 flasks with 15ml large vessel endothelial cell basal medium as per supplier instructions. After approximately 2 days, when cells reached no more than 85% confluency, they were harvested. Cells were washed once with sterile pre-warmed PBS and then coated with 1-2mls of trypsin EDTA 0.25% (Sigma Aldrich). Flasks were gently rocked and viewed down the microscope. When 90% of cells had detached from the plastic, 10mls of pre-warmed large vessel media was washed over the surface of the cell layer to collect all suspended cells. Cells were reseeded at a 1:4 ratio for expansion. HUVEC for co-cultures were used between passage 1 and 4.

HCMEC (Human cerebral microvascular endothelial cells) from ATCC were cultured in DMEM 10% FBS, 100mg/ml L-glutamine, 100μg/ml penicillin and 100μg/ml streptomycin. Cells were grown to confluency before splitting at a ratio of 1:4. HCMEC were used between passage 30-35 for primary ciliogenesis assays.

hTERT RPE-1 (immortalized human retinal pigment epithelial cells) from ATCC were cultured in DMEM 10% FBS, 100mg/ml L-glutamine, 100μg/ml penicillin and 100μg/ml streptomycin. Cells were grown to confluency before splitting before being split at a ratio of 1:5. hTERT-RPE1 cells were used for the ciliogeneis assay between passage 28-35.

HEK-293T (Human embryonic kidney cells) were cultured in DMEM 10% FBS, 100mg/ml L-glutamine, 100μg/ml penicillin and 100μg/ml streptomycin. Cells were stored at passage 4 and brought into culture in collagen I coated T75 tissue culture flasks. Cells were harvested when they reached 90% confluency and split at a 1:6 ratio onto plastic-bottomed tissue culture flasks after first split. Cell were used until passage 11.

All cells were cultured in 5% CO_2 tissue culture incubators at 37^{o}C.

2.1.3 Freezing and thawing cells

All cell stocks were stored at -196˚C in vapour stage liquid nitrogen dewars. Before use cells were stored on dry ice for transit and defrosted quickly in a 37˚C water bath before being added straight to warm media.

To prepare stocks for freezing, cells were harvested when actively proliferating at 70-80% confluency. Cells were washed once with PBS and trypsinised with 0.25% trypsin EDTA and re-suspended in 10ml culture medium. Cells were counted manually with a hemocytometer and pelleted by centrifugation in a bench top centrifuge (at 300 x g for 4 minutes, room temperature (20-22˚C)) the supernatant was discarded and the pellet was re-suspended in pre-chilled freeze medium (90% FBS, 10% DMSO) on ice. 1ml volumes containing between 0.5-1x10^6 (depending on cell type) were transferred to 1.5ml cryovials (Corning) and stored at -80˚C overnight before being transferred to LN2 (-196˚C) for long term storage.

2.1.4 Standard solutions

Standard solutions	Company	Recipe
DMEM (Dulbecco's modified Eagles medium	Sigma-Aldrich	
Freezing medium		90% FBS (Biosera Ltd) with 10% DMSO (Invitrogen)
LB (Luria broth)	Sigma-aldrich	20g LB powder in 1L distilled water. Autoclaved
LVEM (Large vessel endothelial medium)	TCS cellworks	Proprietary preparation
PBS (phosphate buffered saline)	Sigma-Aldrich	
4% [w/v] PFA (paraformaldehyde)	Sigma-Aldrich	4 grams of PFA powder in 100ml PBS (heated to 65 degrees to dissolve)
TE (Tris EDTA) buffer		1 ml of 1 M Tris-HCl (pH 8.0) and 0.2 ml EDTA (0.5 M) up to 100ml with distilled water.
TBS (Tris buffer saline, pH8)		50mM Tris, 150mM NACL
TBST (Tris buffer saline Tween)		TBS with 0.1% Tween 20 (Sigma Aldrich)
0.25% trypsin EDTA (ethylenediaminetetraacetic acid)	Sigma-Aldrich	
Transfer buffer		25mM Tris, 190mM glycine, 20% methanol
Running buffer	Invitrogen	10X solution dilutes with distilled water to 1X
5X siRNA buffer	Thermofisher Scientific	Diluted to 1X with RNAse-free sterile water (Fisher Scientific)

Rac Lysis Buffer		100mM NaCl, 50mM Tris-HCl pH7.4, 10% glycerol, 1% NP-40 5mM $MgCl_2$, EDTA-free complete protease inhibitors (Roche), 1mM DTT.
PBX		PBS with 0.1% [v/v] Triton-X 100
Mounting medium (ProLong Diamond Antifade Mountant)	Thermofisher scientific	
Bovine serum albumin (powder)		
2% [w/v] gelatin solution	Sigma-Aldrich	Diluted to 0.1% in PBS before use
HUVEC optimised medium (Angiogenesis growth medium)	TCS cellworks	
Complete PBS (solutions A and B)		Solution A: 10xPBS. 20x Solution B:18mM CaCl2, 70mM KCl, 18mM MgCl2 2740mM NaCl. Add 50mls of A and 25mls of B to 425ml sterile water to prepare 500mls. Do not refrigerate.

Table 2.1 Standard solutions used throughout this thesis

2.1.5 Bacterial cell culture

DOCK9 and DOCK4 GIPZ shRNA clones for lentiviral knockdown were purchased from Dharmacon and stored at -80°C. All GIPZ shRNA clones were cultured at 37°C in 2xLB broth (low salt) medium plus 100μg/ml ampicillin. shRNA clones were grown according to the manufacturer's protocols. In summary, bacterial stocks were defrosted and vortexed to re-suspend any *E. coli* that may have settled to the bottom of the tube. A 10μl inoculum from the glycerol stock was added to 3-5ml of 2x LB (low salt) plus 100μg/ml ampicillin at 37°C, with shaking, overnight. Overnight cultures were then added to a larger volume of 2xLB at 1:500 dilution of the starter culture. Larger volume was incubated for 18-19hrs with fresh antibiotics and vigorous shaking. Cultures were then pelleted to begin plasmid extraction.

2.1.5.1 DNA plasmid preparation

Plasmid DNA was extracted using an "Invitrogen Purelink Midiprep kit". 0.2-1 μg of the plasmid DNA can be run on a 1% agarose gel. pGIPZ with shRNA is 11774 bp in size. Plasmids were used to prepare lentiviral vectors for shRNA mediated knockdown (3.2.3).

2.1.5.2 DOCK4/9 shRNA sequences

shRNA constructs were from Dharmachon GE life sciences and were used to make lentiviral vectors for DOCK9 knockdown.

DOCK9 shRNA3 (V3LHS_306026) mature antisense "AACAAACAAGCTCTGTGCT"

DOCK9 shRNA4 (V3LHS_306027) mature antisense "TACTTGAGTTGTCACAGCT"

DOCK4 shRNA1 mature antisense "CTCAGTATTTGCAGATATA"

DOCK4 shRNA2 mature antisense "CGCAAGGTCTCTCAGTTAT"

2.2 Cell culture techniques

2.2.1 Production of Lentiviral Vectors in 293T cells

Virus production was according to Tronolab protocols. On day 1 (5pm) $2.5x10^6$ HEK 293T cells were plated in a 10cm plate. On day 2 (5pm) calcium-phosphate precipitate was prepared (1ml/10cm plate) (transfer vector 20μg, packaging plasmid 15μg, Envelope plasmid 6μg) vectors were added to 0.5ml of ddH_2O and 50μgl 2.5M $CaCl_2$ before adding 0.5mls 2xHBS drop by drop to the solution while under vortex agitation. The precipitate was left for 20 minutes at room temperature then added dropwise to plates. The plates were mixed gently by tilting plate from side to side. On day 3 (9-10am) media is discarded and replaced with fresh warm medium. On day 3 (5pm) Media was collected and replaced with fresh as before. Collected media was filtered through a .45μm filter and stored at 4 ^oC before aliquoting in 2ml aliquots and storing at -80 ^oC for long term storage. On day 4 (9-10am) collection step was repeated and fresh media added. On day 4 (5pm) final media was collected, filtered and stored as before. Plates were discarded.

2.2.2 Virus titre assay

Medium containing viral vectors from lentiviral production was collected and used for viral titre assays. $7x10^4$ HEK293T were seeded in 24 well plates and used to titre virus. Virus was added neat and in serial dilutions of 1:5, 1:10 and 1:50 in DMEM with 8μg/μl polybrene for 6 hours or overnight. Virus was replaced with fresh DMEM supplemented with 10% FBS and

grown for 48 hours before expression of GFP was assessed on the EVOS fluorescent microscope. The level of knockdown was assessed by western blotting for proteins of interest (section 3.5.1).

2.2.3 HUVEC lentiviral transduction

$5x10^5$ HUVEC were seeded into T75 tissue culture dishes for transduction. Virus was added in the pre-determined dilution for the viral titre (section 3.2.3) diluted in human large vessel endothelial cell medium with 8μg/μl polybrene for 6 hours or overnight. Expression was assessed with GFP expression on the EVOS microscope and by western blotting for proteins of interest.

2.2.4 HUVEC cell sorting via FACS sort

Transduced HUVEC were trypsinised and collected for fluorescent activated cell sorting. $1x10^6$ cell/ml were collected in LV medium and transferred to polystyrene cell sorter tubes for sorting. The LIMM Cell Sorting Facility sorted the cells based on pre-determined gates based on the level of expression of GFP and knockdown efficiency. Sorted HUVEC were placed back in culture for 24 hours or used directly for experimentation.

2.2.5 HUVEC-HDF coculture assay

$2x10^4$ HDFs at passage 8-11 were plated on plastic or gelatin-coated glass-bottom 24 well plates and cultured for 7 days without medium change until grown to a confluent layer. $1x10^4$ HUVEC were then seeded onto the confluent layer of HDFs and cultured for either 5 days for sprouting assay or 14-16 days for the lumen assay. HDF-HUVEC culture were maintained in 50:50 medium (LV:DMEM) until day 7 before being changed to optimized medium to aid in lumen formation. Media was refreshed every 2 days. Co-cultures were performed with HUVEC that had proteins of interest knocked down via siRNA or shRNA methods (sections 3.1.4, 3.2.4). 5-day assays were washed once with PBS and then fixed in ice cold 70% ethanol for 20 minutes for IHC staining or 4% PFA for immunoflourescent staining.

Angio-tested HDFs at passage 8-11 were plated on gelatin-coated, 24 well, glass bottom plates, at $2x10^4$ cells/well and allowed to grow in DMEM 10% FBS for 7 days without media change. Angiotested HUVEC were then seeded onto confluent HDFs at a density of $1x10^4$ cells/well in 50:50 media (50%DMEM 10%FBS, 50% Large vessel media + supplements + antibiotics). After 7 days, the culture media were changed to 'Optimised' media (TCS Cellworks) and changed

every two days until day 14-16. Cultures were then fixed in 4% PFA for 20 minutes at room temperature and stored in sterile complete PBS at 4°C. Cultures were stained by immunofluorescence for analysis.

2.2.6 In-vitro ciliogenesis assay

Cells to be studied in the ciliogenesis assays were grown on glass cover slips for imaging in 24 well tissue culture plastic plates. Cover slips were sterilized in 70% ethanol before three washes in sterile PBS. Cells were seeded at 70% confluency on cover slips and let grown for 24 hours in 10% DMEM. Cells were then serum starved in 0.2% FBS DMEM for 48hours before fixing with 4% PFA. Inhibitor treatments were added during the 48hours serum starvation period.

2.2.7 Apical membrane initiation site assay (AMIS assay)

HUVEC were seeded on glass cover slips at 60% confluency for the apical domain assay (AMIS). Cells were allowed to adhere for 25 minutes in the incubator before being fixed for immunoflourescent imaging.

2.3 Imaging techniques

2.3.1 Embryo fixation and staining (immunofluorescence)

Embryos were harvested at E12.5 and E13.5 for analysis. E12.5 and E13.5 embryos were fixed in 4% PFA at room temperature for 30 minutes and 4oC for one hour. They were permeabilised in PBS/0.1% Triton X-100 (PBX) for 30 minutes at room temperature before being blocked overnight in 5% BSA/PBX at 4°C. Primary antibodies were incubated overnight at 4°C in 5%BSA/PBX. Embryos were washed 3 x 30 minutes in 1% BSA-PBX at room temperature. Secondary antibody was incubated in 5% BSA-PBX at room temperature for 2 hours. Embryos were washed 3x30 minutes in 1% BSA-PBX at room temperature and incubated with DAPI (1:2000) in final wash. A total of four embryos per embryonic day were analysed with 5 fields per embryo quantified for characterisation studies.

2.3.2 Co-culture fixation and immunofluorescence staining

Co-cultures were washed once with complete PBS and fixed in 4% PFA for 20 minutes at room temperature. Cultures are then washed twice with complete PBS and stored in complete PBS. Cultures were permeabilised in PBX (PBS 0.1% Triton-X 100) for 20 minutes at room

temperature before being blocked in PBX 1% BSA for 20 minutes at room temperature and stored in PBS.

All primary antibodies were incubated in PBX 1% BSA at 4^{o}C overnight. Cultures where washed 3x30 minutes in PBX 1% BSA. Primary antibody dilutions are listed in Table 1.x. Secondary antibodies were incubated for 2 hours at room temp in PBX 1% BSA before washing in in PBX 1% BSA 3x30 minutes. DAPI was added in the final was at a dilution of 1:2000. For phalloidin staining, cultures were incubated for 1 hour at room temperature in PBX 1% BSA at a 1:200 dilution.

2.3.3 Cilia assay fixation and staining

Ciliogenesis assays were carried out using glass cover slips in 24 well dishes. Cover slips were washed once with PBS and fixed in 4%PFA for 15 minutes at room temperature. Monolayers were permeabilised in PBX (PBS 0.1% Triton-X100) for 20 minutes before blocking in PBX 1% BSA for 20 minutes all at room temperature. Cover slips were then stained with primary antibodies for 1 hour at room temperature in PBX 1%BSA before 3x5 minutes washes in PBX. They were then stained for secondary antibodies in PBX 1% BSA for 1 hour at room temperature before 3x5 minutes washes. DAPI nuclear marker was added in the final wash.

2.3.4 AMIS assay fixation and staining

AMIS assays were fixed and stained as above, section (2.3.3)

2.3.5 Immunohistochemistry staining

Co-cultures were washed once with PBS and fixed in 70% Ethanol for 20 minutes at room temperature. Cultures were stained using a commercially available kit from TCS Cellworks (Caltag Med systems) based on binding of an alkaline phosphatase-coupled anti-CD31 antibody linked to an insoluble chromogenic substrate that stains the fixed tubules *in situ*.

2.3.5.1 Embryo immunohistochemistry

Embryos at E13.5 were delivered to the pathology department after genotyping. Embryos were embedded in paraffin blocks and sectioned prior to staining.

2.3.6 Confocal imaging

All confocal imaging was carried out on a Nikon A1R-A1 Confocal Microscope system with Nikon “Elements” software.

2.3.6.1 HUVEC-HDF Co-culture imaging

Co-culture imaging was carried out using an oil immersion x60, x40, or x20 or x10 lenses, and galvano scanning head. Z-stack imaging was used to generate 3D images for analysis. Z-stacks of 15 μm in total thickness were acquired with stacks every 1.0 μm at 1024px resolution. ND2 z-stack image were acquired and used for analysis.

2.3.6.2 Wholemount angiozone embryo imaging

Imaging of E12.5 and E13.5 embryos were taken using a x40 oil immersion lens and a galvano scanner head. Z-stack images were used to generate 3D images and acquired in the angiozone. Z-stacks of 15-30 μm in total thickness were acquired with stacks every 1.0 μm at 1024px resolution.

2.3.6.3 Cilia imaging

Monolayers of ciliated cells were imaged using x20 or x40 (oil immersion) lenses and a galvano scanner head. Z-stacks of 5μm total thickness were acquired with stacks every 0.5μm at 1024px resolution.

2.3.6.4 AMIS imaging

Spreading cells were imaged using x20 or x40 (oil immersion) lenses and a galvano scanner head. Z-stacks of 5μm total thickness were acquired with stacks every 0.5μm at 1024px resolution and used for quantification.

2.3.7 Bright field imaging of Immunohistochemistry stained sections

Phase contrast images of tube formation in the organotypic sprouting assay was acquired using a Nikon light microscope (x4 and x10 images) or an Olympus CKX41 inverted microscope (x40 objective).

Lumen and cilia measurements in the embryo immunohistochemistry sections were carried out using a Nikon Axiovision brightfield microscope (x4, x16, x40 and x100 lenses). Full method is described in sections 3.4.5 and 3.4.6.

2.3.8 Live imaging

Low magnification, long term, time lapse imaging was carried out using a Incucyte Zoom live imaging system. Images of co-culture were taken every 2 hours in phase and GFP channels and combined to make time lapse movies using the Incucyte Zoom software.

High magnification live cell imaging of eGFP-expressing cells and tissues was performed on a Nikon A1R-A1 Confocal Microscope system with a heated chamber and $C0_2$ supply.

Incucyte proliferation assays were performed by seeding GFP expressing HUVEC (Non-S, DOCK9 shRNA 3 and 4) in 24 well plates at 20-30% confluency in triplicate. Cells were imaged in phase and GFP channels at x10 magnification and the increase in confluency was calculated using the Incucyte Zoom software.

2.3.9 Phalloidin staining of cells

Cells to be stained for F-actin visualisation were incubated in a 1:200 dilution of Alexa Fluor 633 phalloidin in PBX (PBS 0.1% Triton-X 100) for 1 hour at room temperature. Wells were washed 3 times with PBX and used for imaging immediately.

Antibody	**Species**	**Supplier**	**Dilution**
CD31 (PECAM1) Sc 31045	Goat	Santa Cruz	1:100
VE-cadherin Sc-6458	Goat	Santa Cruz	1:100
h-Podocalyxin Af-1658	Goat	R + D systems	1:200
Endomucin Sc-65495	Rat	Santa Cruz	1:100
Podocalyxin (mouse AF1556	Goat	R + D systems	1:100
Collagen IV Ab 6586	Rabbit	Abcam	1:200
ARL13B 17711-1-AP	Rabbit	Proteintech	1:1000
DOCK9	Rabbit	Proteintech	1:50
Focal adhesion kinase (FAK) ab40794	Goat	Abcam	1:200

Table 2.2 List of primary antibodies used for immunofluorescence

Antibody	Species	Supplier	Dilution
Alexa Fluor 488	Donkey anti rat IgG	Invitrogen	1:1000
Alexa Fluor 488	Donkey anti rabbit IgG	Invitrogen	1:1000
Alexa Fluor 594	Goat anti rabbit	Invitrogen	1:1000
Alexa Fluor 594	Donkey anti rat	Invitrogen	1:1000
Alexa Fluor 594	Donkey anti goat	Invitrogen	1:1000
Alexa Fluor 633	Goat Anti rabbit	Invitrogen	1:1000
Alexa Fluor 647	Donkey anti goat	Invitrogen	1:1000
DAPI		Sigma-Aldrich	1:2000
Alexa Fluor 633 Phalloidin		Invitrogen	1:200

Table 2.3 List of secondary antibodies used for immunofluorescence

2.4 Image analysis

All immunoflourescent image analysis was carried out using Volocity analysis software (Perkin Elmer). Confocal Z stack rendering of images (Nikon ND2) was carried out using Volocity 3D analysis software version 6.2. "xyz" imaging mode was used to quantify embryo, cilia and co-culture z-stacks. 3D opacity imaging mode was used to view 3D reconstructions of Z stacks.

2.4.1 HUVEC-HDF Co-culture lumen measure

Co-culture assay lumens were measured in "xyz" mode while scrolling through multiple plains of generated z-stacks (15μm deep). The line drawing tool was used to quantify length of lumens vs length of total tubules. Tubules less than 150μm in length, considered to be "growing tips" were not measured in lumen quantifications. Lumenised lengths were compared with total length of tubule within entire Z-stack image to get percentage lumenised length values.

2.4.2 HUVEC-HDF nuclei per length counts

Nuclei per length measures were carried out on z-stack sections from lumen measures above using velocity imaging software. Total length of tubule was measured and intact nuclei along the total length was counted.

2.4.3 Cilia analysis (ciliogenesis assay)

Monolayers of cilia were imaged at x20 and x40 times, and multiple planes taken to generate a Z-stack reconstruction. Image analysis was carried out with the line measuring and counting tool in Volocity software. All cilia within the x20 images were counted and cilia length measured and compared between treatments.

2.4.4 Lumen and filopodia measuring via immunofluorescence (Embryo analysis)

Images of E12.5 and E13.5 embryo "angiozone" at x40 magnification were taken and used to create 3D Z-stack images for analysis (15-30μm deep). Filopodia were measured in z-stack images by scrolling through each Z-stack and counting filopodia on all vessels. Lumens were measured using the line drawing and measuring tool. Podocalyxin staining and presence of circulating blood cells were used to quantify total lumen percentage and measured against total vessel length. Tip cells were counted as cells with a single nucleus, sprouting from a vessel wall, with abundant filopodia.

2.4.5 Cilia count in the embryo immunohistochemistry sections

Transverse sections at the level of the interventricular foramen of Monro were taken for analysis of blood vessel cilia. Cilia were counted as (red) staining for ARL13B within the blood vessels stained for endomucin (brown). Counts were done using the manual count tool in the Axiovision software from images taken at x100 magnification. All lumenised vessels within the parenchyma were imaged and cilia counted.

2.4.6 Lumen measure in the embryo immunohistochemistry sections

Transverse sections at the level of the interventricular foramen of Monro were taken for analysis of blood vessel lumens. Lumens were identified by endomucin staining and radius measured manually using Axiovision software circle tool at x40 and x100 magnification. All lumens within the parenchymal tissue were measured for each section.

2.5 Biochemical techniques

2.5.1 Western blotting analysis

2.5.1.1 Protein quantification by BCA protein assay

Proteins were quantified by the BCA (bicinchoninic acid) method (Smith *et al.*, 1985). This method combines the biuret reaction with the violet-coloured complex formation of copper ions by bicinchoninic acid. A standard curve of BSA ranging from 25μg – 2mg of protein was prepared and used to quantify unknown samples. Protein standards and unknown samples were pipetted in triplicate into a 96 well plate. BCA reagent was added to each well and allowed to react for 30 minutes at 37^{o}C. Protein concentration was then measured on a spectrophotometer at 562nm wavelength and was calculated on Microsoft Excel.

2.5.1.2 SDS-PAGE

To identify proteins of interest quantified protein samples were analysed using Sodium Dodecyl Sulphate Polyacrylamide Gel Electrophoresis (SDS-PAGE). Quantified proteins (3.5.1.1) were resuspended in 4X loading buffer (NuPage, Invitrogen) with 50mM DTT and heated at 70 ^{o}C for 10 minutes before loading. To identify proteins of larger than 100kDa, 3-8% precast acrylamide gels were used (Invitrogen). Electrophoresis was performed at 150V for 1.5 hours in 1X Tris-Acetate SDS Running Buffer (NuPAGE) with added NuPAGE antioxidant (1:500 NuPage, Invitrogen). 5-10μl of protein standard ladder (Dual colour marker, Biorad 10-250kDa) was loaded to compare proteins.

2.5.1.3 Western blotting and detection

After completion of SDS-PAGE electrophoresis the gels were transferred to 50ml of transfer buffer for equilibration. Gels were then transferred to PVDF membrane (pre-activated in methanol for 10 seconds) and sandwiched between 4 sheets of Whatman paper and 4 sponges. The sandwich was then placed in a transfer rig prefilled with 1x transfer buffer (3.1.4). Transfer was at 1A for 2hours at 4^{o}C or 0.1A at 4^{o}C overnight.

Enhanced chemiluminescence (ECL) methods were used to visualize membranes. Membranes were first blocked in 5% milk powder in TBS for 1hour at room temperature. Primary antibody was added in TBST 1% BSA overnight at 4^{o}C. After three 5 minute washes in TBST, at room temperature, secondary antibody (horseradish peroxidase enzyme conjugated) was added in 5% milk powder for 2 hours at room temp. Primary and secondary antibodies are listed in table 2.4. Membranes were then given three 5 minute washes in TBST before adding ECL solution

(Amersham ECL solutions A and B, 1:1 ratio) for 1 minute at room temperature. Membranes were exposed on X-ray film (Amersham Hyperfilm) and band intensities analysed using Image J software.

2.5.1.4 Stripping and reprobing

PVDF membranes were stripped and reprobed for a different antibody or loading controls. To strip membranes, they were washed in ultrapure water for 10 minutes at room temp, then 0.5M sodium hydroxide for 10 minutes and finally ultrapure water for 10 minutes. Membranes were then re-blocked in 5% milk powder and probed with primary antibodies.

Primary antibody	**Company**	**Dilution/ concentration**
Rabbit DOCK9 A300-531A	Bethyl	1:1000
Mouse DOCK4 Ab 85723	Abcam	1:1000
Mouse anti GAPDH	Sigma -Aldrich	1:1000
Rabbit anti GAPDH	Abcam	1:1000
Goat anti VE-cadherin sc-6458	Santa Cruz	1:1000
Secondary antibody	**Company**	**Dilution/ concentration**
Sheep Anti-mouse IgG HRP	Amersham	1:10000
Donkey Anti-Rabbit IgG HRP	Amersham	1:10000
Donkey Anti-Goat HRP	Abcam	1:10000

Table 2.4 List of antibodies used in this thesis for immunoblot assays

2.6 Statistical methods

Normal distribution of data was assessed before parametric test were carried out. Statistical significance was determined using the two tailed student T-test on Microsoft Excel assuming a two-tailed distribution with unequal variance between sample means. All error bars in primary data represent S.E.M. for 3 or more biological replicates.

Chapter 3

Rac GEF DOCK4 and Cdc42 GEF DOCK9 Control Tubule Lumen Formation

3.1 Introduction

Blood vessel growth from pre-existing vessels largely takes place through the process of sprouting angiogenesis. During sprouting angiogenesis tip cells sprout from a vessel wall and migrate towards growth factors and other cells in the surrounding microenvironment. Tip cells have abundant actin-rich filopodial protrusions that sense the extracellular environment and allow response to directional ques. The actin cytoskeleton controls several fundamental endothelial cell functions during angiogenesis; including migration, spreading and cell division. Cell motility and intricate changes in cell shape are particularly important during sprouting and also during the later stages of alignment, elongation and lumen formation. The Rho family of small GTPases cycle between active, GTP-bound forms and inactive, GDP-bound forms to transmit signals from growth factors receptors, and are known to play major roles in controlling and modulating the actin cytoskeleton (Hall, 1998). Guanine nucleotide exchange factors, or GEFs, catalyse the exchange of GDP for GTP thus activating the GTPases, while GTPase activating proteins, or GAPs, increase the intrinsic hydrolysis rate of the GTPase thus inactivating it (Kather and Kroll, 2013). In previous work, described in "Preliminary work leading to this thesis", it had been shown that knockdown of the Rac1 GEF DOCK4 in endothelial cells led to disruption of VEGF-driven filopodia in developing tubules in an organotypic angiogenesis assay, and that VEGF stimulated formation of a complex between DOCK4 and the Cdc42 GEF DOCK9. DOCK9 knockdown blocked filopodia formation. Preliminary work had also shown that DOCK4 knockdown may impact on lumen formation in the assay. This Chapter aims to further investigate the role of DOCK4 and DOCK9 in lumen formation, and assess how cytoskeletal changes early in tubule morphogenesis can affect later stages of lumen formation.

3.2 Optimisation of the organotypic coculture assay to model angiogenesis in vitro

To study the roles of DOCK4 and DOCK9 in angiogenesis, we used an in vitro co-culture model that recapitulates distinct stages of tubule formation. This model involves the coculture of human dermal fibroblasts (HDF) with primary human umbilical vein endothelial cells (HUVEC); endothelial cells are seeded onto a confluent layer of HDF that have grown for seven days (Figure 3.1). The HDF produce a natural 3D environment including matrix and growth factors that enables the development of capillary-like tubules as shown in Figure 3.2 and reported previously (Bishop et al., 1999; Donovan et al., 2001; Mavria et al, 2006). HUVEC may be marked with EGFP by means of lentiviral transduction followed by FACS sorting (Mavria et al

2006; Hetheridge et al, 2011), so that different stages of tubule morphogenesis can be monitored by live cell imaging or by timelapse microscopy (Figure 3.3). At the start of the project, the number of cells was varied for optimal tubule formation which was seen with $1x10^4$ HUVEC and $2.0x10^4$ HDF (Figure 3.2), and therefore these cell numbers were used in subsequent experiments.

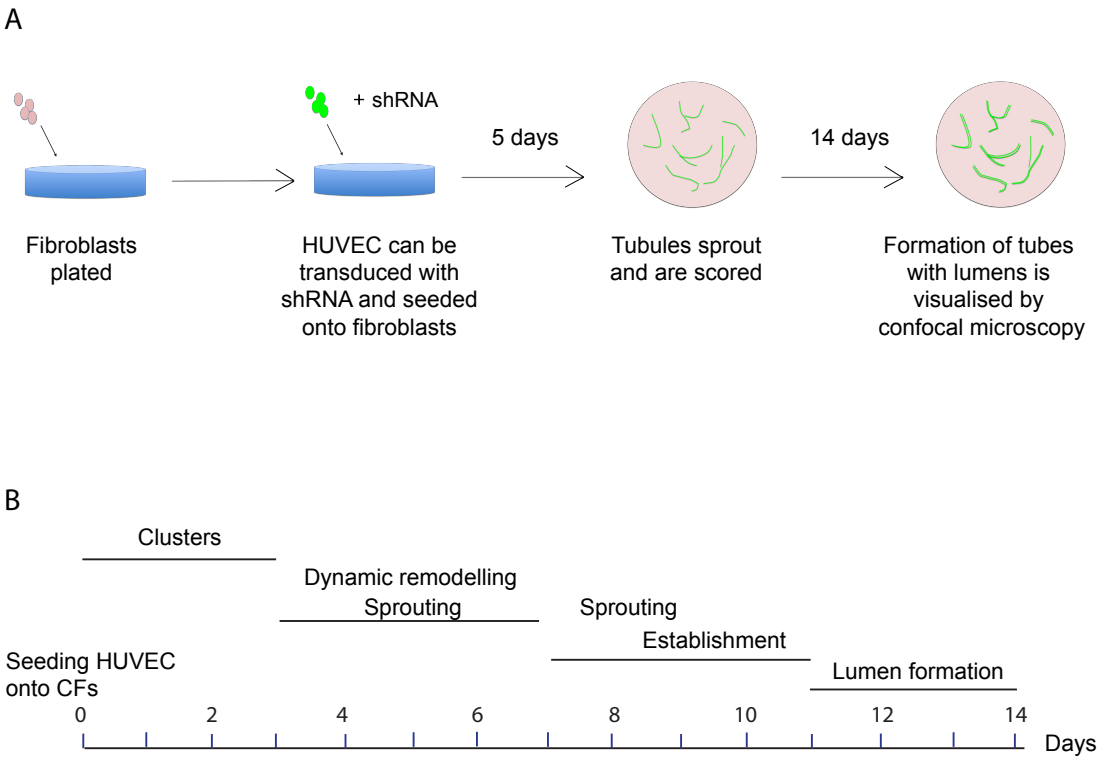

Figure 3.1 Organotypic angiogenesis assay and overview of stages leading to tube formation
(A) Coculture assay setup schematic. $2x10^4$ fibroblasts are plated and let grow to confluence for seven days after which time $1x10^4$ HUVEC, unmodified, marked with EGFP, or transduced with lentiviruses harbouring shRNAs and EGFP are seeded onto the fibroblasts. (B) Stages of tubule formation observed in the coculture Sprouting tubules can be observed 5 days after seeding and quiescent tubules at 11 days (Abraham et al, 2009). The cocultures are analysed for lumen formation 14 days after seeding of HUVEC onto the fibroblasts.

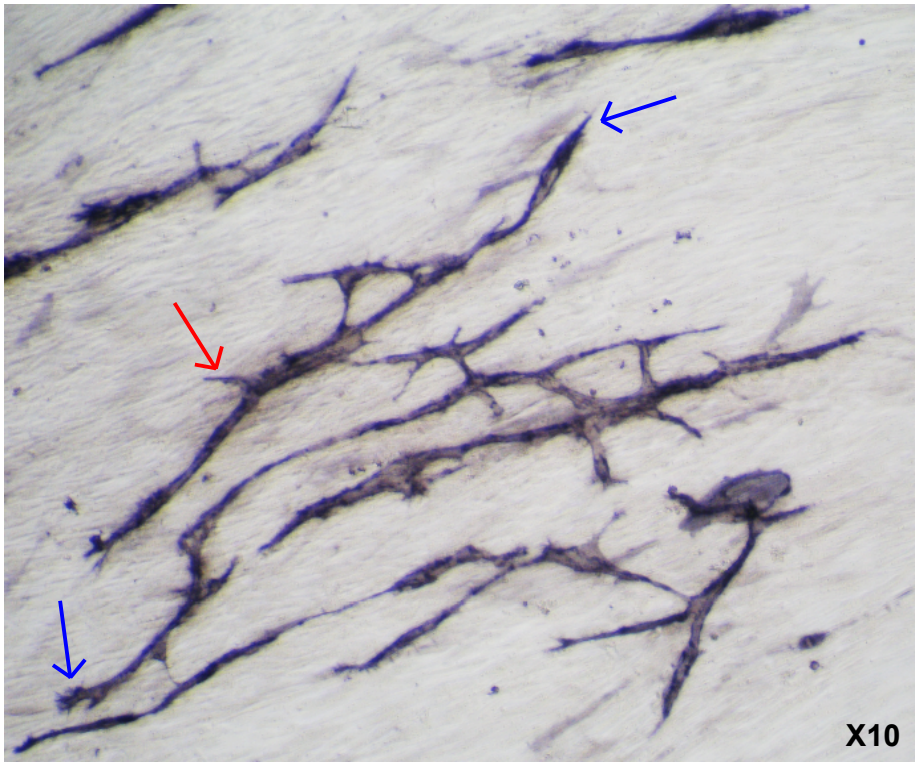

Figure 3.2 Tubule growth in the HUVEC-HDF coculture assay at 5 days
$2x10^4$ fibroblasts were plated and let grow to confluence for seven days after which time $1x10^4$ HUVEC were seeded and let grow for 5 days after which they were fixed with 4% PFA. Cultures were stained using IHC for the endothelial marker CD31 to visualise developing tubules (chapter 2 section 2.3.5). Arrows point to tip cells (blue) and developing sprouts (red). Magnification X10.

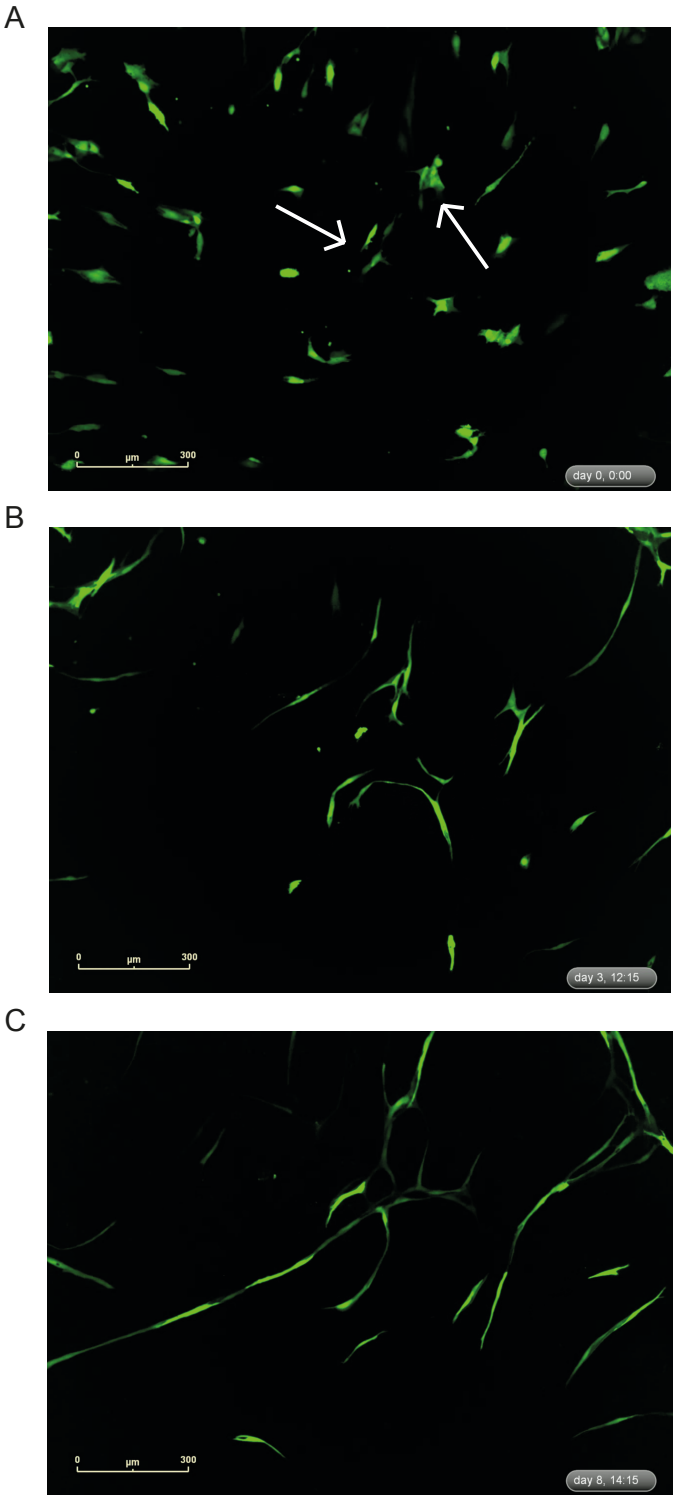

Figure 3.3 Still images from time-lapse movies depicting stages of tubule growth
$2x10^4$ fibroblasts are plated and let grow to confluence for seven days after which time $1x10^4$ EGFP-HUVEC are seeded and imaged using the Incucyte live cell imaging system. GFP images were taken every 2 hours for 14 days. Shown are still images at day 0 (A), day 2 (B), and day 8 (C). Arrows indicate cells moving towards each other into clusters. Scale bar = 350µm.

3.3 Analysis of lumen formation in the coculture assay

As HUVEC develop tubules in the coculture assay, they go through distinct stages of morphogenesis. Early after seeding, HUVEC may aggregate into clusters (Figure 3.3A), while single cells start to migrate along the fibroblast tracts towards other HUVEC (Hetheridge, Mavria and Mellor, 2011). Clusters form (Figure 3.3B) and being to remodel dynamically and sprout for approximately 8 days (Figure 3.3C) by which stage they are still immature and do not form lumens. In order to form lumens, stalk endothelial cells behind the leading tip cell must downregulate their response to angiogenic growth factors and establish lateral cell-cell adhesions (Strilić *et al.*, 2010; Blanco and Gerhardt, 2013; Hayashi *et al.*, 2013). To promote the development of lumens in the coculture assay media were changed at day 7 to optimised media that contain a lower concentration of growth factors (personal communication; Tim Almond TCS Cell Works) and the tubules were monitored up to 18 days after seeding onto confluent fibroblasts. High power confocal imaging on day 11 show that the endothelial cells take on an elongated shape and align next to each other in elaborate branched networks (Figure 3.4) while lumens start to form at sites of opposing cell-cell adhesion (Figure 3.4). Moreover, the cells are joined by mature adherens junctions (Figure 3.5) as shown by continuous distribution of vascular endothelial (VE) cadherin (Abraham et al., 2009). Formation of an apical membrane was also observed at this stage, marked by expression of the apical marker podocalyxin, which later localises at the apical surface of a developed lumen (Strilić *et al.*, 2009). By observing the tubules at different stages beyond day 11, it was determined that 14 day-old cocultures show the greatest abundance of lumens as marked by apical podocalyxin localisation (Figure 3.6), and therefore the assays were routinely taken to this stage. For quantification, tubules showing apical podocalyxin staining were compared with total tubule length, and around 40% of tubules were lumenised in the assay at day 14.

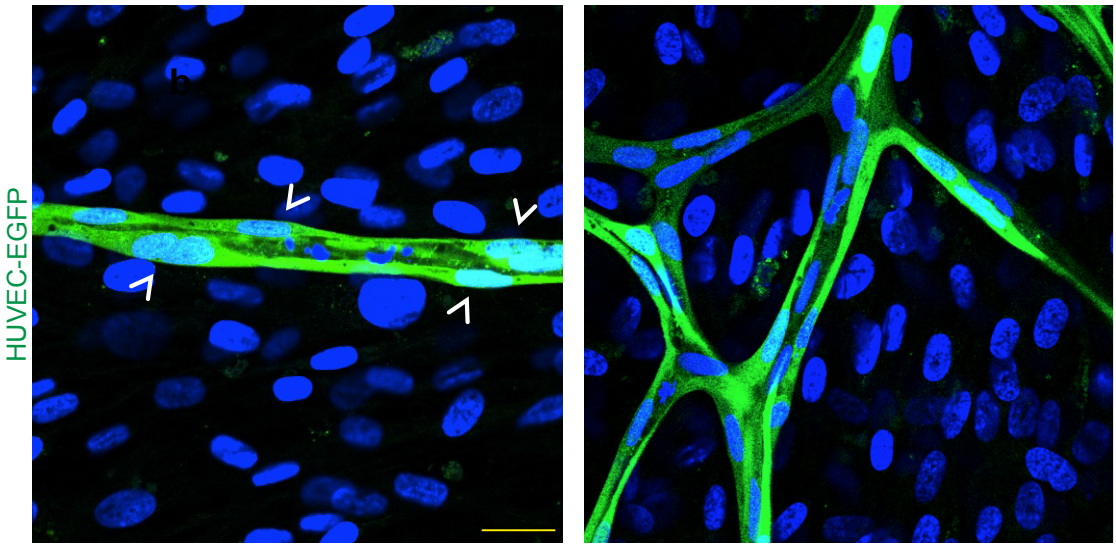

Figure 3.4 Onset of lumen formation in mature tubules in the coculture assay
$2x10^4$ fibroblasts are plated and let grow to confluence for seven days after which time $1x10^4$ EGFP-HUVEC are seeded onto the fibroblasts. The cocultures were fixed on day 11, nuclei were marked with DAPI (blue) and tubules were imaged using confocal microscopy. White arrowheads point to elongated and juxtaposed endothelial cells lining the developing lumens. x40 confocal images with oil-immersion lens. Scale bar 50μm.

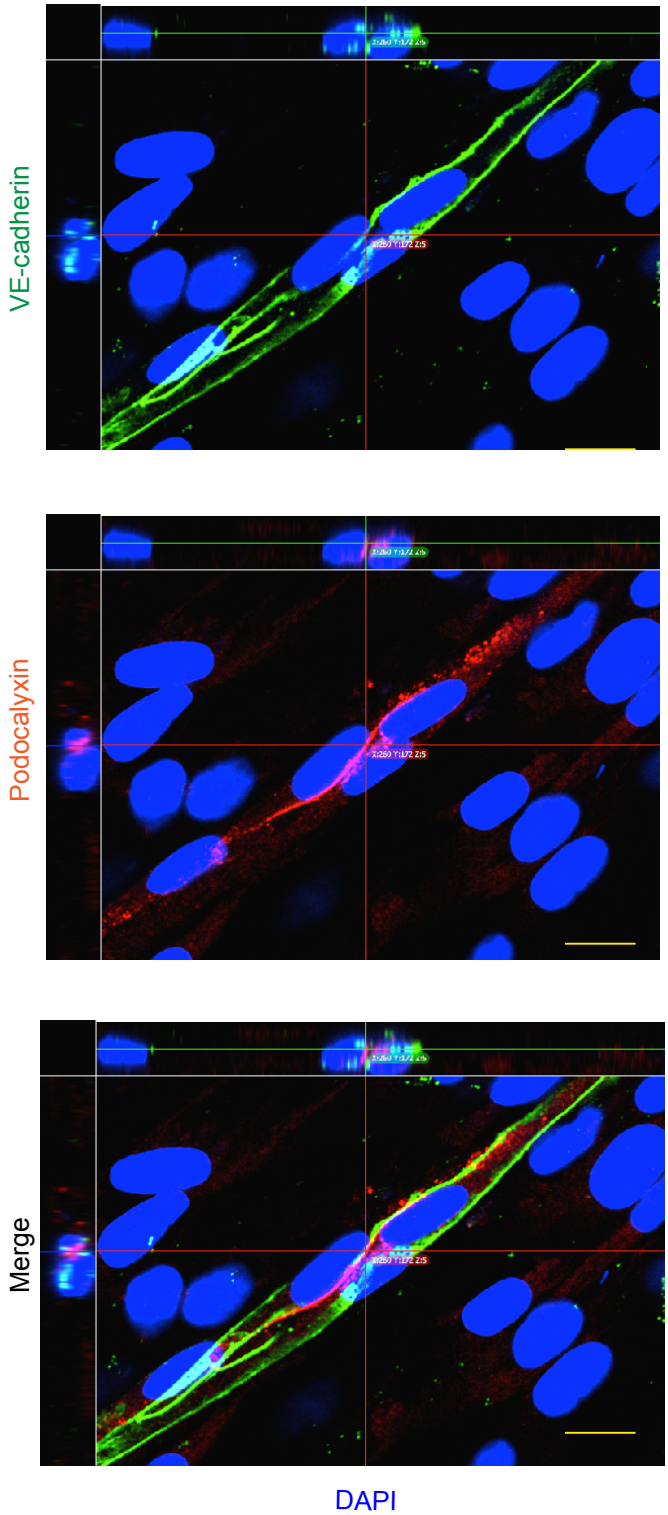

Figure 3.5 VE-cadherin and podocalyxin localization in mature tubules in the coculture assay
$2x10^4$ fibroblasts are plated and let grow to confluence for seven days after which time $1x10^4$ HUVEC are seeded onto the fibroblasts. The cocultures were fixed on day 11, nuclei were marked with DAPI (blue) and tubules were imaged using confocal microscopy. Adherens junctions were marked with VE-cadherin (green), apical membrane with podocalyxin (red) and nuclei with DAPI (blue). The tubules were imaged by confocal microscopy. Note the displacement of VE-cadherin at the site of lumen formation and the staining of the site of displacement with podocalyxin. Scale bar = 15 µm.

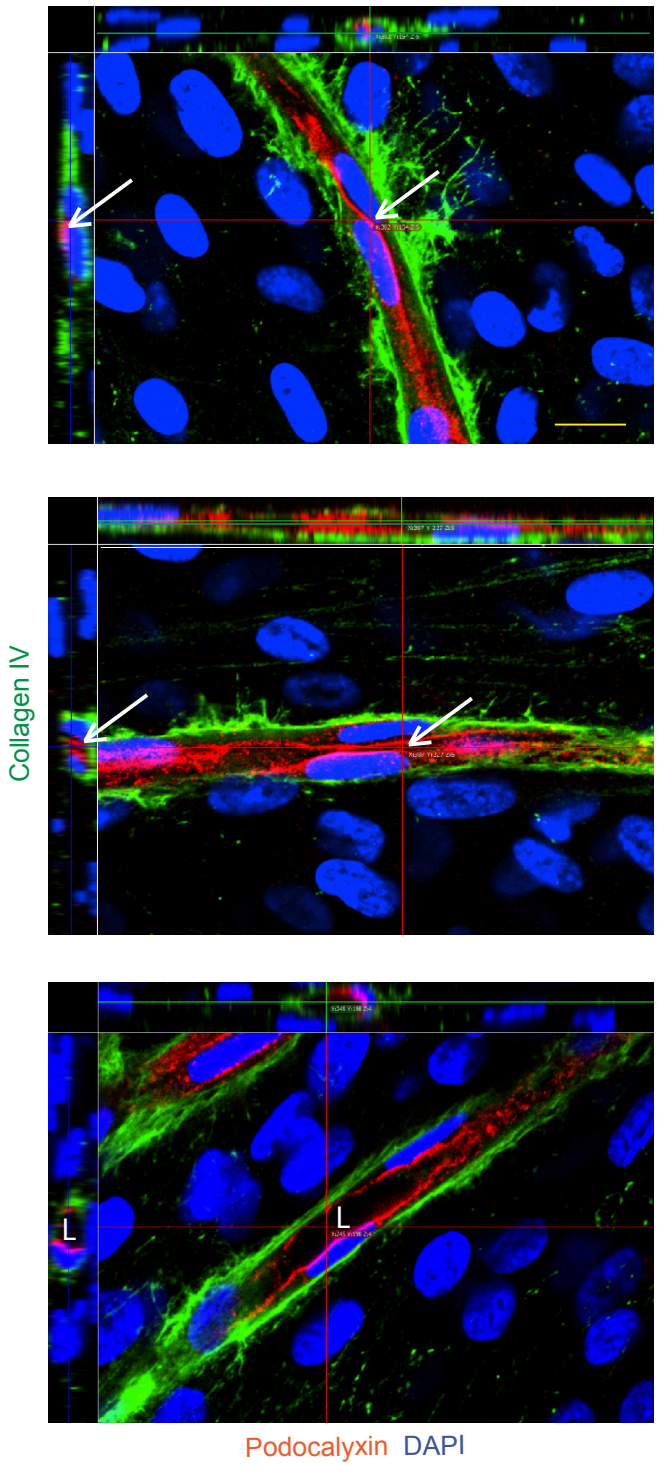

Figure 3.6 Lumen formation in the coculture assay
$2x10^4$ fibroblasts are plated and let grow to confluence for seven days after which time $1x10^4$ HUVEC are seeded onto the fibroblasts. The cocultures were fixed on day 14, nuclei were marked with DAPI (blue) and tubules were imaged using confocal microscopy. Three stages of lumen opening can be seen using podocalyxin staining (red). Apical localization of podocalyxin can be seen between elongated endothelial cells; collagen IV marks basement membrane (green). Arrows point to apical podocalyxin and opening leading to formation of the lumen (L). Scale bar 15µm.

3.4 DOCK4 is necessary for lumen formation in the coculture assay

In order to assess the role of DOCK4 in lumen formation, primary HUVEC were transduced with lentiviruses harbouring DOCK4 shRNAs. This is because, unlike siRNA knockdown which is transient, lentiviral shRNAs achieve long-term, stable knockdown. This is required in order to assess the degree of lumen formation at 14 days after seeding HUVEC onto the fibroblasts. In addition to shRNAs the lentiviruses also express EGFP, which allows FACS sorting of transduced cells for live cell imaging. Initial experiments therefore assessed the degree of correlation between the level of EGFP expression and knockdown efficiency. Cells expressing high and low EGFP levels were sorted, and the level of knockdown in those populations was determined by western blotting. Analysis showed that higher levels of knockdown occurred in cells expressing higher EGFP levels, compared to cells expressing lower EGFP levels. Two different shRNAs that target different sequences within the same gene are routinely used in experiments to eliminate the possibility that the observed phenotypes are due to off-target effects. Accordingly, HUVEC were transduced with two different lentiviral DOCK4 shRNAs (shRNA1 and shRNA2) or negative control shRNA, and were seeded onto confluent HDFs (cell sorting gates in appendix). The cocultures were fixed at 14 days after seeding HUVEC onto HDF and stained for podocalyxin. Multiple Z-stack images were acquired as described in Methods (Chapter 2, Section 2.3.6.1) in order to image the three-dimensional lumens forming over multiple confocal planes. Single Z-plane images from a 3D Z-stack showed that tubules lacking DOCK4 elongated but became thin and failed to acquire sufficient lateral adhesions (Figure 3.7A). There were no changes in the expression level of VE-cadherin which is an important molecule in EC-EC adhesion and early lumen formation (Figure 3.7 B). To further assess the extent of lateral adhesions and loss of thickening within the DOCK4 knockdown tubules, a measurement of nuclei per tubule length was taken in control and DOCK4 shRNA tubules. Consistent with the long thin elongated tubules that lack lumens seen in the DOCK4 knockdown (Figure 3.9), DOCK4 tubules showed less nuclei per length of tubule when compared to the thicker control tubules (Figure 3.8). Quantification of lumenised length showed that there was a marked decrease in lumenised length with DOCK4 knockdown by both shRNA1 and shRNA2 when compared with control tubules (Figure 3.10).

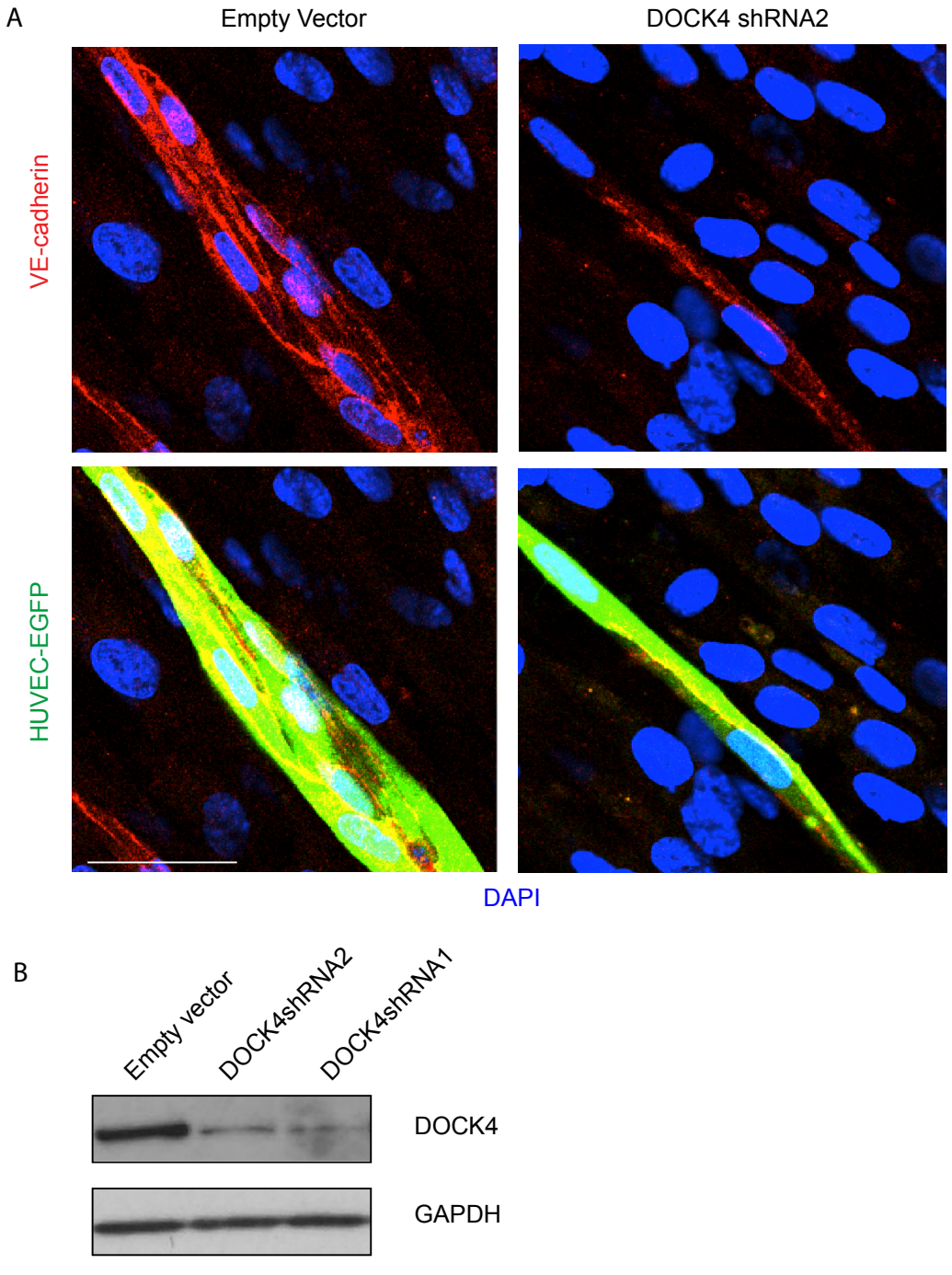

Figure 3.7 The effect of DOCK4 knockdown on tubule lateral adhesions
(A) $2x10^4$ fibroblasts are plated and let grow to confluence for seven days after which time $1x10^4$ HUVEC transduced with non-silencing control shRNA or DOCK4 shRNA 2 were seeded onto the fibroblasts. Cultures were then fixed and stained as before for immunoflourescent imaging. EGFP HUVEC (green), VE-cadherin (red) DAPI (blue). Note loss of lateral adhesions in DOCK4 shRNA2 tubules. Similar effects were observed with an additional DOCK4 shRNA. Scale bar = 25µm. (B) Western blot of the junctional protein VE-cadherin assessed after DOCK4 knockdown and normalised to GAPDH levels.

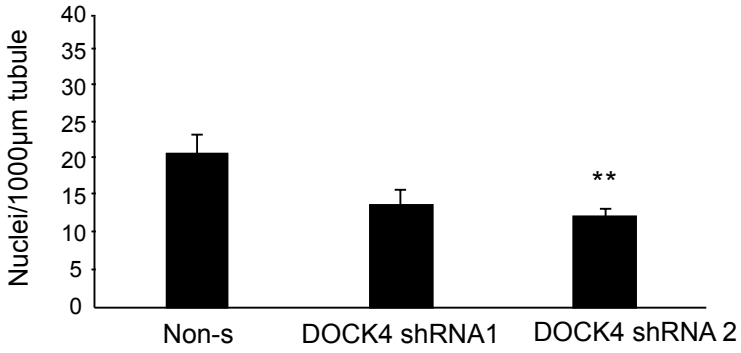

Figure 3.8 DOCK4 knockdown controls endothelial cell numbers in tubules
$2x10^4$ fibroblasts are plated and let grow to confluence for seven days after which time $1x10^4$ HUVEC transduced with negative control shRNA or DOCK4 shRNA 1 or shRNA 2 were seeded onto the fibroblasts. Tubule length was assessed by measuring length of GFP expressing tubules and counting DAPI stained nuclei within. Bar chart shows quantification of nuclei/1000µm length for control, DOCK4 shRNA1 and DOCK4 shRNA2. Quantifications are from multiple images (control n=16 images, DOCK4 shRNA1 n=16, DOCK4 shRNA2 n=18) from two independent experiments, each set up in triplicate. Significance was calculated using a two tailed student T-test. p value for Dock4 shRNA1 =0.0057. ** = $p<0.01$.

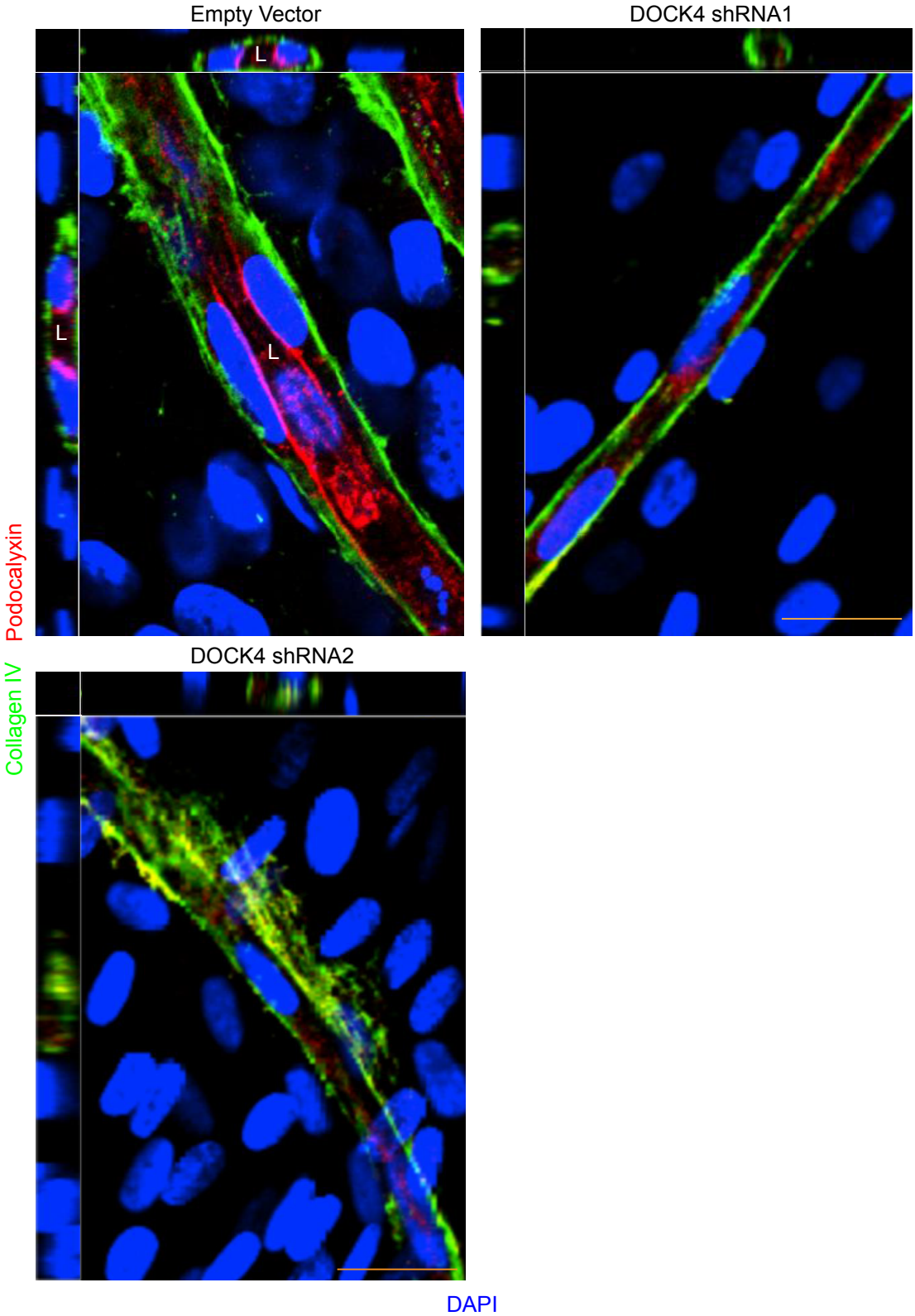

Figure 3.9 DOCK4 knockdown inhibits lumen formation in the coculture assay
$2x10^4$ fibroblasts are plated and let grow to confluence for seven days after which time $1x10^4$ HUVEC transduced with non-silencing control shRNA or DOCK4 shRNA 1 were seeded onto the fibroblasts. The cocultures were fixed on day 14, nuclei were marked with DAPI (blue) and tubules were imaged using confocal microscopy. Apical localization of podocalyxin can be seen between elongated endothelial cells surrounding lumens (L); collagen IV marks the basement membrane. Scale bar 14µm

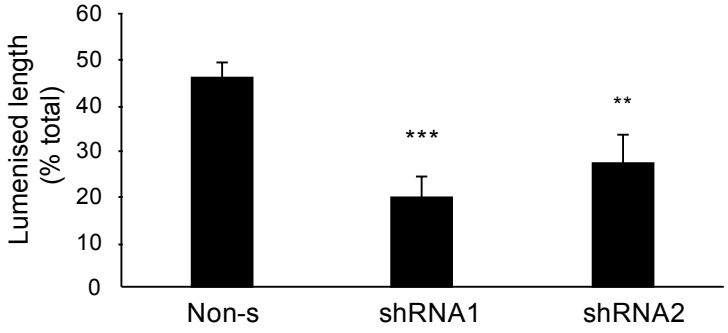

Figure 3.10 Quantification of the effect of DOCK4 knockdown on lumen formation
Bar chart shows quantification of percentage of tubules with lumens compared with total tubule length. Lumen formation was assessed by podocalyxin staining and confocal imaging of mature tubules at 14 days after seeding HUVEC onto fibroblasts. Quantifications are from 2 independent experiments with negative control n=3, shRNA1 n=3 and shRNA2 n=3. 5 images were quantified/well. Scale bar = 14µm. Significance was calculated using a two tailed student T-test. ** = $p<0.01$, ***=$p<0.001$.

3.5 Generation of lentiviral shRNAs for DOCK9 knockdown studies

In the preliminary work leading to this thesis, DOCK4 was found to interact with DOCK9, therefore I set out to investigate the effects of DOCK9 on tubule formation in the coculture system and whether knockdown affects lumen formation. In order to assess lumen formation at 14 days after seeding HUVEC onto fibroblasts, long-term stable DOCK9 knockdown was necessary. Multiple shRNA vectors that also expressed EGFP from Open Biosystems were grown and packaged into lentiviral vectors as described in Methods (Chapter 2, Section 2.2.2-2.2.3). Primary HUVEC were infected with multiple shRNA constructs via lentiviral transduction and were then fluorescence-activated cell sorted based on EGFP fluorescence. Total protein from cell lysates of sorted cells was then quantified and run on a western blotting. The two DOCK9 shRNAs, shRNA3 and shRNA4, gave the best knockdown assessed by western blotting and were used in experiments (Figure 3.11 A). DOCK9 protein levels were compared against a non-silencing negative control shRNA and gave values of 95.2% knockdown for DOCK9 shRNA3 and 97.1% knockdown for shRNA4 (Figure 3.11 B).

A

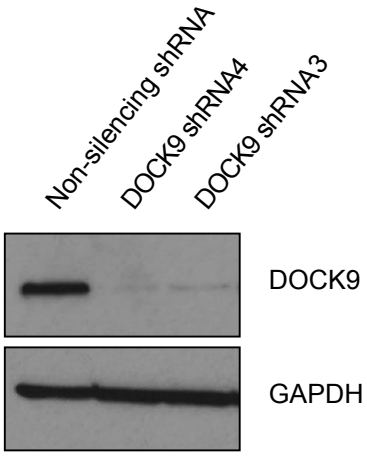

B

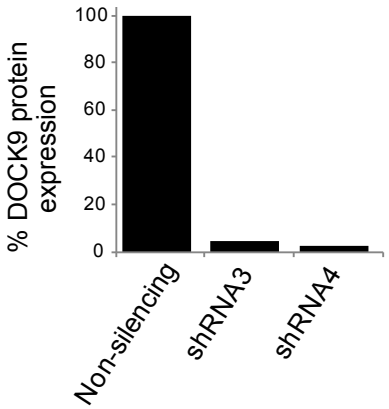

shRNA	Knockdown
DOCK9 shRNA3	95.2%
DOCK9 shRNA4	97.1%

Figure 3.11 Stable knockdown of DOCK9 by means of lentiviral transduction
(A) Lysate was made with HUVEC transduced with non-silencing control shRNA or DOCK9 shRNA 3 or shRNA 4 10 days after transfection. Levels of the Cdc42 GEF DOCK9 were assessed by western blotting where expression of DOCK9 in the knockdown samples (shRNA3 and shRNA4) was compared with DOCK9 levels in the negative control sample (non-silencing). (B) Values shown are expressed as a percentage of control expression, normalised against the housekeeping gene GAPDH.

3.6 Analysis of the effect of DOCK9 knockdown on endothelial cell shape and proliferation

Since Cdc42 is known to control spreading and proliferation (Barry *et al.*, 2015), first I examined whether DOCK9 knockdown affects endothelial cell shape and proliferation. Cell spreading was analysed in control cells and DOCK9 knockdown cells by seeding onto culture dishes and imaged by phase contrast imaging (Figure 3.12 A). No significant difference in spreading area was found between control shRNAs and DOCK9 shRNA knockdown cells (Figure 3.12 A). To account for any similarities in area between spreading cells and elongated cells, circularity measurements were also carried out using ImageJ software. No significant difference was found between the circularity of control shRNAs and DOCK9 shRNA knockdown cells, suggesting that spreading and cell shape changes are not under control of DOCK9 (Figure 3.12 C). Cdc42 has also been shown to play a role in proliferation in many cell types (Boe *et al.*, 2012; Melendez *et al.*, 2013). Any potential effect on proliferation might result in differences in cell number in the co-culture assay and ultimately affect lumen quantification results. Two methods were used to assess any potential differences in proliferation due to loss of DOCK9. The Ki-67 protein is commonly used as a proliferation marker and known to be expressed in the nucleus of cells in interphase and in mitotic chromosomes, but not during G0 (Scholzen and Gerdes, 2000). Quantification of Ki67 positive nuclei showed no significant difference in proliferation between empty vector, non-silencing control and DOCK9 shRNA3 or shRNA4 in HUVEC 24 hours after seeding (Figure 3.13 A). Proliferation was also assessed using a live imaging microscope (Incucyte), capable of time-lapse imaging EGFP-HUVEC during proliferation over the course of three days (Described in Chapter 2 section 2.3.8). This experiment considers if there were any differences in cycling speeds of cells lacking DOCK9. Similarly, results showed that there were no proliferation differences in control or DOCK9 knockdown cells when grown to confluence over three days, shown as an increase in GFP fluorescence over time (Figure 3.13 B).

Knockdown of DOCK9 did not affect VE-cadherin localisation in HUVEC growing as a monolayer or in the coculture assay (Figure 3.13 C). DOCK9 knockdown did not have an effect on overall VE-cadherin levels assessed by western blotting. (Figure 3.13 C). These results suggest that DOCK9 is dispensable for VE-cadherin expression and localisation.

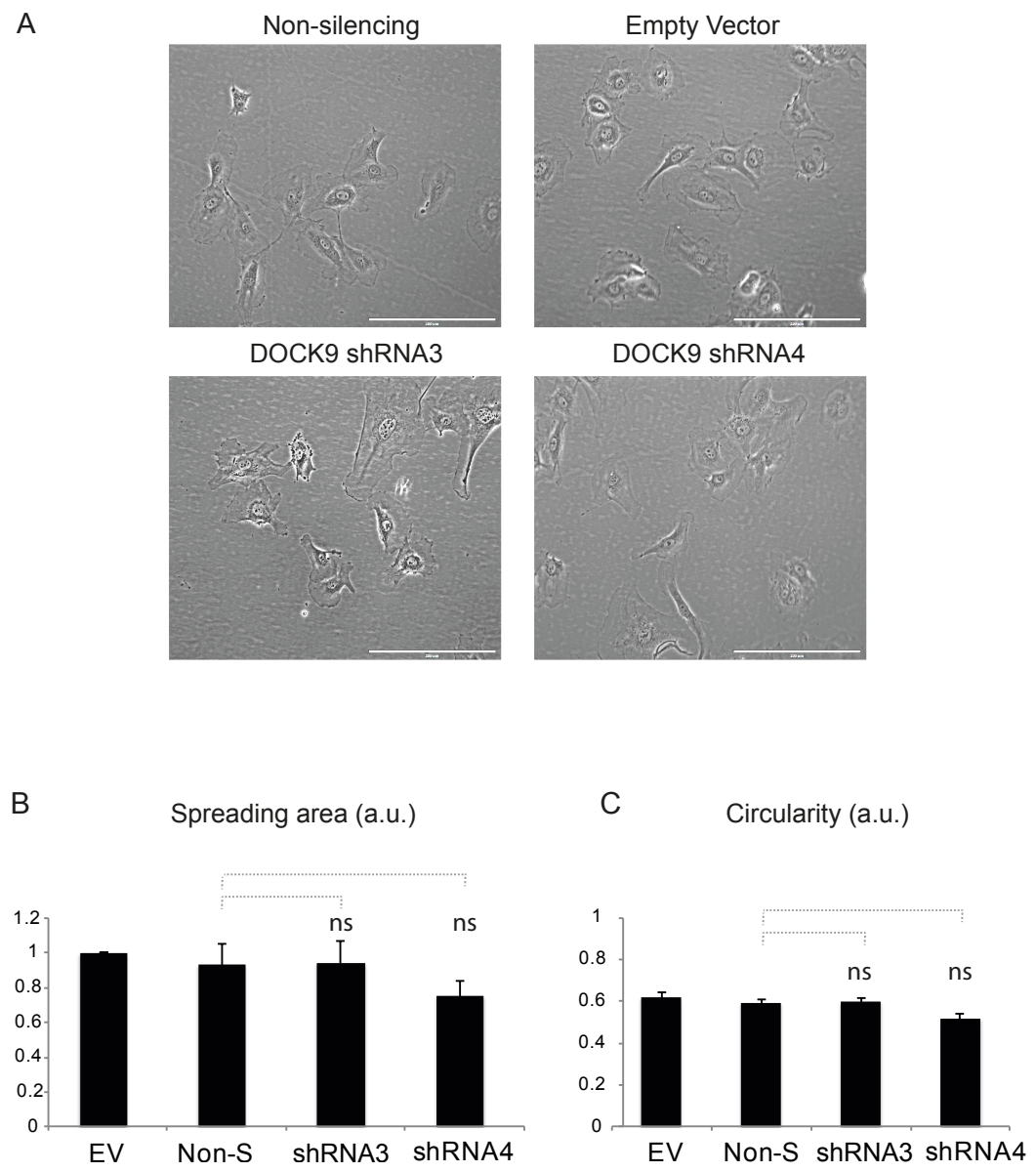

Figure 3.12 DOCK9 knockdown does not affect HUVEC spreading or bipolarity
$1x10^4$ HUVEC transduced with non-silencing control shRNA or DOCK9 shRNA 3 or shRNA4 were seeded onto glass cover slips in 24 well dishes and let adhere overnight before fixing with PFA and Imaging with ImageJ. (A) Representative images of cells spreading and circularity in control and DOCK9 shRNA3 and DOCK9 shRNA4. Scale bar = 200um. (B) Spreading area was measured and compared to control non-silencing shRNA. (C) Circularity was measured using ImageJ where a value of 1 represents a perfect circle (round cell). Significance was calculated using a two tailed student T-test. EV, empty vector; Non-S, non-silencing; ns, non-significant; a.u. (arbitrary units).

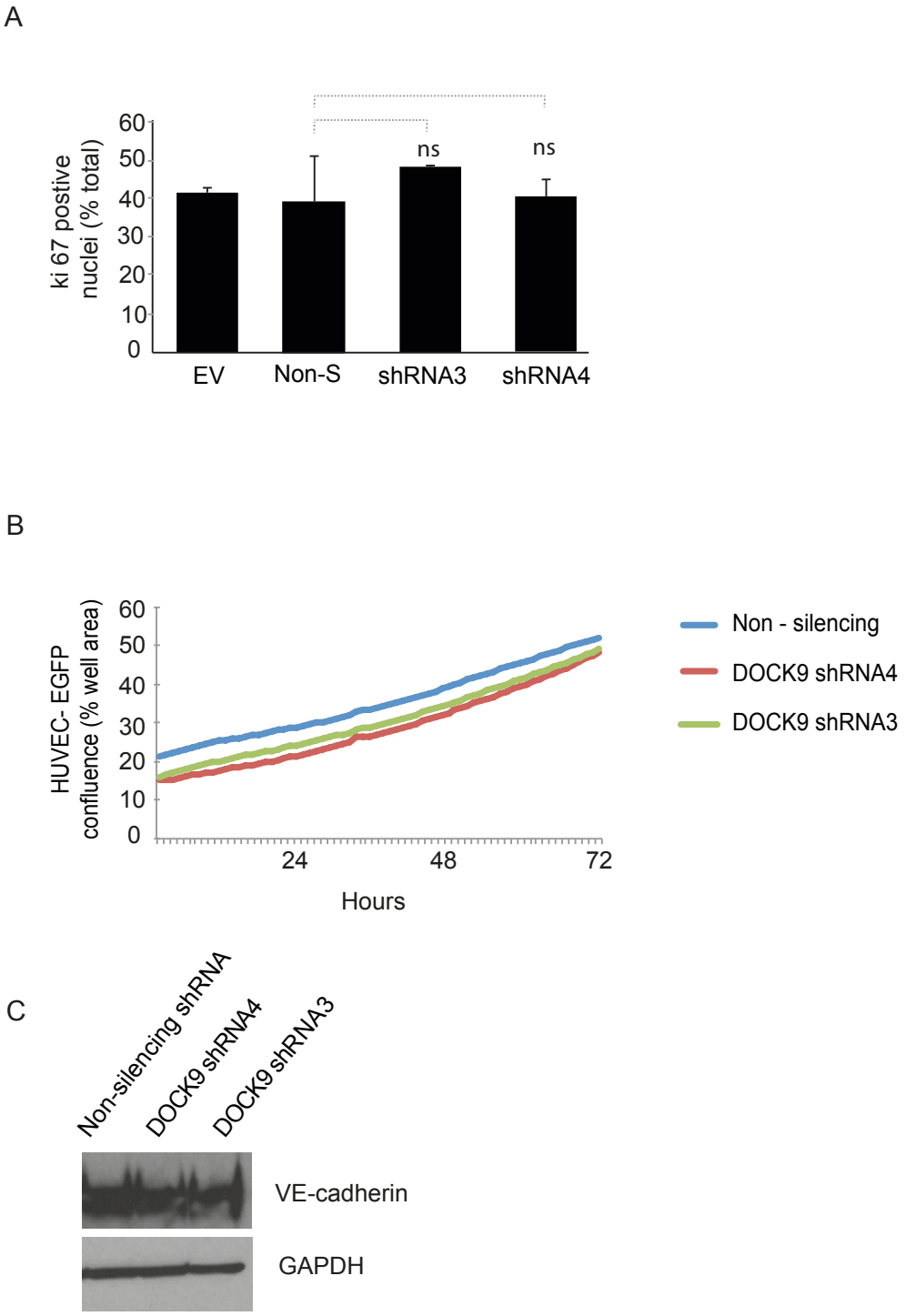

Figure 3.13 DOCK9 does not control endothelial cell proliferation or VE-cadherin expression
(A) 1x10^4 HUVEC transduced with non-silencing and EV control shRNA or DOCK9 shRNA 3 or shRNA4 were seeded onto glass cover slips in 24 well dishes and let adhere overnight before fixing with PFA. Proliferation was assessed by means of Ki-67 staining. Bar chart shows percentage of cell nuclei positive for Ki-67. Ns, non-significant. (B) Increase in confluence over 3 days as measured by EGFP fluorescence on the Incucyte live imaging system. No significant difference was found between proliferation rates as measured by increasing confluence. (C) VE-Cadherin after DOCK9 knockdown western blot. Significance was calculated using a two tailed student T-test. EV, empty vector; Non-S, non-silencing; ns, non-significant.

3.7 DOCK9 knockdown inhibits lumen formation in the coculture assay

To investigate the role DOCK9 plays in lumen formation, the previously optimized lumen assay was employed. Primary HUVEC were transduced with lentiviruses harboring non-silencing control and DOCK9 shRNAs as described in section 3.5 above. Cocultures were grown for 14 days and stained for immunofluorescence microscopy. Lumen formation was assessed by podocalyxin localization at apical sites as before. Tubules lacking DOCK9 had a long thin morphology and less branching when compared with control tubules. This result suggests a role for DOCK9 in branching of developing tubules but no role in tip dynamics. When stained for podocalyxin control, tubules showed strong and defined stain for podocalyxin at lateral sites between elongated cells (Figure 3.14). There was a twofold decrease in lumen formation in tubules lacking DOCK9 with both shRNAs tested (Figure 3.15). These results suggest that DOCK9 is dispensable for tubule elongation but necessary for lumen. Studies on the role of DOCK4 in lumen formation had shown an association between a defect in lumen formation and lateral adhesions with DOCK4 knockout (Abraham *et al.*, 2015). However, when the formation of lateral adhesions was assessed with DOCK9 knockdown by measuring the number of nuclei per unit length, no differences were seen between control tubules and tubules with DOCK9 (Figure 3.16). This suggests that in addition to cytoskeletal rearmaments evidenced by the control of filopodial protrusions regulated by DOCK4 and DOCK9, DOCK4 may play additional roles in the control of lateral cell-cell contacts, which are not shared by DOCK9.

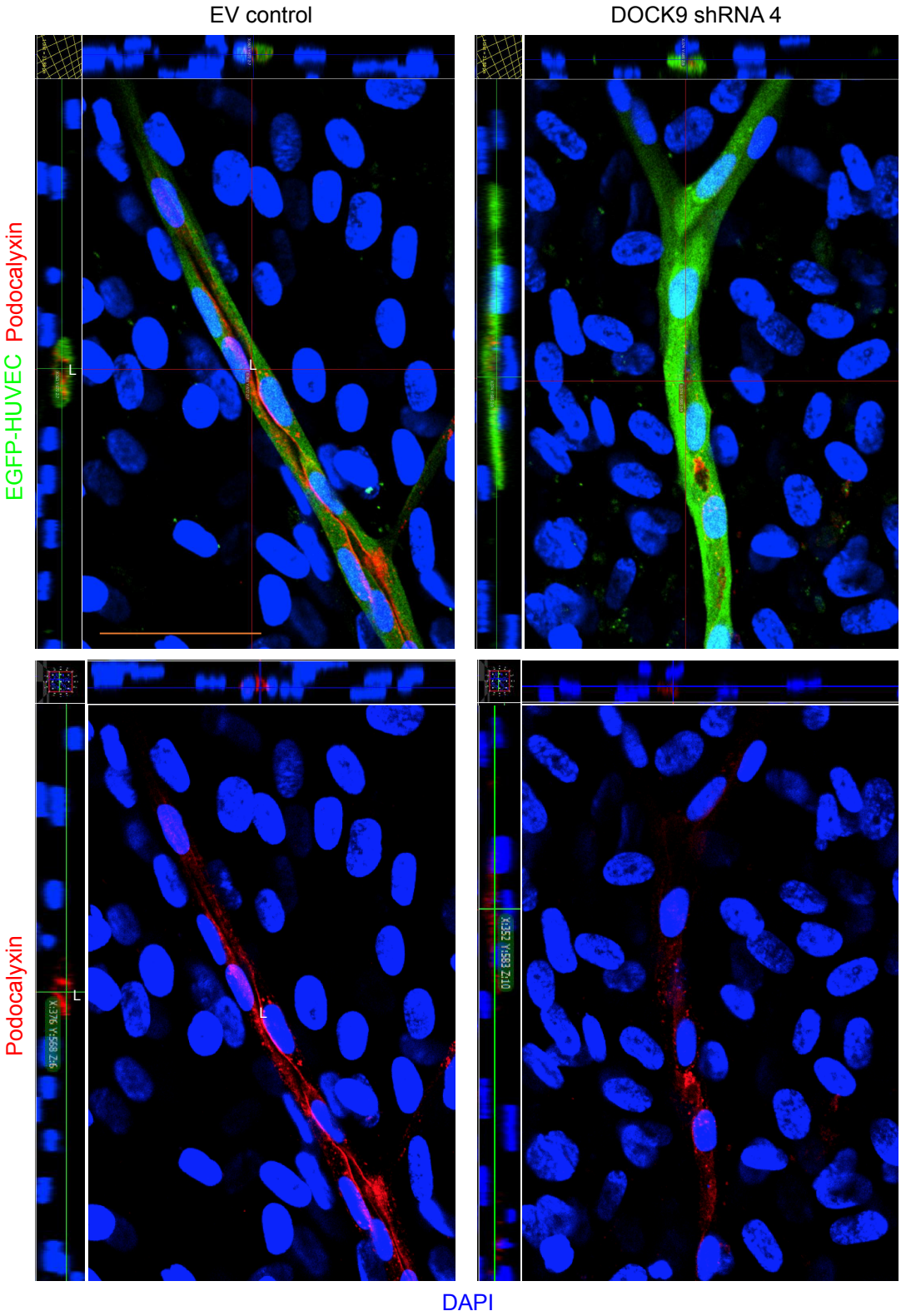

Figure 3.14 EGFP-HUVEC forming tubules in the coculture
$2x10^4$ fibroblasts are plated and let grow to confluence for seven days after which time $1x10^4$ HUVEC transduced with non-silencing control shRNA or shRNA 4 were seeded onto the fibroblasts. The cocultures were fixed on day 14, nuclei were marked with DAPI (blue) and tubules were imaged using confocal microscopy. Apical localization of podocalyxin can be seen between elongated endothelial cells surrounding lumens (L); collagen IV marks basement membrane. Scale bar 16µm.

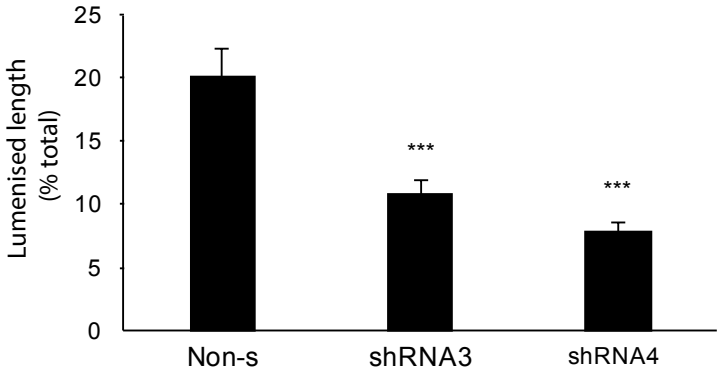

Figure 3.15 DOCK9 controls lumen formation in the coculture assay
$2x10^4$ fibroblasts are plated and grown to confluency for seven days, after which time $1x10^4$ HUVEC transduced with non-silencing control shRNA, or DOCK9 shRNA 3 or shRNA 4 were seeded onto the fibroblasts. The cocultures were fixed on day 14, and lumen formation was assessed by podocalyxin staining and confocal imaging of mature tubules. Bar chart shows quantification of percentage of tubules with lumens compared with total tubule length. Quantifications are from 4 independent experiments, n=number of images, (Non-silencing n=12, shRNA3 n=12 and shRNA4 n=12). Significance was calculated using a two tailed student T-test. *** = $p<0.001$. Non-S, non-silencing.

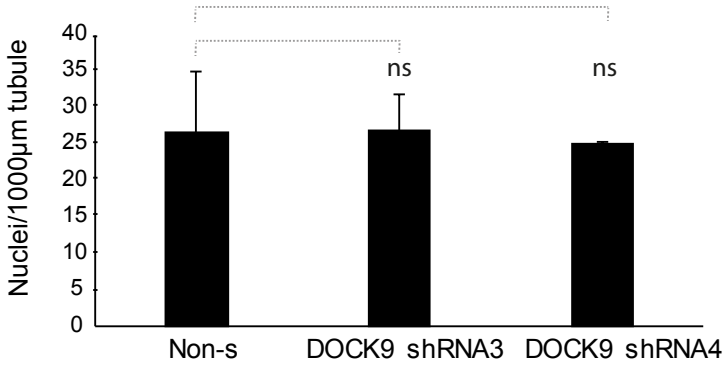

Figure 3.16 DOCK9 knockdown does not affect endothelial density in tubules
$2x10^4$ fibroblasts are plated and grown to confluency for seven days after which time $1x10^4$ HUVEC transduced with non-silencing control shRNA or DOCK9 shRNA 3 or shRNA 4 were seeded onto the fibroblasts. Tubule length was assessed by measuring length of GFP expressing tubules and counting DAPI stained nuclei within. Bar chart shows quantification of nuclei/1000µm length for Non-silencing, DOCK9 shRNA3 and DOCK9 shRNA4. Quantifications are from multiple images (Non-silencing n=16 images, DOCK9 shRNA3 n=16, DOCK9 shRNA4 n=18) from two independent experiments, each set up in triplicate. Significance was calculated using a two tailed student T-test. Non-S, non-silencing, ns, non-significant.

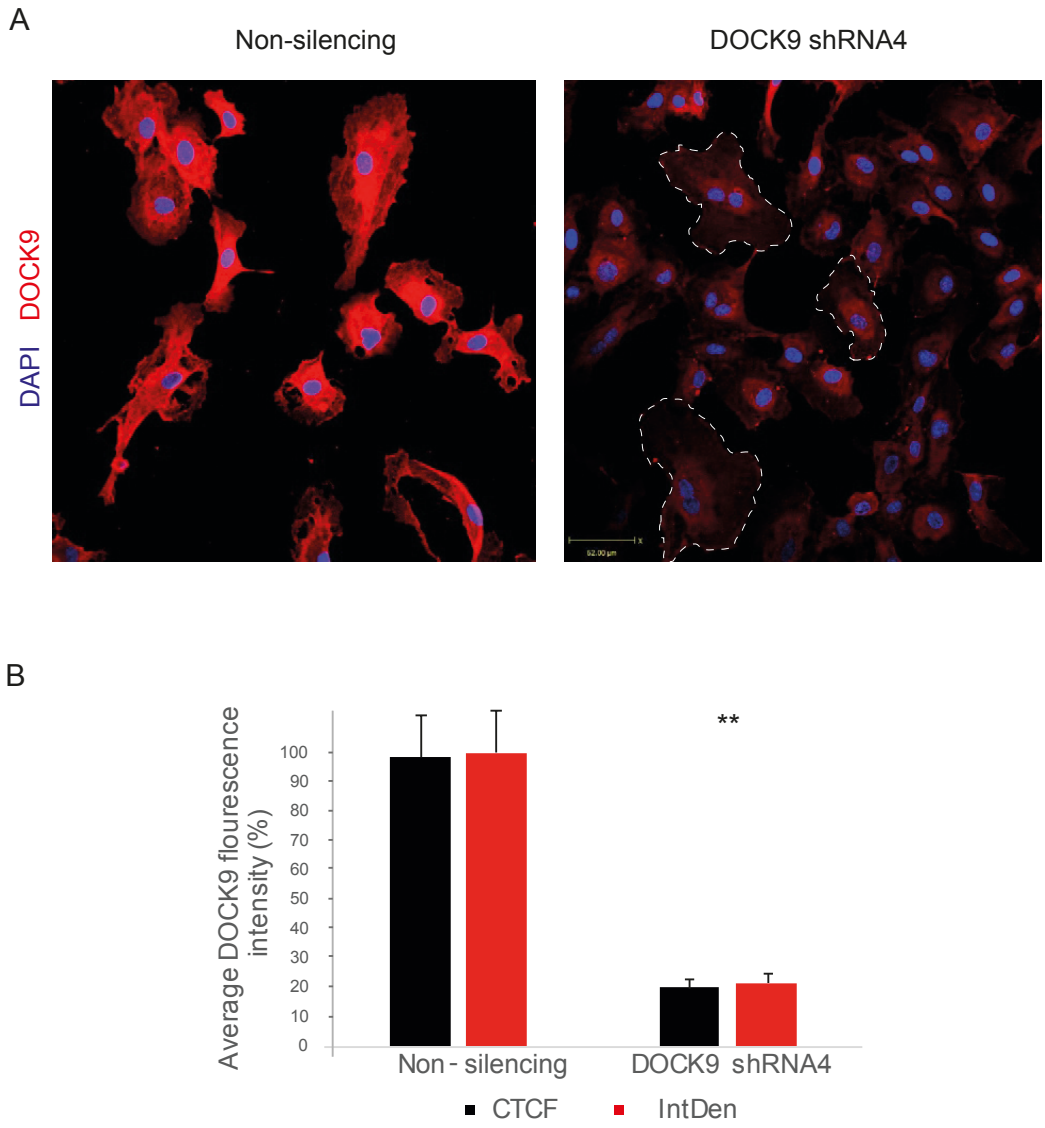

Figure 3.17 Validation of the DOCK9 antibody in HUVEC

$1x10^4$ HUVEC transduced with non-silencing control shRNA or DOCK9 shRNA4 were seeded onto glass cover slips in 24 well dishes and let adhere overnight before fixing with 70% ethanol after. (A) Representative immunofluorescence images of HUVEC stained with DOCK9 antibody. Scale bar = 62μm. (B) Bar chart shows corrected total cell fluorescence (CTCF) and integrated density (IntDen) measured using the ImageJ software. N= number of cells quantified (Non-silencing = 40, DOCK9 shRNA4 = 42) from 5 images per condition. Dashed lines indicate cell boundaries. Significance was calculated using a two tailed student T-test. ** = $p<0.01$.

3.8 DOCK9 localises with the apical surface in spreading HUVEC in vitro

To investigate the localisation of DOCK9 in endothelial cells by immunofluorescence microscopy, staining with a newly available antibody (Proteintech) was optimized in HUVEC. DOCK9 was knocked down using lentiviral shRNAs against DOCK9 in HUVEC and knockdown efficiency was confirmed using western blotting. Cells were then seeded for 24 hours before trying two different fixation methods, 4% PFA and 70% ethanol. Immunofluorescence was then carried out to look at levels of DOCK9 in cells with shRNA compared with non-silencing negative control virus. 70% ethanol fixation was the only method that resulted in a decreased whole cell intensity for DOCK9 stain in shRNA4 knockdown cells compared with control (Figure 3.17). These results were consistent with levels of knockdown seen by western blotting (Figure 3.11).

As shown in section 3.4, DOCK4 tubules failed to acquire sufficient lateral adhesions to form lumens as evident by the nuclei per unit length measures. However, DOCK9 tubules showed no difference in nuclei per length measures when compared with control. To investigate the potential mechanism by which DOCK9 is controlling lumen formation and podocalyxin localisation in tubules, the localisation of podocalyxin to the apical surface during polarisation was assessed.

In endothelial cells, as with many other cells types, acquisition of polarity plays a major role in many of their functions. Acquiring apical-basal (luminal-abluminal) polarity is one of the necessary steps in order to form vascular lumens (Iruela-Arispe and Davis, 2009). Galvagni et al. showed that during the early stages of spreading in vitro, endothelial cells display an F-actin rich domain on their apical surface which is found to be enriched for many proteins usually found on the apical surface. Consequently, they called this site of accumulation of apical proteins in spreading cells in 2D culture apical membrane insertion site (AMIS) (Galvagni *et al.*, 2012). Recent research has also shown that the transport and accumulation of important apical proteins at this AMIS is a process that mimics stages prior to lumen formation when HUVEC again accumulate apical proteins at the newly developing lumen (Richards, Hetheridge and Mellor, 2015).

During spreading, endothelial cells form this apical domain which can be seen by staining of actin filaments (phalloidin). Importantly, podocalyxin can be seen to localize at the AMIS along with the endothelial junctional protein VE-cadherin (Figure 3.18). After optimization of staining

with the DOCK9, I investigated the localisation of DOCK9 during this process and found it was concentrated at the apical surface, as previously reported for other apical proteins (Figure 3.19).

To elucidate a potential role of DOCK9 in localisation of proteins to the apical membrane, siRNA knockdown was carried out on HUVEC, and cells lacking DOCK9 were seeded for the AMIS assay. Knockdown of DOCK9 did not affect localisation of podocalyxin to the apical membrane suggesting it may regulate a different process in lumen formation (Figure 3.20).

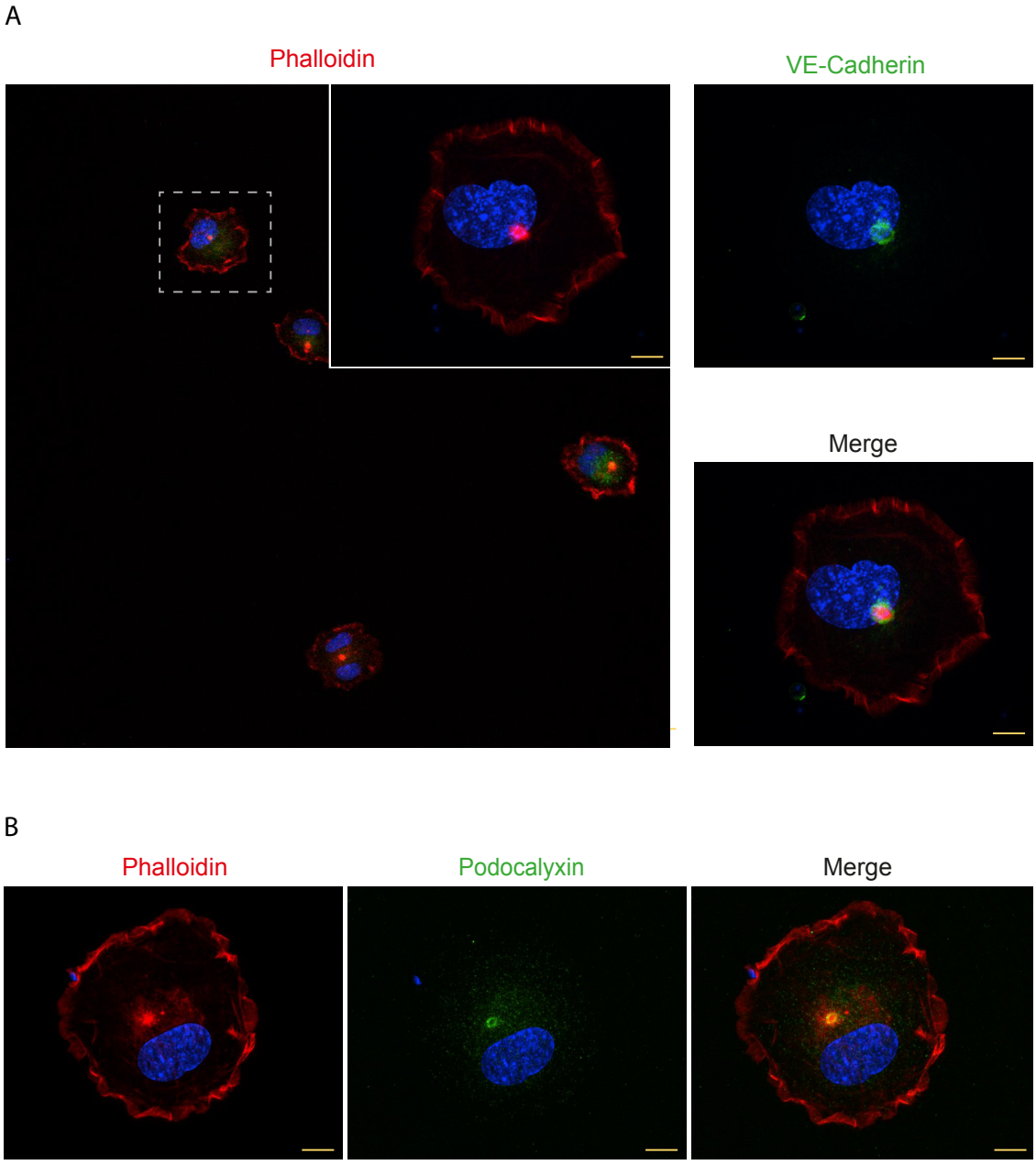

Figure 3.18 Apical proteins localise to the AMIS domain during early spreading in HUVEC
$1x10^4$ HUVEC were seeded onto glass cover slips in 24 well dishes and let spread for 25 minutes before fixing. (A) Cells were stained for apical proteins and imaged by confocal microscopy to generate Z-stacked images. Zoomed area; Phalloidin (red), VE-cadherin (green), DAPI (blue). (B) Phalloidin (red), podocalyxin (green), DAPI (blue). Scale bar = 12um

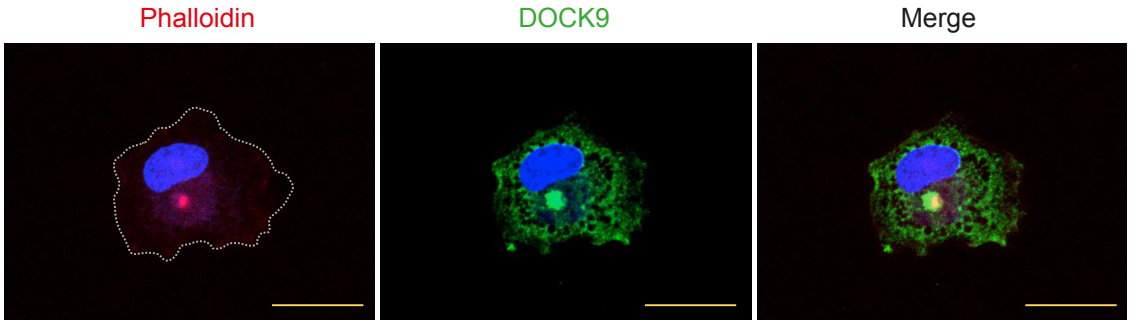

Figure 3.19 DOCK9 localises with the AMIS apical domain in spreading HUVEC
$1x10^4$ HUVEC were seeded onto glass cover slips in 24 well dishes and let spread for 25 minutes before fixing. Cells were stained for apical proteins and imaged by confocal microscopy to generate Z-stacked images. Phalloidin (red), DOCK9 (green), DAPI (blue). Dashed line indicates cell boundary. Scale bar = 31µm

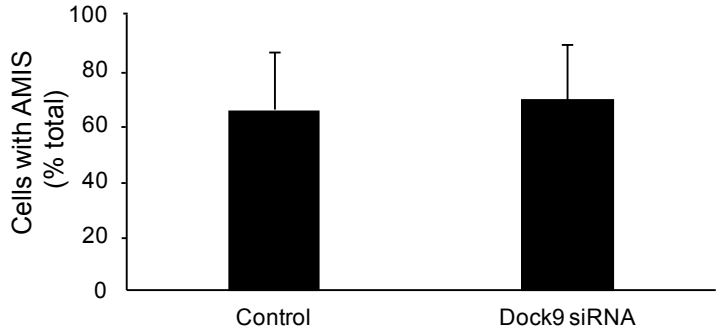

Figure 3.20 DOCK9 knockdown does not affect apical localisation of podocalyxin
HUVEC transduced with control (Non-silencing) and DOCK9 siRNA were seeded on glass slides and let spread for 25 minutes before fixing. Cells were stained for the apical protein podocalyxin and imaged by confocal microscopy to generate Z-stacked images. Bar chart shows quantification of the localization of podocalyxin to the apical domain (AMIS) in control (Non-silencing) and DOCK9 siRNA.

3.9 Conclusions

Vascular lumen formation is a vital step in order to confer functionality to developing blood vessels. The process of tube formation in other cell types has been well studied to date and diverse mechanisms have been described, for example in epithelial cells multiple mechanisms exist based on the size, location, and function of the resulting lumen to be formed (section 1.5.2) (see reviews (Chung and Andrew, 2008; Sigurbjörnsdóttir, Mathew and Leptin, 2014). However, endothelial lumen formation remains to be fully understood since conflicting and contradictory theories exist. Blood vessel lumens have been shown to form via two key mechanisms (Iruela-Arispe and Davis, 2009): expansion of an intracellular vacuoles within endothelial cells to form seamless lumens (Kamei, W Brian Saunders, *et al.*, 2006); or cord hollowing, whereby a lumen forms by opposing endothelial cells with lateral adhesions followed by re-distribution of the cell junctions to the edge of the newly formed tube (Strilić *et al.*, 2009; Pelton *et al.*, 2014). Both of these mechanisms demand an intricate control of actin dynamics and cell shape. A third key mechanism describes the expansion of blood vessel lumens in response to blood flow by inverse blebbing, (Gebala *et al.*, 2016) which also involves intricate in cytoskeletal dynamics and actomyosin contraction.

Rho GTPases are known to be involved in many cellular functions including controlling the actin cytoskeleton and cell shape changes. Guanine nucleotide exchange factors (GEFs) and GTPase activating proteins (GAPs) which activate and deactivate GTPases, respectively, can provide another level of control based on their expression patterns by regulating activity in context-specific situations and also in a spacio-temporal manner (Kather and Kroll, 2013). Therefore, the importance of understanding the role of individual GEFs during angiogenesis is imperative, as they may result in very specific targetable molecules in situations where angiogenesis is deregulated.

In this chapter I have demonstrated that: (i) lumens form in the co-culture assay via lateral cell-cell adhesions and cord hollowing; (ii) DOCK4 and DOCK9 play vital roles in early tubule morphogenesis and actin rearrangement, and both are necessary for lumen formation; (iii) the Cdc42 GEF, DOCK9, localises with the apical surface of spreading HUVEC in vitro. The co-culture assay is an ideal method to visualise the effect of loss of GEFs such as DOCK4 or DOCK9 on tubule morphogenesis as it provides the opportunity to investigate many stages of tubule growth. As seen using CD31 IHC staining, endothelial cells went through multiple stages of angiogenic growth and tubule morphogenesis as previous described (Figure 3.1) (Hetheridge,

Mavria and Mellor, 2011). Tubules then rearrange further and endothelial cells acquire lumenal-ablumenal polarity at sites of cell-cell adhesions. This is consistent with previously described mechanisms and podocalyxin staining patterns seen *in vivo* (Strilić *et al.*, 2009; Robbins and Beitel, 2016).

DOCK9 is a GEF for the Rho GTPase Cdc42, which is known to regulate many cellular functions related to actin dynamics and filopodia formation (Krugmann *et al.*, 2001; Meller *et al.*, 2004). Activation of Cdc42 can be achieved by a number of exchange factors in diverse signalling pathways. As a driver of so many important and distinct cellular functions, the specificity of its action is achieved through the spatial abundance of GEFs in distinct regions of the cell and also through competition between GEFs and GAPs at difference sites.

When DOCK9 was knocked down in the coculture assay, the result was a two-fold decrease in lumenisation seen when compared with control tubules (Figure 3.15). However, nuclei/ length measurements showed no difference in lateral adhesions or abundance of endothelial cells, as seen with DOCK4 knockdown.

Polarisation and acquisition of apical-basal (luminal-abluminal) identity are essential during the early stages of tubule growth. Defects in apical luminal identity could result in defects in tubule rearrangement during lumen formation. Interestingly, activation of Cdc42 by DOCK9 at the cell membrane has previously been shown to have lateral influences on cells, for example the control of dendrite outgrowth in rat hippocampal neurons (Kuramoto, Negishi and Katoh, 2009). I have shown that DOCK9 localises with the apical surface of polarising endothelial cells in the AMIS assay, along with a range of other important apical proteins in vitro (Figure 3.18, 3.17). Loss of DOCK9 at this stage did not affect polarisation of cells or expression of podocalyxin at the AMIS.

These results show that DOCK9, like DOCK4 controls lumen formation. While both control cytoskeletal rearrangements thus regulating a yet unidentified site in the formation of a tube, such as establishment of a curvature for example, DOCK4 also regulates lateral cell-cell contacts, a function that is not shared by DOCK9 according to the data presented in this thesis.

Chapter 4

The role of ROCK2 in Sprouting and Lumen Formation *in vivo*

4.1 Introduction

The Rho associated coiled-coil-containing protein serine/threonine kinases of which there are two isoforms, ROCK1 and ROCK2, are highly conserved serine threonine kinases that are involved in signalling cascades that control actin dynamics down stream of RhoA/C signalling. Rho kinase signalling has been implicated in different aspects of angiogenesis and lumen formation (Bryan *et al.*, 2010; M. Kim *et al.*, 2015). The exact role of ROCK signalling in endothelial cell biology is not completely understood with multiple and conflicting roles having been reported in the literature potentially due to the use of different assays and model systems and the lack of studies in ROCK knockout mouse models. ROCK plays important roles in cardiovascular disease and endothelial dysfunction with a function in smooth muscle cell contraction and vasodilation of blood vessels (Yao *et al.*, 2010). This is supported by the use of ROCK inhibitors for the treatment of cardiovascular disease. Small molecule ROCK inhibitors against ROCK are currently being tested in clinical trials and used to treat many vascular diseases looking at their effect on hypercontraction of vascular smooth muscle cells and endothelial dysfunction (Lin *et al.*, 2007; Surma, Wei and Shi, 2011). Some of these trials have shown promising results for example the use of Fasudil in acute ischemic stroke (Shibuya *et al.*, 2005) and Y27632 in vasospasm (Disli *et al.*, 2009), however it is not known whether their effects are solely due to inhibition of ROCK. A number of new more potent and selective ROCK inhibitors have been developed however their effects on angiogenesis are yet unknown. For a better understanding of the effects of targeting ROCK in disease, it is necessary to elucidate the fundamental roles of ROCK in endothelial cells and for this purpose the use of *in-vivo* models can offer the best insights. In this chapter I investigate the role of the ROCK2 in new blood vessel formation and lumen formation *in-vivo* using a *Rock2* knockout mouse model. A better understanding of ROCK signalling in the vasculature may influence the way we administer therapeutic agents aimed to inhibit ROCK and improve the outcome of these treatments.

4.2 Loss of global *ROCK2* is embryonically lethal at E13.5

Earlier work by Thumkeo and colleagues (Thumkeo *et al.*, 2003) had identified that global loss of the mouse Rho associated kinase 2 gene (*Rock2*) was embryonically lethal, with less than 10% of *Rock2*$^{-/-}$ embryos surviving beyond E13.5 while surviving mice were born runts but subsequently developed normally and were fertile. Embryonic lethality was associated with placental dysfunction and intrauterine growth retardation before foetal death (Thumkeo *et al.*,

2003). The architecture of the endothelium-free placental labyrinth layer of the *Rock2* $^{-/-}$ mice was disrupted with extensive thrombus formation forming throughout. These findings helped elucidate a role for ROCK2 in inhibiting blood coagulation and maintaining blood flow. Later work by the same group had led to the discovery that loss of Rock1 was less severe than Rock2 but *Rock1*$^{-/-}$ embryos experienced failure of eyelid closure and closure of the ventral body wall leading to omphalocele with intestine and liver protruding outside the abdomen (Shimizu *et al.*, 2005). These defects were as a results of loss of organisation of actomyosin bundles at the eye and the umbilical ring. Most *Rock1*$^{-/-}$ mice died as a result of cannibalisation by the mother soon after birth.

Work employing a new *Rock2* knockout line generated more recently in the late Christopher J Marshall's laboratory at the Institute of Cancer Research and described in 'Preliminary work leading to this thesis' had also identified that loss of *Rock2* globally was lethal after E13.5. In order to investigate a potential involvement of placental defects in the embryonic lethality of *Rock2* knockout embryos, the *Rock2* null preimplantation embryos were transferred to a wild type mother and their development compared that of the *Rock2* null embryos in the *Rock2* heterozygous background. It was found that the embryonic lethality could not be rescued with the wild type uterus (McCarthy et al, unpublished data).

Rock2$^{-/-}$ embryos showed disorganised vasculature as observed macroscopically with haemorrhages in the head, neck and trunk region and occasionally pooled blood in the paws and feet (Figure 4.1), in addition to omphalocele as observed previously (Thumkeo *et al.*, 2003). *Rock2* knockout embryos also appeared paler when compared with wild type littermates (Figure 4.1). Sections taken from the Interventricular foramen of Monro (the channel between the lateral ventricles and the third ventricle) high expression of ROCK2 in blood vessels and confirmed complete loss of expression of ROCK2 in the knockout mice (Figure 4.2 A, B). The apparent haemorrhages in the *Rock2* knockout embryos suggested improper blood flow and perfusion, potentially resulting from defects in blood vessel organisation and/or potential heart defects, which prompted further investigation of the role of ROCK2 in angiogenesis during development.

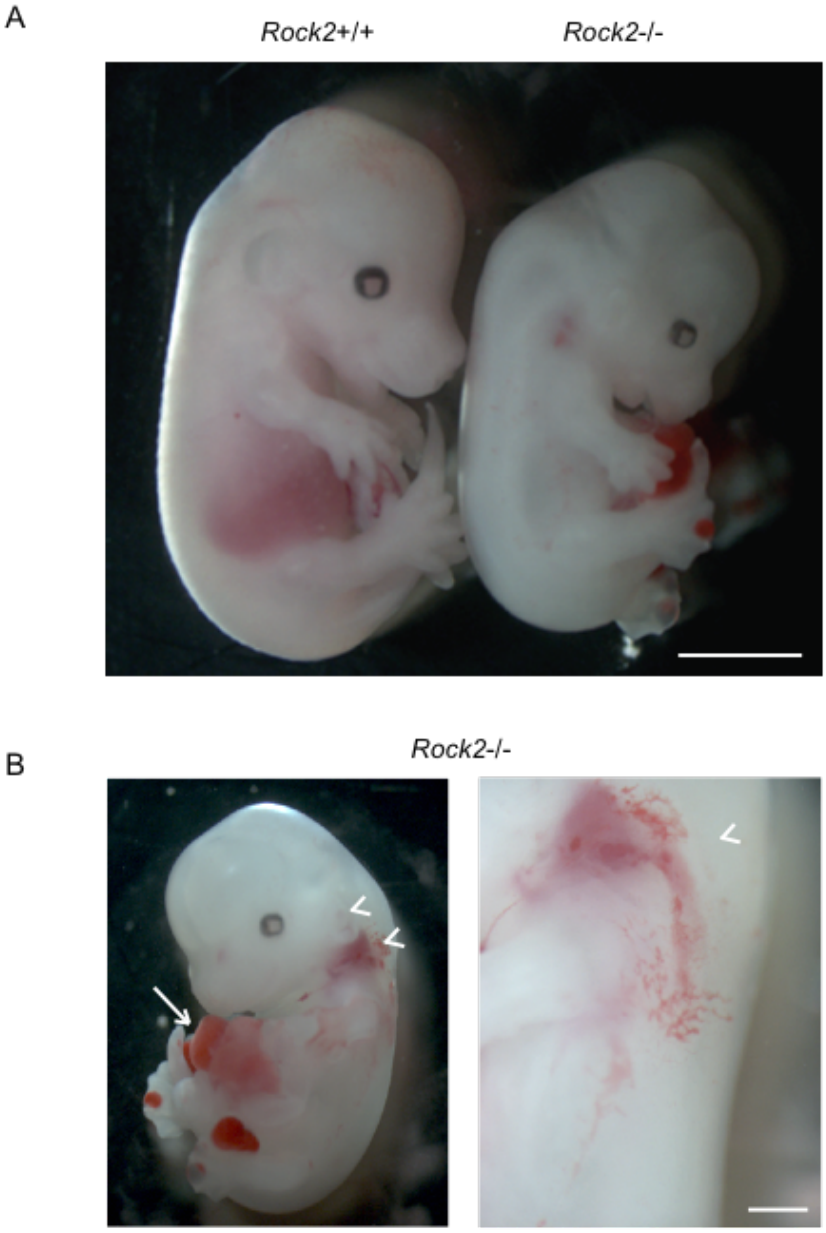

Figure 4.1 Morphology of embryos with global *Rock2* deletion at E13.5
Whole mount bright field images of *Rock2* $^{+/+}$ (wild type) and *Rock2* $^{-/-}$ (knockout) littermates at embryonic day 13.5. (A) Images show smaller size and hutched posture of E13.5 *Rock2*$^{-/-}$ littermates. Scale bar = 2mm (B) Image of *Rock2* $^{-/-}$ embryo showing incomplete closing (arrow) of the abdominal wall (omphalocele) and exhibiting haemorrhages in the head and neck area (arrowhead). Note that blood vessels appear disorganised. Scale bar = 1mm. Images taken by Dr Afshan McCarthy, ICR.

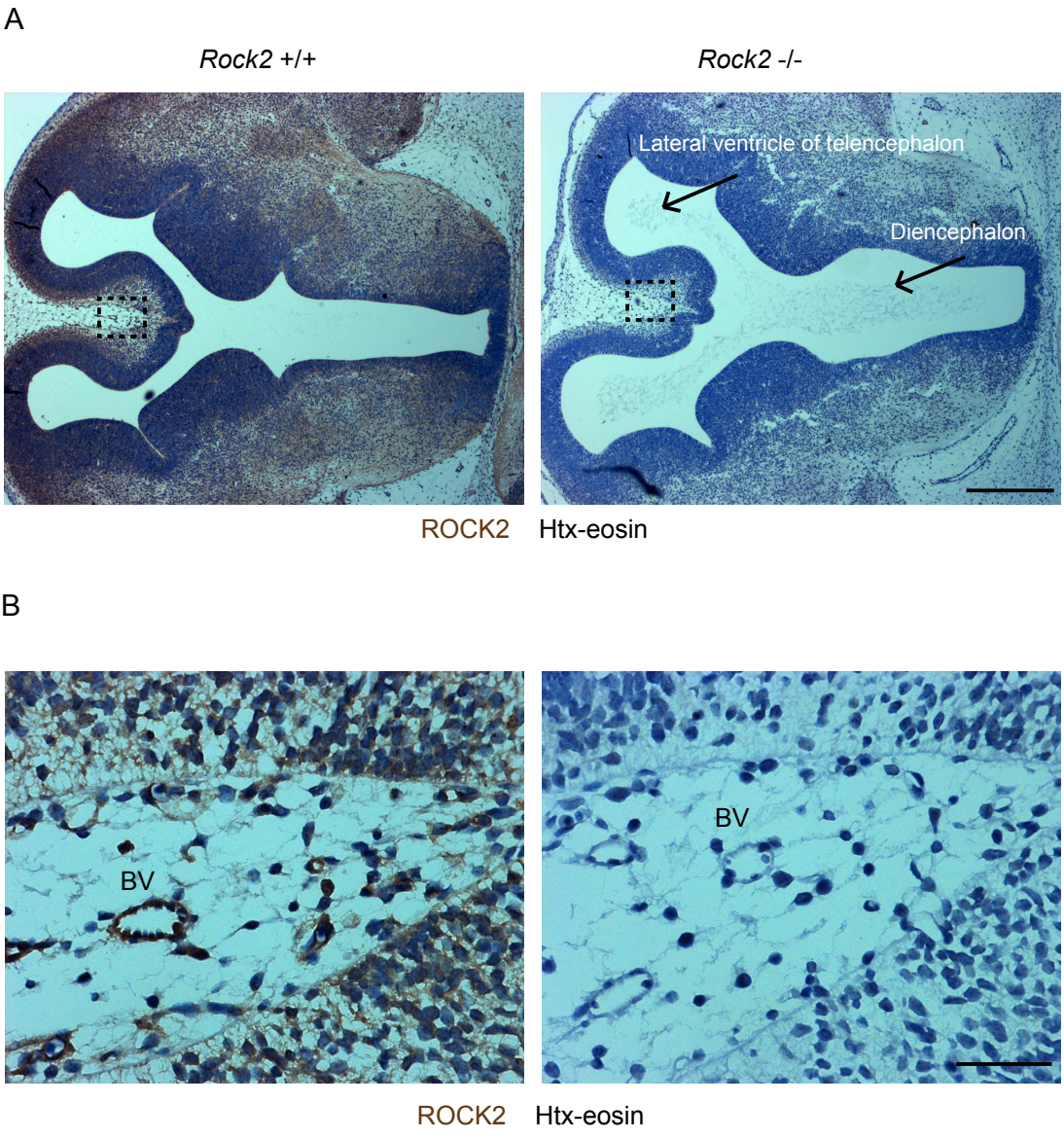

Figure 4.2 ROCK2 staining of sections from wild type and *Rock2* knockout embryos.
Transverse (horizontal) sections taken at the level of the interventricular foramen of Monro stained for ROCK2 expression in embryos at E13.5. (A) Immunohistochemical staining for ROCK2 expression in the brain parenchyma of wild type embryos (*Rock2*$^{+/+}$), and loss of ROCK2 expression in Rock2 knockout embryos (*Rock2*$^{-/-}$*).* Scale bar = 10 μm (B) Dashed box zoomed region from (A) showing strong ROCK2 expression and normal development of blood vessels in brain connective tissue surrounding the parenchyma. Scale bar =100μm. BV = blood vessel.

4.3 Characterising of embryonic brain blood vessels E12.5 vs E13.5

As significant haemorrhaging was seen in the head and neck regions of the ROCK2$^{-/-}$ embryos and high expression of ROCK2 in the vasculature, this led me to investigate blood vessel morphology and blood vessel lumen integrity at this developmental stage. Previously, most studies of *in vivo* developmental angiogenesis relied on dissection of the retina or the hindbrain for staining and quantification of angiogenic functions. The disadvantage of using these areas is the extensive dissection needed and the flat-mounting required for imaging. This results in loss of 3D tissue structure and collapse of lumens. To investigate if there were vascular abnormalities prior to lethality at E13.5 I characterised a previously described area of developmental angiogenesis in the brain (Lim *et al.*, 2010) termed the angiozone from hereon. A network of angiogenic vessel growth branching off the carotid artery was selected as it was in close proximity to the brain region showing haemorrhages and imaged with ease in the wholemount embryos (Figure 4.3 A). The advantage of imaging the angiozone is that embryos can be stained and imaged wholemount without the need for dissection and importantly, the blood vessels remain intact with perfused lumens.

Wild type embryos at two embryonic stages prior to lethality were chosen for characterisation, E12.5 and E13.5 (Figure 4.3 B). Angiogenic functions between the two developmental days were quantified and compared. Analysis indicated angiogenic growth in the brain at this stage of development. There were significant increases in the total number of filopodia, vessel length and lumenised length between E12.5 and E13.5 (Table 4.1).

A

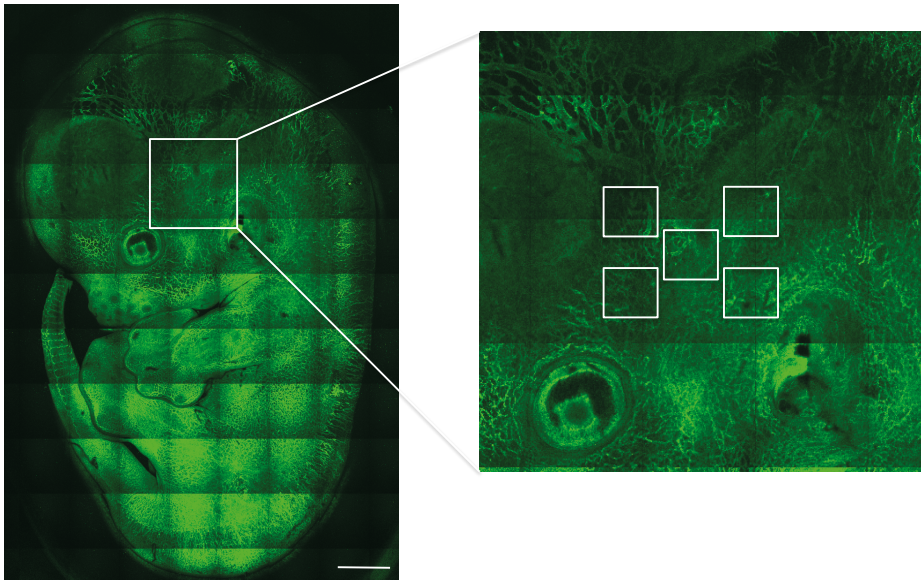

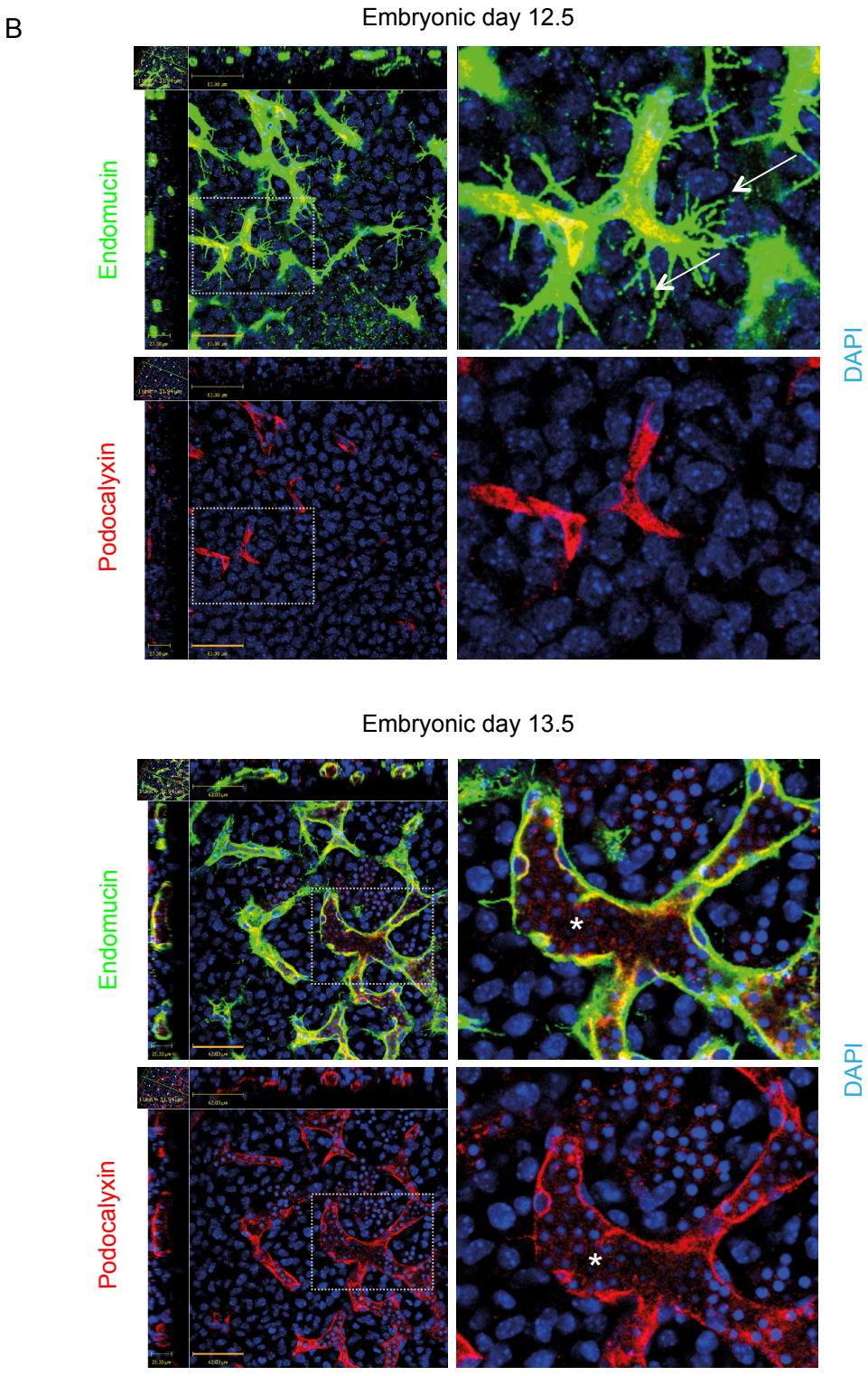

Figure 4.2 Sprouting and lumen formation at E12.5 and E13.5 in wild type embryos
Whole mount confocal imaging of immunofluorescent staining of E12.5 and E13.5 wild type mouse embryos. (A) Left hand image, whole mount tile imaging of a E13.5 embryo stained for endomucin (green) (the image was assembled from XYZ images using Volocity software, Perkin Elmer). Scale bar = 1mm. Right hand image shows the position of the 5 areas quantified for analysis. (B) Endomucin (green) and podocalyxin (red) staining of angiozone for analysis. White arrows point to filopodia, stars mark blood vessel lumens. Scale bar = 62μm

Counts per 40x image	**E12.5**	**E13.5**	***p value***
Filopodia	47.4 (+/- 3.19)	69.2 (+/- 3.05)	1.60E-05
Tip cells	0.95 (+/- 0.184)	1.2 (+/- 0.186)	0.347
Filopodia per tip cell	5.2(+/- 0.36)	6.8(+/- 0.35)	0.003
Branch points	14.3 (+/- 1.4)	17.7 (+/- 1.6)	0.115
Lateral filopodia per length	0.051	0.059	0.326
Total vessel length (μm)	872.3	1080.9	0.003
Total lumenised length (μm)	283.1	568.6	2.10E-05
Lumenised length (% total)	34.4	52.9	0.003

Table 4.1. Angiogenic growth and lumen formation at embryonic days E12.5 and E13.5
Measures of angiogeneic functions at embryonic days 12.5 and 13.5 in the wild type mouse embryo. Confocal images in the angiozone were analysed for angiogenic functions. Values represent measurements within a 30μm z-stack image for each image. n=number of Z-stacks: E12.5 n=20, E13.5 n=20; 4 embryos per embryonic day, 5 images per angiozone. p values calculated from student T tests.

4.4 ROCK2 controls endothelial cell filopodia formation and vascular integrity

To investigate the influence of ROCK2 on actin dynamics I determined the abundance of filopodia on the developing vessels within the angiozone in knockout embryos and wild type littermate controls. Filopodia are actin-rich structures that sense the external environment during endothelial tip migration and sprouting (Mattila and Lappalainen, 2008). As with the angiozone characterisation, 3D Z-stack reconstructions of areas within the angiozone were generated using confocal microscopy and filopodia in each image counted by scrolling through the entire z-stack. Characterisation of the blood vessels closer to the skin in the angiozone showed increased endothelial filopodia in the *Rock2*$^{-/-}$ mice compared with the wild type littermate controls (Figure 4.3). ROCK is a known kinase for LIMK 1 and 2 and also controls MLC 2 phosphorylation (Maekawa *et al.*, 1999) which in turn phosphorylate the actin binding and severing protein cofilin (Ohashi *et al.*, 2000), and controls actomyosin contractility respectively. It is therefore expected that loss of ROCK activity may lead to an abundance of, and slower turnover or defective retraction of actin based filopodia.

Evidence of defects in vascular integrity were also seen in the angiozone with blood cells found outside the blood vessels in the *Rock2*$^{-/-}$ embryos only (Figure 4.4). These observations were consistent with points of haemorrhage identified through earlier macroscopic observations in the E13.5 Rock2$^{-/-}$ embryos.

Embryo sections at the level of the heart stained for endomucin by immunohistochemistry also showed increased filopodial-like structures supporting further the idea that in the absence of ROCK2 endothelial cells are defective in turning over or retracting filopodial protrusions and consequently the vasculature of the Rock2$^{-/-}$ embryos retains a sprouting phenotype when compared with wild type controls (Figure 4.5).

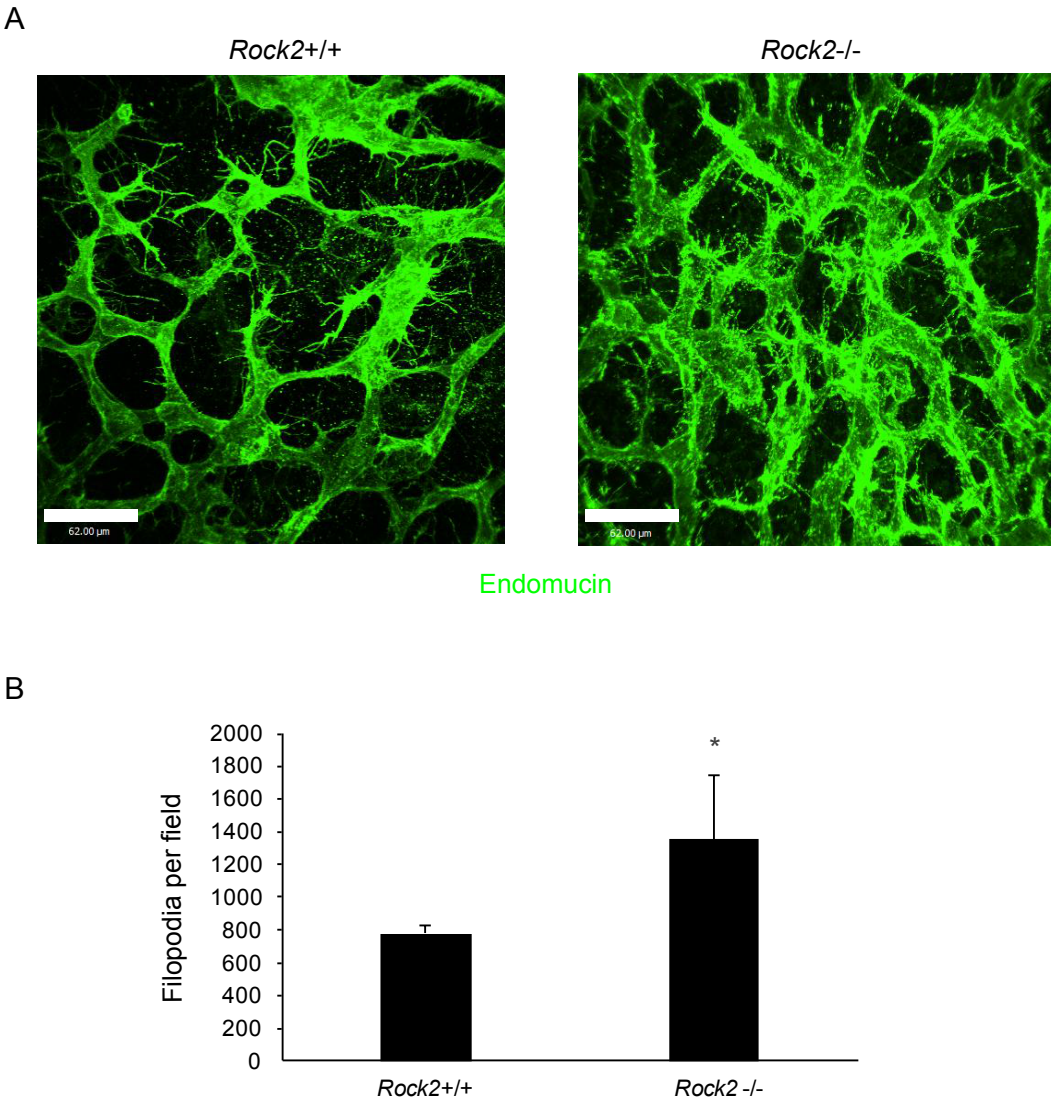

Figure 4.3 Increased filopodial sprouting in cerebral blood vessel in *Rock2* knockout embryos
Filopodial protrusions were assessed by wholemount confocal imaging of the angiozone in E13.5 *Rock2*$^{+/+}$ and *Rock2*$^{-/-}$ mouse embryos stained for endomucin. (A) Representative images of filopodia in *Rock2*$^{+/+}$ versus *Rock2*$^{-/-}$ embryos. Scale bar = 15µm. (B) Bar chart of filopodia counts of E13.5 *Rock2*$^{+/+}$ versus *Rock2*$^{-/-}$, n=15 images (Z-stacks) from embryos from each genotype *Rock2*$^{-/-}$ versus *Rock2*$^{+/+}$ littermate controls. Statistical significance was calculated using a two tailed student T-test. * = $p<0.05$.

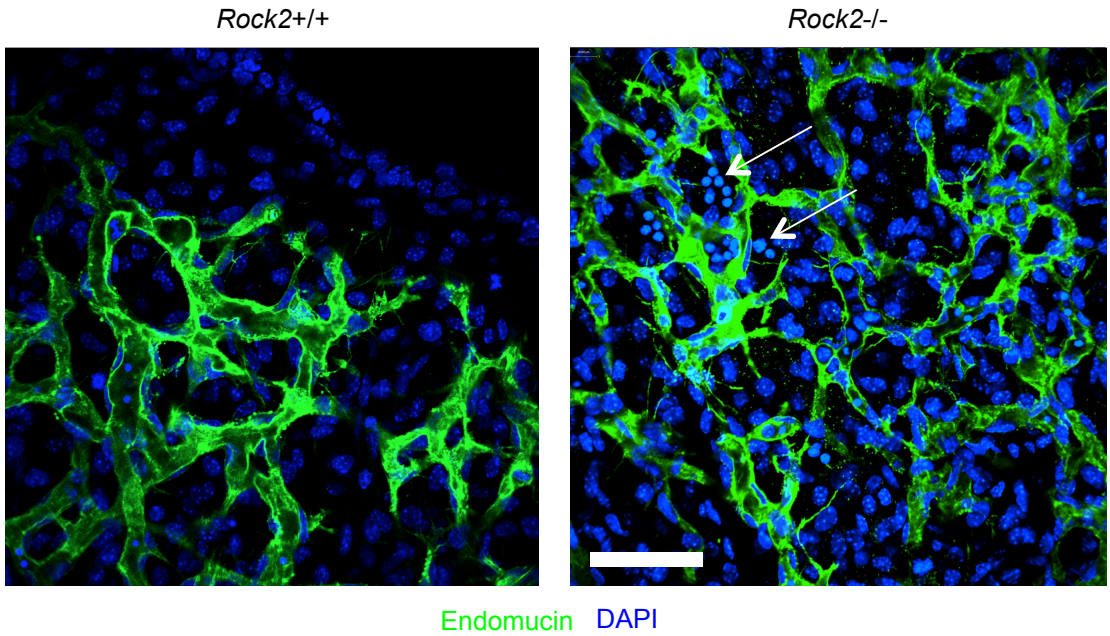

Figure 4.4 Altered vascular integrity in cerebral blood vessel in *Rock2* knockout embryos
Representative images of blood vessels in *Rock2*$^{+/+}$ versus *Rock2*$^{-/-}$ embryos show blood cells outside the vasculature in *Rock2*$^{-/-}$ embryos only. Scale bar = 15μm.

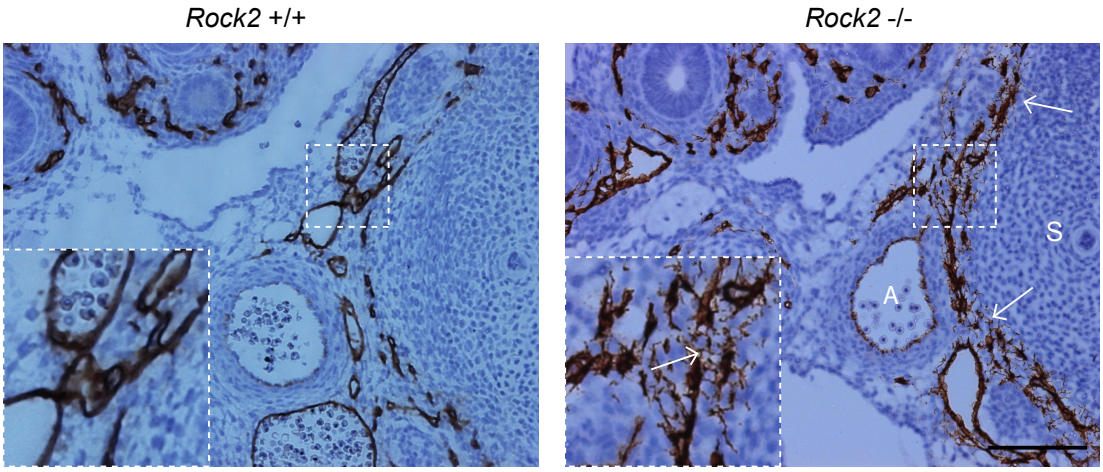

Figure 4.5 *Rock2* knockout embryos show increased filopodia formation in developing blood vessels at the heart level

Transverse sections taken at the level of the heart stained for vascular marker endomucin in embryos at E13.5. Immunohistochemical staining for endomucin in the major vessels at the heart level in *Rock2* $^{-/-}$ and *Rock2* $^{+/+}$. Note the prominent filopodial like structures in nascent blood vessels stained for endomucin (white arrows). Dashed box; zoomed region of hyper-filopodia phenotype. Note increased sprouting in the vessels around the aorta and spinal column in the *Rock2*$^{-/-}$ embryo. A= Aorta, S=spinal column. Scale bar = 30μm.

4.5 ROCK2 controls the morphology of the major vessels during development

To further determine the effect of loss of *Rock2* in blood vessel development, sections from the heart were stained for endomucin and CD31 to assess any effect on major blood vessels. These blood vessels differ significantly from vessels in the parenchyma as they experience a much greater flow rate and pressure and must withstand greater forces. They are also encompassed within numerous levels of mural cells which are known to play important roles in vasodilation and vasoconstriction.

Sections taken at the level of the heart confirmed loss of ROCK2 expression in the *Rock2*$^{-/-}$ mice (Figure 4.6). As with the haemorrhaging seen in the neck and head, it was immediately evident that there was significant haemorrhage in the pericardial cavity of majority of the *Rock2*$^{-/-}$ animals, with blood cells found outside the vascular network and heart and within the cavity itself (Figure 4.6 A-B). High levels of ROCK2 expression are seen in the heart and especially in the epicardium outer layer of the heart wall (Figure 4.6 A-B). Intriguingly, the epicardium layer in the *Rock2*$^{-/-}$ mice is seen to be fractured and discontinuous which may be contributing to the haemorrhaging and leaking of blood cells seen around the heart and in the pericardial cavity.

To assess the effect of loss of *Rock2* on the major blood vessels, analysis of the aorta was carried out. Aortas were measured for diameter, area and circularity in both wild type and *Rock2* knockout embryos. *Rock2* knock-out aortas showed increased aortic area and abnormal circularity when compared with wild type (Figure 4.7A-B). Increased aortic diameter is associated with aortic abnormalities, aneurisms and cardiovascular degeneration as a result of old age (Daugherty and Cassis, 2004). Staining also showed inconsistent mural cell coverage of the aorta (Figure 4.7A) with some areas of the aorta completely lacking mural cell coverage and other areas showing increased mural cell layers surrounding the vessel.

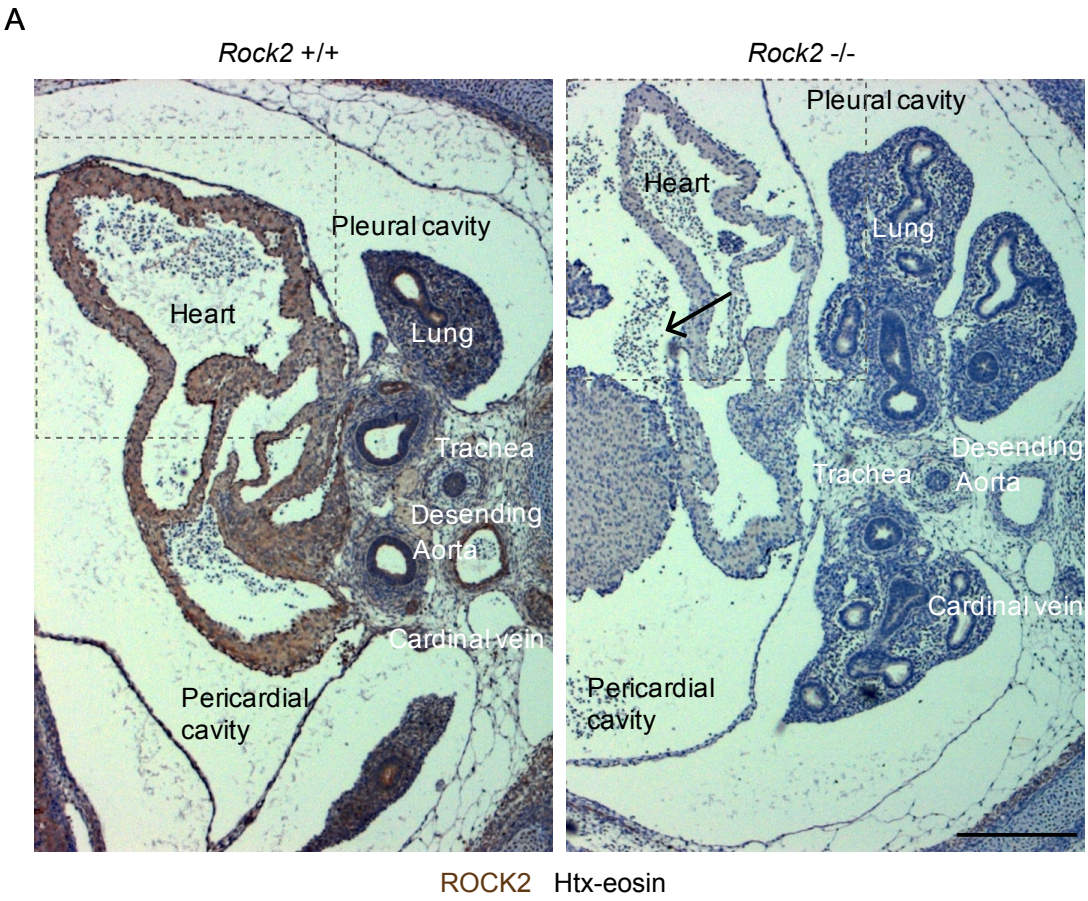

Figure 4.6 *Rock2* controls vascular integrity in the heart
Transverse sections taken at the level of the heart stained for ROCK2 expression in embryos at E13.5. (A) Immunohistochemical staining for ROCK2 expression in the major vessels of the heart in ROCK2 $^{-/-}$ and ROCK2 $^{+/+}$. The heart and the major vessels show strong ROCK2 expression. Black arrow shows blood cells found outside the heart chambers. Scale bar = 100μm. (B) Zoomed inserts from (A) showing heart High levels of ROCK2 expression in *Rock2*$^{+/+}$ sections. Black arrow indicated blood cells outside heart chambers. Scale bar 50μm.

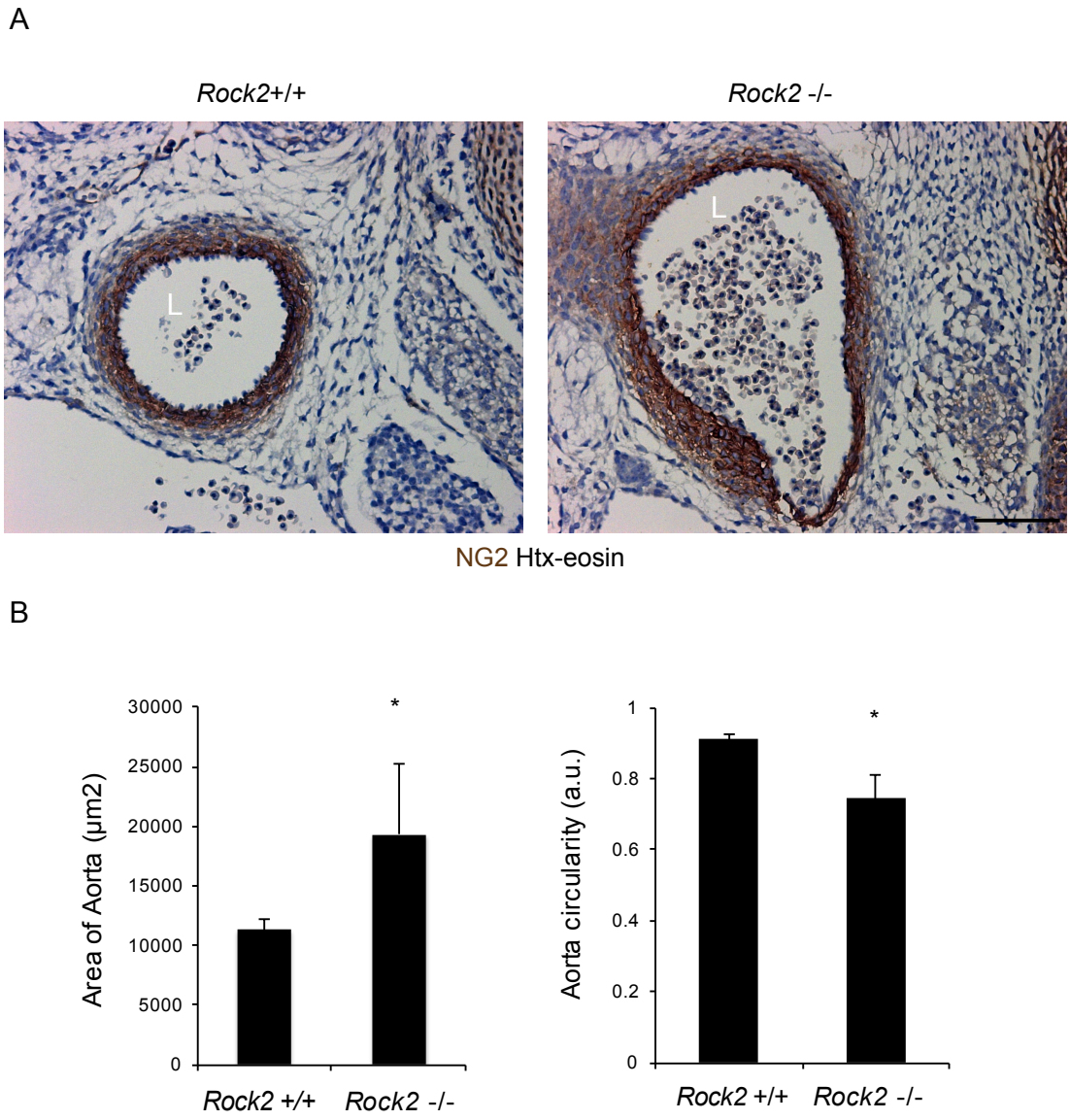

Figure 4.7 Loss of *Rock2* affects aortic diameter and expansion
Transverse section taken at the level of the heart showing the descending aorta stained for the mural cell marker NG2. (A) Representative images of the aorta of wild type and *Rock2* $^{-/-}$ E13.5 embryos. (B) Bar graphs of aorta area and circularity (n=number of embryos *Rock2*$^{+/+}$; n=4, *Rock2*$^{-/-}$; n=4). Significance was calculated using a two tailed equal variance student T-test. * = $p<0.05$. Scale bar = 100µm.

4.6 ROCK2 controls blood vessel diameter and lumen density during angiogenic development

Filopodia are associated with active and dynamic endothelial cell tips cells during sprouting angiogenesis. However, in order to mature and form functional lumens capable of carrying blood, endothelial cells must downregulate sprouting activity. Given that filopodial protrusions persisted in the *Rock2* knockout embryos this led me to assess any potential effects on lumen formation. For this purpose, I chose to look at blood vessel lumens in the brain parenchyma by immunohistochemistry as this provides a large amount of lumens for study and multiple sections for different anti body staining. Sections at the foramen of Monro were sectioned and stained by immunohistochemistry for endothelial blood vessel marker CD31. Transverse sections at the level of the interventricular foramen of Monro were taken and blood vessels within the entire parenchyma of both hemispheres were measured (Figure 4.8). There were no differences in the overall numbers of vessels in the *Rock2*$^{-/-}$ mice compared to wild type controls (Figure 4.9), however, *Rock2*$^{-/-}$ embryos showed reduced numbers of blood vessels with open lumens when compared with wild type littermate controls (Figure 4.9). On further investigation, the lumens that persisted in the *Rock2*$^{-/-}$ embryos were of larger calibre (Figure 4.9). Given that *Rock2* loss is global in these mice, effects on blood vessel size and stability may have due to loss of *Rock2* in other cell types, such as pericytes. To assess any possible effect of *Rock2* loss on mural cell coverage, NG2 staining was carried out on the same vessels which showed no differences in blood vessel mural cell coverage between *Rock2* knockout mice and wild type controls (Figure 4.10).

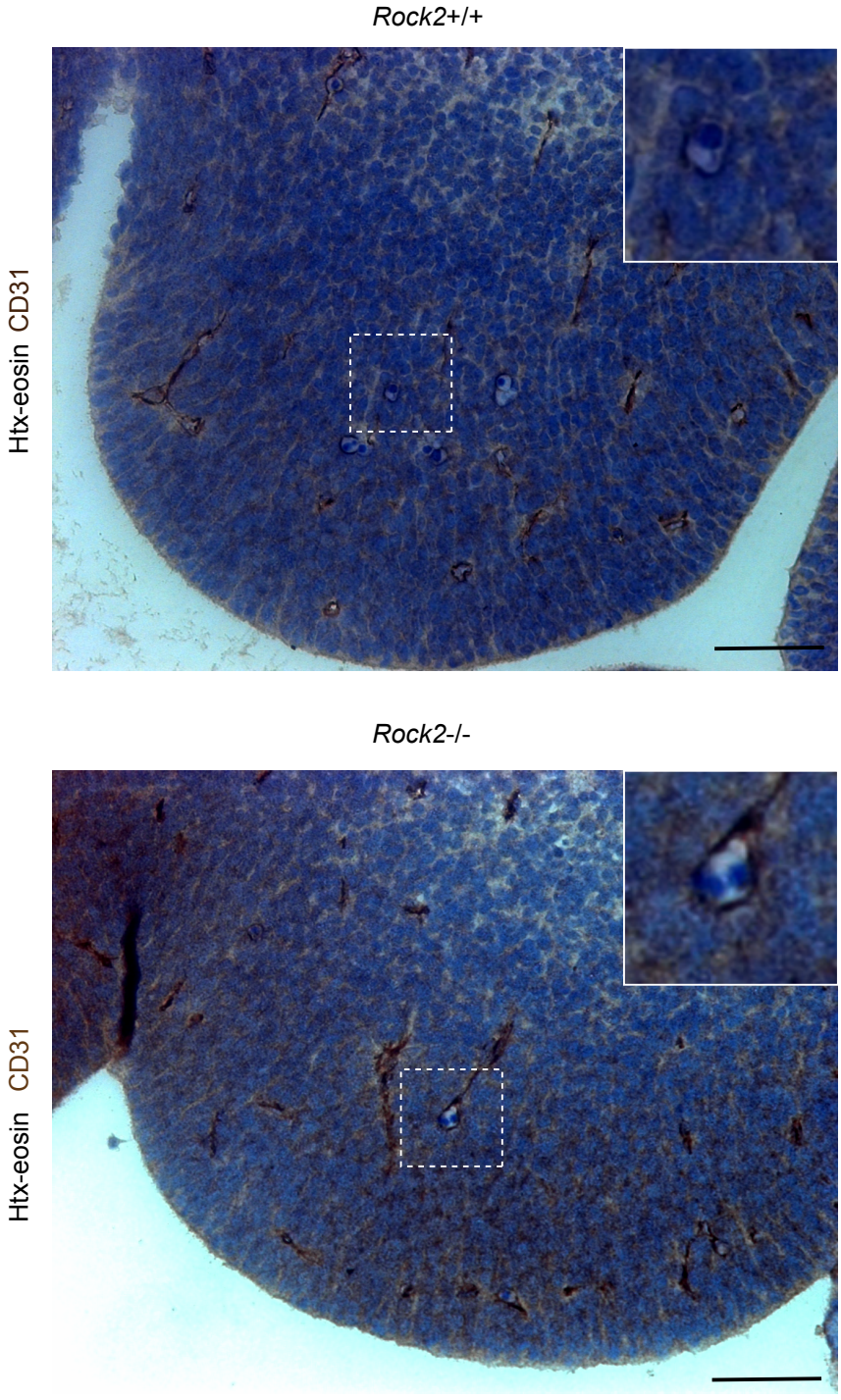

Figure 4.8 *Rock2* controls blood vessel diameter in the parenchyma during development
Transverse sections were taken at the level of the interventricular foramen of Monro and stained for blood vessel marker CD31. Images show representative images of lobes of the parenchyma from sections stained for CD31. Zoomed box inserts shows high magnification example of perfused blood vessel lumens within the parenchyma. Scale bar = 50μm

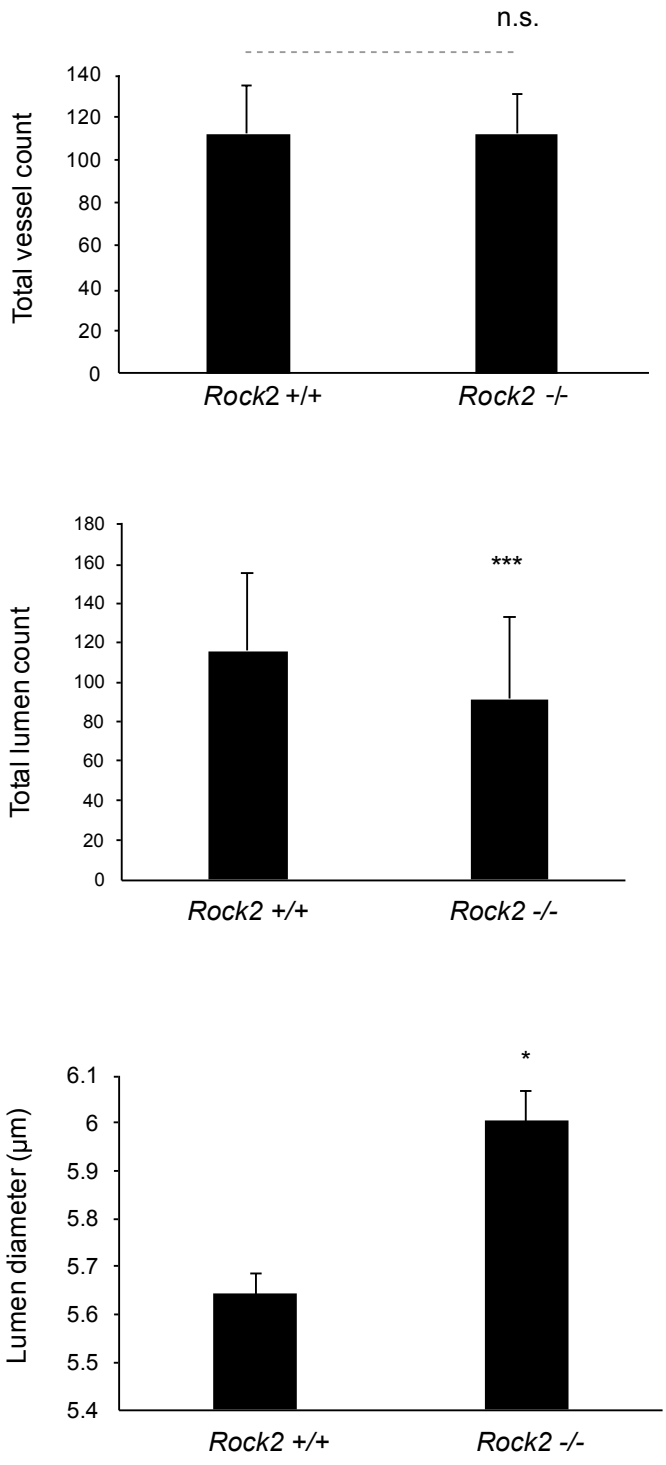

Figure 4.9 *Rock2* controls lumen opening and lumen dynamics during development
Transverse sections taken at the level of the interventricular foramen of Monro, stained for blood vessels marker CD31 were used to measure lumens between *Rock2* $^{+/+}$ and *Rock2*$^{-/-}$. Bar charts show total vessel count, total lumen counts and total lumen diameters. Asterisk indicates significant values assessed by T Test with paired values. n= 3 embryos per genotype (*Rock2* $^{+/+}$, *Rock2* $^{-/-}$ littermate controls). Statistical significance of pair-wise comparisons was calculated using a two-tailed student T-test. * = $p<0.05$, ***=$p<0.001$.

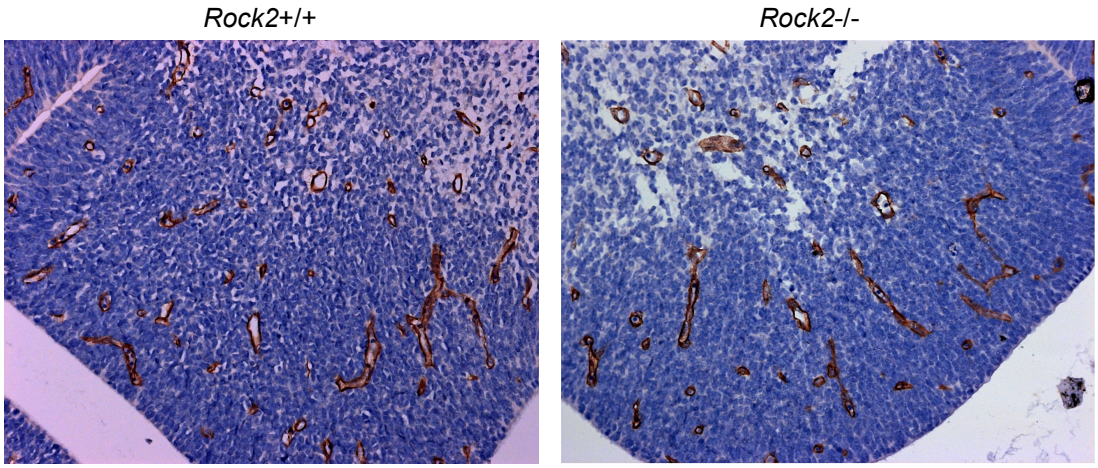

Figure 4.10 Mural cell coverage is not affected in *Rock2*$^{-/-}$ parenchymal vessels
Transverse sections taken at the level of the interventricular foramen of Monro and stained for mural cell marker NG2. Representative images of NG2 coverage in vessels of the parenchyma in *Rock2*$^{-/-}$ and *Rock2* $^{+/+}$ littermate controls.

4.7 Conclusions

Rho signalling through the Rho kinases results in diverse changes in the organisation of the actin cytoskeleton that controls shape and movement of all cells. Precise regulation of the actin cytoskeleton is essential for endothelial cells as they adopt intricate morphologies during migration, sprouting and the process of lumen formation. Rho Kinases (ROCKs) act downstream of Rho and convert its kinase activity into multiple different actin-related outputs including the regulation of MLC, stress fibre formation and contractility (Riento and Ridley, 2003).

There is growing evidence that Rho/ROCK plays an important pathophysiological role in cardiovascular disease. Increased ROCK activity has been shown to play roles in vascular smooth muscle cell contraction, endothelial dysfunction, recruitment of inflammatory cells and in vascular remodelling which are hallmarks of a range of vascular diseases (Surma, Wei and Shi, 2011). Those phenotypes are also commonly followed by extensive neovascularization, a process of new growth in damaged areas to overcome blockage or restriction of blood flow. A range of small molecule inhibitors that target ROCKs are available, and early results have shown positive effects in treating some of the features of vascular diseases including vaso-hyper constriction, hypertension and artery stiffness (Shimokawa and Rashid, 2007; Surma, Wei and Shi, 2011; Shi and Wei, 2013). To fully understand the lasting effect of these inhibitors on vascular diseases, it is important to study ROCK signalling in healthy endothelial cells. As neovascularization is such an important process following a number of these vascular diseases, it is imperative to understand the fundamental role of ROCKs in endothelial cell biology and ultimately in angiogenesis.

In this chapter I have investigated the role of ROCK2 in angiogenesis and blood vessel development in the mouse embryo. In previous *Rock2* genetic deletion studies, 10% of ROCK2 KO mice survived and were born as runts (Thumkeo *et al.*, 2003). Interestingly the surviving animals reported in those studies showed similar phenotypes to the *Rock2*$^{-/-}$ knockout mice analysed in my own work, with pooled blood in the paws that was due to a significant dilation of vessels eventually leading to haemorrhages at E13.5 and defects in limb development (Thumkeo *et al.*, 2003). Macroscopic observation of the mice in our study revealed that embryonic lethality beyond E13.5 was accompanied with improper closing of the abdomen (omphalocele), disorganized blood vessels and haemorrhages in the head and neck region. Immunoflourescent analysis showed the superficial blood vessels near the developing eye and

ear are highly angiogenic and that there was a considerable degree of lumenisation of blood vessels in this area at this stage of development (Figure 4.2, Table 4.1). *Rock2* knockout mice showed hyper-filopodial protrusions in the angiozone at E13.5 (Figure 4.3). These results show that *Rock2* is required for endothelial cell quiescence and they are in agreement with previous studies using tissue culture organotypic assays (Abraham *et al.*, 2009) which had shown that ROCK2 knockdown stimulates sprouting.

Lumen length measures using podocalyxin at the angiozone in the *Rock2*$^{-/-}$ mice would have been an interesting readout, however, due to the limited number of *Rock2*$^{-/-}$ embryos available from the breedings, immunohistochemical analysis of sectioned embryos provided the best use of available embryos as multiple sections can be stained with different antibodies. When the vessels of the brain parenchyma were analysed for vessel lumen size using immunohistochemistry, *Rock2* knock-out mice showed a significant decrease in the abundance of blood vessels with open lumens. On the other hand, the overall number of blood vessels within the parenchyma remained the same but a significant decrease in perfused lumens was observed. These experiments show that ROCK2 is necessary for the formation of blood vessel lumens from nascent blood vessels. Interestingly, the persisting lumens were shown to be of somewhat larger lumen diameter when compared the wild type littermates at the same developmental stage. This may suggest that perfused ROCK2 knock-out lumens are attempting to compensate for lack of overall perfused vessels by expanding to meet the oxygen and nutrient demands during this rapid embryonic growth.

One limit of using the global *Rock2* knockout is that loss of *Rock2* is seen in all cell types and it is not endothelial specific. This must be taken under consideration when assessing the effect of loss of *Rock2*. These results show that there are no changes in pericyte coverage (Figure 4.10) of the parenchymal vessels but we cannot exclude the possibility that other cell type may influence angiogenesis. For example, the apparent changes in smooth muscle cells are likely to account for changes in diameter and shape observed in aortas of *Rock2* null mice (Figure 4.7)

Chapter 5

The role of Rho-associated kinases in Cilia Formation in Endothelial Cells

5.1 Introduction

Primary cilia are cellular organelles that are composed of microtubules that play a role in a huge range of mechanosensation, chemosensation, and signal transduction pathways. Endothelial cilia have been implicated in flow sensing in blood vessels and vascular remodelling in the zebrafish (Goetz *et al.*, 2014). They have also been identified in areas of disturbed flow in vasculature linked with atherosclerosis, but their exact role in blood vessels is not fully understood (Van der Heiden *et al.*, 2008). Although primary cilia are mainly microtubule-based structures, the actin cytoskeleton and its regulation seems to play an important role on ciliogenesis and cilia maintenance. Effectors of actin cytoskeletal dynamics have also been shown to have profound effects on cilia and their function. As an effector of actin dynamics, Rho-associated kinase (ROCK1 and 2) signalling has recently been shown to have a significant influence on ciliogenesis. This pathway has also been previously implicated in many aspects of angiogenesis and lumen formation (Bryan *et al.*, 2010; M. Kim *et al.*, 2015). In this chapter I investigate what effect the Rho-associated kinases have on ciliogenesis in endothelial cells and retinal pigment epithelial cells (RPE) *in vitro* and *in vivo*.

5.2 Cultured human vascular endothelial cells ciliate in the organotypic angiogenesis assay

To characterise the role of ROCK signalling within endothelial primary cilia, the presence of primary cilia on endothelial cells *in vitro* was investigated. Primary human umbilical vein endothelial cells (HUVEC) were first tested in culture. To identify cilia, HUVEC were grown to high confluence in monolayers (Iomini *et al.*, 2004) where they take on the expected cobblestone-like appearance associated with ciliogenesis. After reaching cobblestone confluence, HUVEC were serum starved to halt proliferation and induce ciliogenesis (Geerts *et al.*, 2011). To identify primary cilia on HUVEC, an antibody against the small GTPase ARL13B was used. ARL13B is a prenylated cytoplasmic protein that localizes to the ciliary membrane of primary cilia during and after ciliogenesis and known to be involved in cilia maintenance (Larkins *et al.*, 2011). When probed by immunofluorescence for ARL13B, HUVEC showed the positive localized staining characteristic for cilia on a small number (<1%) of cultured cobblestone HUVEC (Figure 5.1 A). The distribution of primary cilia was investigated in the HDF-HUVEC co-culture assay, for which tubes with lumens can be observed as shown in Chapter 3 (Figure 3.6). Investigation of the presence of cilia at two stages of the model system was analysed, prior to and post lumen formation. At day 7 after seeding HUVEC onto confluent fibroblasts, HUVEC show an elongated phenotype and form tubules although they are still

proliferating. Staining for ARL13B at this time point did not detect cilia on tubules, potentially due to the proliferative state of the endothelial cells (not shown). In contrast, at day 14 when lumens formed in the assay as visualized by podocalyxin staining, short cilia (~1-2μm) could be detected on a proportion of HUVEC (Figure 5.1 B). Interestingly, all cilia appeared on the luminal site of the tubes, consistent with the proposed function of cilia in sensing flow in the luminal site. Fibroblasts in the assay showed longer cilia (~5μm) throughout (Figure 5.1 B).

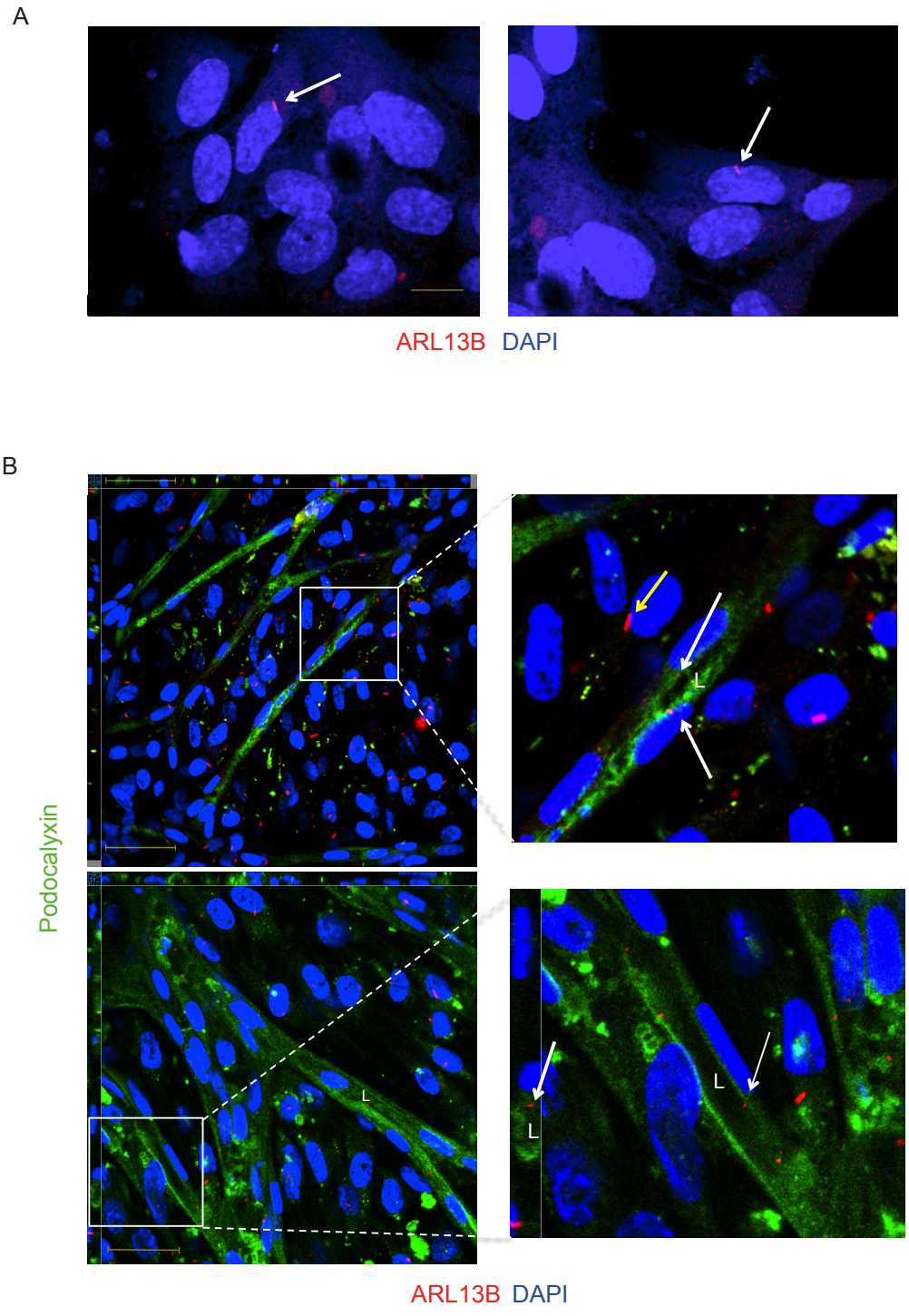

Figure 5.1 Cilia identification on endothelial cells growing in a monolayer and in the HUVEC-HDF coculture model

(A) Confluent HUVEC in monocultures were serum starved for 24 hrs, and then fixed and stained for cilia marker ARL13B and DAPI. Scale bar = 12μm. (B) HUVEC-HDF coculture assay stained for cilia marker ARL13B and luminal marker podocalyxin 14 days after seeding HUVEC onto HDFs. White arrows indicate positive ARL13B cilia staining on HUVEC, yellow arrow indicates positive ARL13B staining on HDF cells; L, lumens. Scale bar = 59μm.

5.3 Microvascular endothelial cells assemble primary cilia during brain development

To assess endothelial cilia in a more physiological environment I looked at the abundance of primary cilia in the vasculature of developing mouse embryos. As described in chapter 4 section 4.2, an area has been identified termed the angiozone that can be stained and imaged for angiogenic blood vessels during brain development. This region shows intact blood vessel lumens in a plexus of blood vessels that sprout from the carotid artery. As previously shown, this is a suitable area for imaging lumens as embryos can be stained wholemount, for endothelial markers, without the need for dissection. This retains the 3D environment in which the lumens are developing, which also provides a model system to visualize vascular cilia *in vivo*. Embryos were harvested and stained at embryonic day 13.5 (E13.5). As shown in chapter 4 section 4.2, both developing and established blood vessels can be seen at this developmental stage in the angiozone area. ARL13B positive cells can also be seen within vessels walls of open lumens and perfused vessels (Figure 5.2A and B). Similar to the *in vitro* angiogenesis model, the surrounding stromal cell population show prominent ARL13B positive cilia (Figure 5.2A). Similarly, as with the co-culture model, the majority of primary cilia face the apical (luminal) side of the vessel.

Transverse sections at the level of the interventricular foramen of Monro, an area previously discussed in chapter 4 section 4.5, were also stained for the cilia marker ARL13B and endothelial marker endomucin (Figure 5.3) by immunohistochemistry, since those embryos were fixed and embedded in paraffin. Blood vessels within the parenchyma identified with endomucin showed positive staining for ARL13B which identified endothelial cell cilia (Figure 5.3). Cilia were observed on the luminal side of these blood vessels shown in Figure 5.3.

Interestingly, primary cilia were not observed in larger, more established vessels such as the aorta, pulmonary vein and the pulmonary artery (Figure 5.4) consistent with the idea that high levels of shear stress generated by blood flow disassemble primary cilia in vascular endothelial cells (Iomini *et al.*, 2004).

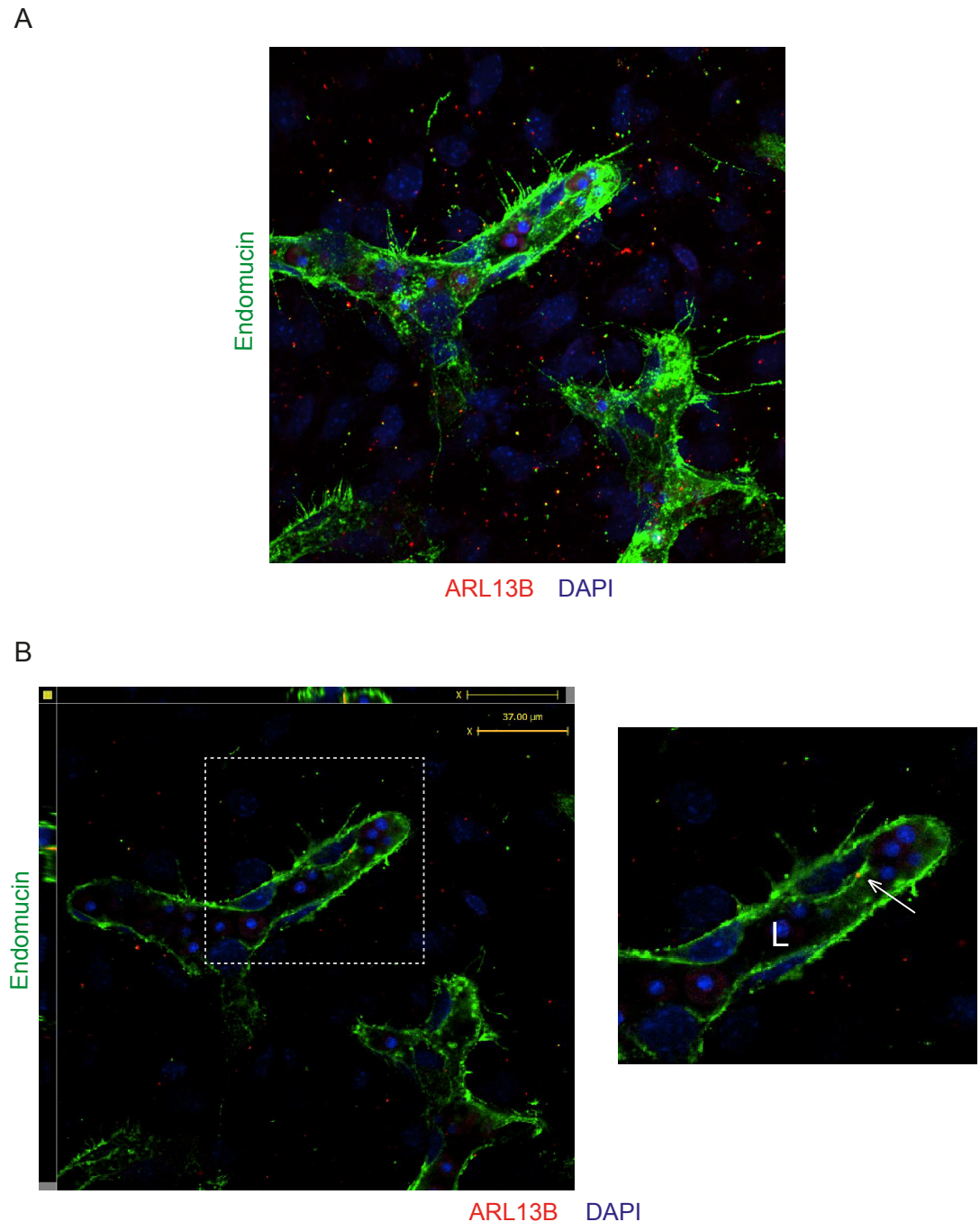

Figure 5.2 Endothelial cilia identification in the angiozone of developing embryos
Angiozone vascular staining in the E13.5 mouse embryo. Immunofluorescence staining of the angiozone for blood vessel marker endomucin (green), cilia marker ARL13B (red) and nuclear marker DAPI (blue). (A) XY compression of angiozone showing total cilia. (B) Single Z-plane showing ARL13B staining in blood vessel. White arrow in the zoomed image points to a cilium in the blood vessel; L, lumen. Scale bar = 37µm.

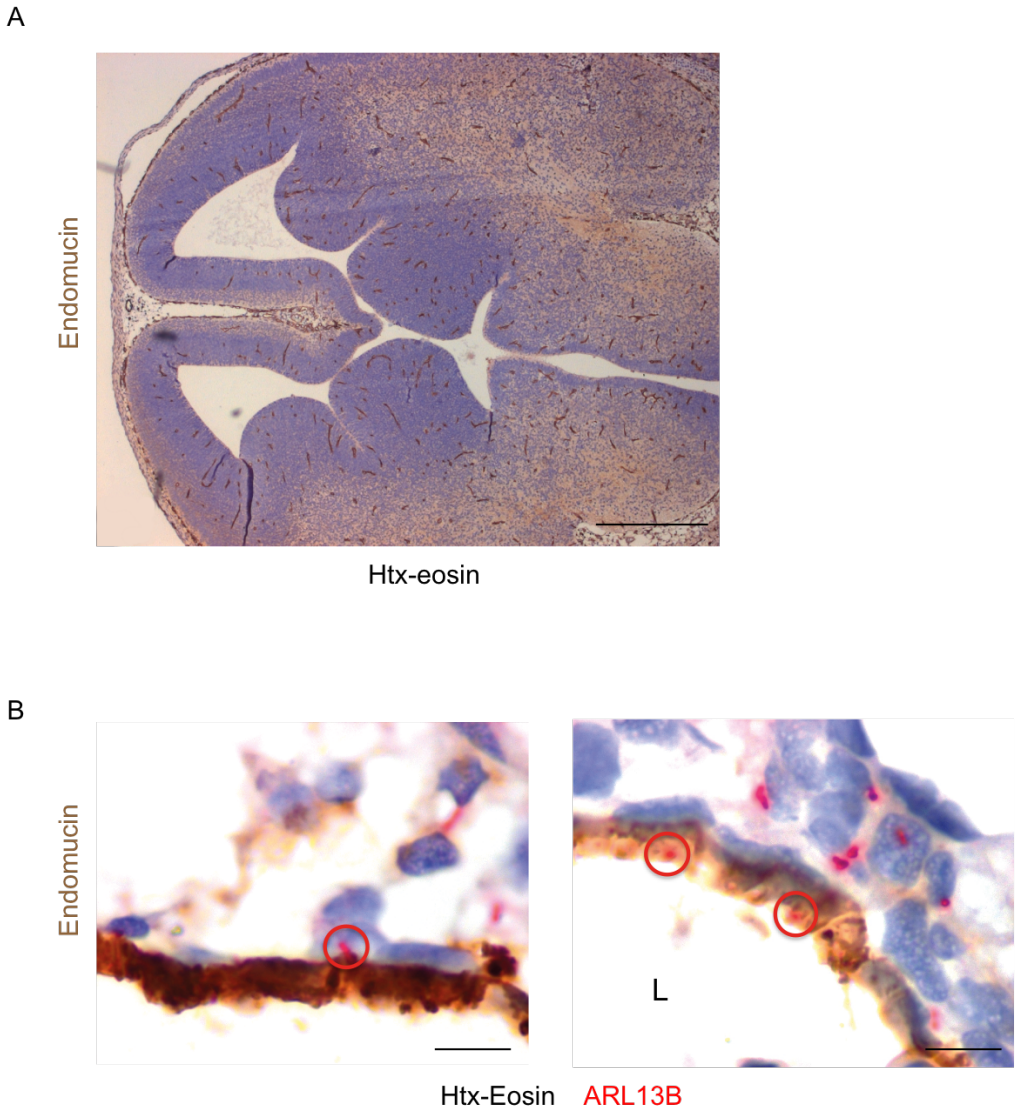

Figure 5.3 Endothelial cilia identification in vessels at the foramen of Monro
Immunohistochemical staining of the brain parenchyma at the level of the foramen of Monro. (A) Transverse section stained for the endothelial marker endomucin (brown), the cilia marker ARL13B (red), and Haematoxylin (Htx) and Eosin. Scale bar = 100μm. (B) Section stained as in (A) visualised at x40 magnification allows detection of ARL13B positive endothelial cell cilia. Note cilia (in red circles) protruding into the lumen. L, Lumen; Scale bar = 10 μm.

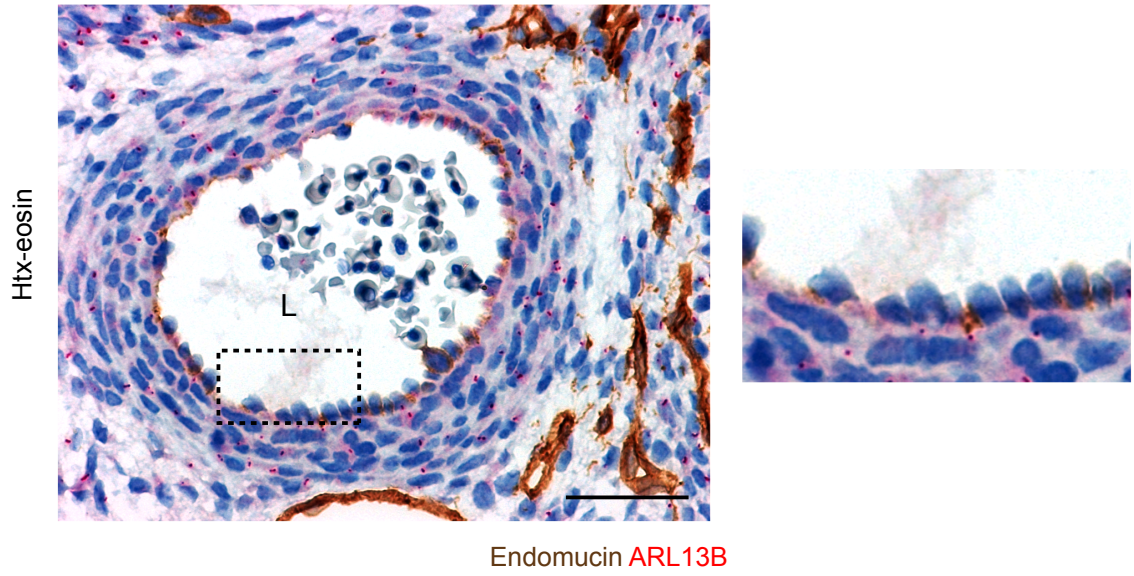

Figure 5.4 Lack of primary cilia in the developing aorta visualised at the heart level
Image shows histology of the developing aorta of a E13.5 embryo from a transverse section taken at the level of the heart, stained for endomucin (brown) and ARL13B (red) by immunohistochemistry. Note the absence of primary cilia within this part of the aorta; L, lumen. Scale bar = 10 μm

5.4 Investigating the role of ROCK in ciliogenesis using an *in vitro* ciliogenesis assay

To analyse the role of ROCK signalling in endothelial cilia, an *in vitro* cilia growth assay was employed (Chapter 2 section 2.2.6). This assay yields monolayers of ciliated cells that can be routinely treated with inhibitors and then stained for immunofluorescence visualization and quantification of cilia. Primary HUVECs were first tested in the cilia growth assay. However, HUVEC *in vitro* produced low and variable numbers of cilia *in vitro* (approximately 1%), which was unsuitable for quantification (Figure 5.1 A).

Since only a small proportion of HUVEC ciliated in monoculture, and in the cocultures only a fraction of tubules developed lumens, alternative endothelial cell lines were acquired and tested. Human cerebral microvascular endothelial cells (HCMECs) and mouse brain endothelial cells (bEnd3) were tested in the assay. Again, only a small proportion of HCMECS (<2%) ciliated. The cells were assessed in the *in vitro* ciliogenesis assay and both cell types were stained for the cilia marker ARL13B and imaged using confocal microscopy. bEnd3 cells showed small perinuclear dots positive for ARL13B in areas expected to display primary cilia at this stage (Figure 5.5). HCMEC were heterogeneous in their morphology, while a small percentage of cells (approximately 1%) showed positive staining for ARL13B (Figure 5.5). Overall, even when grown at higher confluency's and using different serum starvation conditions, the cultured primary endothelial cells and cell lines showed to small a proportion of ciliated cells for routine quantification.

Human retinal pigment epithelial cells (hTERT-RPE1) are commonly used to study cilia *in vitro* as they readily ciliate under appropriate conditions, and their cilia are of a length suitable for measuring and quantification (Rambhatla *et al.*, 2002). RPE1 cells were grown as described in chapter 2 section 2.2.6, and in the assay yielded monolayers of ciliated cells with greater than 90% of all cells extending a cilium (Figure 5.6). Cilia ranging in length from 2-5 μm were observed. This cell line was used for ciliogenesis signalling experiments from hereon.

A

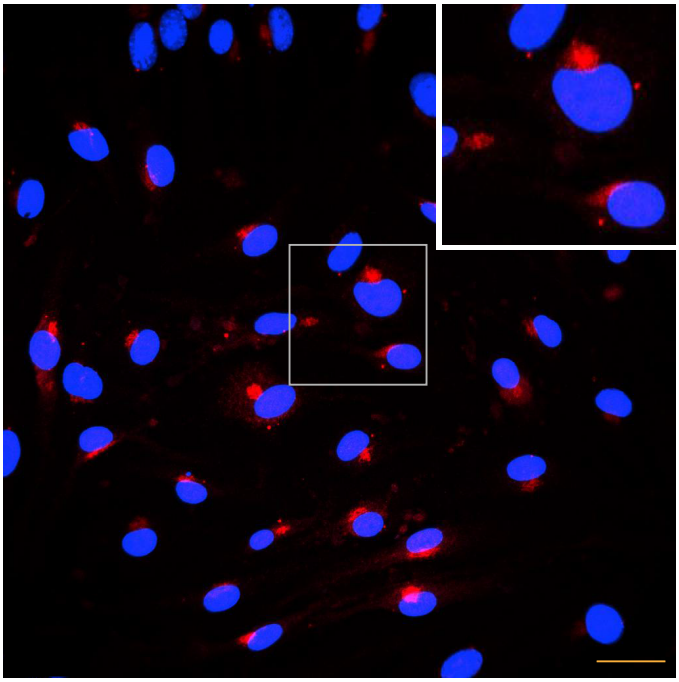

ARL13B DAPI

B

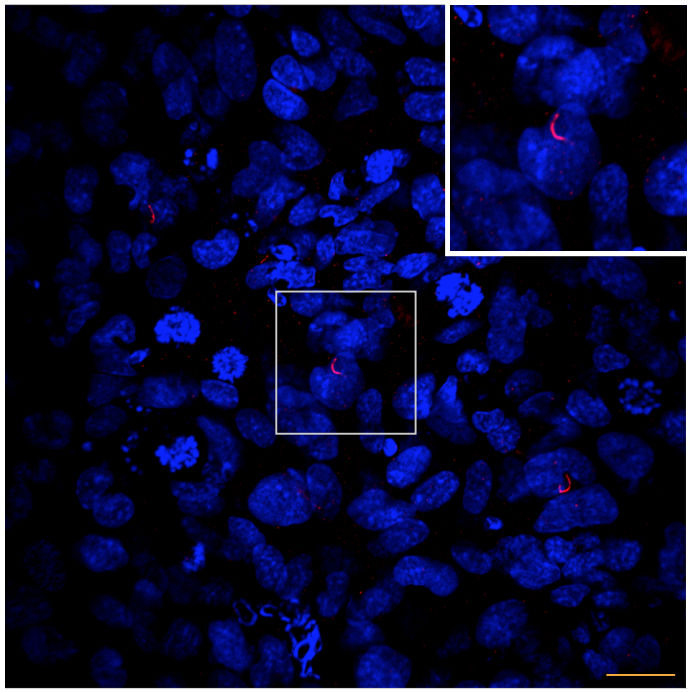

ARL13B DAPI

Figure 5.5 bEnd3 and HCMEC ciliate under serum starvation in culture
bEnd3 and HCMEC cells were seeded at 70 % confluency in 10% FBS DMEM for 24 hours before being serum starved (0.2%FBS) to initiate ciliogenesis for 48 hours prior to fixation. (A) Mouse bEnd3 cells ciliating under serum starvation. (B) Human cerebral microvascular cells ciliating under serum starvation. ARL13B (red), DAPI (blue). Zoomed insets shows individual ARL13B stained cilia. Scale bar = 31μm.

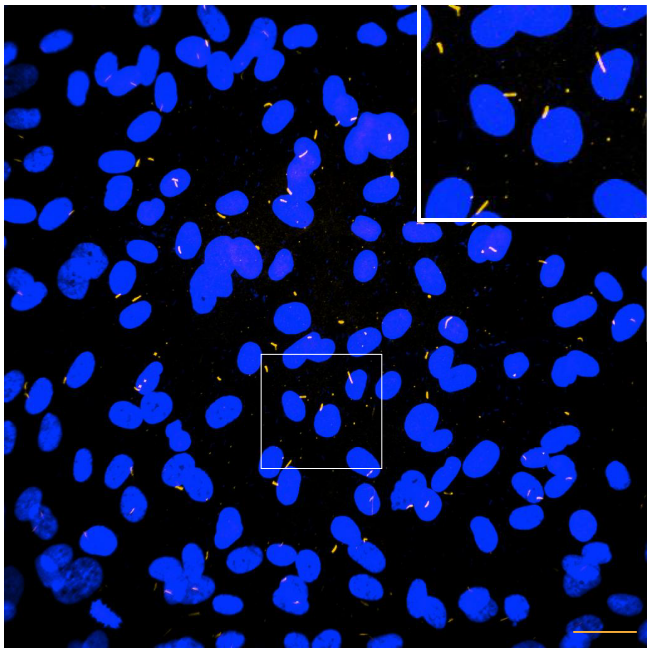

Figure 5.6 hTERT-RPE1 cells ciliate readily under serum starvation in culture
hTERT-RPE1 cells were seeded at 70% confluence in 10% FBS DMEM for 24hr before being serum starved (0.2%) for 48 hours prior to fixation. Image shows ciliated hTERT-RPE1 cells in cilia growth assay, ARL13B (yellow), DAPI (blue). Zoomed inset shows individual ARL13B-stained primary cilia. Scale bar = 31μm.

5.5 Rho kinase (ROCK1/2) controls cilia length and density

Actin plays important roles in cilia maintenance: for example, actin branching activity inhibits ciliogenesis (Malicki and Johnson, 2016). To study the role of the ROCK pathway in ciliogenesis, I used the cilia growth assay and treated the cultures with the commercially available ROCK inhibitor Y27632 (Tocris). The treatment with Y27632 was optimised and showed that treatment on day 2, after the start of serum starvation, gave the highest level of ciliogenesis and two previously optimised doses of 10uM and 50uM were selected. The actin-binding protein cofilin, involved in depolymerising actin, is downstream of ROCK through LIM kinase phosphorylation, and has been shown to enhance cilia formation (Jongshin Kim *et al.*, 2015). Y27632-treated cells stained with the actin marker phalloidin showed a typical ROCK inhibition phenotype (Figure 5.8) with loss of stress fibres. Furthermore, treatment with increasing concentrations of Y27632 gave a significant increase in length of cilia when compared with untreated cells (Figure 5.9). Y27632 treatment at 10μM gave a 20% increase in cilia length compared with control, while treatment with 50μM Y27632 gave mild levels of cytotoxicity in some cells but resulted in a 50% increase in cilia length (Figure 5.10 A). However, there was a corresponding decrease in the number of ciliated cells with both concentrations of Y27632 (Figure 5.10 B). Treatment of cells with 50μM Y27632 gave a 14% decrease in the number of cells ciliated when compared with control (Figure 5.10 B).

Downstream of ROCK signalling, multiple effector proteins influence the actin cytoskeleton through direct effects on actin filaments (Figure 5.7). Blebbistatin inhibits the ATPase activity of non-muscle myosin IIa (Amano *et al.*, 1996). Blebbistatin binds myosin II and blocks its ATPase activity function thereby blocking the effects of MLC2 phosphorylation downstream of Rho signalling. Treatment of hTERT-RPE1 cells with the previously optimised amount of 10μM Blebbistatin in the ciliogenesis assay (Figure 5.11) resulted in significant increases in cilia length compared with control (Figure 5.12). LIM kinase (LIMK) is activated upon ROCK activation and phosphorylates cofilin that in turn inhibits its actin severing ability (Figure 5.7). This results in stabilization of F-actin filaments. Treatment of hTERT-RPE1 cells with a LIM kinase inhibitor (BMS5; SYN kinase (Scott *et al.*, 2010)) in the ciliogenesis assay (Figure 5.11) resulted in increased cilia length (Figure 5.12A). Consistent with results seen in treatment of hTERT-RPE1 cells with Y27632, cells exhibited less cilia when treated with downstream ROCK inhibitors Blebbistatin and Lim kinase inhibitors (5.12B)

To further determine the effect of actin polymerisation on cilia growth, I investigated the effects of treatment with an actin depolymerisation agent for its effect on ciliogenesis. Latrunculin B (Lat B), an actin depolymerising agent that sequesters G-actin and therefore prevents F-actin assembly (McLaughlin, Morton and Ayscough, 2000) was used in these assays. In our published study we optimised Lat B concentrations for blocking actin driven filopodia protrusions without affecting cell viability (Abraham *et al.*, 2015). Treatment of ciliating hTERT-RPE cells with 0.01µg/ml Lat B in the ciliogenesis assay (Figure 5.11) resulted in an increase in cilia length (Figure 5.12A) and decrease in overall cilia numbers (5.12B)

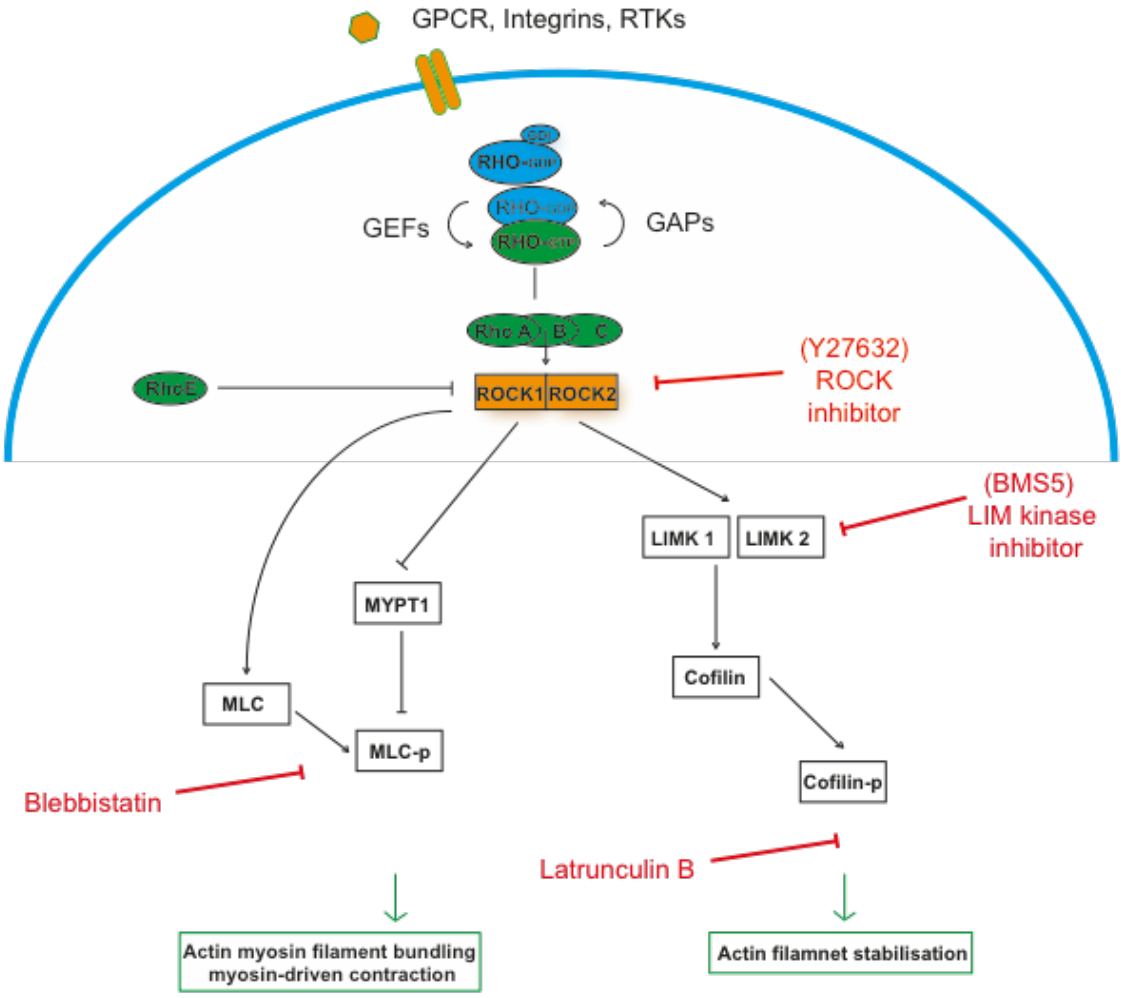

Figure 5.7 Rho/ROCK pathway and inhibitors

The Rho/ROCK signalling pathway indicating the sites of inhibitor activity. Y27632 (ROCK inhibitor) inhibits both isoforms of ROCK (ROCK1/ROCK2) by competing with ATP for binding to the catalytic site. The lim kinase inhibitor, BMS5 inhibits lim kinase 1 and lim kinase 2 equally. Blebbistatin inhibits the ATPase activity of class II myosins. Latrunculin B binds to G-actin and prevents F-actin assembly by reducing the pool of monomeric actin available for filament growth.

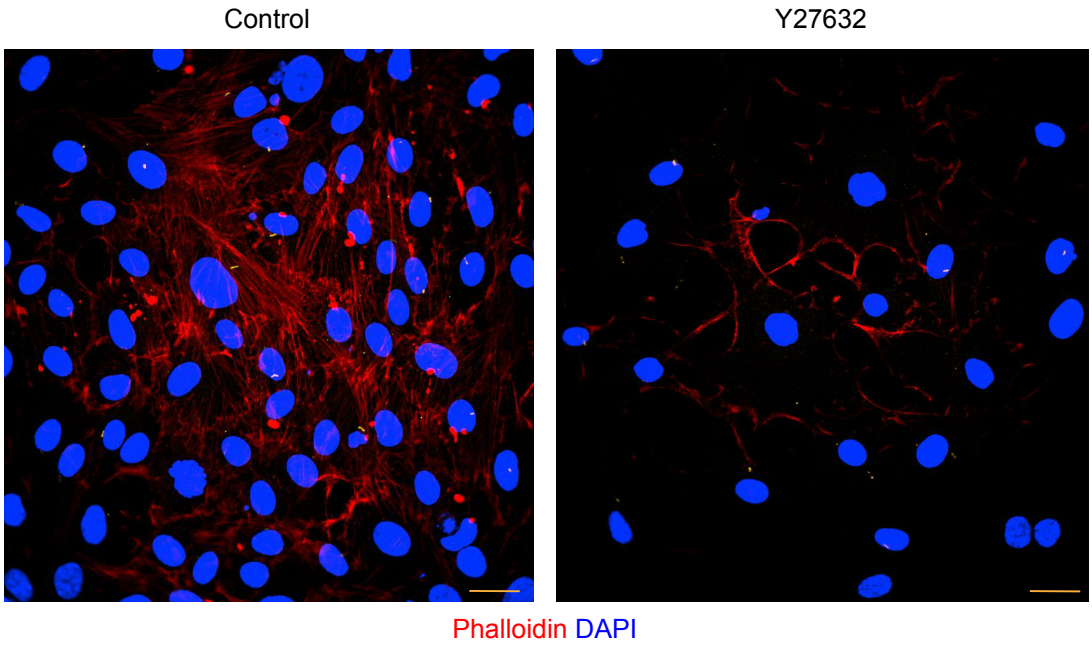

Figure 5.8 Y27632 causes loss of stress fibres in hTERT-RPE1 cells in the *in vitro* ciliogenesis assay

$7x10^4$ hTERT-RPE1 cells were plated in 24 well plates and let grow for 24 hours before being treatment with Y27632 in reduced serum media (0.2% FBS DMEM) to initiate ciliogenesis for 48 hours. Phalloidin stain shows loss of stress fibres in cells treated with Y27632. Scale bar = 31μm.

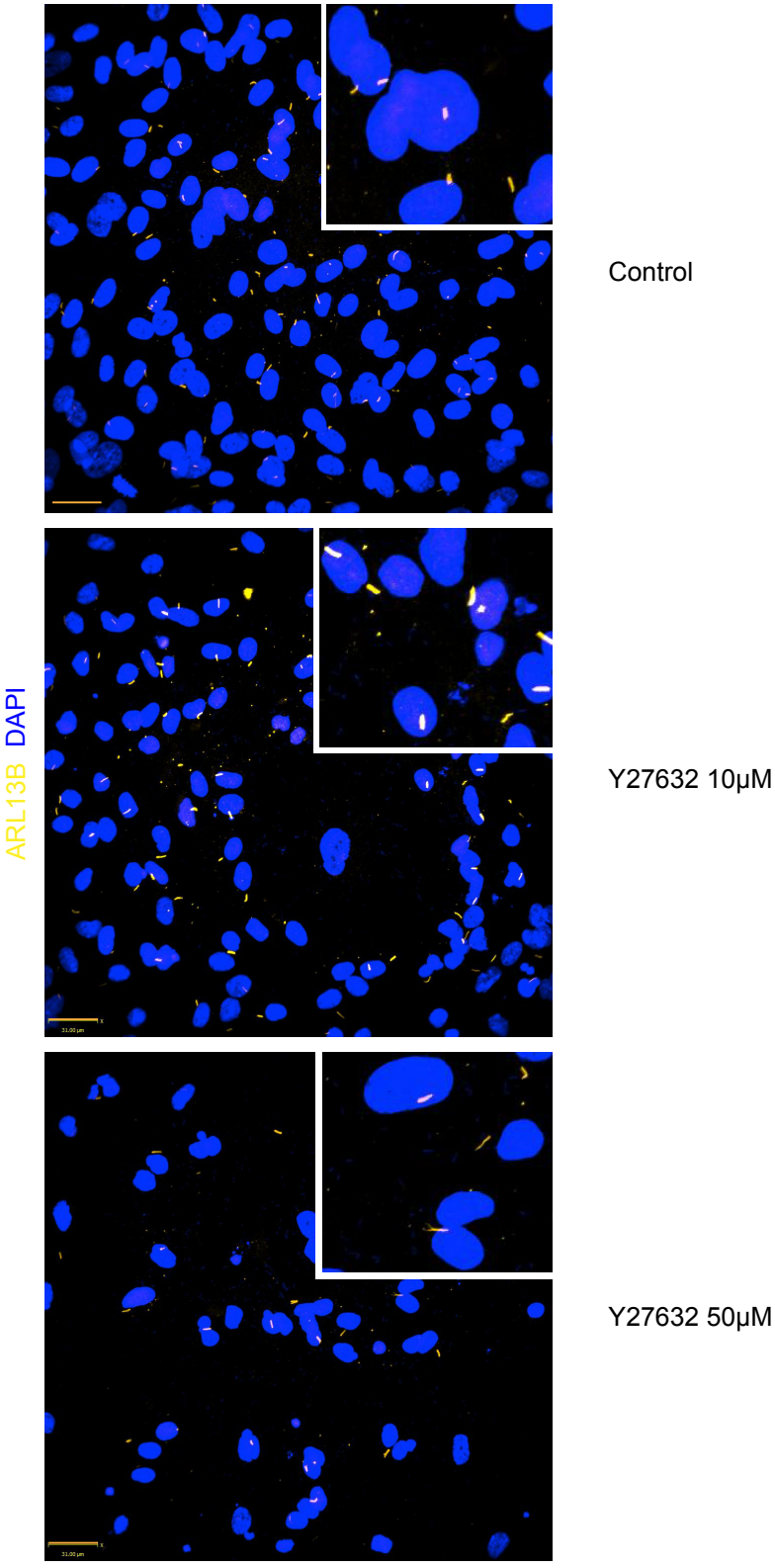

Figure 5.9 Effect of treatment of hTERT-RPE1 cells with the ROCK inhibitor Y27632
$7x10^4$ hTERT-RPE1 cells were plated in 24 well plates and allowed to grow for 24 hours before being treated with Y27632 in reduced serum media (0.2% FBS DMEM) to initiate ciliogenesis for 48 hours. Representative images of ARL13B-stained cilia are shown for control, Y27632 10μM and Y27632 50μM. Zoomed insets show individual ciliated cells. Scale bar = 31μm.

A

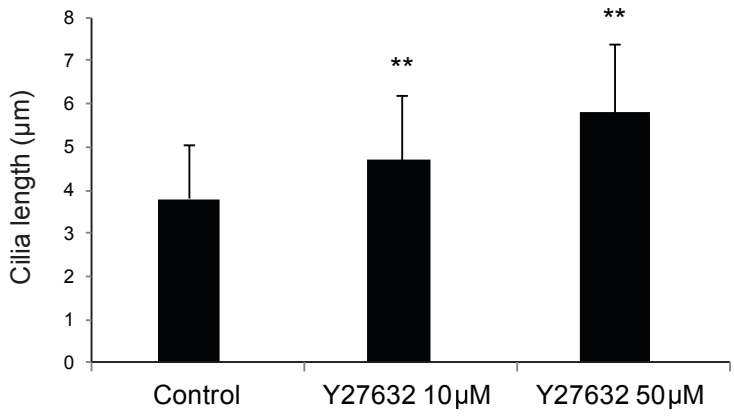

B

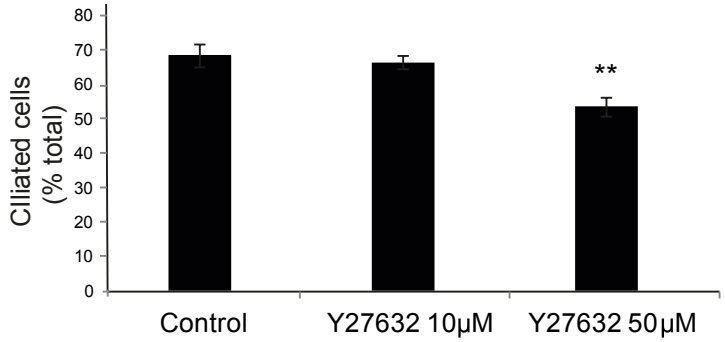

Figure 5.10 Treatment with the ROCK inhibitor Y27632 increases ciliary length and reduces the number of ciliated hTERT-RPE1 cells

$7x10^4$ hTERT-RPE1 cells were plated in 24 well plates and allowed to grow for 24 hours before being treated with Y27632 in reduced serum media (0.2% FBS DMEM) to initiate ciliogenesis for 48 hours. (A) Bar chart shows average cilia length in cells within a 20x microscopic field. Error bars represent S.E.M; N=number of fields (control, 17; Y27632 10µM, 18; Y27632 50µM, 19); from four independent experiments; at least 100 cells were counted per condition in each experiment. (B) Bar chart shows percentage ciliated cells within a 20x microscopic field; Error bars represent S.E.M; N=number of fields (control, 17; Y 10µM, 18; Y 50µM, 19); from four independent experiments; minimum of 100 cells were counted per condition in each experiment. Significance was calculated using a two tailed student T-test. **, $p<0.01$.

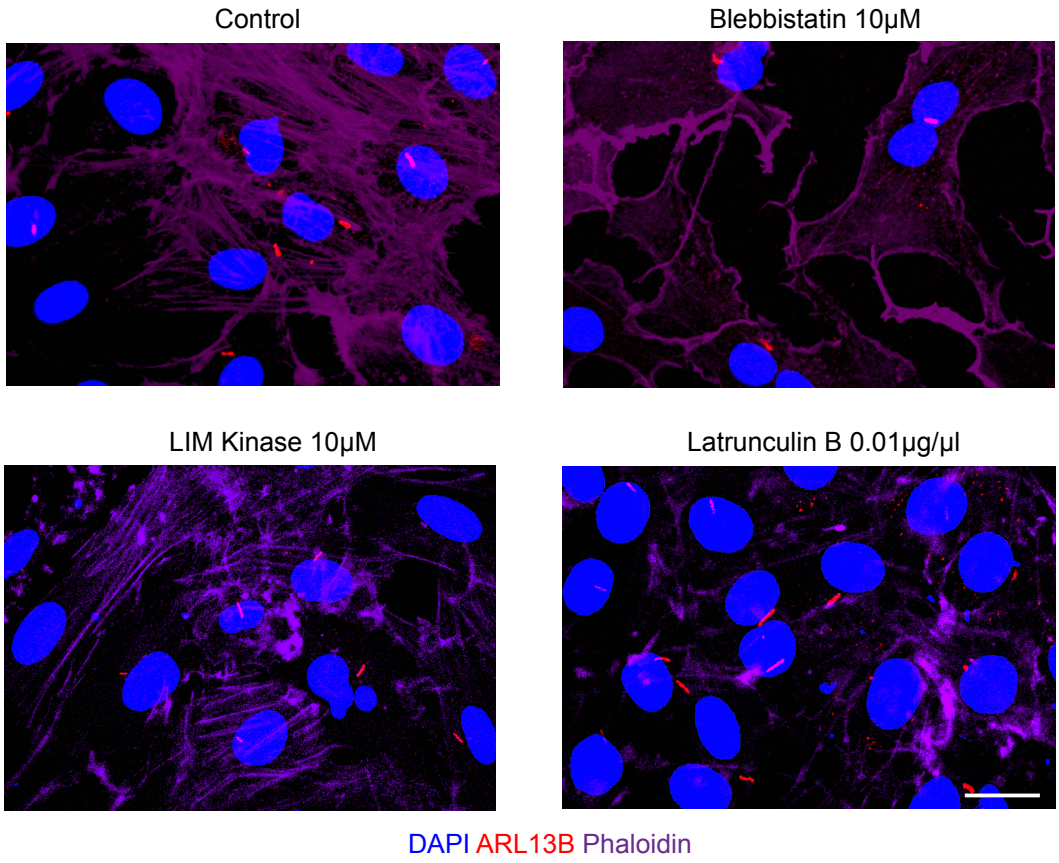

Figure 5.11 Treatment with LIM kinase inhibitors, blebbistatin, or the actin depolymerising agent, latrunculin B increases ciliary length in hTERT-RPE1 cells

$7x10^4$ hTERT-RPE1 cells were plated in 24 well plates and allowed to grow for 24 hours before being treated with either (blebbistatin 10μM, LIM kinase inhibitor 10μM, or latrunculuin B (0.01μg/μl) in reduced serum media (0.2% FBS DMEM) to initiate ciliogenesis for 48 hours. Representative images of ARL13B-stained cilia are shown for control, Blebbistatin 10μM, LIM kinase inhibitor 10μM and latrunculin B 0.01μg/μl. Scale bar = 15μm.

A

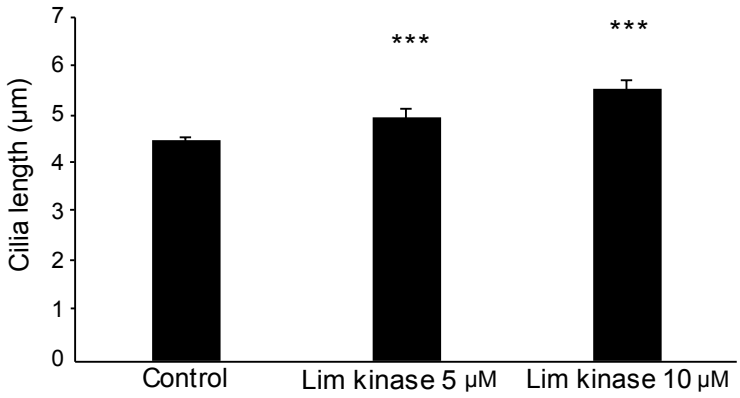
Cilia length (µm)
0
1
2
3
4
5
6
7
***
***
Control
Lim kinase 5 µM
Lim kinase 10 µM

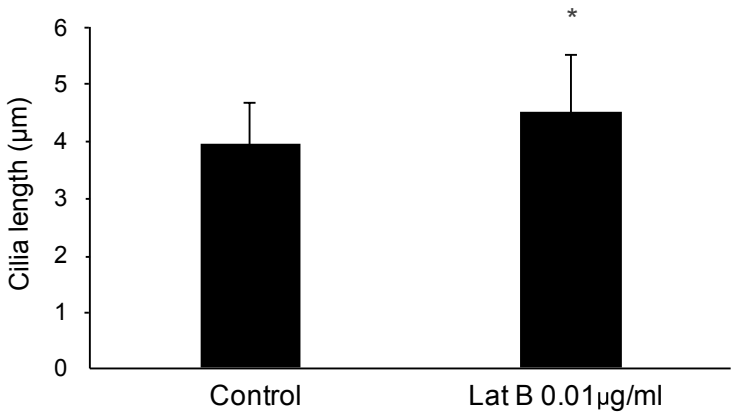
Cilia length (µm)
0
1
2
3
4
5
6
*
Control
Lat B 0.01µg/ml

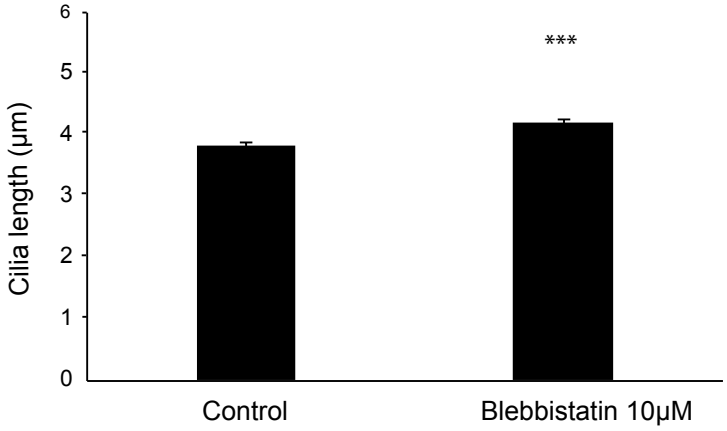
Cilia length (µm)
0
1
2
3
4
5
6
***
Control
Blebbistatin 10µM

B

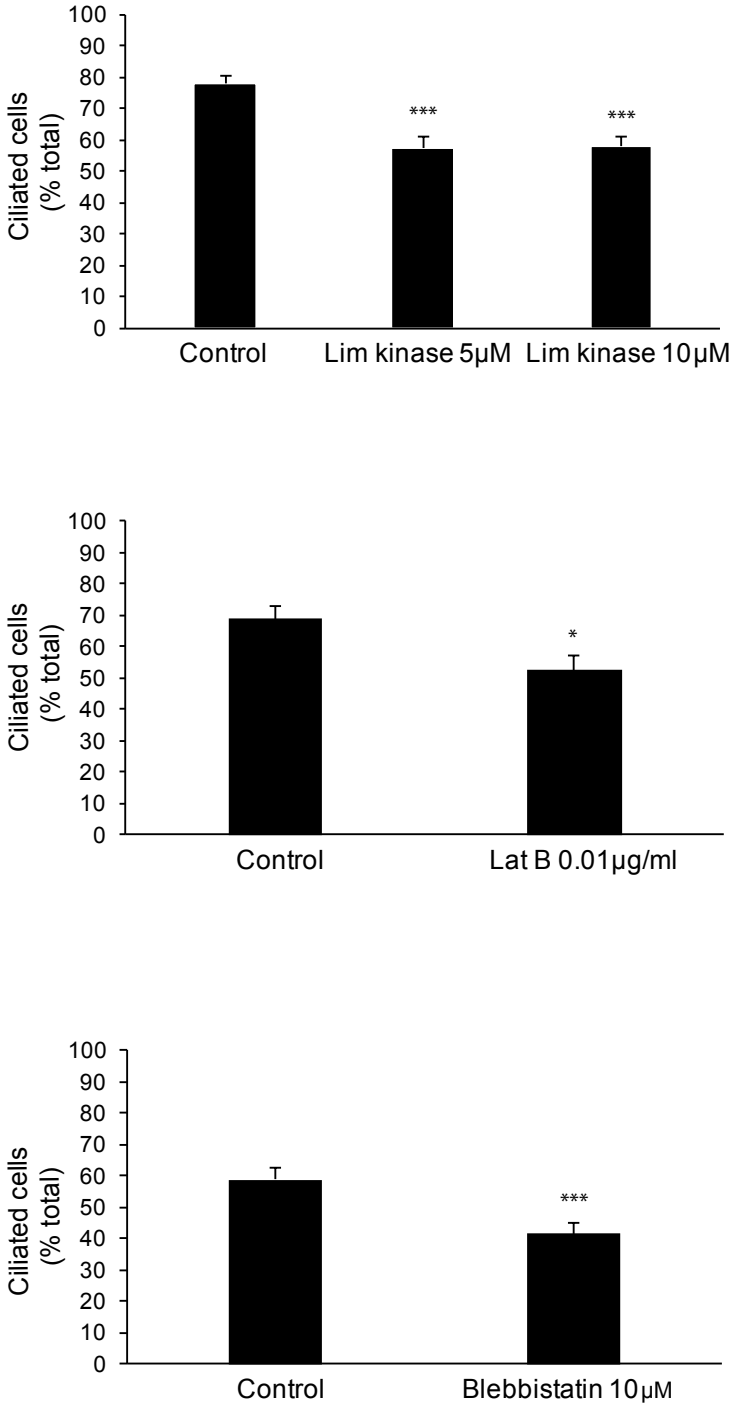

Figure 5.12 Treatment with LIM kinase inhibitors, blebbistatin or the actin depolymerising agent, latrunculin B increases ciliary length in hTERT-RPE cells

$7x10^4$ hTERT-RPE1 cells were plated onto 24 well plates on glass cover slips and allowed grow for 24 hours before being treated with LIMK inhibitor (5μM,10μM) or latrunculin B (0.01μg/μl) or Blebbistatin (10μM) in reduced serum media (0.2% FBS DMEM) to initiate ciliogenesis for 48 hours. (A) Bar charts show average cilia length in cells treated with inhibitors within a x20 field. Lim Kinase inhibitor: N=number of fields (control, 12; LIM kinase inhibitor 5μM, 15; LIM kinase inhibitor 10μM, 15) from three independent experiments; at least 50 cells were counted per condition in each experiment. Latrunculin B at 0.01μg/μl: within a field of view from three

independent experiments. N=number of fields (control, 10; Lat B 0.01μg, 10); at least 50 cells were counted per condition in each experiment. Blebbistatin 10μM: N=number of fields (control, 12; Blebbistatin 10μM, 12) from four independent experiments; at least 50 cells were counted per condition in each experiment. Significance was calculated using a two tailed student T-test. ***=p<0.001. *=p<0.05. Error bars represent S.E.M. (B) Bar charts show percentage ciliated cells within a 20x microscopic field; Lim Kinase inhibitor: N=number of fields (control, 12; LIM kinase inhibitor 5μM, 15; LIM kinase inhibitor 10μM, 15) from three independent experiments; at least 50 cells were counted per condition in each experiment. Latrunculin B at 0.01μg/μl: within a field of view from three independent experiments. N=number of fields (control, 10; Lat B 0.01μg, 10); at least 50 cells were counted per condition in each experiment. Blebbistatin 10μM: N=number of fields (control, 12; Blebbistatin 10μM, 12) from four independent experiments; at least 50 cells were counted per condition in each experiment. Significance was calculated using a two tailed student T-test. ***=p<0.001. *=p<0.05. Error bars represent S.E.M.

5.6 Inhibition of components of the ROCK pathway in *Rock2* $^{-/-}$ MEFs

Chemical inhibitor may act on multiple targets. In order to verify the differences in cilia length and abundance observed with Y27632 treatment was due to inhibition of ROCK, I sought to assess ciliogenesis in mouse embryonic fibroblasts (MEFs) isolated from the *Rock2* knockout mice. First, wild-type MEFs were cultured in the *in vitro* ciliogenesis assay to see if the effect of treatment with Y27632 on ciliogenesis held for this cell type. Wild-type MEFs exhibit smaller cilia (~2-3μm) than RPE1 cells but ciliate sufficiently to be quantified. Indeed, wild-type MEFs treated with Y27632 exhibited the same phenotype as seen before with an increase in cilia length (Figure 5.13 A). The proportion of ciliated cells was also decreased, as observed with the hTERT-RPE1 cells (Figure 5.13 B). MEFs were then isolated from the null and wild-type mice and ciliogenesis was assessed in cilia growth assay. Wild-type and *Rock2* $^{-/-}$ MEFs were seeded and allowed to grow 48 hours as before without the use of inhibitors. Cilia length quantifications showed that *Rock2*$^{-/-}$ MEFs exhibited longer cilia when compared with wild-type MEFs (Figure 5.14), consistent with results seen with the ROCK inhibitor. They also showed a decreased number of total ciliated cells when compared with wild type MEFs.

A

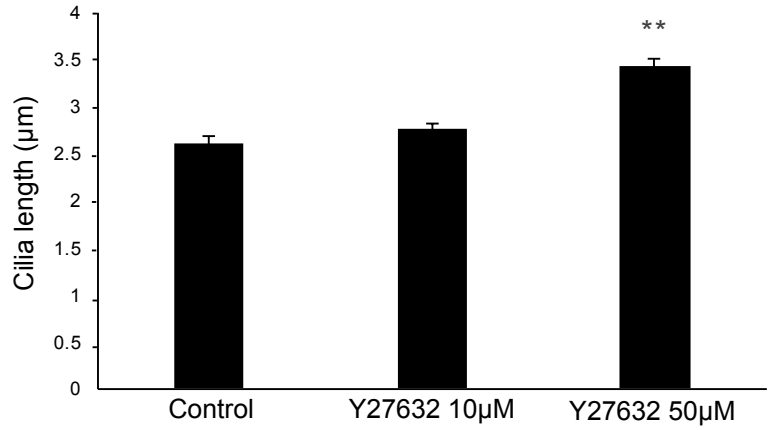

B

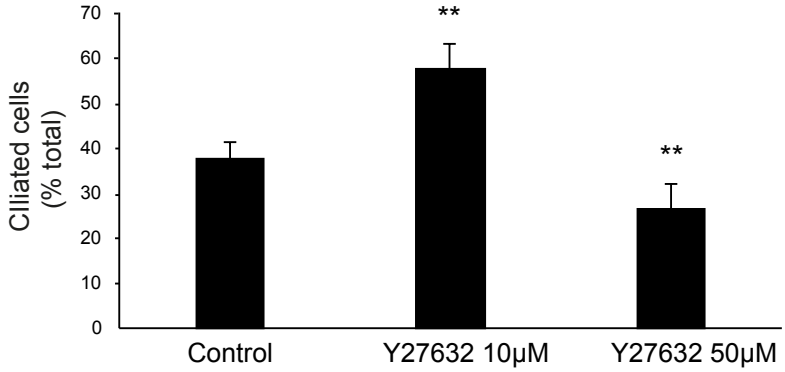

Figure 5.13 Effect of ROCK pathway inhibitors on wild-type mouse embryonic fibroblasts (MEFs)

$5x10^4$ wild type MEFs were plated onto 24 well plates and let grow for 24 hours before being treatment with Y27632 in reduced serum media (0.2% FBS DMEM) to initiate ciliogenesis, for 48 hours. (A) Bar chart shows average cilia length in cells within a microscopic field. Error bars represent S.E.M; N=number of fields (control, 20; 10µM Y27632, 17; 50µM Y27632, 10) from three independent experiments; at least 50 cells were counted per condition in each experiment. (B) Bar chart shows percentage ciliated cells per field of view with Y27632 treatment; Error bars represent S.E.M; N=number of fields; (control, 20 fields; Y27632 10µM, 17; Y27632 50µM, 10) from three independent experiments; minimum of 100 cells were counted per condition in each experiment. Significance was calculated using a two tailed student T-test. ** = $p<0.01$.

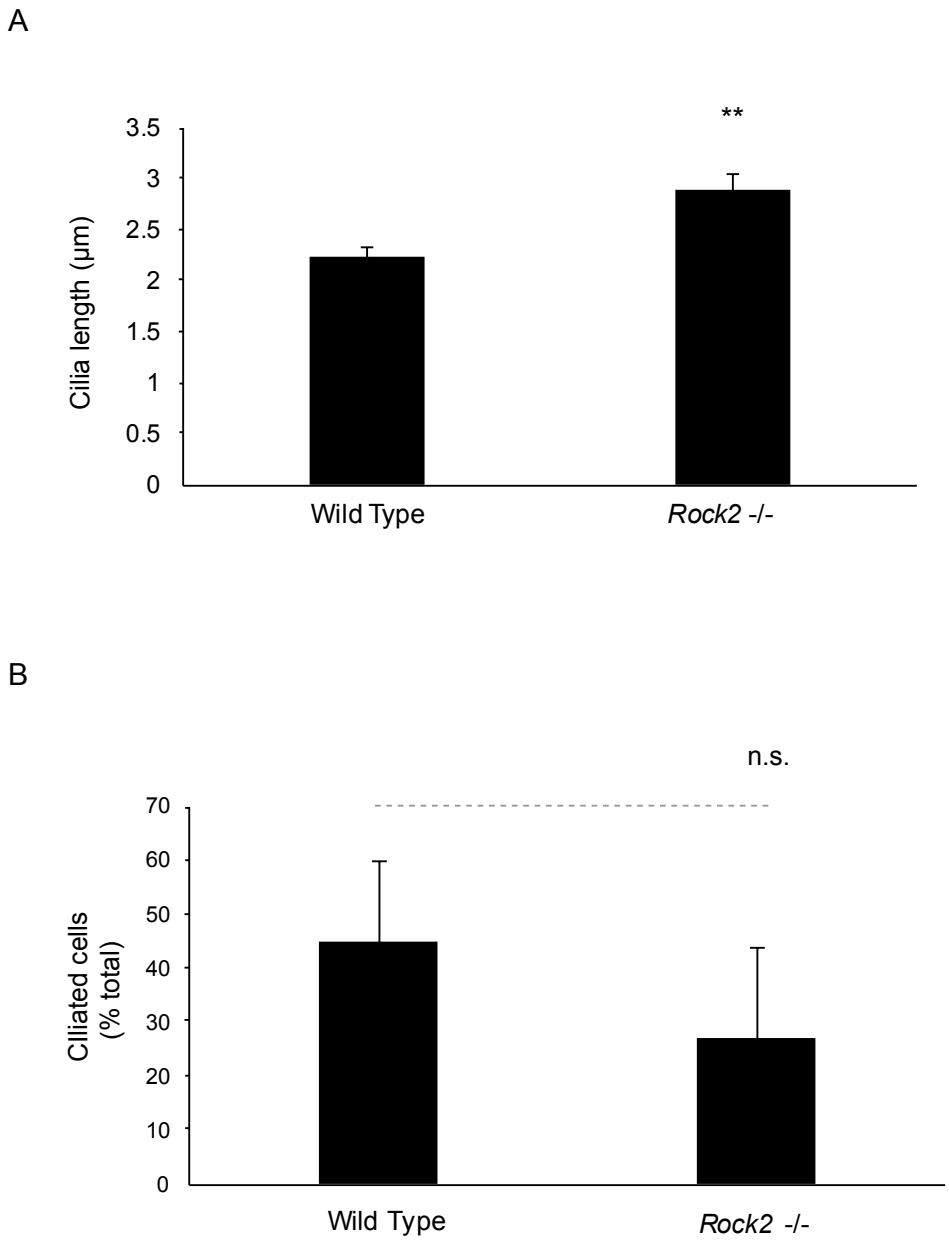

Figure 5.14 Isolated *Rock2* $^{-/-}$ mouse embryonic fibroblasts (MEFs) have increased ciliary length and fewer ciliated cells compared with wild-type MEFs

$5x10^4$ mouse embryonic fibroblasts (MEFs) isolated from *Rock2* $^{-/-}$ embryos cells were plated onto 24 well plates and allowed to grow for 24 hours before being grown in reduced serum media (0.2% FBS DMEM) to initiate ciliogenesis for 48 hours. (A) Bar chart shows average cilia length in cells within microscopic field. Error bars represent S.E.M; N=number of fields; (WT, 20; *Rock2* $^{-/-}$, 20); from three independent experiments; at least 50 cells were counted per genotype in each experiment. (B) Bar chart shows percentage ciliated cells per field of view. Error bars represent S.E.M; N=number of fields; (WT, 20; *Rock2* $^{-/-}$, 20) from three independent experiments. Significance was calculated using a two tailed student T-test. ** = $p<0.01$.

5.7 ROCK2 controls endothelial ciliogenesis and orientation in blood vessels

The *in vitro* experiments using chemical inhibitors and analyses of cilia length and abundance in RPEs and MEFs showed that ROCK2 controls ciliogenesis in cell culture since inhibition or loss of *Rock2* results in decreased ciliary abundance and deregulated ciliary length. It was then of interest to assess whether ROCK inhibition affected ciliogenesis in endothelial cells and whether this correlated with the observed vascular phenotypes of the ROCK2 knockout.

To investigate whether ROCK2 controls ciliogenesis in endothelial cells in blood vessels *in vivo*, I measured the abundance of cilia in the blood vessels of the brain parenchyma of wild type and *Rock2*$^{-/-}$ mouse embryos at E13.5 (Chapter 4 section 4.2) where I had found that cilia are abundant in blood vessels (Figure 5.3). *Rock2*$^{-/-}$ and wild type littermate controls at E13.5 were fixed, sectioned and stained for the cilia marker ARL13B. Cilia were counted within endothelial stained vessels throughout the parenchyma of the entire brain section from each slide (Figure 5.15). Given the defects observed in the regulation of cilia length and abundance in cell culture with ROCK inhibition in order to assess whether in the absence of *Rock2* there were any changes in primary cilia location in the blood vessels, cilia were classified according to their location in relation to the vessel wall and orientation as luminal (protruding into the vessel lumen), internal (within the vessel wall) or external (protruding outside the vessel wall) as (Figure 5.16A). The *Rock2* knockout embryos showed reduced overall cilia numbers (approximately 20% less cilia) in the blood vessels of the developing brain when compared with the wild-type embryos (Figure 5.16B). When location of cilia was taken into consideration, *Rock2* $^{-/-}$ embryos had fewer cilia in the internal and luminal compartments (29.6%) compared with *Rock2* $^{+/+}$ embryos (42.1%), and an increase in the percentage of external cilia form 57.9% in wild type to 70.4% in *Rock2* knockout embryos (Figure 5.16B).

Although cilia counts were reduced in the *Rock2*$^{-/-}$ embryos when compared with *Rock2*$^{+/+}$, accurate measurement of their length was not feasible through sectioned IHC slides. To address this, HCMECs (human cerebral microvascular endothelial cells) were treated with Y27632 in culture and the small number of cells that ciliated were measured. Indeed, inhibition of ROCK using Y27632 resulted in an increase in ciliary length in the HCMEC (Figure 5.17).

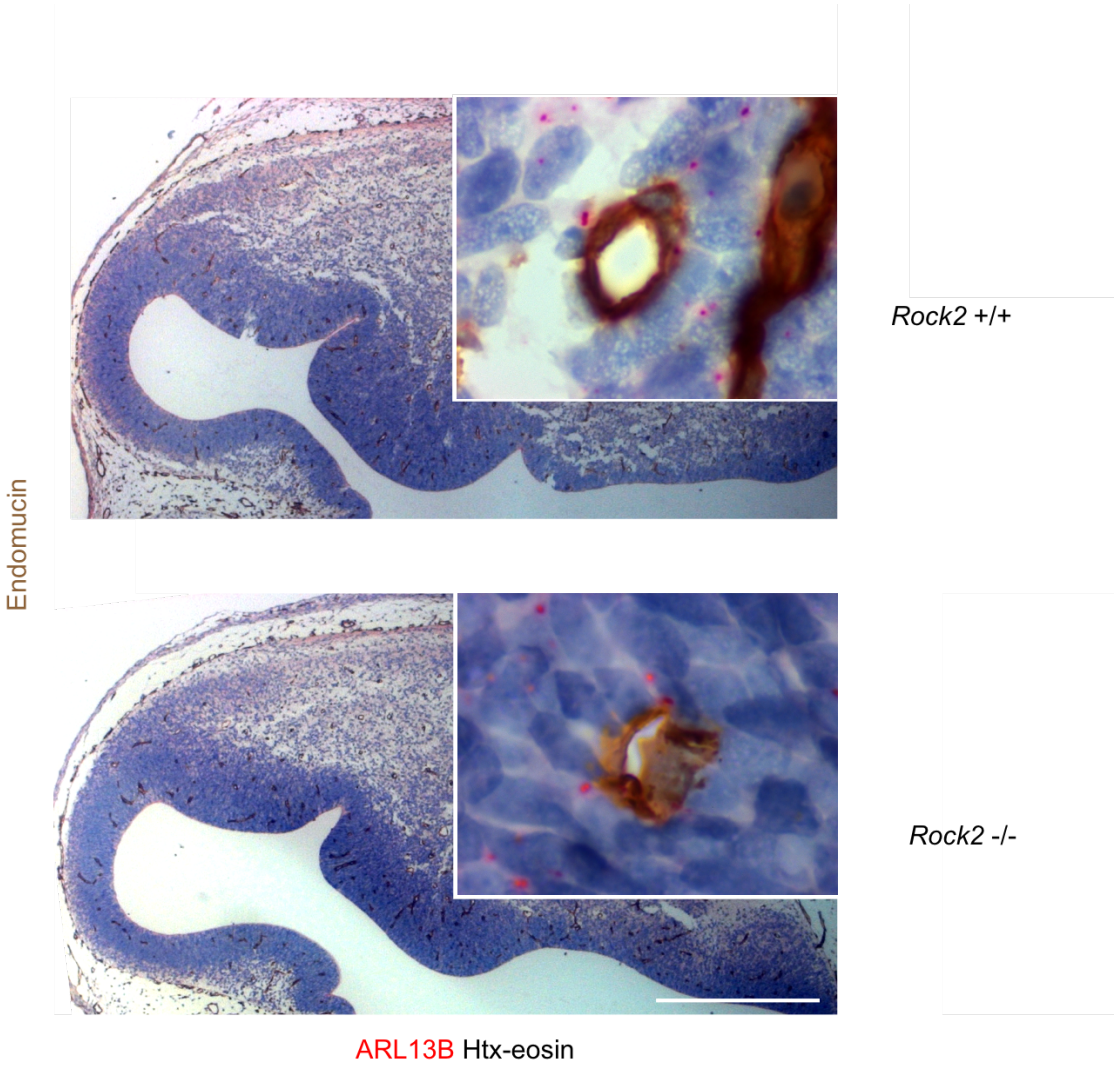

Figure 5.15 Endothelial cell cilia of the vasculature of the E13.5 *Rock2* $^{-/-}$ mice
Transverse sections taken at the level of the interventricular foramen of Monro of E13.5 embryos were stained for endomucin, ARL13B and Htx-eosin. Representative images of section at the interventricular foramen of Monro level stained for Endomucin and ARL13B, H&E stain with endomucin (brown) and ARL13B (red) in *Rock2*$^{+/+}$ and *Rock2*$^{-/-}$. Zoomed inset of vessels stained for endomucin and ARL13B. Scale bar = 100μm.

A

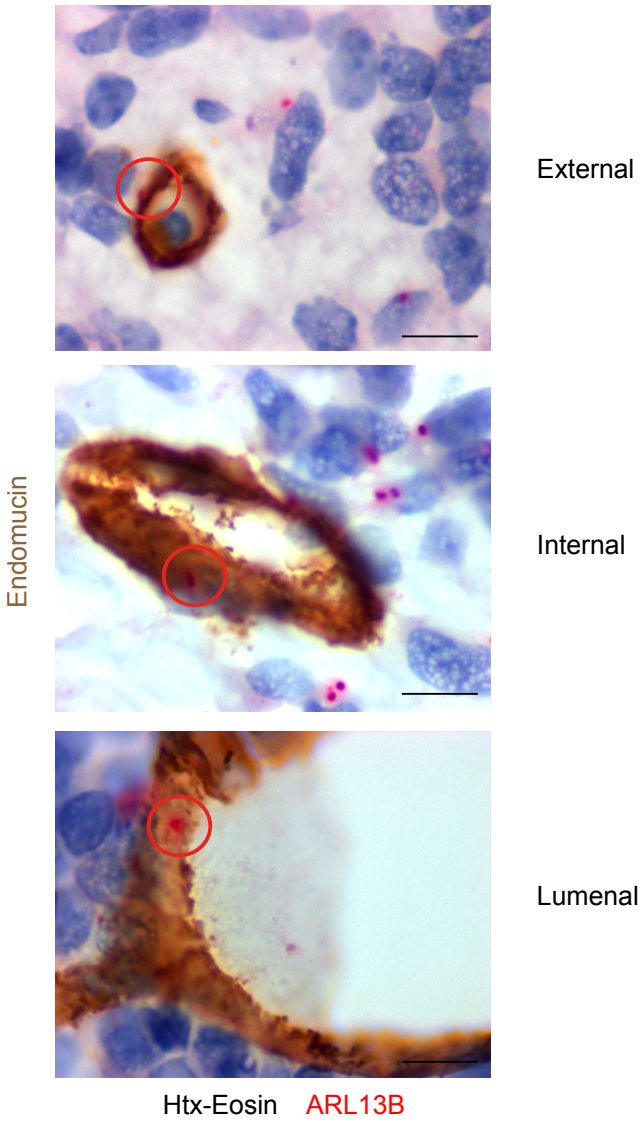

B

	Cilia number		% Total cilia	
	Rock2 $^{+/+}$	***Rock2*** $^{-/-}$	***Rock2*** $^{+/+}$	***Rock2*** $^{-/-}$
Lumenal	20	6	7.6%	2.9%
Internal	91	56	34.5%	26.7%
External	153	148	57.9%	70.4%
Total cilia	264	210	100%	100%

Figure 5.16 Endothelial cell cilia are reduced in the vasculature of the E13.5 *Rock2* $^{-/-}$ mice
Transverse sections taken at the level of the interventricular foramen of Monro of E13.5 embryos were stained for endomucin, ARL13B and Htx-eosin (A) Representative images of

sections at the interventricular foramen of Monro level stained for Endomucin and ARL13B, H&E stain with endomucin (brown) and ARL13B (red) showing lumenal, internal, and externally located endothelial cilia within vessels. Scale bar = 10μm (B) Table shows blood vessel cilia counts in *Rock2*$^{+/+}$ and *Rock2*$^{-/-}$ blood vessels within the embryo parenchyma. N= number of embryos; (*Rock2* $^{-/-}$, 3; *Rock2* $^{+/+}$, 3).

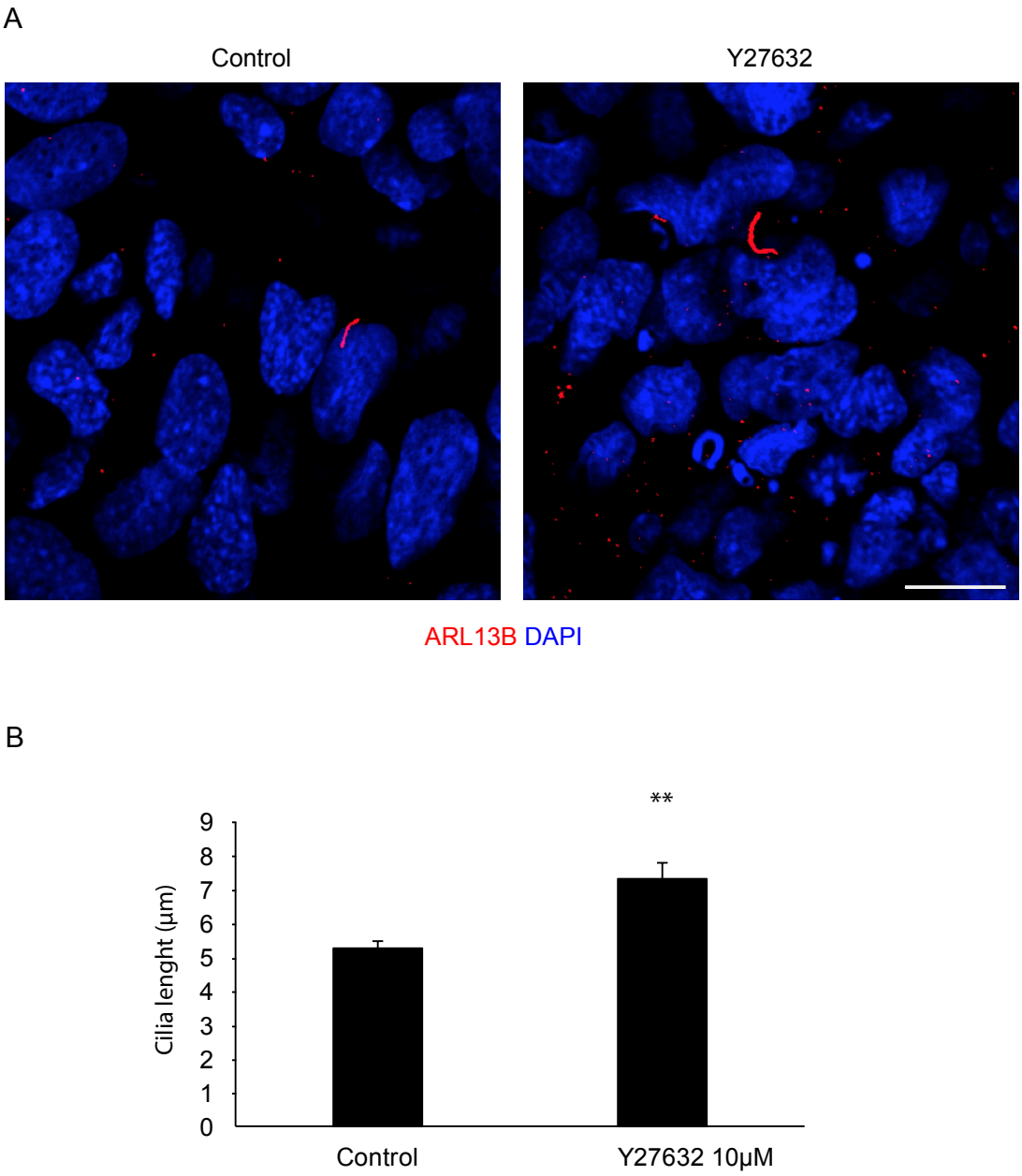

Figure 5.17 Treatment with the ROCK inhibitor Y27632 increases ciliary length in HCMEC
$5x10^4$ HCMEC cells were plated in 24 well plates and allowed to grow for 24 hours before treatment with Y27632 in reduced serum media (0.2% FBS DMEM) to initiate ciliogenesis for 48 hours. (A) Representative images of ciliated HCMEC cells (B) Bar chart shows average cilia length of ciliated HCMECs cells within a 20x field. Error bars represent S.E.M; N=number of fields (control, 5; 5µM Y27632, 5; 10µM Y27632, 5); from three independent experiments; at least 30 cells were counted per condition in each experiment. Significance was calculated using a two tailed student T-test. ** = $p<0.01$.

5.8 Conclusions

Endothelial cells were once thought to be one of the few cell types that did not develop a primary cilium. However, a number of recent published studies have shown that cilia can be found in the apical luminal site of blood vessels in zebrafish, where they sense blood flow and play an active role in vascular remodelling (Goetz *et al.*, 2014) . In the studies presented in this thesis, primary cilia were found only on a subset of endothelial cells both *in vitro* for cultured cell-lines and *in vivo* (Figure 5.1 and 5.2). This finding correlates with the few numbers of endothelial cilia on HUVEC, identified in other published studies (Iomini *et al.*, 2004). The reason for such sparse cilia incidence on endothelial cells may be explained by the nature of imaging analyses, which only gives a single time-point for a population of ciliated cells. It is possible that endothelial cells respond dynamically to local environmental cues that control the precise timing of ciliary growth and dissolution. Indeed, recent evidence shows that cilia appear more or less readily in certain positions within blood vessels in response to surrounding environmental cues: disturbed flow promotes greater cilia incidence compared to laminar flow; and onset of blood flow promotes more cilia compared to continuous unbroken flow (Dinsmore and Reiter, 2016). Therefore, it is possible that primary endothelial cilia only assemble transiently in endothelial cells within blood vessels. Another intriguing hypothesis is that important ciliary functions, such as calcium signalling for vasodilation induced by flow sensing by endothelial cells, may be sufficiently carried out by a small number of ciliated cells within a blood vessel (Egorova *et al.*, 2012).

In this chapter I have shown that control of the actin cytoskeleton plays a fundamental role in the process of primary cilia lengthening and, furthermore, that it controls cilia incidence in endothelial cells. The role of the ROCK signalling pathway and its effect on actin is well-studied and as an effector of Rho signalling, ROCK phosphorylates downstream kinases, the majority of which have a direct effect on actin dynamics. Y27632 is widely used as a ROCK1 and ROCK2 inhibitor. In this chapter I have shown that inhibition of ROCK signalling with Y27632 results in longer primary cilia (Figure 5.9, Figure 5.10). Further investigation in the studies herein revealed that similar effects to inhibition of ROCK on ciliary length are also seen with inhibition of the downstream effectors such as LIM kinase and myosin II (Figure 5.11, Figure 5.12). By phosphorylating cofllin, LIM kinase inhibits its actin severing ability, resulting in longer more stable actin filaments. Inhibition of this activity with a commercially available inhibitor for LIM kinase (BMS5-SYN1024) resulted in longer cilia. However, disruption of cofilin activity and the subsequent lengthening of the cilium may not yield functional cilia, since published evidence

has shown that cofilin knockout causes malpositioning of embryonic node cilia and hence defects in planar cell polarity defects (Mahaffey *et al.*, 2013). Further evidence supporting this regulatory role of actin on cilia formation was also observed with the actin depolymerising agent latrunculin B. The ability of latrunculin B to sequester G-actin and prevent the formation of F-actin filaments resulted in an increase in ciliary length in hTERT-RPE1 cells (Figure 5.11, Figure 5.12).

It has been demonstrated previously that actin branching and nucleating factors inhibit ciliogenesis (Bershteyn *et al.*, 2010; Kim *et al.*, 2010; Cao *et al.*, 2012; Malicki and Johnson, 2016). As seen in the results presented in this chapter, this holds true in my assay, since a decrease in the proportion of ciliated endothelial cells occurred after treatment with the ROCK inhibitor. Furthermore, I have shown that treatment of cells with inhibitors of effectors of the ROCK pathway have fewer cilia (Table 6.1). The cilia that persisted were of an abnormal length, a feature which may impede their function, as cilia length is known to be an important determinant in ciliary functionality (Avasthi and Marshall, 2012) .

Assays employing *Rock2* knockout MEFs showed differences in ciliary length consistent with the treatment of RPE cells, endothelial cells and MEFs with Y27632, confirming that the observed effects resulted from inhibition of ROCK2, rather than off target effects of the inhibitor. This was further supported by inhibition of downstream effectors resulting in a similar phenotype. In Rock2$^{-/-}$ MEFs, the trend towards reduction in cilia abundance was not significant. This could be due to insufficient number of images analysed, given the small differences anticipated. The effects of inhibition of downstream effectors argue that this is true as there was a significant decrease in ciliated cells with loss of all downstream effectors. Consistently, results from the *Rock2*$^{-/-}$ embryo studies showed differences in cilia incidence, with fewer cilia in the mutant null animals (Figure 5.16).

The loss of only one isoform of ROCK (ROCK2) and possible compensation by ROCK1, may also explain why a trend rather than statistically significant difference was observed in the knockout MEFs when compared with treatment with Y27632-treated cells, in which both ROCK isoforms are inhibited by the inhibitor. It is possible that both ROCK1 and ROCK2 are involved are required for regulation of downstream effectors necessary for maintenance of the correct ciliary length.

Pharmacological inhibitor	Target	Effect on primary cilia
Y27632	Rho kinase inhibitor	Increased length, decrease in abundance
Blebbistatin	Myosin II inhibitor	Increased ciliary length
BMS5	Lim kinase inhibitor	Increased ciliary length
Latrunculin B	Actin depolymerising agent	Increased ciliary length

Table 6.1 Summary of effect of Pharmacological inhibitors on ciliary length and abundance in ciliogenesis assay

Chapter 6

Final discussion

6.1 Introduction

Actin based cytoskeletal rearrangements are vital for most aspects of endothelial cell behaviour during angiogenesis. An intricate control of the actin machinery through actin nucleation, branching and severing proteins orchestrated by the Rho family of small GTPases is necessary for the changes in cell shape endothelial cells adopt during sprouting and migration. However, at the start of this project it was not known whether Rho proteins play a role in the development of blood vessel lumens, which are essential for blood flow.

As referred to in Conclusions of Chapter 4, two key mechanisms have been put forward for the formation of blood vessel lumens (Iruela-Arispe & Davis, 2009). Expansion of intracellular vacuoles within endothelial cells to form seamless lumens (Kamei et al., 2006); and cord hollowing, whereby a lumen forms by opposing endothelial cells with lateral adhesions (Pelton, Wright, Leitges, & Bautch, 2014; Strilić et al., 2009). It has been suggested that a cord hollowing mechanism operates predominately during the development of larger vessels such as the aorta, while the cell hollowing mechanism of lumen formation operates during the development of smaller blood vessels (Phng *et al.*, 2015).

Early findings by the Davis group had shown that the Rho GTPases Rac1 and Cdc42, control the process of cell hollowing via regulation of intracellular vacuoles in an in vitro collagen assay of lumen formation (Bayless and Davis, 2002). Further work by Davis and colleagues showed the presence of intracellular vacuoles *in vivo* within zebrafish intersegmental vessels (ISVs) during lumen formation (Kamei, W. Brian Saunders, *et al.*, 2006). However, the continued use of the zebrafish ISVs as a model of lumen formation, and improvement in imaging techniques, led to the finding that the actual architecture of the ISVs conflicted with earlier discoveries. In most regions, complex cell arrangements led to paired endothelial cells forming the ISVs, with luminal spaces found between juxtaposing endothelial cells (Blum *et al.*, 2008) and therefore forming *via* a chord hollowing mechanism. In the ISVs VE-cadherin has been shown to be distributed alongside lateral cell-cell contacts and to be essential for cell polarity and lumen opening (Blum *et al.*, 2008). VE-cadherin levels at lateral adhesions are upregulated in areas of lower VEGFR2 signalling following dephosphorylation of VEGFR2 via VE-PTP. Reduced VEGFR2 signalling within the ISV mediated by VEGFR1 in turn maintains VE-cadherin lateral localisation in the stalk cells (Hayashi *et al.*, 2013).

Additional evidence for the importance of cell-cell junctions in lumen opening was recently shown by the involvement of VE-cadherin and AmotL2 in linking to contractile actin fibres necessary for aortic lumen expansion in the mouse (Hultin *et al.*, 2014). Gebala and co-workers also recently showed that the majority of blood vessel lumens arise at sites of lateral cell-cell adhesions in both the zebrafish and the mouse models, where vacuoles may only provide a small influence on lumen expansion (Gebala *et al.*, 2016). In this project I set out to investigate the role of the Rac1 and Cdc42 GEFs, DOCK4 and DOCK9, in lumen formation using an *in vitro* angiogenesis assay where lumens form *via* a cord hollowing mechanism. I also investigated the role of the Rho effector ROCK2 in lumen formation *in vivo,* and ciliogenesis using a *Rock2* knockout model.

6.2 Rac GEF DOCK4 and Cdc42 GEF DOCK9 control lumen formation

Results presented in this thesis agree with previous work implicating lateral adhesions in lumen formation, and outline a role for DOCK4 and DOCK9 in the process of cord hollowing through control of their respective GTPases, Rac1 and Cdc42. Previous work from this lab (discussed in the 'preliminary work leading to this thesis' section 1.8.1) showed that Rac1 activation mediated by DOCK4, controlled lateral filopodial protrusions in endothelial cells within tubules through an interaction with the Cdc42 GEF, DOCK9. Early experiments had suggested that DOCK4 may be involved in lumen formation through cytoskeletal rearrangements and loss of lateral adhesions.

Loss of DOCK4 in HUVEC, in the angiogenesis coculture model, indeed affected dynamic protrusions and lateral filopodia (Abraham *et al.*, 2015), and led to defects in lumen formation (Figure 3.10). Tubules with DOCK4 knockdown were thinner with fewer nuclei per length and fewer lateral adhesions when compared with control (Figures 3.7 and 3.8). These lateral adhesions appear important for deposition of apical proteins such as podocalyxin prior to the opening of lumens in the co-culture assay (Figure 3.5). Due to the reduction in lateral adhesions, tubules showed fewer nuclei per unit length indicating that fewer cells were making up the tubules.

Investigations in this thesis showed that DOCK9 is also required for lumen formation as knocking down DOCK9 resulted in 50% reduction in lumenised vessels compared with control (Figure 3.15). This further supports the notion that DOCK4-Rac and DOCK9-Cdc42 operate in

the same signalling pathway (Abraham et al, 2015). However, knockdown of DOCK9 did not affect tubule thickness, while lateral adhesions also appeared unaffected (Figure 3.16). Therefore, while DOCK4 and DOCK9 operate in the same pathway to control cytoskeletal rearrangements and filopodia formation which can impact on lumen formation, DOCK4 appears to additionally control lateral adhesions through an unknown mechanism (Figure 6.1).

Results from the AMIS assay showed that DOCK9 does not affect podocalyxin apical localisation and therefore may be involved in subsequent steps of lumen formation such as repulsion and or the establishment of curvature of cells to surround a lumen. On the other hand, DOCK9 may be involved in the actin organisation of the apical membrane prior to lumen formation (Figure 6.1), as supported by its localisation at the early apical membrane initiation site (AMIS); together with the apical proteins podocalyxin and VE-cadherin known to control lumen formation (Strilić *et al.*, 2009; Richards, Hetheridge and Mellor, 2016). It is also possible that localisation of podocalyxin in 3D cultures and *in vivo* is a short-term event prior to formation of a lumen. This idea is supported by the 2D AMIS experiments (Figure 3.18) during which the appearance of an apical membrane is a transient event, as the AMIS appears shortly after plating (25 mins) and disappears ~6 minutes after attachment to the substratum. It would be interesting to investigate whether DOCK4 also localises at the AMIS and controls actin reorganisation at the apical membrane, an experiment that was not carried out due to time constraints.

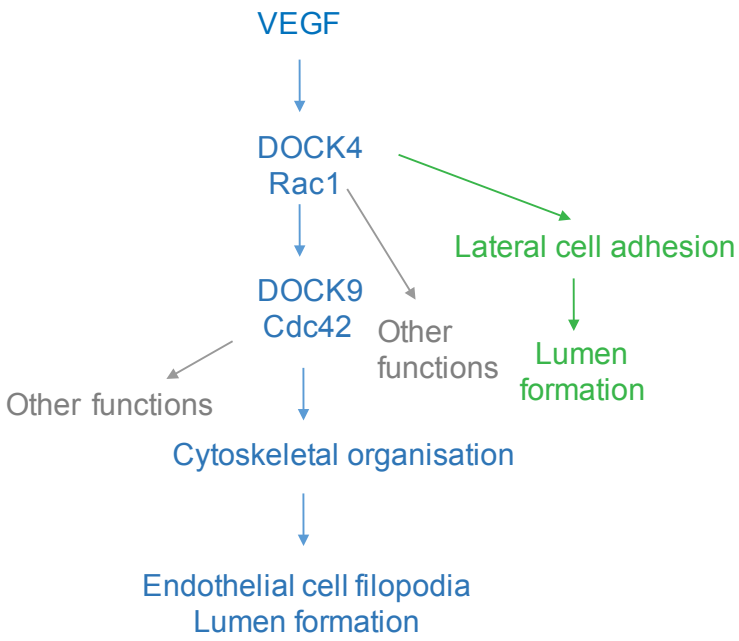

Figure 6.1 Model for the roles of DOCK4 and DOCK9 in blood vessel lumen formation

of pathway downstream of VEGF controlling lumen formation.
Downstream of VEGF signalling the guanine nucleotide exchange factor DOCK4 activates Rac1 which interacts with the Cdc42 GEF DOCK9. Cdc42 activation by DOCK4 and DOCK9 controls filopodia formation while cytoskeletal rearrangements coordinated by DOCK4 driven Rac1 activation and DOCK9 driven Cdc42 activation control lumen formation. DOCK4 is also required for lateral cell-cell adhesions which also impact on lumen formation.

Unlike previous studies where complete loss/knockdown of major Rho GTPases affected lumen formation, here we have shown individual activators (GEFs) responsible for control of some of these lumen formation behaviours. This more specific approach provides a more complete picture of the complex signalling involved in lumen formation and may uncover more realistic targeting opportunities in the future.

During the course of this study, a global *Dock4* knockout mouse model was generated by our lab. Homozygous deletion of DOCK4 led to early embryonic lethality before E7.5, prior to the onset of vascularisation which precluded analysis of vascular phenotypes. However, studies carried out in the heterozygous *Dock4*$^{+/-}$ mice showed perturbed blood vessel lumen formation during development and in tumours grown in heterozygous Dock4 knockout mice, supporting the findings in the organotypic angiogenesis model (Abraham et al, 2015). Since this was carried out in a heterozygous mouse due to the lethality of the homozygous mutant, future studies *in vivo* will utilize a conditional *Dock4* knockout model to delete both *Dock4* alleles and confirm the endothelial cell autonomous role of Dock4 during *in vivo* blood vessel lumen formation.

6.3 Role of Rock2 in blood vessel morphogenesis

Previous work had shown that genetic deletion of *Rock2* was embryonically lethal at E13.5 (Thumkeo *et al.*, 2003). In agreement, the *Rock2* knockout embryos analysed in this thesis exhibited haemorrhages in the head and neck, and occasionally pooled blood in the limb buds (Figure 4.1). Further investigation of the angiozone in the head region revealed that this was a site of ongoing angiogenesis at E12.5 with vessels beginning to lumenise at E13.5 (Figure 4.2 and Table 4.1). Loss of *Rock2* led to a hyperfilopodial phenotype in that region, and loss of normal blood vessel patterning and blood vessel integrity, with blood cells found outside the vessels of the knockout mouse. The hypersprouting phenotype supports earlier findings which

had shown loss of tubule quiescence with ROCK inhibition in tissue culture organotypic assays (Abraham *et al.*, 2009).

This hypersprouting phenotype and loss of integrity could explain the hemorrhages seen in the *Rock2* knockout embryos. Previous studies had shown that reduced quiescence of endothelial cells within blood vessels is an indicator of vascular defects (Liu *et al.*, 2003). This result confirms the findings by Abraham et al which showed that in the tissue culture organotypic model, cell-cell interaction mediated by VE-cadherin activation of RhoC and ROCK is necessary for suppression of sprouting and generation of functional vasculature (Abraham *et al.*, 2009). It has also been shown that ROCK regulates matrix stiffness (Fischer *et al.*, 2009; Samuel *et al.*, 2011) and that stimulation of sprouting with ROCK inhibition is also associated with changes in matrix stiffness (Fischer, Gardel, Ma, Adelstein, & Waterman, 2009).

ROCK2 genetic deletion did not appear to influence blood vessel integrity in the brain parenchyma. However, analysis of blood vessels in the brain parenchyma of developing embryos showed a significant decrease in blood vessels with lumens. To investigate the effect of Rock2 loss on vascular lumen diameter, transverse sections of the developing parenchyma provided large areas of brain parenchyma suitable for the measuring of lumen parameters, including diameter and cilia number. Blood vessel lumen diameter was altered in the *Rock2*$^{-/-}$ embryos with fewer lumenised vessels in the parenchyma. Vessels that did lumenise had a larger diameter compared with wild type. Significant haemorrhage may be due to increases in intravascular pressure due to the defects seen in numbers of lumenised vessels. A proportion of vessels within *Rock2*$^{-/-}$ embryos retained a normal phenotype when compared with littermate wild type controls. An explanation for differences see amongst different vascular beds in terms of requirement for ROCK2 for vessel integrity could be that the actin cytoskeleton may be regulated to different extends by ROCK1 and ROCK2 in different vascular beds, or may be under the control of different cytoskeletal regulators (Lubarsky and Krasnow, 2003). Also, in these studies we cannot exclude the contribution of loss of ROCK2 expression in perivascular cells in the observed defects in integrity and blood vessel lumen formation, although no apparent changes were observed in these cells macroscopically. Conditional deletion of *Rock2* will be necessary to confirm an endothelial cell autonomous nature of any of the observed defects.

Aorta diameter and patterning was also affected in the *Rock2* $^{-/-}$ embryos, with knockout embryos showing increases in vessel diameter and abnormal circularity. However, this may be due to an effect of loss of ROCK2 in smooth muscle cells involved in aorta integrity which would need further investigation, as changes in smooth muscle cells were observed upon macroscopic observation of the aortas of the *Rock2* knockout embryos (Figure 4.7A). Altogether, the results presented in chapter 4 show that ROCK signalling plays a role in angiogenesis, and may highlight the beneficial effects of therapeutic use of ROCK inhibitors in cardiovascular disease. While these findings identify ROCK2 as playing a role in lumen formation *in vivo,* it will be important to also elucidate the functional roles of the closely related isoform ROCK1.

A recently developed Rock1$^{f/f}$/ROCK2$^{f/f}$ double knockout mouse model available in our lab may provide more insights into the role of ROCK1/2 s in angiogenesis and lumen formation. The overall homology of the two isoforms of 68%, and the 92% homology they share in their kinase domain, may allow a level of compensation to take place in the absence of ROCK2, so that ROCK1 may provide sufficient kinase activity for downstream targets in the absence of ROCK2, but the tissue dependency of this potential compensation remains unknown. Differences in the phenotypes observed with *Rock2* genetic deletion in different vascular beds could be attributed to differential compensation by *Rock1* in different tissues. Furthermore, different tissues may have a different requirement for the two different isoforms as exemplified by the high expression levels of ROCK2 found in brain compared to ROCK1 (Nakagawa *et al.*, 1996).

The majority of inhibitors currently being trialed in cardiovascular therapies target both ROCK isoforms. A need for isoform-specific inhibitors is evident with diverging roles for ROCK1 and ROCK2 becoming more evident (Shi *et al.*, 2013). Results shown here elucidate the potential roles of a ROCK2 in angiogenesis using a single isoform knockout mouse model, and pave the way for understanding the effect of single isoform specific inhibitors will have on angiogenesis and lumen formation. These results support the early clinical results seen in treating contraction or stiffness, for example arterial hyperconstriction seen in heart failure associated vascular resistance and contraction, which were attenuated with treatment with the ROCK inhibitor Fasudil. This holds relevance with findings in this study as loss of *Rock2* led to expansion of both parenchymal vessels (Figure 4.6) and the aorta (Figure 4.5).

6.4 Role of Rock2 in ciliogenesis

Recent studies has suggested roles for modulators of actin dynamics such as ROCK2 in the control of primary ciliogenesis (Wheway *et al.*, 2015). With the growing evidence for a role of primary cilia in blood vessel morphology and development (Goetz *et al.*, 2014; Dinsmore and Reiter, 2016), I explored the role for ROCK2 in endothelial primary cilia. How cilia are formed and how parameters such as length and abundance of cilia are maintained within different cell types is still not clear. However, an essential role of endothelial cells is to sense mechanical forces and react to fluid flow induced by the blood, and this may be influenced by primary cilia (Praetorius and Spring, 2003; Van der Heiden *et al.*, 2008; Goetz *et al.*, 2014). An important aspect of cilia maintenance with regards to flow is how cells maintain cilia length and flexibility (Avasthi and Marshall, 2012). Vascular endothelial cells appear to be amongst the smallest cilia in length, falling in the 1 to 5μm range, whereas some neuronal cilia can extend to 9μm (Dummer *et al.*, 2016). The effect of length on flow recognition is important, as the longer a cilium grows, the more sensitive it will become to flow and also more responsive to lower levels of flow-induced sheer stress (Resnick and Hopfer, 2007).

Results from the ROCK2 knockout mouse showed a decrease in primary cilia in the vessels of the brain parenchyma when compared with wild type controls (Figure 5.13). As seen in chapter 4, *Rock2*$^{-/-}$ embryos at E13.5 had lower abundance of bigger diameter lumens when compared with wild-type mouse embryos (Figure 4.7). I have also shown in this chapter that cerebral blood vessels in Rock2$^{-/-}$ embryos displayed less primary cilia than in wild type embryos (Figure 5.13). This suggests that bigger or more established lumens contain less primary cilia. This agrees with published data and supports the hypothesis that primary cilia are early flow sensors involved in detecting low levels of flow during the initial stages of angiogenesis (Goetz et al., 2014) but disassemble under continuous flow (Iomini *et al.*, 2004).

The findings *in vivo* corroborated the findings in the *in vitro* ciliogenesis model. In those assays the ROCK inhibitor Y27632 decreased cilia number, but increased cilia length. Consistently, isolated *Rock2*$^{-/-}$ MEFs also showed shorter and less abundant primary cilia when cultured in the ciliogenesis assay.

As cilia length seems to be a cell-type specific parameter, it seems evident that length plays a role in their function. The findings in chapter 5 demonstrate a role for ROCK2 signalling in primary ciliogenesis by controlling both cilia growth which is important for flow sensing, and

overall cilia abundance. This suggests that ROCK2 may affect lumen formation both directly through control of endothelial cell shape, and indirectly through control of ciliogenesis. However, more work is needed to address whether cilia formation directly affects blood vessel lumen morphogenesis (Figure 6.2). In future studies, it would be interesting to explore whether increase in ciliary length affects flow recognition by endothelial cells, thus affecting lumen expansion (Gebala *et al.*, 2016). As the *Rock2* knockout model employed in these studies is a global *Rock2* knockout model, it presents the opportunity to look the effects of loss of *Rock2* in other cell types and tissues where ciliary roles are better understood, for example in the kidney, where cilia sense urinary flow and modulate kidney tubule development (Yoder, 2007).

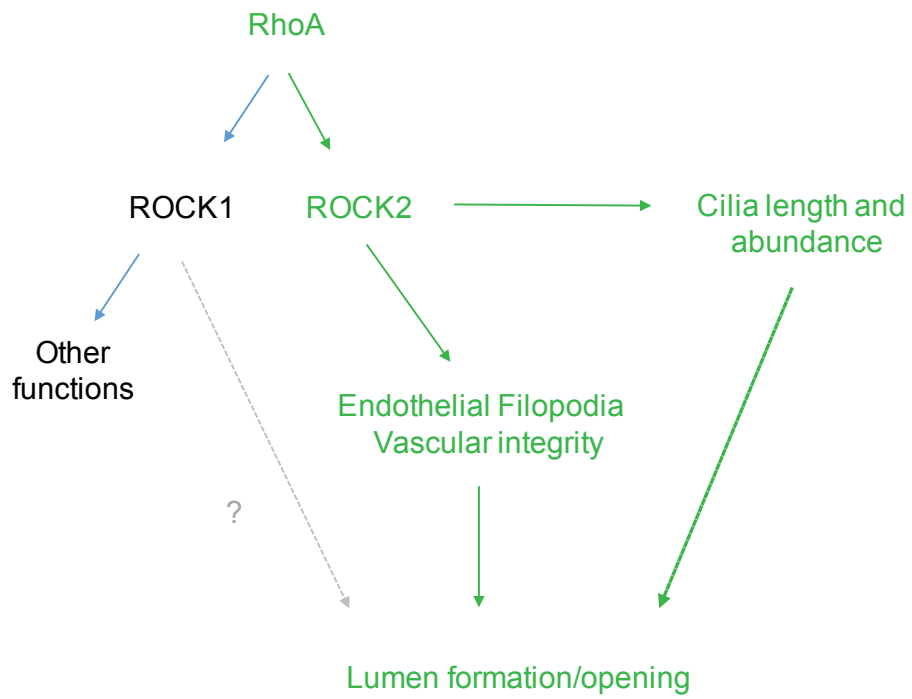

Figure 6.2 Model for the role of ROCK2 in ciliogenesis and lumen formation
ROCK2 activity downstream of Rho signalling influences endothelial cell filopodia formation, vascular integrity and lumen formation through modulation of cytoskeletal organisation. Furthermore, ROCK2 controls cilia length and abundance which may have additional effects on lumen expansion.

6.5 Concluding remarks

In this thesis, I have demonstrated how lumen formation is controlled by the Rac GEF DOCK4 and Cdc42 GEF DOCK9 in a tissue culture angiogenesis model; and how lumen formation and ciliogenesis are regulated by ROCK2. The analyses have shown the importance of cytoskeletal rearrangements controlled by DOCK4 and DOCK9 in the process of lumenogenesis; as well as the importance of lateral cell-cell adhesions controlled by DOCK4 for lumen formation. Work by other members of the laboratory showed that loss of lateral adhesions results from unidirectional sprouting (elongation), and loss of dynamic lateral remodelling in the absence of DOCK4 (Abraham et al., 2015). Defects in lumen formation in response to loss of *Rock2* were associated with i) cytoskeletal rearrangements as evidenced by changes in filopodial protrusions and ii) the regulation of primary cilia which are known to sense blood flow (Goetz *et al.*, 2014; Kallakuri *et al.*, 2014), thus potentially affecting lumen expansion (Gebala *et al.*, 2016). Understanding the cellular and molecular mechanisms of lumen formation and acquisition of blood vessel functionality may help in the future develop protocols for therapeutic angiogenesis, for example to overcome ischemic disease.

The association between cilia and the circulatory system is supported by the presence of vascular defects in many ciliopathies, for example in polycystic kidney disease there is increased hypertension at an early age, and increased incidence of vascular defects later in life including blood vessel abnormalities and aneurisms (Torres, Harris and Pirson, 2007). Recent published studies suggest a role for primary cilia in blood vessel development and homeostasis (Goetz *et al.*, 2014; Dinsmore and Reiter, 2016). The recent findings that loss of primary cilia can promote development of atherosclerosis provides unequivocal evidence of the importance of this sensory organelle for blood vessel homeostasis. Further to this, many ciliopathies show abnormal cilia length with both increases and decreases in primary cilia length seen (Husson *et al.*, 2016). More recent studies have shown shortening of ciliary length to be associated with cystic kidney disease (Husson *et al.*, 2016). Results described herein may lead to a better understanding of the influence of the actin cytoskeleton on ciliary structure and function, and may provide new therapeutic approaches to regulate length and abundance of primary cilia.

References

Abdelhamed, Z. A., Natarajan, S., Wheway, G., Inglehearn, C. F., Toomes, C., Johnson, C. A. and Jagger, D. J. (2015) 'The Meckel-Gruber syndrome protein TMEM67 controls basal body positioning and epithelial branching morphogenesis via the non-canonical Wnt pathway', *Disease Models & Mechanisms*, 67, p. dmm.019083-. doi: 10.1242/dmm.019083.

Abdelhamed, Z. A., Wheway, G., Szymanska, K., Natarajan, S., Toomes, C., Inglehearn, C. and Johnson, C. A. (2013) 'Variable expressivity of ciliopathy neurological phenotypes that encompass Meckel - Gruber syndrome and Joubert syndrome is caused by complex de-regulated ciliogenesis, Shh and wnt signalling defects', *Human Molecular Genetics*, 22(7), pp. 1358–1372. doi: 10.1093/hmg/dds546.

AbouAlaiwi, W. A., Ratnam, S., Booth, R. L., Shah, J. V and Nauli, S. M. (2011) 'Endothelial cells from humans and mice with polycystic kidney disease are characterized by polyploidy and chromosome segregation defects through survivin down-regulation.', *Human molecular genetics*, 20(2), pp. 354–67. doi: 10.1093/hmg/ddq470.

AbouAlaiwi, W. A., Takahashi, M., Mell, B. R., Jones, T. J., Ratnam, S., Kolb, R. J. and Nauli, S. M. (2009) 'Ciliary polycystin-2 is a mechanosensitive calcium channel involved in nitric oxide signaling cascades.', *Circulation research*, 104(7), pp. 860–9. doi: 10.1161/CIRCRESAHA.108.192765.

Abraham, S., Scarcia, M., Bagshaw, R. D., McMahon, K., Grant, G., Harvey, T., Yeo, M., Esteves, F. O. G. G., Thygesen, H. H., Jones, P. F., Speirs, V., Hanby, A. M., Selby, P. J., Lorger, M., Dear, T. N., Pawson, T., Marshall, C. J. and Mavria, G. (2015) 'A Rac/Cdc42 exchange factor complex promotes formation of lateral filopodia and blood vessel lumen morphogenesis', *Nature Communications*. Nature Research, 6, p. 7286. doi: 10.1038/ncomms8286.

Abraham, S., Yeo, M., Montero-Balaguer, M., Paterson, H., Dejana, E., Marshall, C. J. and Mavria, G. (2009) 'VE-Cadherin-mediated cell-cell interaction suppresses sprouting via signaling to MLC2 phosphorylation.', *Current biology : CB*. Elsevier Ltd, 19(8), pp. 668–74. doi: 10.1016/j.cub.2009.02.057.

Adams, R. H. and Alitalo, K. (2007) 'Molecular regulation of angiogenesis and lymphangiogenesis.', *Nature reviews. Molecular cell biology*. Nature Publishing Group, 8(6), pp. 464–78. doi: 10.1038/nrm2183.

Alkam, D., Feldman, E. Z., Singh, A. and Kiaei, M. (2016) 'Profilin1 biology and its mutation, actin(g) in disease', *Cellular and Molecular Life Sciences*, pp. 1–15. doi: 10.1007/s00018-016-2372-1.

Amano, M., Ito, M., Fukata, Y., Chihara, K., Nakano, T., Matsuura, Y. and Kaibuchi, K. (1996) 'Phosphorylation and Activation of Myosin by Rho-associated', *The Journal of biological chemistry*, 271, pp. 20246–20249. doi: 10.1074/jbc.271.34.20246.

Ando, J. and Yamamoto, K. (2013) 'Flow detection and calcium signalling in vascular endothelial cells.', *Cardiovascular research*, 99(2), pp. 260–8. doi: 10.1093/cvr/cvt084.

Andrianantoandro, E. and Pollard, T. D. (2006) 'Mechanism of Actin Filament Turnover by Severing and Nucleation at Different Concentrations of ADF/Cofilin', *Molecular Cell*, 24(1), pp. 13–23. doi: 10.1016/j.molcel.2006.08.006.

Avasthi, P. and Marshall, W. F. (2012) 'Stages of ciliogenesis and regulation of ciliary length.', *Differentiation; research in biological diversity*. Elsevier, 83(2), pp. S30-42. doi: 10.1016/j.diff.2011.11.015.

Barry, D. M., Xu, K., Meadows, S. M., Zheng, Y., Norden, P. R., Davis, G. E. and Cleaver, O. (2015) 'Cdc42 is required for cytoskeletal support of endothelial cell adhesion during blood vessel formation in mice', *Development (Cambridge, England)*. The Company of Biologists, 142(17), pp. 3058–3070. doi: 10.1242/dev.125260.

Bayless, K. J. and Davis, G. E. (2002) 'The Cdc42 and Rac1 GTPases are required for capillary lumen formation in three-dimensional extracellular matrices.', *Journal of cell science*, 115(Pt 6), pp. 1123–36.

Bayless, K. J. and Davis, G. E. (2004) 'Microtubule Depolymerization Rapidly Collapses Capillary Tube Networks in Vitro and Angiogenic Vessels in Vivo through the Small GTPase Rho', *Journal of Biological Chemistry* , 279(12), pp. 11686–11695. doi: 10.1074/jbc.M308373200.

Bayless, K. J., Salazar, R. and Davis, G. E. (2000) 'RGD-Dependent Vacuolation and Lumen Formation Observed during Endothelial Cell Morphogenesis in Three-Dimensional Fibrin Matrices Involves the αvβ3 and α5β1 Integrins', *The American Journal of Pathology*. Elsevier, 156(5), pp. 1673–1683. doi: 10.1016/S0002-9440(10)65038-9.

Bazzoni, G. and Dejana, E. (2004) 'Endothelial Cell-to-Cell Junctions: Molecular Organization and Role in Vascular Homeostasis', *Physiological Reviews*, 84(3).

Bershteyn, M., Atwood, S. X., Woo, W.-M., Li, M. and Oro, A. E. (2010) 'MIM and cortactin antagonism regulates ciliogenesis and hedgehog signaling.', *Developmental cell*, 19(2), pp. 270–83. doi: 10.1016/j.devcel.2010.07.009.

Bishop, A. L. and Hall, A. (2000) 'Rho GTPases and their effector proteins', *Biochem. J*, 348, pp. 241–255.

Blanchoin, L., Boujemaa-Paterski, R., Sykes, C. and Plastino, J. (2014) 'Actin Dynamics, Architecture, and Mechanics in Cell Motility', *Physiological Reviews*, 94(1).

Blanco, R. and Gerhardt, H. (2013) 'VEGF and Notch in tip and stalk cell selection', *Cold Spring Harbor Perspectives in Medicine*, 3(1), pp. 1–20. doi: 10.1101/cshperspect.a006569.

Blum, Y., Belting, H.-G., Ellertsdottir, E., Herwig, L., Lüders, F. and Affolter, M. (2008) 'Complex cell rearrangements during intersegmental vessel sprouting and vessel fusion in the zebrafish embryo', *Developmental Biology*, 316(2), pp. 312–322. doi: 10.1016/j.ydbio.2008.01.038.

Bodle, J. C. and Loboa, E. G. (2016) 'Concise Review: Primary Cilia: Control Centers for Stem Cell Lineage Specification and Potential Targets for Cell-Based Therapies.', *Stem cells (Dayton, Ohio)*, 34(6), pp. 1445–54. doi: 10.1002/stem.2341.

Boe, E. D., Dsjujdbm, B. B. S. F., Sakamori, R., Das, S., Yu, S., Feng, S., Stypulkowski, E., Guan, Y., Douard, V., Tang, W., Ferraris, R. P., Harada, A., Brakebusch, C., Guo, W. and Gao, N. (2012) 'Cdc42 and Rab8a are critical for intestinal stem cell division, survival, and differentiation in mice', *The Journal of Clinical Investigation*, 122(3). doi: 10.1172/JCI60282DS1.

Bolz, S., Pieperhoff, S., De Wit, C. and Pohl, U. (2000) 'Chronic increases in transmural pressure reduce NO-mediated dilations in isolated resistance arteries of the hamster.', *Acta physiologica Scandinavica*, 168(1), pp. 113–7. doi: 10.1046/j.1365-201x.2000.00633.x.

Bravo-Cordero, J. J., Magalhaes, M. A. O., Eddy, R. J., Hodgson, L. and Condeelis, J. (no date) 'Functions of cofilin in cell locomotion and invasion'. doi: 10.1038/nrm3609.

Breitsprecher, D. and Goode, B. L. (2013) 'Formins at a glance', *Journal of Cell Science*, 126(1).

Brugnera, E., Haney, L., Grimsley, C., Lu, M., Walk, S. F., Tosello-Trampont, A.-C., Macara, I. G., Madhani, H., Fink, G. R. and Ravichandran, K. S. (2002) 'Unconventional Rac-GEF activity is mediated through the Dock180–ELMO complex', *Nature Cell Biology*, 4(8), pp. 574–82. doi: 10.1038/ncb824.

Bryan, B. A. and D'Amore, P. A. (2007) 'What tangled webs they weave: Rho-GTPase control of angiogenesis', *Cellular and Molecular Life Sciences*, 64(16), pp. 2053–2065. doi: 10.1007/s00018-007-7008-z.

Bryan, B. A., Dennstedt, E., Mitchell, D. C., Walshe, T. E., Noma, K., Loureiro, R., Saint-Geniez, M., Campaigniac, J.-P., Liao, J. K. and D'Amore, P. A. (2010) 'RhoA/ROCK signaling is essential for multiple aspects of VEGF-mediated angiogenesis', *The FASEB Journal* ,

24(9), pp. 3186–3195. doi: 10.1096/fj.09-145102.

Bryant, D. M. and Mostov, K. E. (2008) 'From cells to organs: building polarized tissue', *Nature reviews. Molecular cell biology*, 9(11), pp. 887–901. doi: 10.1038/nrm2523.

Bugyi, B. and Carlier, M.-F. (2010) 'Control of Actin Filament Treadmilling in Cell Motility', *Annual Review of Biophysics*, 39(1), pp. 449–470. doi: 10.1146/annurev-biophys-051309-103849.

Burri, P. H., Hlushchuk, R. and Djonov, V. (2004) 'Intussusceptive angiogenesis: its emergence, its characteristics, and its significance.', *Developmental dynamics : an official publication of the American Association of Anatomists*, 231(3), pp. 474–88. doi: 10.1002/dvdy.20184.

Bystrevskaia, V. B., Antonov, A. S. and Perov, N. A. (1987) '[Primary cilium in the endothelial cells of the human aorta].', *Doklady Akademii nauk SSSR*, 297(5), pp. 1233–6.

Cai, S., Pestic-Dragovich, L., O'Donnell, M. E., Wang, N., Ingber, D., Elson, E. and De Lanerolle, P. (1998) 'Regulation of cytoskeletal mechanics and cell growth by myosin light chain phosphorylation.', *The American journal of physiology*, 275(5 Pt 1), pp. C1349-56.

Campellone, K. G. and Welch, M. D. (2010) 'A nucleator arms race: cellular control of actin assembly', *Nature Reviews Microbiology*. Nature Publishing Group, 11(4), pp. 237–251. doi: 10.1038/nrm2867.

Cao, J., Shen, Y., Zhu, L., Xu, Y., Zhou, Y., Wu, Z., Li, Y., Yan, X. and Zhu, X. (2012) 'miR-129-3p controls cilia assembly by regulating CP110 and actin dynamics', *Nature Cell Biology*. Nature Research, 14(7), pp. 697–706. doi: 10.1038/ncb2512.

Carlsson, L., Nyström, L.-E., Lindberg, U., Kannan, K. K., Cid-Dresdner, H., Lövgren, S. and Jörnvall, H. (1976) 'Crystallization of a non-muscle actin', *Journal of Molecular Biology*. Academic Press, 105(3), pp. 353–366. doi: 10.1016/0022-2836(76)90098-X.

Carmeliet, P. and Jain, R. K. (2011) 'Molecular Mechanisms and and clinical applications of angiogenesis', *Nature*, 473(7347), pp. 298–307. doi: 10.1038/nature10144.Molecular.

Carmeliet, P., Lampugnani, M.-G., Moons, L., Breviario, F., Compernolle, V., Bono, F., Balconi, G., Spagnuolo, R., Oosthuyse, B., Dewerchin, M., Zanetti, A., Angellilo, A., Mattot, V., Nuyens, D., Lutgens, E., Clotman, F., de Ruiter, M. C., Gittenberger-de Groot, A., Poelmann, R., Lupu, F., Herbert, J.-M., Collen, D. and Dejana, E. (1999) 'Targeted Deficiency or Cytosolic Truncation of the VE-cadherin Gene in Mice Impairs VEGF-Mediated Endothelial Survival and Angiogenesis', *Cell*. Elsevier, 98(2), pp. 147–157. doi: 10.1016/S0092-8674(00)81010-7.

Caroni, P., Arber, S., Barbayannis, F. A., Hanser, H., Schneider, C., Stanyon, C. A. and Bernard,

O. (1998) ‘Regulation of actin dynamics through phosphorylation of cofilin by LIM-kinase’, *Nature*. Nature Publishing Group, 393(6687), pp. 805–809. doi: 10.1038/31729.

Chapouly, C., Yao, Q., Vandierdonck, S., Larrieu-Lahargue, F., Mariani, J. N., Gadeau, A.-P. and Renault, M.-A. (2016) ‘Impaired Hedgehog signalling-induced endothelial dysfunction is sufficient to induce neuropathy: implication in diabetes.’, *Cardiovascular research*, 109(2), pp. 217–27. doi: 10.1093/cvr/cvv263.

Chappell, J. C., Mouillesseaux, K. P. and Bautch, V. L. (2013) ‘Flt-1 (Vascular Endothelial Growth Factor Receptor-1) Is Essential for the Vascular Endothelial Growth Factor–Notch Feedback Loop During AngiogenesisSignificance’, *Arteriosclerosis, Thrombosis, and Vascular Biology*, 33(8).

Chen, F., Ma, L., Parrini, M. C., Mao, X., Lopez, M., Wu, C., Marks, P. W., Davidson, L., Kwiatkowski, D. J., Kirchhausen, T., Orkin, S. H., Rosen, F. S., Mayer, B. J., Kirschner, M. W. and Alt, F. W. (2000) ‘Cdc42 is required for PIP2-induced actin polymerization and early development but not for cell viability’, *Current Biology*, 10(13), pp. 758–765. doi: 10.1016/S0960-9822(00)00571-6.

Cheng, H.-Y., Lin, Y.-Y., Yu, C.-Y., Chen, J.-Y., Shen, K.-F., Lin, W.-L., Liao, H.-K., Chen, Y.-J., Liu, C.-H., Pang, V. F. and Jou, T.-S. (2005) ‘Molecular Identification of Canine Podocalyxin-Like Protein 1 as a Renal Tubulogenic Regulator’, *Journal of the American Society of Nephrology* , 16(6), pp. 1612–1622. doi: 10.1681/ASN.2004121145.

Christensen, S. T., Pedersen, L. B., Schneider, L. and Satir, P. (2007) ‘Sensory cilia and integration of signal transduction in human health and disease.’, *Traffic (Copenhagen, Denmark)*, 8(2), pp. 97–109. doi: 10.1111/j.1600-0854.2006.00516.x.

Chrzanowska-Wodnicka, M. and Burridge, K. (1996) ‘Rho-stimulated contractility drives the formation of stress fibers and focal adhesions.’, *The Journal of Cell Biology*, 133(6).

Chung, S. and Andrew, D. J. (2008) ‘The formation of epithelial tubes’, *Journal of Cell Science*, 121(21).

Cooper, G. M. (2000) ‘Actin, Myosin, and Cell Movement’. Sinauer Associates.

Côté, J.-F. and Vuori, K. (2002) ‘Identification of an evolutionarily conserved superfamily of DOCK180-related proteins with guanine nucleotide exchange activity.’, *Journal of cell science*, 115(Pt 24), pp. 4901–13.

D’Amico, G., Jones, D. T., Nye, E., Sapienza, K., Ramjuan, A. R., Reynolds, L. E., Robinson, S. D., Kostourou, V., Martinez, D., Aubyn, D., Grose, R., Thomas, G. J., Spencer-Dene, B., Zicha, D., Davies, D., Tybulewicz, V. and Hodivala-Dilke, K. M. (2009) ‘Regulation of lymphatic-blood vessel separation by endothelial Rac1’, *Development (Cambridge, England)*.

Company of Biologists, 136(23), pp. 4043–4053. doi: 10.1242/dev.035014.

Daugherty, A. and Cassis, L. A. (2004) 'Mouse Models of Abdominal Aortic Aneurysms', *Arteriosclerosis, Thrombosis, and Vascular Biology*, 24(3), pp. 429–434. doi: 10.1161/01.ATV.0000118013.72016.ea.

Davis, G. E. and Camarillo, C. W. (1996) 'An α2β1 Integrin-Dependent Pinocytic Mechanism Involving Intracellular Vacuole Formation and Coalescence Regulates Capillary Lumen and Tube Formation in Three-Dimensional Collagen Matrix', *Experimental Cell Research*. Academic Press, 224(1), pp. 39–51. doi: 10.1006/excr.1996.0109.

Davis, G. E., Koh, W. and Stratman, A. N. (2007) 'Mechanisms controlling human endothelial lumen formation and tube assembly in three-dimensional extracellular matrices.', *Birth defects research. Part C, Embryo today : reviews*, 81(4), pp. 270–85. doi: 10.1002/bdrc.20107.

Davis, G. E. and Senger, D. R. (2005) 'Endothelial Extracellular Matrix', *Circulation Research*, 97(11).

Davis, G. E. and Senger, D. R. (2008) 'Extracellular matrix mediates a molecular balance between vascular morphogenesis and regression', *Current Opinion in Hematology*, 15(3).

Dawe, H. R., Adams, M., Wheway, G., Szymanska, K., Logan, C. V., Noegel, A. A., Gull, K. and Johnson, C. A. (2009) 'Nesprin-2 interacts with meckelin and mediates ciliogenesis via remodelling of the actin cytoskeleton', *Journal of Cell Science*, 122(15).

Derivery, E. and Gautreau, A. (2010) 'Generation of branched actin networks: assembly and regulation of the N-WASP and WAVE molecular machines.', *BioEssays : news and reviews in molecular, cellular and developmental biology*, 32(2), pp. 119–31. doi: 10.1002/bies.200900123.

Deveza, L., Choi, J. and Yang, F. (2012) 'Therapeutic angiogenesis for treating cardiovascular diseases', *Theranostics*, 2(8), pp. 801–814. doi: 10.7150/thno.4419.

Dinsmore, C. and Reiter, J. F. (2016) 'Endothelial primary cilia inhibit atherosclerosis', *EMBO reports*, 17(2), p. 156 LP-166.

Disli, O. M., Ozdemir, E., Berkan, O., Bagcivan, I., Durmus, N. and Parlak, A. (2009) 'Rho-kinase inhibitors Y-27632 and fasudil prevent agonist-induced vasospasm in human radial artery', *Canadian Journal of Physiology and Pharmacology*. NRC Research Press, 87(8), pp. 595–601. doi: 10.1139/Y09-043.

Djonov, V., Schmid, M., Tschanz, S. A. and Burri, P. H. (2000) 'Intussusceptive Angiogenesis', *Circulation Research*, 86(3).

Doyonnas, R., Kershaw, D. B., Duhme, C., Merkens, H., Chelliah, S., Graf, T. and McNagny, K. M.

(2001) ‘Anuria, Omphalocele, and Perinatal Lethality in Mice Lacking the Cd34-Related Protein Podocalyxin’, *Journal of Experimental Medicine*, 194(1).

Drake, C. J., Davis, L. A. and Little, C. D. (1992) ‘Antibodies to beta 1-integrins cause alterations of aortic vasculogenesis, in vivo.’, *Developmental dynamics : an official publication of the American Association of Anatomists*, 193(1), pp. 83–91. doi: 10.1002/aja.1001930111.

Dummer, A., Poelma, C., DeRuiter, M. C., Goumans, M.-J. T. H. and Hierck, B. P. (2016) ‘Measuring the primary cilium length: improved method for unbiased high-throughput analysis.’, *Cilia*. BioMed Central, 5, p. 7. doi: 10.1186/s13630-016-0028-2.

Dvorak, H. F., Brown, L. F., Detmar, M. and Dvorak, A. M. (1995) ‘Vascular Permeability FactorNascular Endothelial Growth Factor, Microvascular Hyperpermeability, and Angiogenesis’, *American Journal ofPathology*, 146(5).

Egile, C., Rouiller, I., Xu, X. P., Volkmann, N., Li, R. and Hanein, D. (2005) ‘Mechanism of filament nucleation and branch stability revealed by the structure of the Arp2/3 complex at actin branch junctions’, *PLoS Biology*, 3(11), pp. 1902–1909. doi: 10.1371/journal.pbio.0030383.

Egorova, A. D., van der Heiden, K., Poelmann, R. E. and Hierck, B. P. (2012) ‘Primary cilia as biomechanical sensors in regulating endothelial function’, *Differentiation*, 83(2), pp. S56–S61. doi: 10.1016/j.diff.2011.11.007.

Eisenmann, K. M., Peng, J., Wallar, B. J. and Alberts, A. S. (2005) ‘Rho GTPase-formin pairs in cytoskeletal remodelling.’, *Novartis Foundation symposium*, 269, pp. 206-218–30.

El-Kenawi, A. E. and El-Remessy, A. B. (2013) ‘Angiogenesis inhibitors in cancer therapy: mechanistic perspective on classification and treatment rationales’, *British Journal of Pharmacology*, 170, pp. 712–729. doi: 10.1111/bph.12344.

Elliott, H., Fischer, R. S., Myers, K. A., Desai, R. A., Gao, L., Chen, C. S., Adelstein, R. S., Waterman, C. M. and Danuser, G. (2015) ‘Myosin II controls cellular branching morphogenesis and migration in three dimensions by minimizing cell-surface curvature’, *Nature Cell Biology*. Nature Research, 17(2), pp. 137–147. doi: 10.1038/ncb3092.

Erickson, J. W. and Cerione, R. A. (2001) ‘Multiple roles for Cdc42 in cell regulation’, *Current Opinion in Cell Biology*, 13(2), pp. 153–157. doi: 10.1016/S0955-0674(00)00192-7.

Etienne-Manneville, S. (2004) ‘Cdc42 - the centre of polarity’, *Journal of Cell Science*, 117(8).

Fantin, A., Vieira, J. M., Gestri, G., Denti, L., Schwarz, Q., Prykhozhij, S., Peri, F., Wilson, S. W. and Ruhrberg, C. (2010) ‘Tissue macrophages act as cellular chaperones for vascular anastomosis downstream of VEGF-mediated endothelial tip cell induction’, *Blood*, 116(5).

Ferrara, N., Gerber, H.-P. and LeCouter, J. (2003) 'The biology of VEGF and its receptors.', *Nature medicine*, 9(6), pp. 669–76. doi: 10.1038/nm0603-669.

Fischer, R. S., Gardel, M., Ma, X., Adelstein, R. S. and Waterman, C. M. (2009) 'Local cortical tension by myosin II guides 3D endothelial cell branching.', *Current biology : CB*. NIH Public Access, 19(3), pp. 260–5. doi: 10.1016/j.cub.2008.12.045.

Forsythe, J. A., Jiang, B. H., Iyer, N. V, Agani, F., Leung, S. W., Koos, R. D. and Semenza, G. L. (1996) 'Activation of vascular endothelial growth factor gene transcription by hypoxia-inducible factor 1.', *Molecular and cellular biology*, 16(9), pp. 4604–13.

Galkin, V., Orlova, A. and Kudryashov, D. (2011) 'Remodeling of actin filaments by ADF/cofilin proteins', *Proceedings of the*.

Galvagni, F., Baldari, C. T., Oliviero, S. and Orlandini, M. (2012) 'An apical actin-rich domain drives the establishment of cell polarity during cell adhesion', *Histochemistry and Cell Biology*, 138(3), pp. 419–433. doi: 10.1007/s00418-012-0965-9.

Gavard, J. and Gutkind, J. S. (2006) 'VEGF controls endothelial-cell permeability by promoting the beta-arrestin-dependent endocytosis of VE-cadherin.', *Nature cell biology*, 8(11), pp. 1223–34. doi: 10.1038/ncb1486.

Gebala, V., Collins, R., Geudens, I., Phng, L.-K. and Gerhardt, H. (2016) 'Blood flow drives lumen formation by inverse membrane blebbing during angiogenesis in vivo', *Nature Cell Biology*. Nature Research, advance on(4), pp. 443–450. doi: 10.1038/ncb3320.

Geerts, W. J. C., Vocking, K., Schoonen, N., Haarbosch, L., van Donselaar, E. G., Regan-Klapisz, E. and Post, J. A. (2011) 'Cobblestone HUVECs: a human model system for studying primary ciliogenesis.', *Journal of structural biology*. Elsevier Inc., 176(3), pp. 350–9. doi: 10.1016/j.jsb.2011.09.013.

Gelberg H1, Healy L, Whiteley H, Miller LA, V. E. (1996) 'In vivo enzymatic removal of alpha 2-->6-linked sialic acid from the glomerular filtration barrier results in podocyte charge alteration and glomerular injury', *Lab Invest.*, 74(5), pp. 907–20.

Gerhardt, H., Golding, M., Fruttiger, M., Ruhrberg, C., Lundkvist, A., Abramsson, A., Jeltsch, M., Mitchell, C., Alitalo, K., Shima, D. and Betsholtz, C. (2003) 'VEGF guides angiogenic sprouting utilizing endothelial tip cell filopodia.', *The Journal of cell biology*, 161(6), pp. 1163–77. doi: 10.1083/jcb.200302047.

GG, B. (1999) 'Arp2/3 complex and actin depolymerizing factor/cofilin in dendritic organization and treadmilling of actin filament array in lamellipodia', *J. Cell Biol.*, 145, p. 1009.

Goetz, J. G. G., Steed, E., Ferreira, R. R. R., Roth, S., Ramspacher, C., Boselli, F., Charvin, G., Liebling, M., Wyart, C., Schwab, Y. and Vermot, J. (2014) 'Endothelial cilia mediate low

flow sensing during zebrafish vascular development.', *Cell reports*. Elsevier, 6(5), pp. 799–808. doi: 10.1016/j.celrep.2014.01.032.

Goldschmidt-Clermont, P. J., Furman, M. I., Wachsstock, D., Safer, D., Nachmias, V. T. and Pollard, T. D. (1992) 'The control of actin nucleotide exchange by thymosin beta 4 and profilin. A potential regulatory mechanism for actin polymerization in cells', *Mol Biol Cell*, 3(9), pp. 1015–1024. doi: 10.1091/mbc.3.9.1015.

Goley, E. D. and Welch, M. D. (2006) 'The ARP2/3 complex: an actin nucleator comes of age', *Nature Reviews Molecular Cell Biology*. Nature Publishing Group, 7(10), pp. 713–726. doi: 10.1038/nrm2026.

Gore, A. V., Monzo, K., Cha, Y. R., Pan, W. and Weinstein, B. M. (2012) 'Vascular Development in the Zebrafish', *Cold Spring Harbor Perspectives in Medicine*, 2(5), pp. a006684–a006684. doi: 10.1101/cshperspect.a006684.

Gory-Faure, S., Prandini, M. H., Pointu, H., Roullot, V., Pignot-Paintrand, I., Vernet, M. and Huber, P. (1999) 'Role of vascular endothelial-cadherin in vascular morphogenesis', *Development*, 126(10).

Goto, H., Inoko, A. and Inagaki, M. (2013) 'Cell cycle progression by the repression of primary cilia formation in proliferating cells.', *Cellular and molecular life sciences : CMLS*, 70(20), pp. 3893–905. doi: 10.1007/s00018-013-1302-8.

Gupta, M. K. and Qin, R.-Y. (2003) 'Mechanism and its regulation of tumor-induced angiogenesis.', *World journal of gastroenterology*, 9(6), pp. 1144–55.

Hall, A. (1998) 'Rho GTPases and the actin cytoskeleton.', *Science (New York, N.Y.)*, 279(5350), pp. 509–14.

Hartmann, S., Ridley, A. J. and Lutz, S. (2015) 'The function of rho-associated kinases ROCK1 and ROCK2 in the pathogenesis of cardiovascular disease', *Frontiers in Pharmacology*, 6(NOV), pp. 1–16. doi: 10.3389/fphar.2015.00276.

Haust, M. D. (1987) 'Endothelial cilia in human aortic atherosclerotic lesions.', *Virchows Archiv. A, Pathological anatomy and histopathology*, 410(4), pp. 317–26.

Hayashi, M., Majumdar, A., Li, X., Adler, J., Sun, Z., Vertuani, S., Hellberg, C., Mellberg, S., Koch, S., Dimberg, A., Koh, G. Y., Dejana, E., Belting, H.-G., Affolter, M., Thurston, G., Holmgren, L., Vestweber, D. and Claesson-Welsh, L. (2013) 'VE-PTP regulates VEGFR2 activity in stalk cells to establish endothelial cell polarity and lumen formation.', *Nature communications*. Nature Publishing Group, 4, p. 1672. doi: 10.1038/ncomms2683.

He, M., Agbu, S. and Anderson, K. V (2016) 'Microtubule Motors Drive Hedgehog Signaling in Primary Cilia.', *Trends in cell biology*. doi: 10.1016/j.tcb.2016.09.010.

Van der Heiden, K., Hierck, B. P., Krams, R., de Crom, R., Cheng, C., Baiker, M., Pourquie, M. J. B. M., Alkemade, F. E., DeRuiter, M. C., Gittenberger-de Groot, A. C. and Poelmann, R. E. (2008) 'Endothelial primary cilia in areas of disturbed flow are at the base of atherosclerosis.', *Atherosclerosis*, 196(2), pp. 542–50. doi: 10.1016/j.atherosclerosis.2007.05.030.

Herbert, S. P. and Stainier, D. Y. R. (2011) 'Molecular control of endothelial cell behaviour during blood vessel morphogenesis.', *Nature reviews. Molecular cell biology*, 12(9), pp. 551–64. doi: 10.1038/nrm3176.

Herwig, L., Blum, Y., Krudewig, A., Ellertsdottir, E., Lenard, A., Belting, H.-G. and Affolter, M. (2011) 'Distinct Cellular Mechanisms of Blood Vessel Fusion in the Zebrafish Embryo', *Current Biology*. Elsevier, 21(22), pp. 1942–1948. doi: 10.1016/j.cub.2011.10.016.

Herzog, D., Loetscher, P., van Hengel, J., Knusel, S., Brakebusch, C., Taylor, V., Suter, U. and Relvas, J. B. (2011) 'The Small GTPase RhoA Is Required to Maintain Spinal Cord Neuroepithelium Organization and the Neural Stem Cell Pool', *J Neurosci*, 31(13), pp. 5120–5130. doi: 10.1523/JNEUROSCI.4807-10.2011.

Hetheridge, C., Mavria, G. and Mellor, H. (2011) 'Uses of the in vitro endothelial–fibroblast organotypic co-culture assay in angiogenesis research', *Biochemical Society Transactions*, 39(6).

Hierck, B. P., Van der Heiden, K., Alkemade, F. E., Van de Pas, S., Van Thienen, J. V, Groenendijk, B. C. W., Bax, W. H., Van der Laarse, A., Deruiter, M. C., Horrevoets, A. J. G. and Poelmann, R. E. (2008) 'Primary cilia sensitize endothelial cells for fluid shear stress.', *Developmental dynamics : an official publication of the American Association of Anatomists*, 237(3), pp. 725–35. doi: 10.1002/dvdy.21472.

van Hinsbergh, V. W. M. and Koolwijk, P. (2008) 'Endothelial sprouting and angiogenesis: matrix metalloproteinases in the lead.', *Cardiovascular research*, 78(2), pp. 203–12. doi: 10.1093/cvr/cvm102.

Hiramoto, K., Negishi, M. and Katoh, H. (2006) 'Dock4 is regulated by RhoG and promotes Rac-dependent cell migration', *Experimental Cell Research*, 312(20), pp. 4205–4216. doi: 10.1016/j.yexcr.2006.09.006.

Hirata, E., Yukinaga, H., Kamioka, Y., Arakawa, Y., Miyamoto, S., Okada, T., Sahai, E. and Matsuda, M. (2012) 'In vivo fluorescence resonance energy transfer imaging reveals differential activation of Rho-family GTPases in glioblastoma cell invasion.', *Journal of cell science*, 125(Pt 4), pp. 858–68. doi: 10.1242/jcs.089995.

Hoang, M. V, Whelan, M. C. and Senger, D. R. (2004) 'Rho activity critically and selectively

regulates endothelial cell organization during angiogenesis', *Proceedings of the National Academy of Sciences of the United States of America*. National Academy of Sciences, 101(7), pp. 1874–1879. doi: 10.1073/pnas.0308525100.

Hoffman, G. R. and Cerione, R. A. (2013) 'Regulation of the RhoGTPases by RhoGDI'. Landes Bioscience.

Hood, J. D., Frausto, R., Kiosses, W. B., Schwartz, M. A. and Cheresh, D. A. (2003) 'Differential ??v integrin-mediated Ras-ERK signaling during two pathways of angiogenesis', *Journal of Cell Biology*, 162(5), pp. 933–943. doi: 10.1083/jcb.200304105.

Hu, G. D., Chen, Y. H., Zhang, L., Tong, W. C., Cheng, Y. X., Luo, Y. L., Cai, S. X. and Zhang, L. (2011) 'The generation of the endothelial specific cdc42-deficient mice and the effect of cdc42 deletion on the angiogenesis and embryonic development', *Chinese Medical Journal*, 124(24), pp. 4155–4159. doi: 10.3760/cma.j.issn.0366-6999.2011.24.007.

Hultin, S., Zheng, Y., Mojallal, M., Vertuani, S., Gentili, C., Balland, M., Milloud, R., Belting, H.-G., Affolter, M., Helker, C. S. M., Adams, R. H., Herzog, W., Uhlen, P., Majumdar, A. and Holmgren, L. (2014) 'AmotL2 links VE-cadherin to contractile actin fibres necessary for aortic lumen expansion', *Nature Communications*, 5, p. 3743. doi: 10.1038/ncomms4743.

Husson, H., Moreno, S., Smith, L. A., Smith, M. M., Russo, R. J., Pitstick, R., Sergeev, M., Ledbetter, S. R., Bukanov, N. O., Lane, M., Zhang, K., Billot, K., Carlson, G., Shah, J., Meijer, L., Beier, D. R. and Ibraghimov-Beskrovnaya, O. (2016) 'Reduction of ciliary length through pharmacologic or genetic inhibition of CDK5 attenuates polycystic kidney disease in a model of nephronophthisis.', *Human molecular genetics*. Oxford University Press, 25(11), pp. 2245–2255. doi: 10.1093/hmg/ddw093.

Ichetovkin, I., Grant, W. and Condeelis, J. (2002) 'Cofilin produces newly polymerized actin filaments that are preferred for dendritic nucleation by the Arp2/3 complex', *Current Biology*, 12(1), pp. 79–84. doi: 10.1016/S0960-9822(01)00629-7.

Iden, S., Rehder, D., August, B., Suzuki, A., Wolburg-Buchholz, K., Wolburg, H., Ohno, S., Behrens, J., Vestweber, D., Ebnet, K., Baumeister, U., Funke, R., Ebnet, K., Vorschmitt, H., Koch, S., Vestweber, D., Bilder, D., Schober, M., Perrimon, N., Chen, X., Macara, I., Ebnet, K., Suzuki, A., Horikoshi, Y., Hirose, T., Brickwedde, M. M. Z., Ohno, S., Vestweber, D., Ebnet, K., Aurrand-Lions, M., Kuhn, A., Kiefer, F., Butz, S., Zander, K., Brickwedde, M. M. zu, Suzuki, A., Imhof, B., Vestweber, D., Hurd, T., Gao, L., Roh, M., Macara, I., Margolis, B., Itoh, M., Sasaki, H., Furuse, M., Ozaki, H., Kita, T., Tsukita, S., Lemmers, C., Michel, D., Lane-Guermonprez, L., Delgrossi, M., Medina, E., Arsanto, J., Bivic, A. Le, Macara, I.,

Mertens, A., Rygiel, T., Olivo, C., Kammen, R. van der, Collard, J., Plant, P., Fawcett, J., Lin, D., Holdorf, A., Binns, K., Kulkarni, S., Pawson, T., Ruffer, C., Strey, A., Janning, A., Kim, K., Gerke, V., Simionescu, M., Simionescu, N., Palade, G., Suzuki, A., Ohno, S., Suzuki, A., Ishiyama, C., Hashiba, K., Shimizu, M., Ebnet, K., Ohno, S., Takekuni, K., Ikeda, W., Fujito, T., Morimoto, K., Takeuchi, M., Monden, M., Takai, Y., Tanentzapf, G., Tepass, U., Vorbrodt, A., Dobrogowska, D., Yamanaka, T., Horikoshi, Y., Sugiyama, Y., Ishiyama, C., Suzuki, A., Hirose, T., Iwamatsu, A., Shinohara, A. and Ohno, S. (2006) 'A distinct PAR complex associates physically with VE-cadherin in vertebrate endothelial cells.', *EMBO reports*. EMBO Press, 7(12), pp. 1239–46. doi: 10.1038/sj.embor.7400819.

Inaba, N., Ishizawa, S., Kimura, M., Fujioka, K., Watanabe, M., Shibasaki, T. and Manome, Y. (2010) 'Effect of inhibition of the ROCK isoform on RT2 malignant glioma cells.', *Anticancer research*, 30(9), pp. 3509–14.

Iomini, C., Tejada, K., Mo, W., Vaananen, H. and Piperno, G. (2004) 'Primary cilia of human endothelial cells disassemble under laminar shear stress.', *The Journal of cell biology*, 164(6), pp. 811–7. doi: 10.1083/jcb.200312133.

Iruela-Arispe, M. L. and Davis, G. E. (2009) 'Cellular and molecular mechanisms of vascular lumen formation.', *Developmental cell*. Elsevier Inc., 16(2), pp. 222–31. doi: 10.1016/j.devcel.2009.01.013.

Ito, M., Nakano, T., Erdödi, F. and Hartshorne, D. J. (2004) 'Myosin phosphatase: Structure, regulation and function', *Molecular and Cellular Biochemistry*. Kluwer Academic Publishers, 259(1/2), pp. 197–209. doi: 10.1023/B:MCBI.0000021373.14288.00.

Jackson, B., Peyrollier, K., Pedersen, E., Basse, A., Karlsson, R., Wang, Z., Lefever, T., Ochsenbein, A. M., Schmidt, G., Aktories, K., Stanley, A., Quondamatteo, F., Ladwein, M., Rottner, K., van Hengel, J. and Brakebusch, C. (2011) 'RhoA is dispensable for skin development, but crucial for contraction and directed migration of keratinocytes.', *Molecular biology of the cell*, 22(5), pp. 593–605. doi: 10.1091/mbc.E09-10-0859.

Jaffe, A. B. and Hall, A. (2005) 'RHO GTPASES: Biochemistry and Biology', *Annual Review of Cell and Developmental Biology*, 21(1), pp. 247–269. doi: 10.1146/annurev.cellbio.21.020604.150721.

John O. Connolly‡ , Nandi Simpson,* Lindsay Hewlett, and A. H. (2002) 'Rac Regulates Endothelial Morphogenesis and Capillary Assembly', *Molecular Biology of the Cell*, 13, pp. 2474–2485.

Johnson, D. I. and Pringle, J. R. (1990) 'Molecular characterization of CDC42, a Saccharomyces cerevisiae gene involved in the development of cell polarity.', *The Journal of cell biology*,

111(1), pp. 143–52.

Jones, E. a V, le Noble, F. and Eichmann, A. (2006) 'What determines blood vessel structure? Genetic prespecification vs. hemodynamics.', *Physiology (Bethesda, Md.)*, 21, pp. 388–95. doi: 10.1152/physiol.00020.2006.

Kallakuri, S., Yu, J. a, Li, J., Li, Y., Weinstein, B. M., Nicoli, S. and Sun, Z. (2014) 'Endothelial Cilia Are Essential for Developmental Vascular Integrity in Zebrafish.', *Journal of the American Society of Nephrology : JASN*, pp. 1–12. doi: 10.1681/ASN.2013121314.

Kamei, M., Brian Saunders, W., Bayless, K. J., Dye, L., Davis, G. E. and Weinstein, B. M. (2006) 'Endothelial tubes assemble from intracellular vacuoles in vivo', *Nature*, 442(7101), pp. 453–456.

Kamei, M., Brian Saunders, W., Bayless, K. J., Dye, L., Davis, G. E. and Weinstein, B. M. (2006) 'Endothelial tubes assemble from intracellular vacuoles in vivo', *Nature*, 442(7101), pp. 453–456. doi: 10.1038/nature04923.

Kather, J. N. and Kroll, J. (2013) 'Rho guanine exchange factors in blood vessels: Fine-tuners of angiogenesis and vascular function', *Experimental Cell Research*, 319(9), pp. 1289–1297. doi: 10.1016/j.yexcr.2012.12.015.

Kaur, S., Leszczynska, K., Abraham, S., Scarcia, M., Hiltbrunner, S., Marshall, C. J., Mavria, G., Bicknell, R. and Heath, V. L. (2011) 'RhoJ/TCL Regulates Endothelial Motility and Tube Formation and Modulates Actomyosin Contractility and Focal Adhesion Numbers', *Arteriosclerosis, Thrombosis, and Vascular Biology*, 31(3), pp. 657–664. doi: 10.1161/ATVBAHA.110.216341.

Kelly, A. E., Kranitz, H., Dötsch, V. and Mullins, R. D. (2006) 'Actin binding to the central domain of WASP/Scar proteins plays a critical role in the activation of the Arp2/3 complex', *Journal of Biological Chemistry*, 281(15), pp. 10589–10597. doi: 10.1074/jbc.M507470200.

Kendall, R. L. and Thomas, K. A. (1993) 'Inhibition of vascular endothelial cell growth factor activity by an endogenously encoded soluble receptor.', *Proceedings of the National Academy of Sciences of the United States of America*, 90(22), pp. 10705–9.

Kim, J., Hsia, E. Y. C., Brigui, A., Plessis, A., Beachy, P. A. and Zheng, X. (2015) 'The role of ciliary trafficking in Hedgehog receptor signaling.', *Science signaling*, 8(379), p. ra55. doi: 10.1126/scisignal.aaa5622.

Kim, J., Jo, H., Hong, H., Kim, M. H., Kim, J. M., Lee, J.-K., Heo, W. Do, Kim, J., Gerdes, J. M., Davis, E. E., Katsanis, N., Goetz, S. C., Anderson, K. V., Kim, S., Li, A., Pugacheva, E. N., Jablonski, S. A., Hartman, T. R., Henske, E. P., Golemis, E. A., Rieder, C. L., Jensen, C. G.,

Jensen, L. C., Santos, N., Reiter, J. F., Tucker, R. W., Pardee, A. B., Fujiwara, K., Mori, Y., Akedo, H., Tanigaki, Y., Tanaka, K., Okada, M., Huangfu, D., Ishikawa, H., Marshall, W. F., Pitaval, A., Tseng, Q., Bornens, M., Théry, M., Kim, J., Bershteyn, M., Atwood, S. X., Woo, W.-M., Li, M., Oro, A. E., Cao, J., Hernandez-Hernandez, V., Halder, G., Johnson, R. L., Zhao, B., Tumaneng, K., Guan, K.-L., Halder, G., Dupont, S., Piccolo, S., Aragona, M., Dupont, S., Habbig, S., Habbig, S., Kim, M., Lee, M.-S., Kim, C.-H., Lim, D.-S., Knödler, A., Westlake, C. J., Wada, K.-I., Itoga, K., Okano, T., Yonemura, S., Sasaki, H., Zhao, B., Choi, J. W., Yu, F.-X., Zhao, B., Zhao, B., Gise, A. von, Lee, K. H., Inoko, A., Gerstein, M. B., Mizuno, K., Ross-Macdonald, P., Piccolo, S., Dupont, S., Cordenonsi, M., Schmidt, K. N., Ridley, A. J., Pan, J., You, Y., Huang, T., Brody, S. L., Park, T. J., Haigo, S. L., Wallingford, J. B., Park, T. J., Mitchell, B. J., Abitua, P. B., Kintner, C., Wallingford, J. B., Adams, M., Hossain, Z., Makita, R., Tian, Y., Yim, H., Sung, C. K., You, J., Tian, Y., Benjamin, T., Kim, I., Shalom, O., Shalva, N., Altschuler, Y., Motro, B., White, M. C., Quarmby, L. M., Evangelista, M., Thiel, C., Pollard, T. D., Cooper, J. A., Rottner, K., Hänisch, J., Campellone, K. G., Hattula, K., Yoshizaki, H., Ye, J., Schmittgen, T. D., Livak, K. J., Carpenter, A. E., Valcu, M. and Valcu, C.-M. (2015) 'Actin remodelling factors control ciliogenesis by regulating YAP/TAZ activity and vesicle trafficking', *Nature Communications*. Nature Publishing Group, 6, p. 6781. doi: 10.1038/ncomms7781.

Kim, J., Lee, J. E., Heynen-Genel, S., Suyama, E., Ono, K., Lee, K., Ideker, T., Aza-Blanc, P. and Gleeson, J. G. (2010) 'Functional genomic screen for modulators of ciliogenesis and cilium length.', *Nature*, 464(7291), pp. 1048–51. doi: 10.1038/nature08895.

Kim, M., M. Shewan, A., Ewald, A. J., Werb, Z. and Mostov, K. E. (2015) 'p114RhoGEF governs cell motility and lumen formation during tubulogenesis through a ROCK–myosin-II pathway', *Journal of Cell Science*, 128(23).

Ko, S. H. and Bandyk, D. F. (2014) 'Therapeutic angiogenesis for critical limb ischemia', *Seminars in Vascular Surgery*, 27(1), pp. 23–31. doi: 10.1053/j.semvascsurg.2014.10.001.

Koenigs, V., Jennings, R., Vogl, T., Horsthemke, M., Bachg, A. C., Xu, Y., Grobe, K., Brakebusch, C., Schwab, A., Baehler, M., Knaus, U. G. and Hanley, P. J. (2014) 'Mouse macrophages completely lacking Rho (RhoA, RhoB and RhoC) have severe lamellipodial retraction defects, but robust chemotactic navigation and increased motility', *Journal of Biological Chemistry* . doi: 10.1074/jbc.M114.563270.

Koh, W., Mahan, R. D. and Davis, G. E. (2008) 'Cdc42- and Rac1-mediated endothelial lumen formation requires Pak2, Pak4 and Par3, and PKC-dependent signaling', *Journal of Cell Science*, 121(7).

Kotsis, F., Boehlke, C. and Kuehn, E. W. (2013) 'The ciliary flow sensor and polycystic kidney disease.', *Nephrology, dialysis, transplantation : official publication of the European Dialysis and Transplant Association - European Renal Association*, 28(3), pp. 518–26. doi: 10.1093/ndt/gfs524.

Kovar, D. R. and Pollard, T. D. (2004) 'Insertional assembly of actin filament barbed ends in association with formins produces piconewton forces.', *Proceedings of the National Academy of Sciences of the United States of America*, 101(41), pp. 14725–14730. doi: 10.1073/pnas.0405902101.

Kozma, R., Ahmed, S., Best, A. and Lim, L. (1995) 'The Ras-related protein Cdc42Hs and bradykinin promote formation of peripheral actin microspikes and filopodia in Swiss 3T3 fibroblasts.', *Molecular and Cellular Biology*, 15(4), pp. 1942–1952.

Krugmann, S., Jordens, I., Gevaert, K., Driessens, M., Vandekerckhove, J. and Hall, A. (2001) 'Cdc42 induces filopodia by promoting the formation of an IRSp53:Mena complex', *Current Biology*. Elsevier, 11(21), pp. 1645–1655. doi: 10.1016/S0960-9822(01)00506-1.

Kuramoto, K., Negishi, M. and Katoh, H. (2009) 'Regulation of dendrite growth by the Cdc42 activator Zizimin1/Dock9 in hippocampal neurons', *Journal of Neuroscience Research*, 87(8), pp. 1794–1805. doi: 10.1002/jnr.21997.

Kwei, S., Stavrakis, G., Takahas, M., Taylor, G., Folkman, M. J., Gimbrone, M. A. and García-Cardeña, G. (2004) 'Early adaptive responses of the vascular wall during venous arterialization in mice.', *The American journal of pathology*, 164(1), pp. 81–9. doi: 10.1016/S0002-9440(10)63099-4.

Lampugnani, M. G., Orsenigo, F., Rudini, N., Maddaluno, L., Boulday, G., Chapon, F. and Dejana, E. (2010) 'CCM1 regulates vascular-lumen organization by inducing endothelial polarity', *Journal of Cell Science*, 123(7).

Larkins, C. E., Aviles, G. D. G., East, M. P., Kahn, R. A. and Caspary, T. (2011) 'Arl13b regulates ciliogenesis and the dynamic localization of Shh signaling proteins', *Molecular Biology of the Cell* , 22(23), pp. 4694–4703. doi: 10.1091/mbc.E10-12-0994.

Lassing, I. and Lindberg, U. (1985) 'Specific interaction between phosphatidylinositol 4,5-bisphosphate and profilactin.', *Nature*, 314(6010), pp. 472–4.

di Lauro, R., De Ruggiero, P., di Lauro, R., di Lauro, M. T. and Romano, M. R. (2010) 'Intravitreal bevacizumab for surgical treatment of severe proliferative diabetic retinopathy', *Graefe's Archive for Clinical and Experimental Ophthalmology*. Springer-Verlag, 248(6), pp. 785–791. doi: 10.1007/s00417-010-1303-3.

Lenard, A., Ellertsdottir, E., Herwig, L., Krudewig, A., Sauteur, L., Belting, H. G. and Affolter, M.

(2013) 'In vivo analysis reveals a highly stereotypic morphogenetic pathway of vascular anastomosis', *Developmental Cell*, 25(5), pp. 492–506. doi: 10.1016/j.devcel.2013.05.010.

Leong, S. Y., Faux, C. H., Turbic, A., Dixon, K. J. and Turnley, A. M. (2011) 'The Rho Kinase Pathway Regulates Mouse Adult Neural Precursor Cell Migration', *STEM CELLS*, 29(2), pp. 332–343. doi: 10.1002/stem.577.

Li, J., Hou, B., Tumova, S., Muraki, K., Bruns, A., Ludlow, M. J., Sedo, A., Hyman, A. J., McKeown, L., Young, R. S., Yuldasheva, N. Y., Majeed, Y., Wilson, L. a., Rode, B., Bailey, M. a., Kim, H. R., Fu, Z., Carter, D. a. L., Bilton, J., Imrie, H., Ajuh, P., Dear, T. N., Cubbon, R. M., Kearney, M. T., Prasad, R. K., Evans, P. C., Ainscough, J. F. X. and Beech, D. J. (2014) 'Piezo1 integration of vascular architecture with physiological force', *Nature*. Nature Publishing Group. doi: 10.1038/nature13701.

Li, X. and Eriksson, U. (2001) 'Novel VEGF family members: VEGF-B, VEGF-C and VEGF-D.', *The international journal of biochemistry & cell biology*, 33(4), pp. 421–6.

Lim, S.-T., Chen, X. L., Tomar, A., Miller, N. L. G., Yoo, J. and Schlaepfer, D. D. (2010) 'Knock-in mutation reveals an essential role for focal adhesion kinase activity in blood vessel morphogenesis and cell motility-polarity but not cell proliferation.', *The Journal of biological chemistry*. American Society for Biochemistry and Molecular Biology, 285(28), pp. 21526–36. doi: 10.1074/jbc.M110.129999.

Lin, G., Craig, G. P., Zhang, L., Yuen, V. G., Allard, M., McNeill, J. H. and MacLeod, K. M. (2007) 'Acute inhibition of Rho-kinase improves cardiac contractile function in streptozotocin-diabetic rats', *Cardiovascular Research*, 75(1).

Liu, Z.-J., Shirakawa, T., Li, Y., Soma, A., Oka, M., Dotto, G. P., Fairman, R. M., Velazquez, O. C. and Herlyn, M. (2003) 'Regulation of Notch1 and Dll4 by vascular endothelial growth factor in arterial endothelial cells: implications for modulating arteriogenesis and angiogenesis.', *Molecular and cellular biology*, 23(1), pp. 14–25.

Lizama, C. O. and Zovein, A. C. (2013) 'Polarizing pathways: balancing endothelial polarity, permeability, and lumen formation.', *Experimental cell research*. Elsevier, 319(9), pp. 1247–54. doi: 10.1016/j.yexcr.2013.03.028.

Lubarsky, B. and Krasnow, M. A. (2003) 'Tube Morphogenesis', *Cell*. Elsevier, 112(1), pp. 19–28. doi: 10.1016/S0092-8674(02)01283-7.

Madaule, P. and Axel, R. (1985) 'A novel ras-related gene family.', *Cell*, 41(1), pp. 31–40.

Maekawa, M., Ishizaki, T., Boku, S., Watanabe, N., Fujita, A., Iwamatsu, A., Obinata, T., Ohashi, K., Mizuno, K. and Narumiya, S. (1999) 'Signaling from Rho to the actin cytoskeleton

through protein kinases ROCK and LIM-kinase.', *Science (New York, N.Y.)*, 285(5429), pp. 895–8.

Maffucci, T. and Falasca, M. (2001) 'Specificity in pleckstrin homology (PH) domain membrane targeting: a role for a phosphoinositide–protein co-operative mechanism', *FEBS Letters*, 506(3), pp. 173–179. doi: http://dx.doi.org/10.1016/S0014-5793(01)02909-X.

Mahaffey, J. P., Grego-Bessa, J., Liem, K. F. and Anderson, K. V. (2013) 'Cofilin and Vangl2 cooperate in the initiation of planar cell polarity in the mouse embryo', *Development*, 140(6).

Malicki, J. J. and Johnson, C. A. (2016) 'The Cilium: Cellular Antenna and Central Processing Unit.', *Trends in cell biology*. doi: 10.1016/j.tcb.2016.08.002.

Martin, M., Geudens, I., Bruyr, J., Potente, M., Bleuart, A., Lebrun, M., Simonis, N., Deroanne, C., Twizere, J.-C., Soubeyran, P., Peixoto, P., Mottet, D., Janssens, V., Hofmann, W.-K., Claes, F., Carmeliet, P., Kettmann, R., Gerhardt, H. and Dequiedt, F. (2013) 'PP2A regulatory subunit Bα controls endothelial contractility and vessel lumen integrity via regulation of HDAC7', *The EMBO Journal*. Nature Publishing Group, 32(February), pp. 2491–2503. doi: 10.1038/emboj.2013.187.

Matsuoka, T. and Yashiro, M. (2014) 'Rho/ROCK signaling in motility and metastasis of gastric cancer', *World Journal of Gastroenterology*, 20(38), pp. 13756–13766. doi: 10.3748/wjg.v20.i38.13756.

Mattila, P. K. and Lappalainen, P. (2008) 'Filopodia: molecular architecture and cellular functions.', *Nature reviews. Molecular cell biology*, 9(6), pp. 446–54. doi: 10.1038/nrm2406.

Mavria, G., Vercoulen, Y., Yeo, M., Paterson, H., Karasarides, M., Marais, R., Bird, D. and Marshall, C. J. (2006) 'ERK-MAPK signaling opposes Rho-kinase to promote endothelial cell survival and sprouting during angiogenesis', *Cancer Cell*, 9(1), pp. 33–44. doi: 10.1016/j.ccr.2005.12.021.

Mayer, B. J. (2001) 'SH3 domains: complexity in moderation.', *Journal of cell science*, 114(Pt 7), pp. 1253–63.

McKenzie, J. A. G. and Ridley, A. J. (2007) 'Roles of Rho/ROCK and MLCK in TNF-alpha-induced changes in endothelial morphology and permeability.', *Journal of cellular physiology*, 213(1), pp. 221–8. doi: 10.1002/jcp.21114.

McLaughlin, P. J., Morton, W. M. and Ayscough, K. R. (2000) 'Latrunculin alters the actin-monomer subunit interface to prevent polymerization.', *Nature Cell Biology*, 2(6), pp. 376–378. doi: 10.1038/35014075.

Meder, D., Shevchenko, A., Simons, K. and Füllekrug, J. (2005) 'Gp135/podocalyxin and NHERF-2 participate in the formation of a preapical domain during polarization of MDCK cells', *Journal of Cell Biology*, 168(2), pp. 303–313. doi: 10.1083/jcb.200407072.

Melendez, J., Liu, M., Sampson, L., Akunuru, S., Han, X., Vallance, J., Witte, D., Shroyer, N. and Zheng, Y. (2013) 'Cdc42 coordinates proliferation, polarity, migration, and differentiation of small intestinal epithelial cells in mice', *Gastroenterology*. Elsevier, Inc, 145(4), pp. 808–819. doi: 10.1053/j.gastro.2013.06.021.

Melendez, J., Stengel, K., Zhou, X., Chauhan, B. K., Debidda, M., Andreassen, P., Lang, R. A. and Zheng, Y. (2011) 'RhoA GTPase Is Dispensable for Actomyosin Regulation but Is Essential for Mitosis in Primary Mouse Embryonic Fibroblasts', *Journal of Biological Chemistry* , 286(17), pp. 15132–15137. doi: 10.1074/jbc.C111.229336.

Meller, N., Irani-Tehrani, M., Kiosses, W. B., Del Pozo, M. A. and Schwartz, M. A. (2002) 'Zizimin1, a novel Cdc42 activator, reveals a new GEF domain for Rho proteins', *Nature Cell Biology*. Nature Publishing Group, 4(9), pp. 639–647. doi: 10.1038/ncb835.

Meller, N., Irani-Tehrani, M., Ratnikov, B. I., Paschal, B. M. and Schwartz, M. A. (2004) 'The Novel Cdc42 Guanine Nucleotide Exchange Factor, Zizimin1, Dimerizes via the Cdc42-binding CZH2 Domain', *Journal of Biological Chemistry* , 279(36), pp. 37470–37476. doi: 10.1074/jbc.M404535200.

Meller, N., Merlot, S. and Guda, C. (2005) 'CZH proteins: a new family of Rho-GEFs', *Journal of Cell Science*, 118(21).

MF, C. (2003) 'ATP hydrolysis on actin-related protein 2/3 complex causes debranching of dendritic actin arrays', *Proc. Natl. Acad. Sci. USA*, 100, p. 6337.

Miyamoto, Y., Yamauchi, J., Sanbe, A. and Tanoue, A. (2007) 'Dock6, a Dock-C subfamily guanine nucleotide exchanger, has the dual specificity for Rac1 and Cdc42 and regulates neurite outgrowth', *Experimental Cell Research*, 313(4), pp. 791–804. doi: 10.1016/j.yexcr.2006.11.017.

Mong, P. Y. and Wang, Q. (2009) 'Activation of Rho Kinase Isoforms in Lung Endothelial Cells during Inflammation', *The Journal of Immunology*, 182(4), pp. 2385–2394. doi: 10.4049/jimmunol.0802811.

Montalvo, J., Spencer, C., Hackathorn, A., Masterjohn, K., Perkins, A., Doty, C., Arumugam, A., Ongusaha, P. P., Lakshmanaswamy, R., Liao, J. K., Mitchell, D. C. and Bryan, B. A. (2013) 'ROCK1 & 2 perform overlapping and unique roles in angiogenesis and angiosarcoma tumor progression.', *Current molecular medicine*, 13(1), pp. 205–19.

Montana, V. and Sontheimer, H. (2011) 'Bradykinin Promotes the Chemotactic Invasion of

Primary Brain Tumors', *Journal of Neuroscience*, 31(13).

Nagy, J., Chang, S.-H., Dvorak, A. and Dvorak, H. (2009) 'Why are tumour blood vessels abnormal and why is it important to know?', *British Journal of Cancer*, 100, pp. 865–869. doi: 10.1038/sj.bjc.6604929.

Nakagawa, O., Fujisawa, K., Ishizaki, T., Saito, Y., Nakao, K. and Narumiya, S. (1996) 'ROCK-I and ROCK-II, two isoforms of Rho-associated coiled-coil forming protein serine/threonine kinase in mice.', *FEBS letters*, 392(2), pp. 189–93.

Nauli, S. M., Kawanabe, Y., Kaminski, J. J., Pearce, W. J., Ingber, D. E. and Zhou, J. (2008) 'Endothelial cilia are fluid shear sensors that regulate calcium signaling and nitric oxide production through polycystin-1.', *Circulation*, 117(9), pp. 1161–71. doi: 10.1161/CIRCULATIONAHA.107.710111.

Nielsen, J. S. and McNagny, K. M. (2008) 'Novel functions of the CD34 family', *Journal of Cell Science*, 121(22).

van Nieuw Amerongen, G. P., Koolwijk, P., Versteilen, A. and van Hinsbergh, V. W. M. (2003) 'Involvement of RhoA/Rho Kinase Signaling in VEGF-Induced Endothelial Cell Migration and Angiogenesis In Vitro', *Arteriosclerosis, Thrombosis, and Vascular Biology*, 23(2).

Niwa, R., Nagata-Ohashi, K., Takeichi, M., Mizuno, K. and Uemura, T. (2002) 'Control of actin reorganization by slingshot, a family of phosphatases that dephosphorylate ADF/cofilin', *Cell*, 108(2), pp. 233–246. doi: 10.1016/S0092-8674(01)00638-9.

Nobes, C. D. and Hall, A. (1995) 'Rho, Rac, and Cdc42 GTPases Regulate the Assembly of Multimolecular Focal Complexes Associated with Actin Stress Fibers, Lamellipodia, and Filopodia', *Cell*. Elsevier, 81(1), pp. 53–62. doi: 10.1016/0092-8674(95)90370-4.

le Noble, F., Moyon, D., Pardanaud, L., Yuan, L., Djonov, V., Matthijsen, R., Bréant, C., Fleury, V. and Eichmann, A. (2004) 'Flow regulates arterial-venous differentiation in the chick embryo yolk sac.', *Development (Cambridge, England)*, 131(2), pp. 361–75. doi: 10.1242/dev.00929.

Ohashi, K., Nagata, K., Maekawa, M., Ishizaki, T., Narumiya, S. and Mizuno, K. (2000) 'Rho-associated kinase ROCK activates LIM-kinase 1 by phosphorylation at threonine 508 within the activation loop', *Journal of Biological Chemistry*, 275(5), pp. 3577–3582. doi: 10.1074/jbc.275.5.3577.

ORLANDO, K., STONE, N. and PITTMAN, R. (2006) 'Rho kinase regulates fragmentation and phagocytosis of apoptotic cells', *Experimental Cell Research*, 312(1), pp. 5–15. doi: 10.1016/j.yexcr.2005.09.012.

Oro, A. E. (2007) 'The primary cilia, a "Rab-id" transit system for hedgehog signaling.', *Current*

opinion in cell biology, 19(6), pp. 691–6. doi: 10.1016/j.ceb.2007.10.008.

Patel-Hett, S. and D'Amore, P. A. (2011) 'Signal transduction in vasculogenesis and developmental angiogenesis', *International Journal of Developmental Biology*, 55(4–5), pp. 353–369. doi: 10.1387/ijdb.103213sp.

Pedersen, L. B. and Rosenbaum, J. L. (2008) 'Intraflagellar transport (IFT) role in ciliary assembly, resorption and signalling.', *Current topics in developmental biology*, 85, pp. 23–61. doi: 10.1016/S0070-2153(08)00802-8.

Pelton, J. C., Wright, C. E., Leitges, M. and Bautch, V. L. (2014) 'Multiple endothelial cells constitute the tip of developing blood vessels and polarize to promote lumen formation', *Development*, 141(21).

Peng, J., Wallar, B. J., Flanders, A., Swiatek, P. J. and Alberts, A. S. (2003) 'Disruption of the Diaphanous-Related Formin Drf1 Gene Encoding mDia1 Reveals a Role for Drf3 as an Effector for Cdc42', *Current Biology*. Elsevier, 13(7), pp. 534–545. doi: 10.1016/S0960-9822(03)00170-2.

Petrovic, N. (2016) 'Targeting Angiogenesis in Cancer Treatments: Where do we Stand?', *Journal of Pharmacy & Pharmaceutical Sciences*, 19(2), pp. 226–238.

Phng, L.-K., Gebala, V., Bentley, K., Philippides, A., Wacker, A., Mathivet, T., Sauteur, L., Stanchi, F., Belting, H.-G., Affolter, M. and Gerhardt, H. (2015) 'Formin-Mediated Actin Polymerization at Endothelial Junctions Is Required for Vessel Lumen Formation and Stabilization', *Developmental Cell*, 32(1), pp. 123–132. doi: 10.1016/j.devcel.2014.11.017.

Phng, L.-K. and Gerhardt, H. (2009) 'Angiogenesis: a team effort coordinated by notch.', *Developmental cell*, 16(2), pp. 196–208. doi: 10.1016/j.devcel.2009.01.015.

Pitaval, A., Tseng, Q., Bornens, M. and Théry, M. (2010) 'Cell shape and contractility regulate ciliogenesis in cell cycle-arrested cells.', *The Journal of cell biology*, 191(2), pp. 303–12. doi: 10.1083/jcb.201004003.

Plank, L. and Ware, B. R. (1987) 'ACANTHAMOEBA PROFILIN BINDING TO FLUORESCEIN-LABELED ACTINS', *BIOPHYS. J.©BiophysicalSociety*, 51, pp. 985–988.

Pollard, T. D. and Cooper, J. A. (1984) 'Quantitative analysis of the effect of Acanthamoeba profilin on actin filament nucleation and elongation', *Biochemistry*. American Chemical Society, 23(26), pp. 6631–6641. doi: 10.1021/bi00321a054.

Praetorius, H. A. and Spring, K. R. (2003) 'Removal of the MDCK cell primary cilium abolishes flow sensing.', *The Journal of membrane biology*, 191(1), pp. 69–76. doi: 10.1007/s00232-002-1042-4.

Pruyne, D., Evangelista, M., Yang, C., Bi, E., Zigmond, S., Bretscher, A. and Boone, C. (2002) 'Role of Formins in Actin Assembly: Nucleation and Barbed-End Association', *Science*, 297(5581).

Pugsley, M. K. and Tabrizchi, R. (2000) 'The vascular system: An overview of structure and function', *Journal of Pharmacological and Toxicological Methods*, 44(2), pp. 333–340. doi: 10.1016/S1056-8719(00)00125-8.

Pyke, K. E. and Tschakovsky, M. E. (2005) 'The relationship between shear stress and flow-mediated dilatation: implications for the assessment of endothelial function.', *The Journal of physiology*, 568(Pt 2), pp. 357–69. doi: 10.1113/jphysiol.2005.089755.

Qi, Y., Liu, J., Saadat, S., Tian, X., Han, Y., Fong, G.-H., Pandolfi, P. P., Lee, L. Y. and Li, S. (2015) 'PTEN induces apoptosis and cavitation via HIF-2-dependent Bnip3 upregulation during epithelial lumen formation', *Cell Death and Differentiation*. Nature Publishing Group, 22(5), pp. 875–884. doi: 10.1038/cdd.2014.185.

Rambhatla, L., Chiu, C.-P., Glickman, R. D. and Rowe-Rendlemen, C. (2002) 'In vitro differentiation capacity of telomerase immortalizes human RPE cells', *Invest. Opthalm. Vis. Sc.*, 43(5), pp. 1622–1630.

Ratcliffe, P. J., Maxwell, P. H., Wiesener, M. S., Chang, G.-W., Clifford, S. C., Vaux, E. C., Cockman, M. E., Wykoff, C. C., Pugh, C. W. and Maher, E. R. (1999) 'The tumour suppressor protein VHL targets hypoxia-inducible factors foroxygen-dependent proteolysis', *Nature*. Nature Publishing Group, 399(6733), pp. 271–275. doi: 10.1038/20459.

RD, M. (2008) 'Capping protein increases the rate of actin-based motility by promoting filament nucleation by the Arp2/3 complex', *Cell*, 133, p. 841.

Resnick, A. and Hopfer, U. (2007) 'Force-Response Considerations in Ciliary Mechanosensation', *Biophysical Journal*. Elsevier, 93(4), pp. 1380–1390. doi: 10.1529/biophysj.107.105007.

Richards, M., Hetheridge, C. and Mellor, H. (2015) 'The Formin FMNL3 Controls Early Apical Specification in Endothelial Cells by Regulating the Polarized Trafficking of Podocalyxin.', *Current biology : CB*, 25(17), pp. 2325–31. doi: 10.1016/j.cub.2015.07.045.

Richards, M., Hetheridge, C. and Mellor, H. (2016) 'The Formin FMNL3 Controls Early Apical Specification in Endothelial Cells by Regulating the Polarized Trafficking of Podocalyxin', *Current Biology*. Elsevier, 25(17), pp. 2325–2331. doi: 10.1016/j.cub.2015.07.045.

Ridley, A. J. and Hall, A. (1992) 'The small GTP-binding protein rho regulates the assembly of focal adhesions and actin stress fibers in response to growth factors.', *Cell*, 70(3), pp.

389–99.

Ridley, A. J., Paterson, H. F., Johnston, C. L., Diekmann, D. and Hall, A. (1992) 'The small GTP-binding protein rac regulates growth factor-induced membrane ruffling.', *Cell*, 70(3), pp. 401–10.

Riento, K. and Ridley, A. J. (2003) 'ROCKs: multifunctional kinases in cell behaviour', *Nat Rev Mol Cell Biol*. Nature Publishing Group, 4(6), pp. 446–456.

Risau, W. (1997) 'Mechanisms of angiogenesis.', *Nature*, 386(6626), pp. 671–4. doi: 10.1038/386671a0.

Risau, W. and Flamme, I. (1995) 'Vasculogenesis.', *Annual review of cell and developmental biology*, 11, pp. 73–91. doi: 10.1146/annurev.cb.11.110195.000445.

Robbins, R. M. and Beitel, G. J. (2016) 'Vascular Lumen Formation: Negativity Will Tear Us Apart', *Current Biology*. Elsevier, 20(22), pp. R973–R975. doi: 10.1016/j.cub.2010.10.032.

Roberto Dominguez and Kenneth C. Holmes (2011) 'NIH Public Access', *Annu Rev Biophys. 2011 Jube 9; 40: 169-186.doi:10.1146/annurev-biophys-042910-155359*, (3), pp. 169–186. doi: 10.1146/annurev-biophys-042910-155359.Actin.

Rossman, K. L., Der, C. J. and Sondek, J. (2005) 'GEF means go: turning on RHO GTPases with guanine nucleotide-exchange factors', *Nature Reviews Molecular Cell Biology*. Nature Publishing Group, 6(2), pp. 167–180. doi: 10.1038/nrm1587.

Samuel, M. S., Lopez, J. I., McGhee, E. J., Croft, D. R., Strachan, D., Timpson, P., Munro, J., Schröder, E., Zhou, J., Brunton, V. G., Barker, N., Clevers, H., Sansom, O. J., Anderson, K. I., Weaver, V. M. and Olson, M. F. (2011) 'Actomyosin-mediated cellular tension drives increased tissue stiffness and β-catenin activation to induce epidermal hyperplasia and tumor growth.', *Cancer cell*. NIH Public Access, 19(6), pp. 776–91. doi: 10.1016/j.ccr.2011.05.008.

Sánchez de Diego, A., Alonso Guerrero, A., Martínez-A, C. and van Wely, K. H. M. (2014) 'Dido3-dependent HDAC6 targeting controls cilium size.', *Nature communications*, 5, p. 3500. doi: 10.1038/ncomms4500.

Satir, P., Pedersen, L. B. and Christensen, S. T. (2010) 'The primary cilium at a glance', *Journal of Cell Science*, 123(4).

Schneider, L., Clement, C. A., Teilmann, S. C., Pazour, G. J., Hoffmann, E. K., Satir, P. and Christensen, S. T. (2005) 'PDGFRalphaalpha signaling is regulated through the primary cilium in fibroblasts.', *Current biology : CB*, 15(20), pp. 1861–6. doi: 10.1016/j.cub.2005.09.012.

Schnittler, H. J., Wilke, A., Gress, T., Suttorp, N. and Drenckhahn, D. (1990) 'Role of actin and myosin in the control of paracellular permeability in pig, rat and human vascular endothelium.', *The Journal of physiology*, 431, pp. 379–401.

Scholzen, T. and Gerdes, J. (2000) 'The Ki-67 protein: From the known and the unknown', *Journal of Cellular Physiology*. John Wiley & Sons, Inc., 182(3), pp. 311–322. doi: 10.1002/(SICI)1097-4652(200003)182:3<311::AID-JCP1>3.0.CO;2-9.

Scott, R. W., Hooper, S., Crighton, D., Li, A., König, I., Munro, J., Trivier, E., Wickman, G., Morin, P., Croft, D. R., Dawson, J., Machesky, L., Anderson, K. I., Sahai, E. A. and Olson, M. F. (2010) 'LIM kinases are required for invasive path generation by tumor and tumor-associated stromal cells.', *The Journal of cell biology*. The Rockefeller University Press, 191(1), pp. 169–85. doi: 10.1083/jcb.201002041.

Semenza, G. L., Jiang, B.-H., Leung, S. W., Passantino, R., Concordet, J.-P., Maire, P. and Giallongo, A. (1996) 'Hypoxia Response Elements in the Aldolase A, Enolase 1, and Lactate Dehydrogenase A Gene Promoters Contain Essential Binding Sites for Hypoxia-inducible Factor 1', *Journal of Biological Chemistry*. American Society for Biochemistry and Molecular Biology, 271(51), pp. 32529–32537. doi: 10.1074/jbc.271.51.32529.

Shi, J. and Wei, L. (2007) 'Rho kinase in the regulation of cell death and survival', *Archivum Immunologiae et Therapiae Experimentalis*, 55(2), pp. 61–75. doi: 10.1007/s00005-007-0009-7.

Shi, J. and Wei, L. (2013) 'Rho kinases in cardiovascular physiology and pathophysiology: the effect of fasudil.', *Journal of cardiovascular pharmacology*, 62(4), pp. 341–54. doi: 10.1097/FJC.0b013e3182a3718f.

Shi, J., Wu, X., Surma, M., Vemula, S., Zhang, L., Yang, Y., Kapur, R. and Wei, L. (2013) 'Distinct roles for ROCK1 and ROCK2 in the regulation of cell detachment', *Cell Death and Disease*. Nature Publishing Group, 4(2), pp. e483-13. doi: 10.1038/cddis.2013.10.

Shibuya, M., Hirai, S., Seto, M., Satoh, S. and Ohtomo, E. (2005) 'Effects of fasudil in acute ischemic stroke: results of a prospective placebo-controlled double-blind trial.', *Journal of the neurological sciences*. Elsevier, 238(1–2), pp. 31–9. doi: 10.1016/j.jns.2005.06.003.

Shimizu, Y., Thumkeo, D., Keel, J., Ishizaki, T., Oshima, H., Oshima, M., Noda, Y., Matsumura, F., Taketo, M. M. and Narumiya, S. (2005) 'ROCK-I regulates closure of the eyelids and ventral body wall by inducing assembly of actomyosin bundles.', *The Journal of cell biology*. The Rockefeller University Press, 168(6), pp. 941–53. doi: 10.1083/jcb.200411179.

Shimokawa, H. and Rashid, M. (2007) 'Development of Rho-kinase inhibitors for cardiovascular

medicine', *Trends in Pharmacological Sciences*. Elsevier, 28(6), pp. 296–302. doi: 10.1016/j.tips.2007.04.006.

Shweiki, D., Itin, A., Soffer, D. and Keshet, E. (1992) 'Vascular endothelial growth factor induced by hypoxia may mediate hypoxia-initiated angiogenesis.', *Nature*, 359(6398), pp. 843–5. doi: 10.1038/359843a0.

Sigurbjörnsdóttir, S., Mathew, R. and Leptin, M. (2014) 'Molecular mechanisms of de novo lumen formation', *Nature Reviews Molecular Cell Biology*. Nature Research, 15(10), pp. 665–676. doi: 10.1038/nrm3871.

Sineva, G. S. and Pospelov, V. A. (2014) 'β-Catenin in pluripotency: adhering to self-renewal or Wnting to differentiate?', *International review of cell and molecular biology*, 312, pp. 53–78. doi: 10.1016/B978-0-12-800178-3.00002-6.

Singla, Veena, and J. F. R. "The primary cilium as the cell's antenna: signaling at a sensory organelle. . science 313. 578. (2006): 629-633. (2006) 'The Primary Cilium as the Cell ' s Antenna : Signaling at a Sensory Organelle Author (s): Veena Singla and Jeremy F . Reiter', *Science*, 313(5787), pp. 629–633.

Smith, P. K., Krohn, R. I., Hermanson, G. T., Mallia, A. K., Gartner, F. H., Provenzano, M. D., Fujimoto, E. K., Goeke, N. M., Olson, B. J. and Klenk, D. C. (1985) 'Measurement of protein using bicinchoninic acid.', *Analytical biochemistry*, 150(1), pp. 76–85. doi: 10.1016/0003-2697(85)90442-7.

Steffen, A., Ladwein, M., Dimchev, G. A., Hein, A., Schwenkmezger, L., Arens, S., Ladwein, K. I., Holleboom, J. M., Schur, F., Small, J. V., Schwarz, J., Gerhard, R., Faix, J., Stradal, T. E. B., Brakebusch, C. and Rottner, K. (2013) 'Rac function is crucial for cell migration but is not required for spreading and focal adhesion formation', *Journal of Cell Science*, 126(20).

Strilić, B., Eglinger, J., Krieg, M., Zeeb, M., Axnick, J., Babál, P., Müller, D. J. and Lammert, E. (2010) 'Electrostatic cell-surface repulsion initiates lumen formation in developing blood vessels.', *Current biology : CB*, 20(22), pp. 2003–9. doi: 10.1016/j.cub.2010.09.061.

Strilić, B., Kucera, T., Eglinger, J., Hughes, M. R., McNagny, K. M., Tsukita, S., Dejana, E., Ferrara, N. and Lammert, E. (2009) 'The molecular basis of vascular lumen formation in the developing mouse aorta.', *Developmental cell*, 17(4), pp. 505–15. doi: 10.1016/j.devcel.2009.08.011.

Surma, M., Wei, L. and Shi, J. (2011) 'Rho kinase as a therapeutic target in cardiovascular disease', *Future Cardiology*, 7(5), pp. 657–671. doi: 10.2217/fca.11.51.Rho.

Tammela, T., Zarkada, G., Nurmi, H., Jakobsson, L., Heinolainen, K., Tvorogov, D., Zheng, W., Franco, C. A., Murtomäki, A., Aranda, E., Miura, N., Ylä-Herttuala, S., Fruttiger, M.,

Mäkinen, T., Eichmann, A., Pollard, J. W., Gerhardt, H. and Alitalo, K. (2011) 'VEGFR-3 controls tip to stalk conversion at vessel fusion sites by reinforcing Notch signalling.', *Nature cell biology*, 13(10), pp. 1202–13. doi: 10.1038/ncb2331.

Tan, W., Palmby, T. R., Gavard, J., Amornphimoltham, P., Zheng, Y. and Gutkind, J. S. (2008) 'An essential role for Rac1 in endothelial cell function and vascular development', *The FASEB Journal* , 22(6), pp. 1829–1838. doi: 10.1096/fj.07-096438.

TD, P. (2006) 'Kinetics of the formation and dissociation of actin filament branches mediated by Arp2/3 complex', *Biophys. J.*, 91, p. 3519.

TD, P. (2009) 'Cofilin dissociates Arp2/3 complex and branches from actin filaments', *Curr. Biol.*, 19, p. 537.

Thumkeo, D., Keel, J., Ishizaki, T., Hirose, M., Nonomura, K., Oshima, H., Oshima, M., Taketo, M. M. and Narumiya, S. (2003) 'Targeted disruption of the mouse rho-associated kinase 2 gene results in intrauterine growth retardation and fetal death.', *Molecular and cellular biology*, 23(14), pp. 5043–55.

Tischer, E., Mitchell, R., Hartman, T., Silva, M., Gospodarowicz, D., Fiddes, J. C. and Abraham, J. A. (1991) 'The human gene for vascular endothelial growth factor. Multiple protein forms are encoded through alternative exon splicing.', *The Journal of biological chemistry*, 266(18), pp. 11947–54.

Tkachenko, E., Gutierrez, E., Saikin, S. K., Fogelstrand, P., Kim, C., Groisman, A. and Ginsberg, M. H. (2013) 'The nucleus of endothelial cell as a sensor of blood flow direction.', *Biology open*, 2(10), pp. 1007–12. doi: 10.1242/bio.20134622.

Torres, V. E., Harris, P. C. and Pirson, Y. (2007) 'Autosomal dominant polycystic kidney disease.', *Lancet*, 369(9569), pp. 1287–301. doi: 10.1016/S0140-6736(07)60601-1.

Toshima, J., Toshima, J. Y., Amano, T., Yang, N., Narumiya, S. and Mizuno, K. (2001) 'Cofilin phosphorylation by protein kinase testicular protein kinase 1 and its role in integrin-mediated actin reorganization and focal adhesion formation.', *Molecular biology of the cell*, 12(4), pp. 1131–45. doi: 10.1091/mbc.12.4.1131.

Valente, E. M., Logan, C. V, Mougou-Zerelli, S., Lee, J. H., Silhavy, J. L., Brancati, F., Iannicelli, M., Travaglini, L., Romani, S., Illi, B., Adams, M., Szymanska, K., Mazzotta, A., Lee, J. E., Tolentino, J. C., Swistun, D., Salpietro, C. D., Fede, C., Gabriel, S., Russ, C., Cibulskis, K., Sougnez, C., Hildebrandt, F., Otto, E. A., Held, S., Diplas, B. H., Davis, E. E., Mikula, M., Strom, C. M., Ben-Zeev, B., Lev, D., Sagie, T. L., Michelson, M., Yaron, Y., Krause, A., Boltshauser, E., Elkhartoufi, N., Roume, J., Shalev, S., Munnich, A., Saunier, S., Inglehearn, C., Saad, A., Alkindy, A., Thomas, S., Vekemans, M., Dallapiccola, B., Katsanis,

N., Johnson, C. A., Attié-Bitach, T. and Gleeson, J. G. (2010) 'Mutations in TMEM216 perturb ciliogenesis and cause Joubert, Meckel and related syndromes', *Nature Genetics*. Nature Research, 42(7), pp. 619–625. doi: 10.1038/ng.594.

Vega, F. M. and Ridley, A. J. (2008) 'Rho GTPases in cancer cell biology.', *FEBS letters*, 582(14), pp. 2093–101. doi: 10.1016/j.febslet.2008.04.039.

Vestweber, D. (2008) 'VE-Cadherin', *Arteriosclerosis, Thrombosis, and Vascular Biology*, 28(2).

Wada, K.-I., Itoga, K., Okano, T., Yonemura, S. and Sasaki, H. (2011) 'Hippo pathway regulation by cell morphology and stress fibers.', *Development (Cambridge, England)*, 138(18), pp. 3907–14. doi: 10.1242/dev.070987.

Wang, C., Baker, B. M., Chen, C. S. and Schwartz, M. A. (2013) 'Endothelial cell sensing of flow direction.', *Arteriosclerosis, thrombosis, and vascular biology*, 33(9), pp. 2130–6. doi: 10.1161/ATVBAHA.113.301826.

Wang, G. L., Jiang, B. H., Rue, E. A. and Semenza, G. L. (1995) 'Hypoxia-inducible factor 1 is a basic-helix-loop-helix-PAS heterodimer regulated by cellular O2 tension.', *Proceedings of the National Academy of Sciences*, 92(12), pp. 5510–5514. doi: 10.1073/pnas.92.12.5510.

Wang, Y., Kaiser, M. S., Larson, J. D., Nasevicius, A., Clark, K. J., Wadman, S. A., Roberg-Perez, S. E., Ekker, S. C., Hackett, P. B., McGrail, M. and Essner, J. J. (2010) 'Moesin1 and Ve-cadherin are required in endothelial cells during in vivo tubulogenesis', *Development*, 137(18).

Watanabe, N., Madaule, P., Reid, T., Ishizaki, T., Watanabe, G., Kakizuka, A., Saito, Y., Nakao, K., Jockusch, B. M. and Narumiya, S. (1997) 'p140mDia, a mammalian homolog of Drosophila diaphanous, is a target protein for Rho small GTPase and is a ligand for profilin', *EMBO Journal*, 16(11), pp. 3044–3056. doi: 10.1093/emboj/16.11.3044.

Wegner, A. and Isenbergt, G. (1983) '2-Fold difference between the critical monomer concentrations of the two ends of actin filaments in physiological salt conditions', *Biochemistry*, 80, pp. 4922–4925.

WHEELER, A. and RIDLEY, A. (2004) 'Why three Rho proteins? RhoA, RhoB, RhoC, and cell motility', *Experimental Cell Research*, 301(1), pp. 43–49. doi: 10.1016/j.yexcr.2004.08.012.

Wheway, G., Schmidts, M., Mans, D. A., Szymanska, K., Nguyen, T.-M. T., Racher, H., Phelps, I. G., Toedt, G., Kennedy, J., Wunderlich, K. A., Sorusch, N., Abdelhamed, Z. A., Natarajan, S., Herridge, W., van Reeuwijk, J., Horn, N., Boldt, K., Parry, D. A., Letteboer, S. J. F., Roosing, S., Adams, M., Bell, S. M., Bond, J., Higgins, J., Morrison, E. E., Tomlinson, D. C.,

Slaats, G. G., van Dam, T. J. P., Huang, L., Kessler, K., Giessl, A., Logan, C. V, Boyle, E. A., Shendure, J., Anazi, S., Aldahmesh, M., Al Hazzaa, S., Hegele, R. A., Ober, C., Frosk, P., Mhanni, A. A., Chodirker, B. N., Chudley, A. E., Lamont, R., Bernier, F. P., Beaulieu, C. L., Gordon, P., Pon, R. T., Donahue, C., Barkovich, A. J., Wolf, L., Toomes, C., Thiel, C. T., Boycott, K. M., McKibbin, M., Inglehearn, C. F., UK10K Consortium, University of Washington Center for Mendelian Genomics, Stewart, F., Omran, H., Huynen, M. A., Sergouniotis, P. I., Alkuraya, F. S., Parboosingh, J. S., Innes, A. M., Willoughby, C. E., Giles, R. H., Webster, A. R., Ueffing, M., Blacque, O., Gleeson, J. G., Wolfrum, U., Beales, P. L., Gibson, T., Doherty, D., Mitchison, H. M., Roepman, R. and Johnson, C. A. (2015) 'An siRNA-based functional genomics screen for the identification of regulators of ciliogenesis and ciliopathy genes.', *Nature cell biology*, 17(8), pp. 1074–87. doi: 10.1038/ncb3201.

Wilkinson, S., Paterson, H. F. and Marshall, C. J. (2005) 'Cdc42-MRCK and Rho-ROCK signalling cooperate in myosin phosphorylation and cell invasion', *Nat Cell Biol*. Nature Publishing Group, 7(3), pp. 255–261.

Witke, W., Sutherland, J. D., Sharpe, A., Arai, M., Kwiatkowski, D. J. and Pollard, T. D. (2001) 'Profilin I is essential for cell survival and cell division in early mouse development', *Proc Natl Acad Sci U S A*, 98(7), pp. 3832–3836.

Xu, K., Sacharidou, A., Fu, S., Chong, D. C., Skaug, B., Chen, Z. J., Davis, G. E. and Cleaver, O. (2011) 'Blood Vessel Tubulogenesis Requires Rasip1 Regulation of GTPase Signaling', *Developmental Cell*. Elsevier, 20(4), pp. 526–539. doi: 10.1016/j.devcel.2011.02.010.

Yajnik, V., Paulding, C., Sordella, R., McClatchey, A. I., Saito, M., Wahrer, D. C. R., Reynolds, P., Bell, D. W., Lake, R., van den Heuvel, S., Settleman, J. and Haber, D. A. (2003) 'DOCK4, a GTPase Activator, Is Disrupted during Tumorigenesis', *Cell*, 112(5), pp. 673–684. doi: 10.1016/S0092-8674(03)00155-7.

Yang, J., Zhang, Z., Roe, S. M., Marshall, C. J. and Barford, D. (2009) 'Activation of Rho GTPases by DOCK Exchange Factors Is Mediated by a Nucleotide Sensor', *Science*, 325(5946).

Yao, L., Romero, M. J., Toque, H. a, Yang, G., Caldwell, R. B. and Caldwell, R. W. (2010) 'The role of RhoA/Rho kinase pathway in endothelial dysfunction.', *Journal of cardiovascular disease research*, 1(4), pp. 165–170. doi: 10.4103/0975-3583.74258.

Yoder, B. K. (2007) 'Role of Primary Cilia in the Pathogenesis of Polycystic Kidney Disease', *Journal of the American Society of Nephrology*, 18(5), pp. 1381–1388. doi: 10.1681/ASN.2006111215.

Zhu, S.-L., Luo, M.-Q., Peng, W.-X., Li, Q.-X., Feng, Z.-Y., Li, Z.-X., Wang, M.-X., Feng, X.-X., Liu, F.

and Huang, J.-L. (2015) 'Sonic hedgehog signalling pathway regulates apoptosis through Smo protein in human umbilical vein endothelial cells.', *Rheumatology (Oxford, England)*, 54(6), pp. 1093–102. doi: 10.1093/rheumatology/keu421.

Zovein, A. C., Luque, A., Turlo, K. A., Hofmann, J. J., Yee, K. M., Becker, M. S., Fassler, R., Mellman, I., Lane, T. F. and Iruela-Arispe, M. L. (2010) 'β1 Integrin Establishes Endothelial Cell Polarity and Arteriolar Lumen Formation via a Par3-Dependent Mechanism', *Developmental Cell*. Elsevier, 18(1), pp. 39–51. doi: 10.1016/j.devcel.2009.12.006.